The role of c-di-AMP in *Listeria monocytogenes* pathogenesis

By

Cheta Siletti

A dissertation submitted in partial fulfillment of

the requirements for the degree of

Doctor of Philosophy

(Microbiology)

at the

UNIVERSITY OF WISCONSIN- MADISON

2024

Date of final oral examination: 08/01/2024
The dissertation is approved by the following members of the Final Oral Committee:

Tu-Anh Huynh, Assistant Professor, Department of Food Science
Mark J. Mandel, Associate Professor, Department of Medical Microbiology and Immunology
Jason M. Peters, Assistant Professor, School of Pharmacy
Wilmara Salgado-Pabón, Associate Professor, Department of Pathobiological Sciences
John-Demian Sauer, Associate Professor, Department of Medical Microbiology and Immunology

ACKNOWLEDGEMENTS

I would like to thank my advisor, Tu Anh Huynh, for her support of my development as a scientist, for encouraging me to pursue my own ideas, and also pushing me to think about things in different ways. Also, I thank my other committee members for their continued support and constructive feedback, especially over the past year as I've been working towards my dissertation.

I would also like to acknowledge my lab members, who have made long days in the lab much easier. Special thanks to Justin Dang for his assistance in producing an acceptable western blot, and Yuxing Chen, for her support and friendship in and out of the lab.

I owe a huge thanks Terra Thiem, and Marcia Verhage for their administrative support and always knowing what form I need to fill out and where it needs to be sent.

I also want to thank the MDTP community for providing a source of friendship and support through the challenges of graduate school.

Finally, I want to thank my friends, family and partner for their unwavering support throughout the past five years.

ABSTRACT

Bacteria are an abundant life form, inhabiting almost every environment on earth. Central to the adaptability of bacteria are second messengers, which are small nucleotide signal transducing molecules. Upon sensing external changes, bacteria fine-tune levels of second-messengers within the cell to modulate the activity of target molecules and elicit an adaptive response. Numerous bacterial second messengers have been discovered to date, including (p)ppGpp and c-di-GMP, and they each have a unique array of biological functions. C-di-AMP is a second messenger well-known for controlling osmolyte homeostasis in bacteria, though since its discovery, research has continued to elucidate novel functions of this molecule, making it regarded as a global regulator. Importantly, c-di-AMP is conditionally essential for many of the bacteria that produce it. One such organism for which c-di-AMP is essential is the pathogen, *Listeria monocytogenes. L. monocytogenes* is the causative agent of Listeriosis, though it also exists as an environmental saprophyte in soil and can persist despite stressors such as high-salt and refrigeration, making it a formidable foodborne pathogen. C-di-AMP in *L. monocytogenes* is synthesized by the diadenylate cyclase (DAC) protein DacA, and degraded by the phosphodiesterase (PDE) proteins PdeA and PgpH. DacA is essential for *L. monocytogenes* growth in rich medium, as the absence of c-di-AMP leads to a signaling cascade causing toxic accumulation of oligopeptides. Despite its importance, accumulation of c-di-AMP can also be toxic. The *ΔpdeAΔpgpH* (ΔPDE) mutant, which accumulates ~4-5x more c-di-AMP than WT has a weakened cell wall, is sensitive to osmotic stress and cell-wall targeting agents, and was previously shown to be attenuated for virulence in a mouse-model of infection, however the underlying mechanisms by which c-di-AMP accumulation exerts these toxic effects remain largely unknown. Upon performing RNAseq to assess transcriptional differences between WT and ΔPDE during basal growth, I found that ΔPDE was diminished for expression of its pathogenicity island, which is activated by the transcriptional regulator PrfA. The work

presented in Chapter 2 presents the finding that c-di-AMP accumulation diminishes levels of the PrfA-activating cofactor, glutathione (GSH). The work presented in Chapter 3 characterizes the transcriptional response of *L. monocytogenes* to GSH, which paves the way for future studies on the effect of c-di-AMP on GSH metabolism. Appendices A and B present preliminary data characterizing c-di-AMP levels under different growth and stress conditions, and the influence of c-di-AMP accumulation and depletion on transcriptional responses to cell-wall stress. These findings represent the discovery of novel c-di-AMP regulated pathways, the knowledge of which will aid in the understanding of *L. monocytogenes* growth and pathogenesis.

TABLE OF CONTENTS

LIST OF TABLES

LIST OF FIGURES

Chapter 1. C-di-AMP homeostasis and signaling in *Listeria monocytogenes* and other bacterial species

INTRODUCTION

C-di-AMP was first identified during crystallization of the *Thermotoga maritima* DNA damage checkpoint protein, DisA[1]. Upon solving the crystal structure of DisA, it was found that an uninterpreted binding pocket within the protein contained c-di-AMP[2]. Following this discovery, in-vitro experiments confirmed that both *T. maritima* and *Bacillus subtilis* DisA possessed diadenylate cyclase activity, and were able to synthesize c-di-AMP from two molecules of ATP[3]. Though c-di-AMP was discovered in 2008, its production by a living organism was not experimentally demonstrated until 2010, when *L. monocytogenes* was discovered to secrete c-di-AMP during infection, triggering a robust host type I interferon (IFN) response[4]. Since this discovery, c-di-AMP synthesis has been identified in a number of other bacteria as well as some archaea, and much has been learned about its biological functions[5]. Today, c-di-AMP is recognized as a regulator of cell-wall and osmolyte homeostasis, central metabolism, virulence, and stringent-response activation[6]. Despite its importance, uncontrolled c-di-AMP accumulation has detrimental consequences such as increased antibiotic susceptibility, sensitivity to osmotic stress, and attenuated virulence, though the mechanisms underlying c-di-AMP toxicity remain largely unexplained[7]. While both the essentiality and toxicity of c-di-AMP has been demonstrated in numerous bacteria, *L. monocytogenes* has remained a gold-standard model for the study of c-di-AMP due to its genetic tractability and well-defined intracellular lifecycle. In this chapter, a summary of current literature on c-di-AMP metabolism, molecular targets, biological functions, and regulation of pathogenesis will be presented. A special focus will be placed on c-di-AMP metabolism in *L. monocytogenes*, the model organism used for work presented in this thesis.

C-DI-AMP SIGNALING IN BACTERIA

Maintenance of c-di-AMP homeostasis

Synthesis of c-di-AMP

C-di-AMP is synthesized from two molecules of ATP by diadenylate-cyclase (DAC) proteins and degraded into 5' pApA by phosphodiesterase (PDE) proteins[8] (**Fig. 1.1**). To date, five distinct DAC proteins have been discovered: DisA, DacA (CdaA), CdaS, CdaM, and CdaZ[6]. Common to all known DACs is a DisA_N (DAC) catalytic domain[7]. DacA is the most widespread DAC protein, and has a DAC domain linked to three N-terminal transmembrane helices which form a homodimer[9]. DacA is inhibited by interactions with the proteins GlmM and DacB (CdaR), both of which are frequently transcribed in the same operon as DacA in *Firmicutes*[10]. In many *Firmicutes,* such as *Listeria monocytogenes*, *Lactococcus lactis*, and *Staphylococcus aureus*, DacA is the only DAC present in the genome[9]. However, in the case of *Bacillus subtilis,* both DacA, CdaS, and DisA are present[11]. Compared to DacA and DisA, distribution of CdaS, CdaM, and CdaZ are more narrowly distributed. CdaM is found exclusively in *Mycoplasma* sp., whereas CdaZ is found in Archaea[12].

Degradation of c-di-AMP

C-di-AMP is degraded to 5' pApA by phosphodiesterase (PDE) proteins (**Fig. 1.1**). To date, three classes of PDEs have been described: GdpP, PgpH, and Pde2, though the presence of these PDEs varies by bacterial species[1]. Furthermore, PDEs contain either a DHH/DHHA1 or HD catalytic domain[13–15]. The GdpP-type PDE PdeA was the first PDE to be characterized[15] and contains two N-terminal transmembrane helices, a Per-Arnt-Sim (PAS) domain, a degenerate GGDEF domain, and a catalytic DHH/DHHA1 domain[16]. The PAS domain is thought to act as a signal receptor that detects nitric oxide, oxygen, and carbon monoxide via a tightly-bound heme-molecule[16]. In addition, (p)ppGpp has been shown to

competitively inhibit PdeA enzymatic activity[15]. Though PdeA has been extensively characterized, it is only found in *Firmicutes* and *Mollicutes*[6].

The PgpH-type PDE was first characterized in *L. monocytogenes*[13], following its discovery as a c-di-AMP binding protein by a chemical proteomics screen[13,17]. Before the discovery of PgpH, only DHH/DHHA1-domain containing proteins had been established as c-di-AMP PDEs. However, structure-function studies following the discovery of PgpH as a c-di-AMP molecular target demonstrated that that the PgpH HD-motif is required for c-di-AMP binding and hydrolysis[13]. To date, only PgpH-class PDEs have been shown to possess an HD catalytic domain, however, similarly to the GdpP class of PDEs, PgpH is a membrane-protein. PgpH contains 7-transmembrane helices as well as an amino-terminal extracellular domain, the latter of which is thought to be involved in signal detection[13]. Extracellular signals which regulate PgpH activity remain unknown, though like GdpP, PgpH is inhibited by the stringent-response alarmone (p)ppGpp[13]. The third class of PDE, Pde2 (DhhP), is cytosolic and contains only the DHH/DHHA1 catalytic domain. The Pde2 homolog NrnA can further degrade 5' pApA, the product of c-di-AMP hydrolysis, to AMP[18,19]. DhhP/NrnA-like PDEs are found in most bacterial species, though some have preferred nano-RNase activity towards 5'pApA or additional short RNA oligonucleotides[6].

Transport of c-di-AMP

In addition to synthesis and degradation, efflux of c-di-AMP is also important for c-di-AMP homeostasis. The multi-drug export family (MDR) transporters MdrM and MdrT are important for c-di-AMP export and induction of host type-I IFN response by *L. monocytogenes*[4,20] (**Fig. 1.1**). In fact, c-di-AMP was first discovered in *L. monocytogenes* by characterization of a strain overexpressing MDRs[4]. Though MdrM and MdrT are present in other bacteria such as *S. aureus*, it is unclear if their function is the same as in *L. monocytogenes*. Overexpression of MdrM and MdrT in *S. aureus* does not cause an increase in c-di-AMP

secretion as it does in *L. monocytogenes*, indicating that the function of these transporters may not be conserved[21].

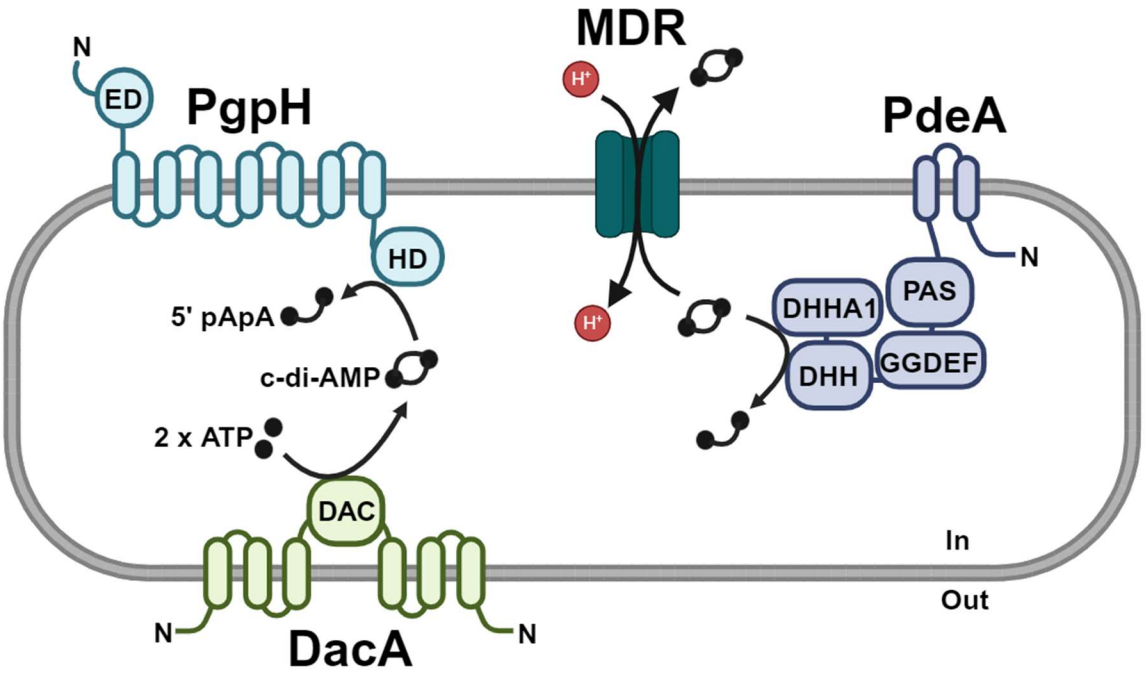

Figure 1.1: Synthesis, degradation, and transport of c-di-AMP in *L. monocytogenes*.

C-di-AMP molecular targets and functions

C-di-AMP has a number of known molecular targets which are outlined in **Table 1.1** and whose biological functions are described in this section. The best-known class of c-di-AMP targets are transporters of osmoprotectants. However, other targets include central metabolic regulators, small RNAs, transcription factors, and several proteins of unknown function. Cellular processes regulated by c-di-AMP molecular targets are outlined in this section.

Table 1.1. Summary of known molecular targets of c-di-AMP and the species in which they have been observed.

Class	Target	Species	Reference
Control of osmolyte homeostasis	**OpuCA**	*S. aureus, L. monocytogenes, B. subtilis*	[22–24]
	KimA	*B. subtilis, S. aureus, L. monocytogenes*	[25–27]
	KtrCD	*M. pneumoniae, B. subtilis, L. monocytogenes*	[27,28]
	KtrA	*S. aureus, B. subtilis, S. agalacticiae*	[28]
	OpuBA	*S. agalacticiae*	[29]
	KdpD	*S. aureus, L. monocytogenes, Synechococcus elongatus*	[27,30,31]
	CpaA	*S. aureus, B. subtilis,*	[25,32]
	BusR	*S. agalacticiae*	[29]
	TrkH	*S. agalacticiae*	[33]
	KupAB	*L. lactis*	[34]
	KhtT	*B. subtilis*	[35]
	YrvC	*B. subtilis*	[25]
	CabP	*S. pneumoniae*	[36]
	MgtE	*B. subtilis*	[25]
Central Metabolism	**PycA**	*L. monocytogenes*	[37]
	DarR	*M. smegmatis*	[38]

Signal transduction	**CbpB (DarB)**	*B. subtilis, L. monocytogenes*	[39,40]
	YdaO	*B. subtilis*	[41]
Mammalian Targets	**RECON**	c-di-AMP targets independent of bacterial species	[42]
	STING	c-di-AMP targets independent of bacterial species	[43]
	DDX41	c-di-AMP targets independent of bacterial species	[44]
Unknown Functions	**NrdR**	*L. monocytogenes*	[17]
	CbpA	*L. monocytogenes*	[17]
	PstA	*L. monocytogenes, S. aureus, B. subtilis*	[17,45,46]

Osmolyte homeostasis

Maintenance of internal turgor pressure is important for bacterial growth[47]. Because the cytosol is composed largely of water, but bacteria lack transporters for water, exchange of osmolytes or compatible solutes is required to maintain turgor pressure[47]. C-di-AMP controls transporters of osmolytes such as K+, Mg+, carnitine, amino acids, and glycine betaine by interacting either directly with transporters, or with signal transduction proteins or riboswitches that control transporter expression[22,23,36,48,49]. To date, one of the most well-characterized functions of c-di-AMP is inhibition of potassium transport. In *S. aureus*, c-di-AMP binds to the RCK_C domain of CpaA, a K+ antiporter, and promotes its activity[32,50]. In *L. lactis*, the K+ transporters KupAB are inhibited by c-di-AMP binding[51]. KimA, a K+/H+ symporter, and KtrCD, a low affinity K+ transporter, are inhibited by c-di-AMP binding in *B. subtilis, S. aureus*, and *L. monocytogenes*[25,49,52]. Furthermore, the K+/H+ antiporter KhtT and the potassium exporter CpaA have been shown to interact with c-di-AMP in *B. subtilis*[25]. In addition to binding directly to membrane transporters, c-di-AMP controls K+ transport by binding to intermediate signaling

molecules that regulate transporters. KdpD is a sensor kinase which, when bound by c-di-AMP, inhibits expression of the Kdp family of K+ transporters[8,23,30,31]. In S. *pneumoniae*, CabP complexes with TrkH to transport K+ when c-di-AMP concentrations are low[36]. Finally, c-di-AMP controls K+ transport by interacting with riboswitches to control transporter expression. in *B. subtilis,* the *ydbO* riboswitch, which is upstream of both *kimA* and *ktrAB,* inhibits translation of KimA when bound to c-di-AMP[53]. In addition to controlling potassium homeostasis, c-di-AMP affects activity of other compatible solute transporters. OpuCA is a high-affinity ATPase carnitine transporter which is inhibited by c-di-AMP binding to its cystathionine beta-synthase (CBS) domain in *S. aureus, L. monocytogenes*, and *B. subtilis*.

Disruption of both c-di-AMP synthesizing and degrading proteins has consequences for bacterial osmoregulation. In a number of bacterial species, including *L. monocytogenes*, c-di-AMP depletion caused by DAC disruption causes cell lysis due to uncontrolled uptake of osmolytes and compatible solutes[29,37,49,54–56].

Stringent response

C-di-AMP is a mediator of signal transduction related to activation of the stringent response. In both *B. subtilis* and *L. monocytogenes*, the c-di-AMP binding protein CbpB binds to and activates the (p)ppGpp synthetase RelA in its apo form, but not when it is bound to c-di-AMP. When c-di-AMP is depleted, uncontrolled activation of RelA by apo-CbpB leads to a sharp increase in (p)ppGpp in c-di-AMP null strains of *L. monocytogenes* and *B. subtilis*. This phenomenon renders c-di-AMP essential for these species in rich media, as (p)ppGpp accumulation leads to decreased levels of GTP, which inhibit the transcriptional repressor CodY[54]. Derepression of the CodY regulon is toxic when nutrients are abundant. This is thought to be due to uncontrolled uptake of oligopeptides by the Opp family of transporters, as mutations in OppA suppress DacA essentiality in rich media[39,54]. The crosstalk between c-di-AMP and the stringent response is complex, as (p)ppGpp inhibits the activity of both PdeA and

PgpH[39]. Indeed, nutritional status can influence c-di-AMP levels. For instance, in *B. subtilis*, c-di-AMP levels change during growth in different types of nitrogen sources[11].

Monitoring of DNA damage

In *B. subtilis*, the DAC protein DisA is inhibited when it encounters double-stranded DNA breaks, lowering intracellular concentrations of c-di-AMP[57]. Indeed, during sporulation, c-di-AMP concentrations are 3-fold higher than during vegetative growth[58]. Similarly, deletion of the DAC CdaS leads to delayed sporulation in *B. thurigiensis*[59]. DisA also interacts with the recombinase RecA by downregulating its activity, which allows for DNA repair to occur before replication is resumed[60].

Central metabolism

The central metabolic protein pyruvate carboxylase (PycA), which synthesizes pyruvate from oxaloacetate, is enzymatically inhibited when bound to c-di-AMP. Indeed, in a c-di-AMP null strain of *L. monocytogenes*, a toxic accumulation of citrate is observed, likely due to uncontrolled flux of oxaloacetate through the TCA cycle[17]. Furthermore, depletion of c-di-AMP results in increased carbon flux into glutamate/glutamine synthesis, which is reliant on the activity of PycA in *L. monocytogenes*[17,61]. In *M. smegmatis*, the transcription factor DarR inhibits expression of genes involved in the synthesis of medium-chain fatty acids when bound to cdi-AMP[38]. Additionally, c-di-AMP binds to the PII-like protein PstA. The PII family of proteins is known to be involved in regulation of nitrogen metabolism[45]. The crystal structure of PstA has been solved, allowing for insight into c-di-AMP binding mechanisms[62,63], though the molecular targets of PstA, as well as the effect c-di-AMP has on PstA function, remain largely unclear.

Cell size and cell-wall homeostasis

In *L. monocytogenes*, elevated c-di-AMP levels are associated with a thinner cell-wall, increased sensitivity to cell-wall targeting antibiotics and salt, and attenuated virulence[13,64]. c-di-

AMP accumulation impairs the synthesis of the cell-wall precursors D-ala-D-ala and UDP-MurNac, which likely contributes to enhanced cell-wall targeting antibiotic sensitivity[64]. Though the relationship between cell-wall synthesis and c-di-AMP remains largely unknown, it is likely that c-di-AMP accumulation reduces intracellular K+ levels by inhibiting K+ importers, which in turn impairs the function of Ddl, the enzyme which synthesizes D-ala-D-ala[64]. Interestingly, c-di-AMP appears to have differential effects on cell-wall homeostasis, depending on the organism. For instance, in *B. subtilis*, c-di-AMP accumulation causes beta-lactam sensitivity to an even greater extent than in *L. monocytogenes*[64]. Conversely, in *Staphylococcus aureus*, c-di-AMP accumulation is associated with increased lipotechoic acid (LTA) crosslinking, and increased resistance to cell-wall targeting antibiotics[65].

C-di-AMP related phenotypes in *L. monocytogenes*

Since *L. monocytogenes* was found to secrete c-di-AMP into the host cell cytosol, C-di-AMP metabolizing proteins in *L. monocytogenes* have been well-characterized. Given its genetic tractability, *L. monocytogenes* is a fantastic model in which to study the functions of c-di-AMP. A summary of *L. monocytogenes* phenotypes associated with aberrant c-di-AMP production, as well as the proposed mechanisms underlying these phenotypes, are presented in this section and summarized in **Table 1.2.**

C-di-AMP depletion and associated phenotypes

One of the first characterized *L. monocytogenes* c-di-AMP metabolic mutants was the c*ΔdacA* strain. Because c-di-AMP is essential for *L. monocytogenes* growth in rich medium, a conditionally-inducible copy of *dacA* must be introduced in order to delete *dacA* from its native locus[66]. In fact, in the absence of a conditional copy of *dacA*, attempts to delete *dacA* in *L. monocytogenes* resulted in spontaneous suppressor mutations in the *oppABCDF* operon, or in *relA*[54]. It was later found that c-di-AMP depletion causes an increase in (p)ppGpp, which is

mediated by RelA, which in turn leads to increased expression of *opp* genes, and uncontrolled uptake of osmolytes which is toxic in complex medium[54]. Decreased c-di-AMP levels also affect bacterial growth and viability by causing increased bacteriolysis both during growth in broth[66]. Increased turgor pressure, due to uncontrolled osmolyte uptake by potassium transporters inhibited by c-di-AMP, contributes to increased lysis, as supplementing growth medium with 2% NaCl reduces lysis of the c∆*dacA* mutant. Increased turgor pressure may also stress the cell-wall, and unsurprisingly, c∆*dacA* mutant exhibits increased sensitivity to the cell-wall targeting antibiotics such cefuroxime, penicillin and ampicillin. c∆*dacA* also exhibits reduced growth and increased lysis in macrophages, and is attenuated for virulence in a mouse model of infection[17]. Despite lower levels of growth in macrophages, release of bacterial DNA by c∆*dacA* during lysis hyper stimulates IFN-β response, leading to increased host-cell proptosis. The AIM2 inflammasome, which is stimulated by bacterial DNA, also causes caspase-1 cleavage and host-cell pyroptosis[67]. Infection of AIM2 deficient macrophages with c∆*dacA* resulted in reduced host-cell death, confirming the involvement of bacterial DNA release in increased pyroptosis[66,68]. The mechanisms underlying increased c∆*dacA* bacteriolysis during infection are complex, and likely mediated by some independent mechanisms. Deletion of citrate synthase (*citZ*) in c∆*dacA* significantly rescues growth in macrophages and in-vivo virulence, but has no effect on growth in broth[17]. The c∆*dacA* mutant exhibits increased synthesis of glutamine/glutamate (Glx, a process which is dependent on activity of the c-di-AMP repressed enzyme pyruvate carboxylase (PycA). Increased PycA activity leads to increased flux through the oxidative branch of the TCA cycle, leading to increased synthesis of Glx, the first step of which is performed by CitZ. Thus, a metabolic imbalance resulting from uncontrolled Glx biosynthesis contributes to attenuated virulence in c∆*dacA,* and this is distinct from the mechanisms contributing the c∆*dacA* growth defect in broth[17].

While reduced *dacA* expression has many consequences for bacterial growth, *dacA* overexpression has a phenotypic effect in the Δ*mdrMTAC* background. The MDR family transporters MdrM and MdrT mediate c-di-AMP secretion[4,20], which triggers host type I IFN response during infection. However, the additional transporters MdrA and MdrC also contribute to modestly to host interferon response during infection[69]. Thus, the *mdrMTAC* quadruple mutant has been used extensively to study the consequences of reduced c-di-AMP secretion. In addition to inducing reduced interferon response during infection, *mdrMTAC* is more susceptible to vancomycin than WT. Interestingly, *dacA* overexpression improved vancomycin resistance in the *mdrMTAC* background, but not in WT[69]. This suggests that there is a complex interplay between c-di-AMP levels, MDR transporters, and cell-wall homeostasis.

C-di-AMP accumulation and associated phenotypes

By and large, function of one PDE is sufficient to compensate for deletion of the other, but there are certain phenotypes that appear to be specific to loss of just one PDE. The Δ*pdeA* mutant exhibits increased acid tolerance, as well as modestly increased tolerance of the cell-wall targeting antibiotics cefuroxime, ampicillin and penicillin[66]. In addition, Δ*pdeA* produces more biofilm than WT or Δ*pgpH* alone, indicating a unique function for PdeA in the context of biofilm formation[70]. Interestingly, ΔPDE was able to form even more biofilm than Δ*pdeA* alone, suggesting that there is an additive effect of c-di-AMP accumulation on biofilm formation. Conversely, cΔ*dacA* was strongly impaired for biofilm formation, further indicating a correlation between c-di-AMP levels and biofilm forming ability[70]. Another study found that *ΔpgpH* was impaired for biofilm formation, and downregulated expression of genes involved in cell-wall homeostasis and motility[71]. It is important to note that this study was performed on a *L. monocytogenes* strain belonging to serotype 4a, in contrast to most studies which utilize strains belonging to serotype 1/2a[72]. Furthermore, the authors of this study did not test a Δ*pdeA,* or a ΔPDE mutant for biofilm forming ability and gene expression, so it is difficult to conclude

whether PgpH function alone is important for biofilm formation. PdeA overexpression was found to enhance *mdrMTAC* vancomycin susceptibility[69]. Interestingly, overexpression of *pdeA* achieved by placing it under control of the PrfA-dependent *actA* promoter (P_{actA}-*pdeA)* in the PrfA* background significantly increased cefuroxime sensitivity compared to PrfA* alone[66].

While *pdeA* or *pgpH* deletions alone have been shown to have only modest effects on *L. monocytogenes* phenotypes, the double Δ*pdeA*Δ*pgpH* (ΔPDE) mutant has many defects. Notably, ΔPDE is highly susceptible to osmotic stress induced by NaCl and sorbitol[23]. In WT, growth under NaCl stress induces uptake of the compatible solute carnitine[23]. C-di-AMP binds to the CBS domain of OpuC, the ATPase component of the carnitine transporter OpuCA, and under NaCl stress, ΔPDE, as well as OpuC mutants abolished for c-di-AMP binding, are severely impaired for uptake of carnitine[23]. Once again, this highlights the importance of c-di-AMP for adaptation to osmotic stress. ΔPDE also exhibits disrupted cell-wall homeostasis, and is susceptible to β-lactams such as cefuroxime, as well as D-cycloserine (DCS), antibiotics targeting distinct steps in cell-wall synthesis[64]. β-lactams inhibit transpeptidation of peptidoglycan[73] whereas DCS inhibits the enzymes Dal and Ddl, which generate D-alanine and the cell-wall precursor molecule D-ala-D-ala, respectively[74]. ΔPDE susceptibility to DCS can be partially restored by addition of potassium to the medium, as this corrects for reduced intracellular potassium and enhances function of the potassium-dependent enzyme Ddl. However, potassium fails to restore ΔPDE resistance to cefuroxime, which targets a later step in cell-wall synthesis[64]. This illustrates that c-di-AMP signaling is highly complex, and affects multiple independent pathways involved in cell-wall homeostasis. In addition to increased sensitivity to cell-wall targeting agents, ΔPDE is attenuated for virulence in a mouse model of infection[13].

Table 1.2: Summary of *L. monocytogenes* c-di-AMP metabolic mutants, and their observed phenotypes.

Genotype	Effect on c-di-AMP levels	Phenotype	References
cΔ*dacA*	Decreased	Increased bacteriolysis	17,66
		Increased cefuroxime, penicillin, ampicillin susceptibility	
		Uncontrolled osmolyte uptake	
		Reduced growth rate	
		Reduced biofilm	
		Impaired growth in macrophages	
		Attenuated virulence in a mouse model.	
***dacA* overexpression**	Not directly measured, presumably increased	restores *mdrMTAC* vancomycin susceptibility	69
***ΔpdeA ΔpgpH* (ΔPDE)**	Increased	Increased cefuroxime, ampicillin, lysozyme, D-cycloserine susceptibility	13,64
		Increased susceptibility to osmotic stress	
		Increased biofilm	
		Thinner cell-wall	
		Reduced peptidoglycan, UDP-MurNac, D-ala-D-ala	
		Reduced intracellular K+	
		Attenuated virulence in a mouse model	
		Reduced growth in macrophages	
		Increased IFN-β induction	
Δ*pdeA*	Unchanged in broth, modestly increased during macrophage infection	increased acid tolerance	69,70
		Modestly increased resistance to cefuroxime, penicillin, ampicilli	
		Enhanced biofilm formation	
***pdeA* overexpression**	Not directly measured, presumably decreased	enhances *mdrMTAC* susceptibility to vancomycin	66,69
		enhances PrfA* susceptibliity to cefuroxime	
Δ*pgpH*	Moderately increased in broth, unchanged during macrophage infection	Decreased biofilm formation (serotype 4b)	71

ROLES OF C-DI-AMP IN BACTERIAL PATHOGENESIS

C-di-AMP is produced by a number of pathogenic bacteria. It is important not just for bacterial growth and survival within the host environment, but can mediate a number of host-responses that affect both bacterial virulence and host-survival. The ways by which c-di-AMP signaling affects virulence potential can be divided into three major categories, 1) Alteration of host immune response, 2) altered expression or activity of bacterial virulence factors 3) Inherent changes in growth or metabolism with pleiotropic effects on virulence potential. A summary of what is currently understood of these mechanisms in relevant bacterial pathogens is summarized in the Table 1.3, and detailed in this section.

Table 1.3: Summary of virulence-related phenotypes in pathogens with altered c-di-AMP metabolism.

Organism	c-di-AMP level of mutant	Effect on virulence	Proposed mechanism(s)	Reference
Listeria monocytogenes	c∆*dacA*, reduced c-di-AMP	Attenuated virulence in macrophages, mice	Increased lysis, metabolic imbalance	[66,75]
	ΔPDE, increased c-di-AMP	Attenuated virulence in macrophages, mice	Reduced glutathione availability, unknown mechanisms	Current study
Staphylococcus aureus		c-di-AMP promotes survival in macrophages	c-di-AMP induces interferon response in macrophages, promotes bacterial growth	[21]
Borrelia burgdorferi	c*ΔdhhP*, increased c-di-AMP	Abolished virulence in a mouse model	cΔdhhP mutant exhibits reduced growth rate, is defective for production of growth-rate dependent virulence factor, OspC	[76]
Streptococcus pneumoniae	*Δpde1, Δpde2, Δpde1pde2, increased c-di-AMP in all mutants*	Attenuated for virulence in a mouse model	General basal growth defect may affect in-vivo virulence	[14]

Streptococcus pyogenes	ΔgdpP, Δpde2 increased c-di-AMP	Reduced virulence in subcutaneous mouse-infection model	ΔgdpP, Δpde2 are defective for post-transcriptional processing, and transcription, respsectively, of virulence factor SpeB.	[77,78]
	ΔcdaA, decreased c-di-AMP	Reduced virulence in subcutaneous mouse-infection model	Reduced SpeB transcription	[78]
Mycobacterium tuberculosis	*ΔcnpB*, increased c-di-AMP	Attenuated for virulence in a mouse model	Increased type-1 IFNR, potentially additional mechanisms	[79]
Borrelia turicatae	ΔcdaA, decreased c-di-AMP	Attenuated in mouse model of infection	Mice failed to seroconvert, ΔcdaA likely cleared early in infection	[80]
Enterococcus faecalis	ΔcdaA, decreased c-di-AMP	Attenuated in mouse and Galleria mellonella models of infection	Impaired biofilm formation in vitro may translate to colonization defect in vivo	[81]
	ΔgdpP, ΔdhhP, ΔgdpPdhhP, increased c-di-AMP	All three mutants attenuated in insect model of infection. ΔdhhP, ΔgdpPdhhP impaired for colonization in mice	Potential hypersensitivity to increased osmolyte concentrations in urine	[81,82]
Porphyromonas gingivalis	Δpde_{PG}, decreased c-di-AMP	Increased virulence in Galleria mellonella	Exhibits higher LPS immunoreactivity, may affect host-immune response	[83]
	ΔcdaR, increased c-di-AMP	Attenuated virulence in Galleria mellonella	Reduced planktonic growth and biofilm formation in vivo may affect virulence potential	[83]
Bacillus anthracis	*ΔgdpP, ΔpgpH-HD, ΔgdpPpgpH-HD,* increased c-di-AMP	All three mutants attenuated in mouse model of infection	Inhibition of potassium uptake causes reduced anthrax toxin expression.	[84,85]
Streptoccus suis	ΔgdpP, increased c-di-AMP	decreased adherence to and invasion of Hep-2 cells, attenuation in a mouse model	Decreased expression of virulence factors	[86]

Streptococcus mitis	Δpde1, effect on c-di-AMP levels not tested	Decreased adherence to oral keratinocytes	Reduced biofilm formation in vitro may contribute to adhesion defect	[87]
Clostridioides difficile	ΔgdpP, increased c-di-AMP	Decreased persistence in mouse GI tract	Decreased osmotic stress tolerance	[88]

Mammalian Targets of c-di-AMP

C-di-AMP is produced by many pathogens, so not surprisingly, mammalian cells have evolved mechanisms for sensing and responding to this second messenger. Three mammalian c-di-AMP receptors, STING, DDX41, and RECON, have been discovered to date (**Fig. 1.2**). STING is a protein found in the membrane of phagocytic cells, and is activated by c-di-AMP, c-di-GMP, or 3',3'-cGAMP released by bacteria, as well as 2',3'-cGAMP produced by the host cell in response to foreign DNA[89]. Once activated by a cognate nucleotide, STING activates a downstream cascade, eventually leading to the production of type I interferons[90]. c-di-AMP also binds to and inhibits the mammalian protein RECON, which negatively regulates NF-kB[42]. During infection, c-di-AMP binds to RECON, resulting in increased NF-kB activity which reduces bacterial survival[42]. Additionally, the pattern recognition receptor (PRR) DDX41 serves as a sensor for c-di-AMP in the host. Upon interacting with c-di-AMP, DDX41 then forms a complex with STING to mediate downstream activation of interferon genes[44]. Activation of mammalian immune receptors by c-di-AMP can have both positive and negative effects on bacterial virulence. In *L. monocytogenes, M. tuberculosis,* and *S. aureus*, Type-1 interferon activation by c-di-AMP via the STING axis promotes bacterial survival[21,75]. Upregulating STING activation in mice by treatment with purified c-di-AMP, or infection with the *L. monocytogenes tetR::tn917* mutant, which hypersecretes c-di-AMP, resulted in decreased protective immunity in a type-I IFN-dependent manner[75]. Similarly, c-di-AMP released by *S. aureus* biofilms induces STING-dependent type-1 IFN response, and this is beneficial for *S. aureus* survival[21]. Conversely, mice

infected with the *M. tuberculosis* Δ*cnpB* mutant, which accumulates higher levels of c-di-AMP than WT, exhibited increased Type-1 IFN response and enhanced survival[79]. However, further research is needed to confirm whether c-di-AMP-activation of Type-1 IFN via STING results in attenuated virulence of the *M. tuberculosis* Δ*cnpB mutant.*

An indicator of host-immune response to the pathogen *B. turicatae* is the development of IgA or IgM antibodies against *Borrelia.* This process is referred to as seroconversion[91]. Interestingly, mice infected with the *B. turicatae* ΔcdaA mutant, which produces low levels of c-di-AMP, failed to seroconvert. It is likely that the *ΔcdaA* mutant was cleared before a full immune response could be achieved, but it represents a novel mechanism by which altered c-di-AMP levels affect host-immune response nonetheless[80].

A determinant of *Porphyromonas gingivalis* pathogenesis is the host-immune response to bacterial lipopolysaccharide (LPS). C-di-AMP metabolism in *P. gingivalis* is atypical, as deletion of the phosphodiesterase pde_{PG} reduces c-di-AMP production, likely due to de-repression of c-di-AMP synthesis[83]. Importantly, LPS of the *P. gingivalis* Δpde_{PG} mutant exhibits increased immunoreactivity, and was enhanced for virulence in the *Galleria mellonella* insect model[83]. This represents yet another potential mechanism by which c-di-AMP signaling affects host-immune response and bacterial pathogenesis.

Effect of c-di-AMP on bacterial virulence factors

Bacterial virulence factors are specific genes, proteins, or pathways whose activity allows for successful colonization of a host-niche[92]. While virulence factors vary across species, their production and activity is affected by c-di-AMP in many pathogenic species, once again illustrating the vast diversity of processes regulated by c-di-AMP.

In *Borrelia burgdorferi,* the causative agent of Lyme disease, upregulation of the σ^s factor RpoS upregulates production of the major virulence factor OspC. OspC is an outer membrane

protein that protects bacteria from host phagocytosis, and is required for infection[93]. In a *B. burgdorferi ΔdhhP* phosphodiesterase mutant, c-di-AMP accumulates to high levels, and this abolishes growth in a mouse-model of infection[76]. Interestingly, the *ΔdhhP* mutant is impaired for RpoS induction, as well as OspC. RpoS induction is in part mediated by the transcriptional regulator BosR, which also exhibited a reduction in the *ΔdhhP* mutant[76]. Thus, in *B. burgdorferi*, c-di-AMP affects signaling cascades important for production of major virulence factors. The exact mechanism of this regulation remains unclear, but additional consequences of diminished BosR activity in the *ΔdhhP* represent an exciting subject of future studies.

Streptococcus pyogenes causes diseases ranging from strep throat, to infective endocarditis and toxic shock syndrome (TSS)[94]. SpeB (secreted pyrogenic exotoxin B) is a secreted cysteine protease and major virulence factor of *S. pyogenes*. SpeB has a number of effects during infection, ranging from damage of host tissue to immunomodulatory activity on host-immune response[95,96]. Both the DAC mutant, *ΔcdaA* and the PDE mutants *ΔgdpP* and *Δpde2,* are severely attenuated for virulence in a mouse model and have reduced levels of SpeB[77,78]. Interestingly, reduced SpeB in *ΔcdaA* and *Δpde2* takes place at the transcriptional level, whereas a posttranscriptional process causes reduced SpeB in the *ΔgdpP* mutant[77,78]. The effect of c-di-AMP signaling on multiple levels of the same pathway once again highlights the incredible diversity of processes regulated by this second messenger.

Bacillus anthracis is the causative agent of anthrax whose virulence is largely dependent on production of the tripartite anthrax toxin. This toxin is composed of the three polypeptides, protective antigen (PA), lethal factor (LF), and edema factor (EF)[97]. In addition, surface associated proteins, collectively referred to as the S-layer, represent an additional virulence factor[98]. Both S-layer proteins and anthrax toxin production are regulated by AtxA[99]. Potassium stimulates SpooA phosphorylation in *B. anthracis*, which represses AbrB, a repressor of anthrax toxin expression[100]. *B. anthracis encodes* two known c-di-AMP phosphodiesterases, GdpP and

PgpH. Both a Δ*gdpP* mutant, a Δ*pgpH*-HD mutant lacking the PgpH catalytic HD-domain, and a double Δ*gdpP*Δ*pgpH*-HD double mutant produce elevated amounts of c-di-AMP and are attenuated for virulence in a mouse model[84]. Expression of toxin genes was significantly downregulated in both the single and double PDE mutants, whereas S-layer formation was only impaired in the double PDE mutant[84]. A later study identified the potassium transport systems KdpFABC and KtrCB/D as molecular targets whose activity is inhibited by c-di-AMP in *B. anthracis*. The study went on to demonstrate that c-di-AMP accumulation inhibits potassium transport and decreases intracellular potassium in *B. anthracis,* and that overexpressing KdpD and KtrC restored toxin expression in the double PDE mutant[85]. Thus, it is speculated that reduced potassium resulting from c-di-AMP accumulation in *B. anthracis* indirectly causes depression of AbrB, which in turn represses toxin expression. However, further studies are needed to confirm this hypothesis.

Streptococcus suis is a major zoonotic pathogen which can cause serious disease in both pigs and humans[101]. *S. suis* serotype 2 (SS2) is able to synthesize c-di-AMP, and possesses the c-di-AMP PDE, GdpP[86]. In-frame deletion of *gdpP* in SS2 resulted in increased c-di-AMP accumulation, reduced hemolytic activity, impaired adhesion to and invasion of the human laryngeal cell-line Hep-2, and attenuated virulence in a mouse model. Remarkably, the same study demonstrated that the expression virulence genes important for hemolysis, adhesion, invasion, and colonization were decreased in the Δ*gdpP* strain[86]. However, the underlying mechanisms by which c-di-AMP accumulation decreases virulence-gene expression and attenuates virulence in *S. suis* have yet to be identified.

Finally, *L. monocytogenes* has a well-defined intracellular lifecycle, beginning with receptor-mediated phagocytic uptake into host cells by InlA and InlB, or uptake by professional phagocyte. PlcA, PlcB, and Mpl enable escape from the phagocytic vacuole, and ActA mediates host-actin polymerization, enabling *L. monocytogenes* to swim through the cytosol and into

neighboring cells[102]. Hpt, another *L. monocytogenes* virulence factor, is a transporter which enables acquisition of glucose-6-phosphate, an important carbon source in the host cell cytosol[103]. Expression of genes encoding these *L. monocytogenes* virulence factors is activated by the transcriptional regulator PrfA[104]. Upon entry into the host cytosol, which is rich in glutathione (GSH), PrfA is activated by allosteric binding to GSH, which primes it for binding to the promoter sequence of its core regulon[105,106] (**Fig. 1.2**). In minimal media, supplementation with GSH or reducing agents such as TCEP, which activate GSH synthesis, also leads to upregulation of PrfA genes[107]. C-di-AMP accumulation in the ΔPDE mutant results in attenuated virulence in a mouse model, and until recently, very little was known of the underlying mechanisms. However, as part of work in presented in this thesis, it was discovered that the ΔPDE mutant is impaired for expression of the core PrfA regulon in minimal media, as well as during activation by GSH and TCEP. The mechanisms underlying this discovery are examined in Chapter 2.

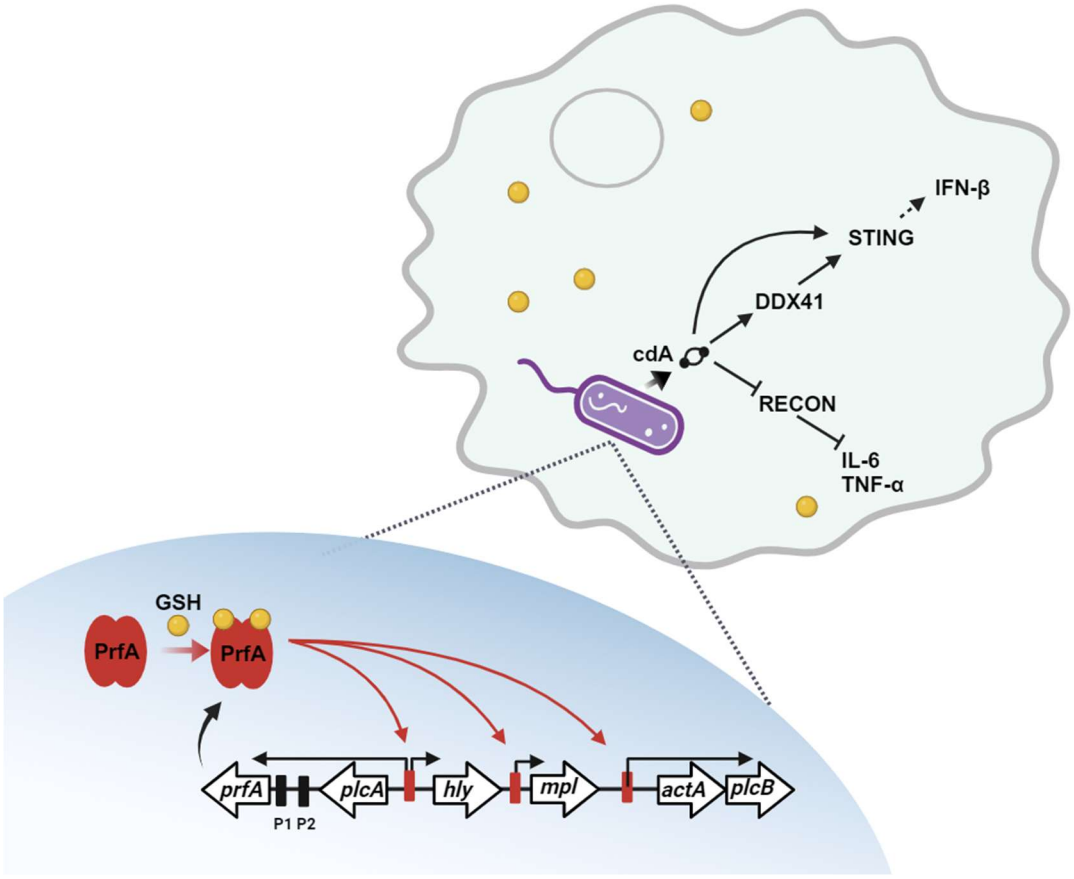

Figure 1.2. Model of virulence-program activation by PrfA, and host-targets of c-di-AMP during *L. monocytogenes* infection.

Effects of c-di-AMP perturbation that indirectly affect virulence

In addition to controlling expression or activity of virulence factors, and modulating host immune-response, c-di-AMP also regulates a number of biological processes which indirectly affect virulence potential. C-di-AMP has been demonstrated to influence biofilm formation, osmotic stress tolerance, acid tolerance, and cell-wall homeostasis in vitro, though for a number of pathogens these traits also affect virulence potential.

Enterococcus faecalis is a commensal member of the human gut microbiome, but is also an opportunistic pathogen. One key trait that allows *E. faecalis* to persist on host-tissues and

resist antibiotic treatment is its biofilm forming ability[108]. Kundra et al. found that *E. faecalis* possesses one DAC (CdaA) and two PDEs (DhhP and GdpP) and that deletion of *cdaA* causes a decrease in c-di-AMP levels, whereas deletion of *dhhP* or *gdpP* alone increased c-di-AMP levels, with deletion of both PDEs having an additive effect. Upon examining the consequences of altered c-di-AMP levels, the authors found that the *ΔcdaA, ΔdhhP, ΔgdpP*, and Δ*dhhPΔgdpP* mutants were all attenuated for virulence in a mouse model[81]. To further explore the underlying mechanisms of these virulence defects, the authors went on to show that biofilm *ebpA* transcription, which is required for robust biofilm formation, was reduced in ΔcdaA[81]. Interestingly, biofilm forming ability was not affected in the PDE mutants, indicating that yet another c-di-AMP regulated process impairs virulence in these strains. The Δ*dhhP*, Δ*gdpP*, and Δ*dhhPΔgdpP* exhibited modestly reduced growth in urine. C-di-AMP levels and *cdaA* transcription have been also been shown to decrease in *E. faecalis* upon growth in urine, whereas *dhhP* and *gdpP* transcripts increase[81,82]. Together, this suggests that c-di-AMP accumulation may be detrimental during *E. faecalis* adaptation to osmotic stressors encountered in urine, or at other points during infection.

Streptococcus mitis is a commensal bacteria in the oral cavity, though it can cause opportunistic disease in immunocompromised individuals[109]. In order to survive in the oral environment. *S. mitis* must be able to withstand changes in pH, form biofilm, and withstand stressors such as antibiotics and oral hygiene products[87]. *S. mitis* synthesizes c-di-AMP via CdaA, and degrades c-di-AMP via Pde1 and Pde2[87]. The Δpde1 mutant was found defective for oral keratinocyte colonization and biofilm formation, indicating yet another link between c-di-AMP, biofilm forming ability, and pathogenesis[87].

Clostridioides difficile is an enteric pathogen which causes severe diarrhea, particularly in the context of dysbiosis following antibiotic treatment[110]. To cause severe infection, *C. difficile* must overcome a number of stressors encountered in the intestinal tract such as low pH, high

osmolarity of the intestinal lumen, and bile salts[111]. As c-di-AMP has been shown to affect response to these stressors in numerous other organisms, Oberkampf et al. explored the role of c-di-AMP in *C. difficile* growth and pathogenesis. They found that the Δ*gdpP* mutant accumulated ~3x more c-di-AMP than WT, whereas neither Δ*disA* nor Δ*cdaA* mutants were altered for c-di-AMP levels[88]. The Δ*gdpP* mutant was also impaired for basal growth, resistance to cell-wall targeting antibiotics, and osmotic stress, and exhibited a strong biofilm phenotype compared to WT[88]. They went on to demonstrate that the Δ*gdpP* mutant is impaired for persistence in the murine GI tract, likely due to impaired tolerance to osmotic stress[88]. However, the contribution of other c-di-AMP mediated defects cannot be excluded.

CONCLUDING REMARKS

C-di-AMP is essential for many of the bacterial species who produce it, highlighting its importance as a regulator of bacterial growth and homeostasis. While enzymes that synthesize and degrade c-di-AMP are well-characterized, the mechanisms by which these enzymes are regulated by environmental signals is not well understood. C-di-Amp also has a number of known molecular targets. These targets affect many aspects of bacterial growth and physiology, including osmolyte homeostasis, central metabolism, and transcriptional regulation. C-di-AMP also has well-characterized effects on the host-immune response. It is a potent inducer of type-1 IFN response, and this occurs through the STING axis. Finally, altered levels of c-di-AMP within the bacterial cell result in several phenotypes for which there is no clear molecular intermediate. Notably, c-di-AMP accumulation causes a defective cell-wall and attenuated virulence in *L. monocytogenes*, though the underlying mechanisms are not known. Through my dissertation work, I discovered that c-di-AMP accumulation impairs *L. monocytogenes* virulence-program activation, and causes diminished levels of the virulence signal GSH. In the following chapters, work will be presented which sheds light on the mechanisms by which c-di-AMP impairs PrfA activation and diminishes GSH levels in *L. monocytogenes*.

Chapter 2. C-di-AMP accumulation disrupts glutathione metabolism and impairs virulence program expression in *Listeria monocytogenes*

Experiments, and writing of this chapter were carried out with the help of Matthew Freeman, Zepeng Tu, David M. Stevenson, Daniel Amador-Noguez, John-Demian Sauer, and Tu Anh N. Huynh

A version of this chapter is being revised for resubmission in *Infection and Immunity*.

ABSTRACT

C-di-AMP is an essential second messenger that regulates many cellular processes within bacterial cells. For bacteria that produce c-di-AMP, maintaining c-di-AMP homeostasis is critical for physiology and pathogenesis. Unregulated c-di-AMP accumulation attenuates the virulence of many bacterial pathogens, including those that do not require c-di-AMP for growth. Nevertheless, the mechanisms by which c-di-AMP regulates bacterial pathogenesis remain poorly understood. For the human pathogen *Listeria monocytogenes*, a mutant lacking both c-di-AMP phosphodiesterases, denoted as the ΔPDE mutant, accumulates ~4x higher levels of c-di-AMP than WT and is significantly attenuated in the mouse model of systemic infection. *L. monocytogenes* is an intracellular pathogen that replicates in the mammalian cell cytosol, and the intracellular lifecyle is dependent on the master transcription factor PrfA, which is activated by reduced glutathione (GSH) during infection. Our transcriptomic analysis revealed that the ΔPDE mutant is significantly impaired for the expression of virulence genes within the PrfA core regulon. Subsequent quantitative gene expression analyses validated this phenotype both at the basal level and upon PrfA activation by GSH. A constitutively active PrfA* variant, PrfA G145S, which mimics the glutathione-bound conformation, restores virulence gene expression in ΔPDE but only partially rescues virulence defect. Through GSH quantification and uptake assays, we found that the ΔPDE strain is significantly depleted for GSH, and that c-di-AMP inhibits GSH uptake. Constitutive expression of *gshF* (encoding a GSH synthetase) does not restore GSH levels in the ΔPDE strain, suggesting that c-di-AMP inhibits GSH synthesis activity or promotes GSH catabolism. Taken together, our data reveals GSH metabolism as another pathway that is regulated by c-di-AMP. C-di-AMP accumulation depletes cytoplasmic GSH levels within *L. monocytogenes* that leads to impaired virulence program expression.

INTRODUCTION

The Gram-positive bacterial pathogen *Listeria monocytogenes* is a leading cause of mortality and hospitalization among foodborne illnesses. Although acquired orally, *L. monocytogenes* can cross the intestinal barrier to cause systemic infection with mortality rates approaching 16% in clinical cases[112]. A hallmark of *L. monocytogenes* pathogenesis is its intracellular life cycle[113]. *L. monocytogenes* can invade many mammalian cell types, including non-phagocytic cells, using surface-anchored internalins such as InlA and InlB. Following host-cell entry, *L. monocytogenes* escapes the vacuole using the pore-forming toxin listeriolysin O (LLO, encoded by the *hly* gene), the phospholipases PlcA and PlcB, and the metalloprotease Mpl. In the cell cytosol, *L. monocytogenes* uses ActA to polymerize host actin, required for intracellular motility and cell-to-cell spread. All virulence genes required for the intracellular lifestyle, including those listed above, are transcriptionally regulated by the master transcription factor PrfA[104].

PrfA belongs to the Crp/Fnr family of transcription factors, which function as homodimers with a DNA-binding helix-turn-helix motif in each monomer[104,114]. Unlike other Crp/Fnr proteins that require a co-factor for DNA binding, apo-PrfA can bind to its consensus palindromic DNA operator, called PrfA box, to maintain a basal expression of some virulence genes in the absence of activating signals. During infection, PrfA is allosterically activated by reduced glutathione (GSH), which is derived from the host or synthesized by *L. monocytogenes*[105]. GSH binds PrfA at the stoichiometry of one GSH per PrfA monomer, inducing an active DNA-binding conformation of the helix-turn-helix motif[106]. A single mutation (G145S) near the GSH binding site renders PrfA constitutively active by mimicking the GSH-bound conformation[106,115] During broth growth in *Listeria* Synthetic Medium (LSM), PrfA can be activated by supplementation with GSH or reducing reagents such as TCEP, which stimulate GSH synthesis[107]. *L. monocytogenes* makes and secretes c-di-AMP, a nucleotide second messenger that regulates many molecular

targets in bacterial cells[4,17]. C-di-AMP-binding proteins within *L. monocytogenes* have different cellular functions, such as potassium and carnitine uptake, central metabolism and ppGpp synthesis, and signal transduction[17,23,27,39,63]. During infection, secreted c-di-AMP is recognized by mammalian cytosolic receptors to activate inflammatory and type I interferon responses[4,42]. Type I interferon response is considered to promote *L. monocytogenes* pathogenesis during systemic infection, but activates an anti-bacterial response in the gastrointestinal tract[116,117].

C-di-AMP homeostasis is critical to *L. monocytogenes* growth and infection. In *L. monocytogenes*, c-di-AMP is synthesized from ATP by a single diadenylate cyclase, DacA, and degraded by the phosphodiesterases PdeA and PgpH into the linear nucleotide pApA[118]. In rich media, such as Brain Heart Infusion (BHI) broth, the Δ*dacA* mutant accumulates a toxic level of ppGpp that inhibits bacterial growth[54]. By contrast, the Δ*pdeA* Δ*pgpH* mutant (hereafter denoted as the ΔPDE mutant) does not exhibit an appreciable growth defect in BHI, but is greatly attenuated for virulence in the mouse model of intravenous infection, despite hyper-activating type I interferon response[13]. These phenotypes indicate that the mechanisms underlying ΔPDE virulence attenuation are related to bacterial defects during infection.

The pathways and molecular targets leading to diminished pathogenesis at high c-di-AMP levels are not clearly defined. Here, we found that c-di-AMP accumulation inhibits the expression of the PrfA core regulon in *L. monocytogenes*, and this defect contributes to virulence attenuation in the ΔPDE strain. We further found that c-di-AMP accumulation impairs GSH uptake, and either inhibits GSH synthesis or promotes GSH catabolism. Combined, these defects result in a cytoplasmic GSH depletion that impairs PrfA function. Our findings reveal GSH metabolism as another pathway that is regulated by c-di-AMP, with implications in *L. monocytogenes* virulence program and nutrient acquisition inside the host.

RESULTS

The ΔPDE mutant is defective for virulence gene expression in the PrfA core regulon

The ΔPDE mutant was previously shown to be highly attenuated for virulence in a mouse model of infection[13]. To identify genes that could contribute to ΔPDE virulence defect, we performed RNAseq to profile the transcriptomes of the wild-type (WT) and ΔPDE strains, grown in LSM to mid-exponential phase[54].The cDNA libraries were sequenced at the depth of 17 – 20 million reads, and had 856x-1042x mapped read coverage. Compared to WT, the ΔPDE strain displayed mostly a transcriptional downshift, with 67 genes being down-regulated by ≥4-fold, and 9 genes being up-regulated by ≥4-fold (P value < 0.05) (**Table S2.1**). Remarkably, the vast majority of down-regulated genes in ΔPDE belong to the 10403S prophage locus (41 genes) or the PrfA core regulon (11 genes) (**Fig. 2.1A**). In addition to the core regulon, PrfA has been shown to putatively or indirectly regulate the expression of up to 145 other genes[119]. We did not observe those genes among the most significantly altered in ΔPDE, except for the upregulation of a cellobiose transporter (*lmo2683*) and two genes of hypothetical function (*lmo0186* and *lmo0019*) **(Table S2.1)**. Furthermore, *kdpA* expression was also reduced by ~6-fold in the ΔPDE strain, consistent with an inhibitory effect of c-di-AMP on the expression of the *kdp* operon, which encodes a potassium uptake system (**Table S2.1**)[27,30].

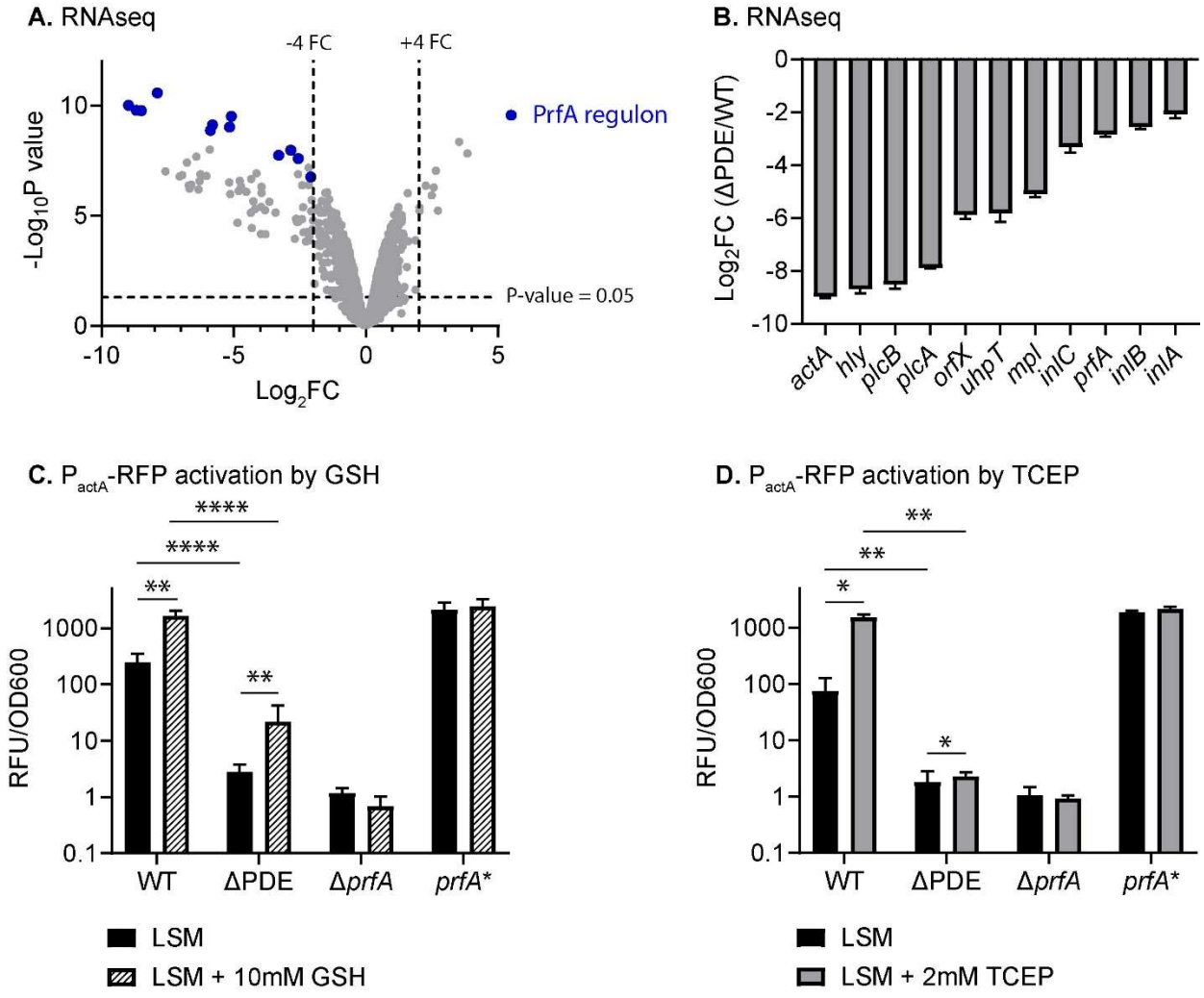

Figure 2.1. C-di-AMP accumulation impairs virulence gene expression in *L. monocytogenes*. A. Volcano plot of differentially expressed genes in the ΔPDE mutant compared to the WT strain. RNAseq was performed on mid-log cultures grown in *Listeria* Synthetic Medium (LSM). Blue dots indicate genes within the PrfA core regulon. **B.** Log_2fold change in PrfA-regulated gene expression was calculated from read counts per million (cpm) of two independent ΔPDE cultures, compared to the average of two independent WT cultures. Data in A and B are from the same RNAseq experiment. **C.** PrfA-regulated gene expression was quantified in *L. monocytogenes* strains carrying P_{actA}::RFP transcriptional reporter. The Δ*prfA* and *prfA** strains were quantified as negative and positive controls, respectively. Cultures were grown to mid-log in LSM or LSM + 10mM GSH. Red fluorescence was normalized to OD600 of each respective culture. **D.** Red fluorescence was quantified as in C. LSM cultures were left untreated or treated with 2mM TCEP for 2 hours. Data in C and D are average of 3-6 independent experiments. Error bars show standard deviations. Statistical analyses were performed by two-way ANOVA with multiple comparisons for the indicated pairs: ns, non-significant; *, $P < 0.05$; **, $P < 0.01$; ****, $P < 0.0001$

PrfA is the master transcription factor that upregulates *L. monocytogenes* virulence gene expression required for the intracellular life cycle[114]. Our RNAseq analysis revealed that the PrfA core regulon was significantly down-regulated in the ΔPDE strain (**Fig. 2.1A-B**). Given the ΔPDE virulence defect, we focused on evaluating PrfA-regulated virulence genes. To validate RNAseq results, we employed RT-qPCR to quantify the expression of three genes in the PrfA core regulon: *prfA*, *hly* (an early gene), and *actA* (a late gene). In LSM cultures, the ΔPDE strain was significantly impaired for the expression of all three genes, reflecting a defect in basal PrfA function (**Fig. S2.1A-C**). To examine gene expression upon PrfA activation, we next performed RT-qPCR for cultures grown in the presence of GSH. Although these genes were up-regulated by GSH in both the WT and ΔPDE strains, their expression levels in ΔPDE remained significantly lower than in WT (**Fig. S2.1A-C**). Furthermore, of the three genes, we noticed that the ΔPDE strain was most impaired for *actA* expression, which was reduced by 10 – 100-fold compared to the basal and activated levels in WT (**Fig. S2.1C**). As an independent method to quantify *actA* expression, we used a red fluorescent reporter fused with the *actA* promoter (P_{actA}-RFP)[107]. This assay confirmed that the ΔPDE strain was significantly defective for *actA* expression both at the basal level and upon PrfA activation by GSH or TCEP (**Fig. 2.1C-D**). To examine PrfA-activation in the context of host-cell infection, we assessed PrfA-protein levels in an ex-vivo model. Western blot against PrfA protein was performed on WT and ΔPDE-infected immortalized bone-marrow-derived-macrophages (iBMMs). We found that PrfA protein was less abundant in ΔPDE during iBMM infection relative to WT, consistent with our prior findings that PrfA cannot be fully activated in ΔPDE. (**Fig. S2.2**). It can be concluded from these results that virulence-program activation is impaired in ΔPDE, resulting in both reduced expression of the PrfA core-regulon and lower levels of PrfA protein levels during ex-vivo infection.

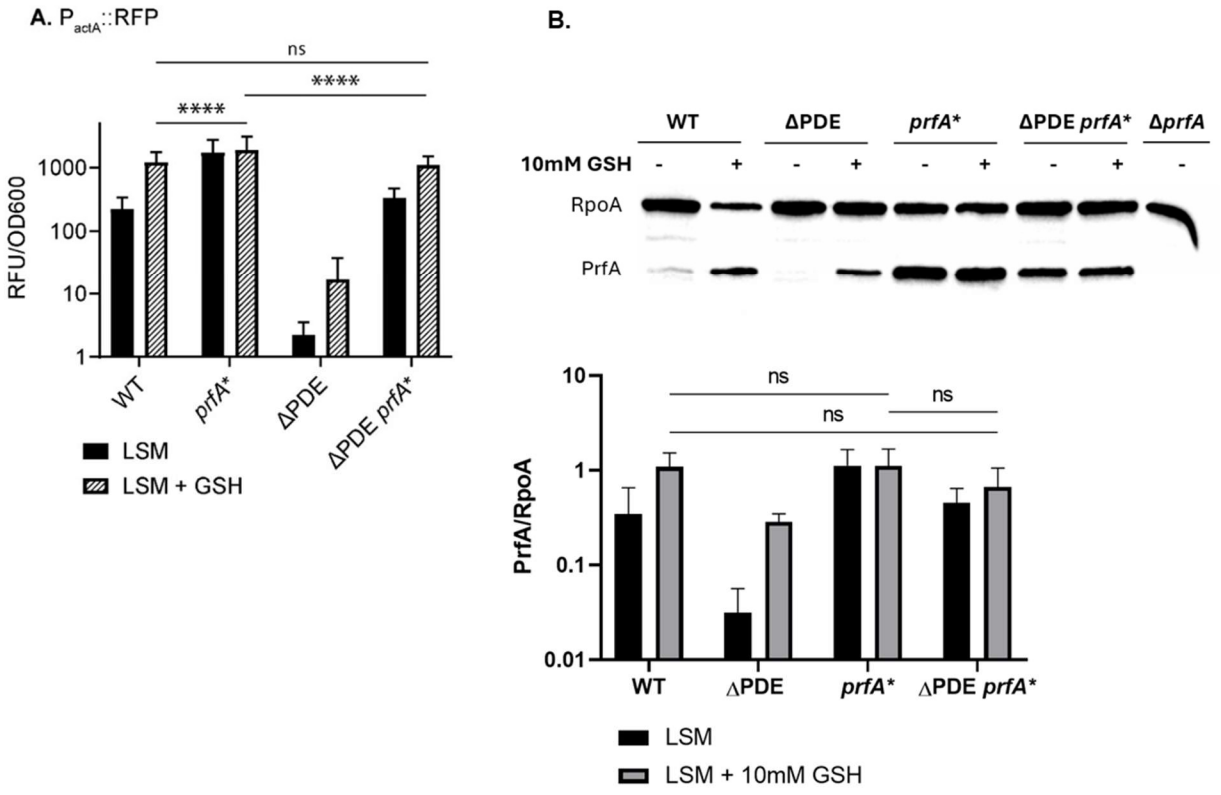

Figure 2.2. A constitutive PrfA variant (PrfA*) restores PrfA activity and *prfA* gene expression upon c-di-AMP accumulation. A. P_{actA}::RFP transcriptional activity was quantified in WT, ΔPDE, and isogenic strains in which the native *prfA* allele is replaced with *prfA** (G145S). Red fluorescence, normalized to OD600, was measured for mid-log cultures grown in LSM or LSM + 10mM GSH, and normalized to OD600. **B.** Representative western blot of PrfA and the loading control RpoA (top panel), measured in cultures grown in LSM or LSM + 10mM GSH. Quantification of PrfA band intensity relative to RpoA (bottom panel) is representative of four independent experiments. Error bars show standard deviations. Statistical analyses were performed by two-way ANOVA with multiple comparisons for the indicated pairs: ns, non-significant; *, $P < 0.05$; **, $P < 0.01$; ****, $P < 0.0001$

Defective PrfA activity contributes to virulence-program activation at high c-di-AMP levels

To assess whether a defect in PrfA activity contributes to the defective ΔPDE virulence-program activation in vitro, we replaced the native *prfA* gene with a constitutive PrfA* variant (G145S) that structurally mimics the GSH-bound form[106,115]. In transcriptional reporter assays with P_{actA}-RFP, the *prfA** strain exhibited constitutive *actA* expression, independent of GSH

supplementation, as expected (**Fig. 2.2A**). In the ΔPDE background, the *prfA** allele restored *actA* expression to the WT level in LSM + 10mM GSH (**Fig. 2.2A**). Interestingly, *actA* expression was not constitutive in ΔPDE *prfA**. Previous studies have always found the activity of PrfA* to be constitutive regardless of GSH availability. To address concerns that the ΔPDE *prfA** strain harbored additional mutations affecting PrfA activity, we whole-genome sequenced the ΔPDE PrfA* strain to confirm no additional mutations were present which could cause PrfA* responsiveness to GSH. Interestingly, WGS results of ΔPDE PrfA* revealed a single SNP not present in the PrfA* parent strain. The SNP was in the 5'UTR region upstream of the gene *lmo0514.* Previously, Quereda *et al.* found that *lmo0514,* an internalin like protein, is upregulated in *L. monocytogenes* upon infection[120]. To verify that this SNP did not affect our transcriptional reporter results, we remade the strain and confirmed via whole-genome sequencing that it acquired no additional mutations compared to the parent strain. Results from the transcriptional reporter assay with P_{actA}-RFP in the new ΔPDE PrfA* were effectively identical to results with our original strain (**Table S2.9**). As an additional readout for PrfA activity in the reconstructed ΔPDE PrfA* strain, we assessed growth on Glucose-6-phosphate (G6P). Hexose-6-phosphates are thought to be one of the major carbon sources during intracellular growth[121] and are imported through Hpt, which is a member of the core PrfA regulon[119]. When hexose-6-phosphates are the sole source of carbon, *L. monocytogenes* can grow only when PrfA is activated. Consistent with our previous data, ΔPDE was unable to utilize G6P as a carbon source when supplemented with 10mM GSH. Interestingly, in the absence of GSH, ΔPDE *prfA** was almost completely abolished for G6P utilization, though its growth was largely improved relative to ΔPDE when the medium was supplied with 10mM GSH (**Figure S2.7**). Together, these data suggest that the observed GSH-responsiveness of PrfA* in the ΔPDE background is a direct consequence of c-di-AMP accumulation.

To further examine PrfA activity in ΔPDE, we next assessed PrfA protein stability. To do this, PrfA protein levels were measured by western blot in the reconstructed ΔPDE *prfA** strain. In the ΔPDE background, the *prfA** allele restored PrfA levels in the presence of 10mM GSH (**Fig. 2.2B).** However, PrfA levels appeared modestly lower in the ΔPDE *prfA** strain in the absence of GSH (**Fig. 2.2B).** Together, these data suggest that in ΔPDE, unidentified factors impair full PrfA activation in the absence of GSH, leading to reduced virulence-gene expression and reduced PrfA protein levels.

We next tested the possibility that factors independent of PrfA repress *prfA* transcription in ΔPDE. Previous studies have shown that the stress-responsive sigma factor SigB influences PrfA expression via the P2 promoter, though this interaction is complex and varies depending on environmental conditions[122]. ΔPDE is susceptible to salt stress[23], a condition that robustly activates SigB[123], suggesting that ΔPDE may be defective for SigB activity, and that this affects *prfA* expression. First, to test whether *sigB* activation in WT is altered upon PrfA activation by 10mM GSH, RT-qPCR was performed on *sigB*, and *opuCA,* which is strongly activated by SigB[124]. There was no significant difference in either *sigB* or *opuCA* expression in either LSM, or LSM + 10mM GSH (**Fig. S2.3A**) This suggests that SigB activity is not upregulated during the PrfA-activating conditions tested. *ActA* expression in Δ*sigB* during growth in LSM and LSM + 10mM GSH was also assessed. Δ*sigB* was not significantly impaired for *actA* expression in either LSM or LSM + 10mM GSH, suggesting that under the conditions tested, SigB is not required for PrfA activity (**Fig. S2.3B**). RsbX is a strong negative regulator of SigB, and inactivation of *rsbX* causes strong upregulation of SigB[125],. Inactivating *rsbX* in the ΔPDE background did not rescue *actA* expression (**Figure S2.3B**). Taken together, these results demonstrate that diminished *prfA* expression in ΔPDE is not influenced by SigB.

Glutathione deficiency impairs PrfA activity in the ΔPDE strain

Given the partial restorative effect of PrfA* on both virulence-gene expression and PrfA protein levels, we hypothesized that the ΔPDE strain might be impaired for PrfA activation by GSH. We found that GSH levels were significantly depleted in the ΔPDE strain compared to WT, in LSM, LSM + GSH, and LSM + TCEP. (**Fig. 2.3A-B)**. The deficiency in GSH was not due to oxidation, since the total glutathione pool and oxidized glutathione (GSSG) were also reduced in ΔPDE (**Fig. S2.4A-B)**. Furthermore, a previous study found that methylglyoxalase is important to maintain a sufficient GSH pool in *L. monocytogenes*[126]. We found no evidence for an impaired methylglyoxalase activity in the ΔPDE strain, since ΔPDE exhibited a comparable methylglyoxal susceptibility to WT (**Fig. S2.4C**). The ΔPDE strain could fully induce *actA* expression to the activated level of WT, but only upon both GSH supplementation and *gshF* over-expression (**Fig. 2.3C**). These data suggest that GSH deficiency contributes to reduced PrfA function in the ΔPDE strain.

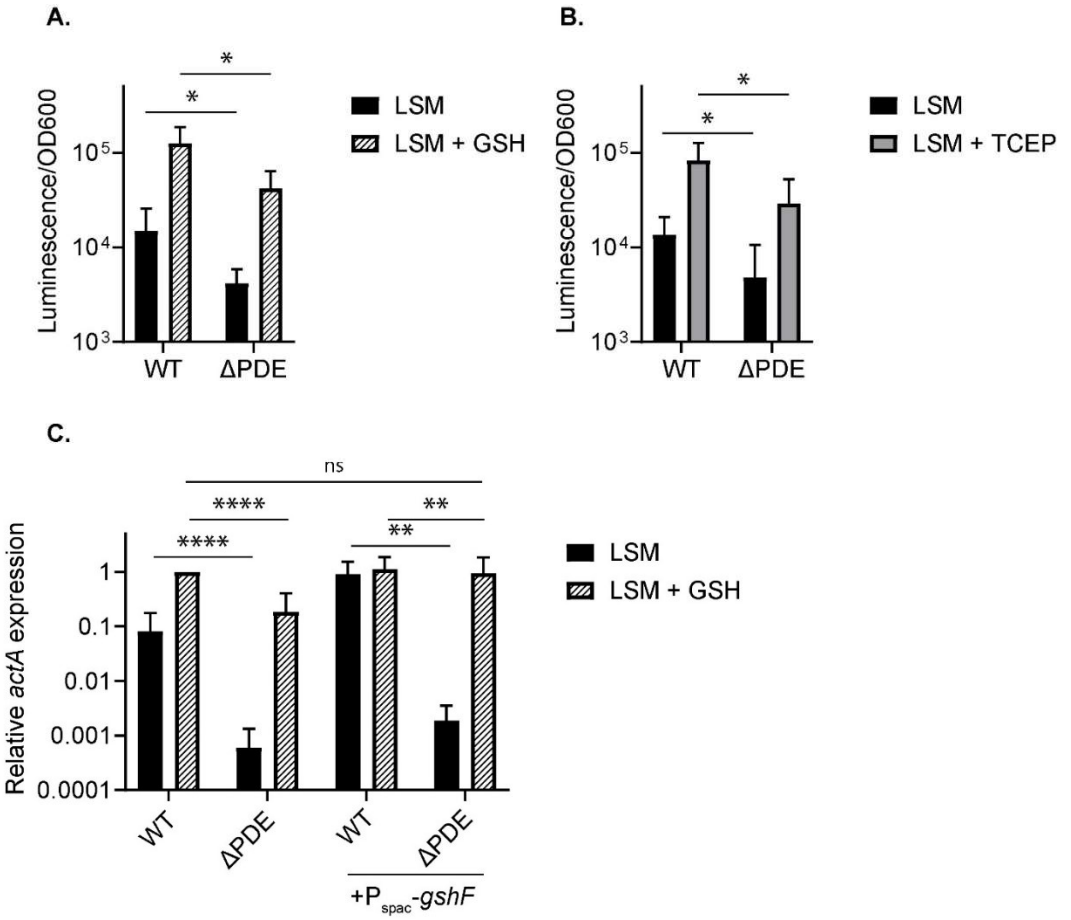

Figure 2.3. A deficiency in reduced glutathione (GSH) contributes to diminished virulence gene expression at high c-di-AMP levels. A. Reduced glutathione (GSH) levels of mid-log cultures grown in LSM or LSM + 10mM GSH. GSH levels are reported by luminescence and normalized to culture OD600. Several GSH standards were quantified to determine the linear range of the assay, and all biological samples were quantified at appropriate dilutions to ensure measurements were within the linear range. **B.** Mid-log LSM cultures were left untreated, or treated with 2mM TCEP for 2 hours, and quantified for GSH levels as in A. **C.** *actA* gene expression by RT-qPCR. Cultures were grown in LSM or LSM + 10mM GSH to mid-log phase. In each culture, the expression level of *actA* was normalized to that of *rplD* as a housekeeping gene. Error bars represent standard deviations. Statistical analyses were performed by two-way ANOVA with multiple comparisons for the indicated pairs: ns, non-significant; *, P < 0.05; **, P < 0.01; ****, P < 0.0001

C-di-AMP accumulation inhibits GSH uptake

We sought to determine how GSH is depleted in the ΔPDE mutant. *L. monocytogenes* synthesizes GSH by the glutathione synthase GshF[127] and also imports GSH via CtaP and OppDF[128]. We evaluated GSH uptake in the Δ*gshF* and ΔPDE Δ*gshF* strains, which cannot

synthesize GSH. These strains were grown in LSM until mid-exponential phase, then supplemented with GSH for ~0.7 doubling times, and quantified for cytoplasmic GSH levels. In these assays, we found that ΔPDE Δ*gshF* accumulated about one third of GSH levels compared to Δ*gshF*, suggesting a GSH uptake defect at high c-di-AMP levels (**Fig. 2.4A**). We further verified this phenotype in ^{3}H-GSH uptake assays for the Δ*gshF* and ΔPDE Δ*gshF* cultures (**Fig. 2.4B**). To assess if GSH transporter expression was impaired in ΔPDE, we performed qRT-PCR on *ctaP* and *oppDF*. In both LSM and LSM + 10mM GSH, neither expression of *ctaP* nor *oppD,* which shares an operon with *oppF,* were lower than WT (**Fig. S2.5A-B**). Interestingly, expression of *ctaP* was downregulated in both WT and ΔPDE during growth in 10mM GSH (**Fig. S2.5A).** Taken together, it can be concluded that GSH uptake in ΔPDE is impaired, though not due to reduced expression of known GSH transporters.

The intracellular lifecycle of *L. monocytogenes*, including cytosolic replication and cell-to-cell spread, can be assessed by a plaque formation assay upon infection of murine fibroblasts (L2 cells)[129]. To evaluate GSH uptake during infection, we performed an L2 plaque formation assay. Consistent with a previous study[105] we found the Δ*gshF* mutant to form significantly smaller plaques than the WT strain (**Fig. 2.4C**). Compared to Δ*gshF*, the ΔPDE Δ*gshF* strain was much further diminished for plaque formation, indicating that c-di-AMP accumulation impairs GSH uptake during infection (**Fig. 2.4C**).

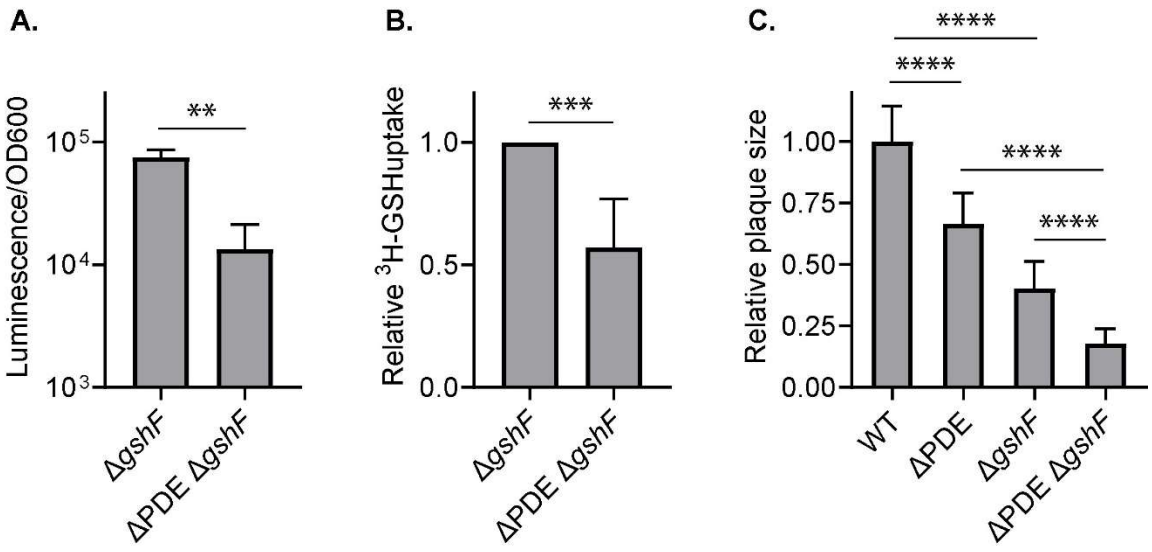

Figure 2.4. C-di-AMP accumulation inhibits GSH uptake in broth culture and ex-vivo infection. A. The Δ*gshF* and ΔPDE Δ*gshF* strains were grown to mid-log phase in LSM and supplemented with 10mM GSH for one hour (approximately 0.7 doublings in LSM). Cultures were thoroughly washed and quantified for intracellular GSH, reported as luminescence normalized to OD600. **B.** ^{3}H-GSH uptake assay. Cultures were grown to mid-log, then supplemented with ^{3}H-GSH for 30 minutes. Uptake activity was assessed by radioactivity normalized to OD600. **C.** Plaque formation at 4 days post infection of L2 fibroblasts. Plaque sizes were quantified by ImageJ. In each experiment, the average plaque size by each strain was normalized to the average WT plaque size, set at 1. Error bars represent standard deviations. Statistical analyses were performed by Student's t-test in A-B and one-way ANOVA in C, with multiple comparisons for the indicated pairs: **, P < 0.01; ***, P < 0.001; ****, P < 0.0001

C-di-AMP depletes cytoplasmic GSH by inhibiting synthesis or promoting catabolism

The ΔPDE mutant was deficient in intracellular GSH during growth in the absence of GSH supplementation, suggesting a defect in GSH synthesis (**Fig. 2.3A**). We first quantified glycine, cysteine, and glutamate, which are substrates for GSH synthesis by GshF[127]. By LC-MS, we found that the ΔPDE strain was moderately reduced for glutamate, but glycine and cysteine levels were comparable to WT (**Fig. S2.6A**). Given that cysteine is the limiting substrate for GshF activity in bacterial cells[130] it is unlikely that the ΔPDE strain is lacking in substrates for GSH synthesis.

The gene expression levels of *gshF* were comparable in the WT and ΔPDE strains, and in the *prfA** and ΔPDE *prfA** strains, with and without exogenous GSH in the culture medium (**Fig. S2.6B**). Therefore, we next examined post-transcriptional regulation of GshF by replacing the native *gshF* gene with a constitutively expressed allele (P_{spac}-*gshF*). Constitutive expression of P_{spac}-*gshF* in WT and the ΔPDE strain was confirmed via qPCR (**Fig. S2.6B**). To evaluate GSH synthesis, we grew cultures in the absence or presence of TCEP, which activates GSH synthesis without adding GSH to the culture medium[107]. Even upon constitutive *gshF* expression, the ΔPDE mutant was still significantly depleted for GSH, both under the basal condition and TCEP activation (**Fig. 2.5A**). Because constitutive *gshF* expression failed to restore GSH synthesis in ΔPDE, we wondered if GshF protein stability was affected in ΔPDE. Native *gshF* was replaced with a constitutively expressed FLAG-tagged protein (P_{spac}-*gshF*-FLAG) in WT and ΔPDE and Western Blot against the FLAG-epitope was performed for cultures grown in LSM. GshF levels in ΔPDE did not differ significantly from those in WT, indicating that diminished GshF protein stability is not the cause of GSH deficiency in ΔPDE (**Fig S2.8**).

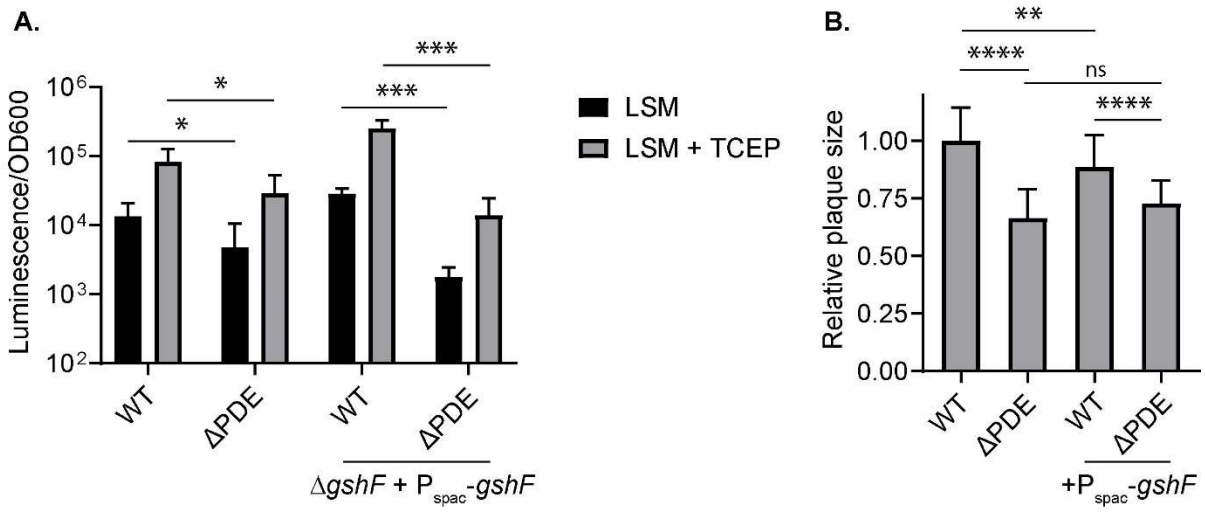

Figure 2.5. Activation of GSH synthesis activity does not restore GSH levels in the ΔPDE strain. A. Intracellular GSH levels. Cultures were left untreated or treated with 2mM TCEP for 2 hours. GSH levels are reported as luminescence normalized to OD600 of each culture. **B.** Plaque formation at 4 days post infection of L2 fibroblasts. Plaque sizes were quantified by

ImageJ. In each experiment, the average plaque size by each strain was normalized to the average WT plaque size, set at 1. Error bars show standard deviations. Statistical analyses were performed by two-way ANOVA in A and one-way ANOVA in B, with multiple comparisons for the indicated pairs: ns, non-significant; *, P < 0.05; **, P < 0.01; ***, P < 0.001; ****, P < 0.0001.

Next, we assessed the contribution of reduced GshF activity to ex-vivo virulence in ΔPDE. In L2 plaque formation assay, *gshF* over-expression only moderately increased the ΔPDE plaque sizes, suggesting that GshF activity might be impaired (**Fig. 2.5B**). However, we noticed that the ΔPDE Δ*gshF* strain formed significantly smaller plaques than the ΔPDE strain, indicating that GSH synthesis is not completely inhibited at high c-di-AMP levels during infection (**Fig. 2.4C**). Together, these data suggest c-di-AMP accumulation impairs GshF activity or promotes GSH catabolism.

Defective PrfA activity contributes to virulence attenuation at high c-di-AMP levels

We next examined the contribution of PrfA defect to ΔPDE virulence attenuation in a mouse model of intravenous infection. In the WT background, *prfA** increased bacterial burdens in both the spleen and liver, as expected (**Fig. 2.6A-B**). Compared to ΔPDE burdens, the media burdens of ΔPDE *prfA** were increased by ~10-fold in the liver, and by ~3-fold in the spleen (**Fig. 2.6A-B**). Thus, a defect in PrfA function partially contributes to ΔPDE virulence attenuation in the liver. However, our data also reveal that there are additional mechanisms underlying the virulence defect of ΔPDE at high c-di-AMP levels.

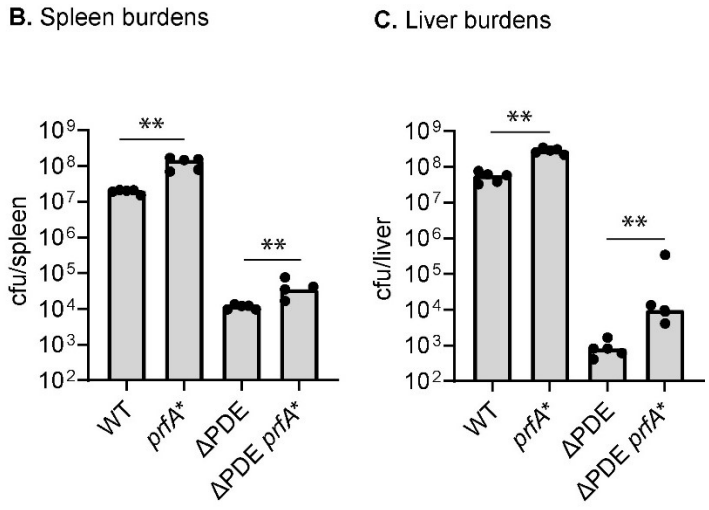

Figure 2.6. A constitutive PrfA variant (PrfA*) partially rescues virulence defect upon c-di-AMP accumulation. A-B. Bacterial burdens in the spleen and liver at 48 hours post-intravenous infection with 1 x 10^5 cfu of *L. monocytogenes*. Each dot represents *L. monocytogenes* burden from one animal. Bars represent medians of the groups. Statistical analyses were performed by Mann-Whitney test, with multiple comparisons for the indicated pairs: ns, non-significant; **, P < 0.01; ****, P < 0.0001.

C-di-AMP accumulation enhances H_2O_2 sensitivity

ΔPDE *prfA** was not fully rescued for in-vivo virulence, which led us to question what additional consequences of c-di-AMP accumulation could impair ΔPDE survival in-vivo. *L. monocytogenes* encounters oxidative stressors such as reactive oxygen species (ROS) during host-cell infection[131] and GshF is important for *L. monocytogenes* resistance to oxidative stressors[132]. Thus, we hypothesized that an additional consequence of GSH deficiency specific to ΔPDE is reduced oxidative stress tolerance. To test this, we first assessed terminal OD_{600} of WT and ΔPDE grown in LSM containing 0.5mM, 0.25mM, and 0.125mM H_2O_2. At 0.5mM and 0.25mM H_2O_2, ΔPDE was more impaired for growth than WT (**Fig. 2.7A**). To test the contribution of GshF to ΔPDE H_2O_2 sensitivity, we repeated growth in 0.25mM and 0.125mM H_2O_2 for WT and ΔPDE strains deleted for and overexpressing *gshF*. While ΔPDE + P_{spac}-*gshF* was still more sensitive to 0.25mM H_2O_2 than WT + P_{spac}-*gshF,* growth of Δ*gshF* and ΔPDE

gshF::tn were statistically equivalent at 0.25mM H_2O_2 (**Fig. 2.7B**). While this data suggests that deleting GshF equalizes WT and ΔPDE H_2O_2 sensitivity, poor growth of both WT and ΔPDE *gshF* deletion strains in 0.25mM H_2O_2 makes these data difficult to reliably interpret. At 0.125mM H_2O_2, which did not inhibit ΔPDE growth relative to WT, neither overexpressing nor deleting *gshF* had a significant influence on relative ΔPDE growth compared to WT (**Fig. 2.7C**). All together, these data demonstrate that c-di-AMP accumulation causes enhanced sensitivity to H_2O_2. However, these results do not provide conclusive evidence about whether reduced GshF activity is responsible for H_2O_2 sensitivity in ΔPDE.

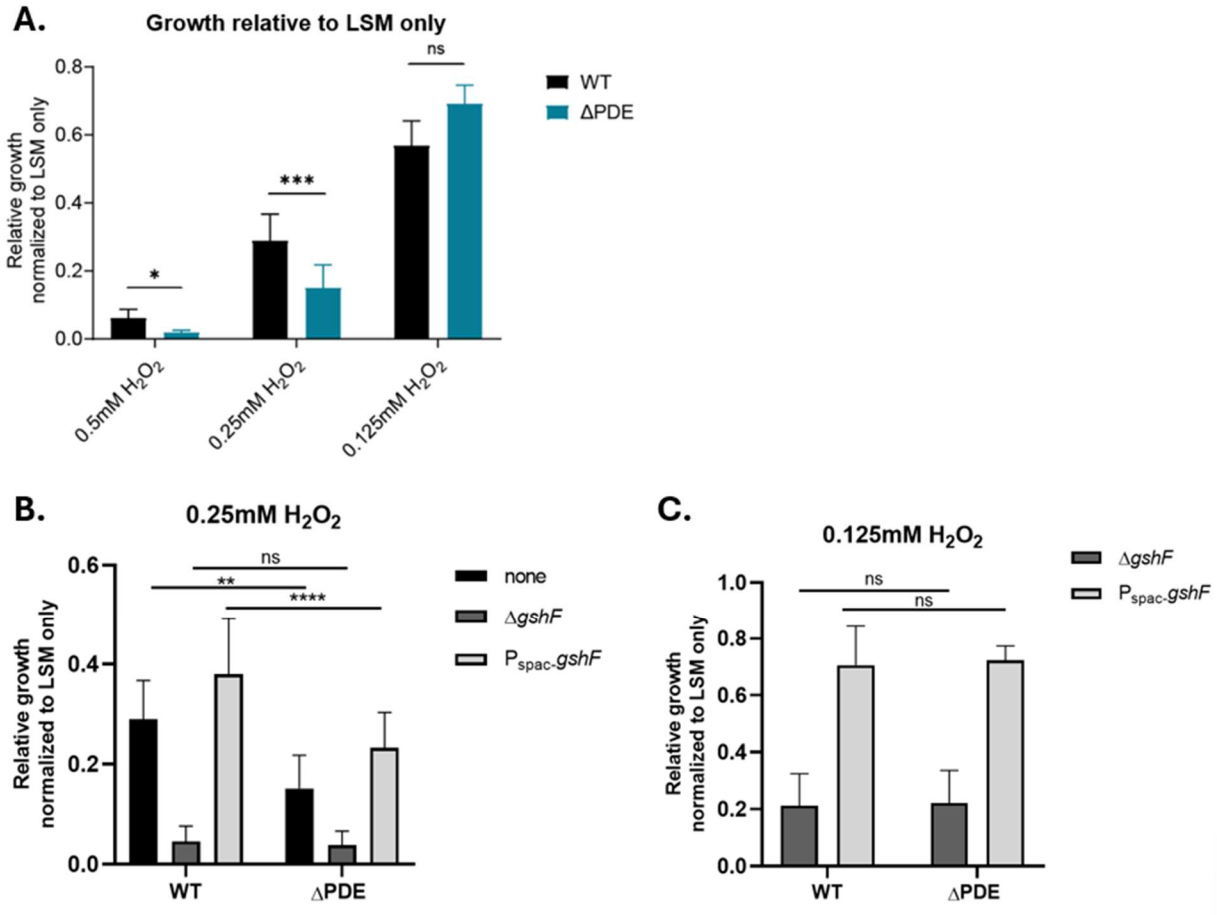

Figure 2.7. C-di-AMP accumulation enhances H_2O_2 susceptibility. A. Terminal OD_{600} of WT and ΔPDE in 0.5, 0.25, and 0.125mM H_2O_2 relative to that of each strain in LSM. **B-C**. Terminal OD_{600} of WT and ΔPDE deleted for or overexpressing *gshF* in 0.25 (B) or 0.125mM (C) H_2O_2 relative to that of each strain in LSM. Statistical analyses were performed by two-way ANOVA,

with multiple comparisons for the indicated pairs: ns, non-significant; *, P < 0.05; **, P < 0.01; ***, P < 0.001.

DISCUSSION

C-di-AMP homeostasis is critical for bacterial growth and pathogenesis. The attenuated virulence conferred by c-di-AMP accumulation is widely observed in many pathogens, including *Mycobacterium tuberculosis*, which does not require c-di-AMP for growth[79,133] and *Borrelia burgdorferi*, which produces a very low level of c-di-AMP[76,134]. In the c-di-AMP phosphodiesterase (Δ*dhhP*) mutant of *B. burgdorferi*, the transcription factor BosR is inhibited, causing reduced expression of the major virulence factor OspC[134]. However, the *B. burgdorferi* Δ*dhhP* mutant also has a significant growth defect, and DhhP might degrade other nucleotides in addition to c-di-AMP[135,136]. For *Bacillus anthracis*, the ΔPDE mutant also grows poorly and is diminished for anthrax toxin production, a defect that is partially attributed to the upregulation of the transcriptional repressor AbrB[84]. The molecular mechanisms by which c-di-AMP inhibits virulence factor expression in these bacteria are unclear, and the mechanisms by which c-di-AMP impairs the virulence of other pathogens are even less understood.

The *L. monocytogenes* c-di-AMP ΔPDE mutant does not have a significant growth defect in rich media, but is attenuated for virulence, suggesting defects that are pertinent to replication and adaptation in the host. Our findings here reveal that c-di-AMP accumulation impairs *prfA* expression and activity during under basal and PrfA activating conditions, as well as in an ex-vivo model of infection. We demonstrated that GSH, an allosteric activator of PrfA, is depleted in the ΔPDE mutant, and that this has implications for ex-vivo virulence. Upon further examination of the mechanisms underlying GSH depletion in ΔPDE, it was found that both synthesis and uptake of GSH is impaired by c-di-AMP accumulation. First, we found that c-di-AMP accumulation inhibits GSH uptake. High affinity GSH transport in *L. monocytogenes* was recently shown to require the Ctp complex and the ATPases OppDF, the latter of which are

components of the Opp complex that transports oligopeptides. Based on the demonstrated function of c-di-AMP in inhibiting potassium, Mg^{2+}, and carnitine transporters[137], it is conceivable that c-di-AMP might also inhibit the OppDF and Ctp ATPase function particularly. As for how c-di-AMP accumulation depletes cytoplasmic GSH, we found that c-di-AMP does not inhibit *gshF* gene expression, or expression of *oppDF* or *ctaP.* However, the possibility remains that allosteric inhibition of GshF, OppDF, or CtaP occurs when c-di-AMP levels are high. Indeed our ex vivo infection data demonstrates that the absence of GshF reduces plaque ΔPDE L2 plaque formation to a greater degree than it does for WT. This suggests that uptake of host-GSH is impaired in ΔPDE. Our L2 plaque data further indicates that GshF is operational in the ΔPDE strain during infection, though its activity might be reduced. One mechanism by which GshF activity could be reduced is lowered substrate abundance. Based on metabolomic analysis of ΔPDE, the GshF substrates cysteine, glycine, and glutamate do not appear to be reduced. However, c-di-AMP is a known regulator of metabolic enzyme function, so while GshF substrates are not reduced in ΔPDE, it is plausible that these substrates are being funneled into different pathways independent of GSH metabolism. Future investigations are necessary to distinguish these mechanisms.

Because GSH is an allosteric activator of the master virulence factor PrfA, the first major implication of GSH depletion is a reduced virulence program expression. In support for this, our data shows that virulence gene expression at high c-di-AMP levels can be restored by a constitutive PrfA* variant, or a combination of increased GSH synthesis and GSH supplementation. However, the PrfA* variant does not fully rescue ΔPDE virulence to the WT level, indicating that c-di-AMP accumulation confers additional defects during infection. We previously reported that the *L. monocytogenes* ΔPDE strain is sensitive to cell wall-targeting antimicrobials, including lysozyme that is abundant in mammalian cell cytosol[64]. Given the requirement of cell wall homeostasis for successful infection by *L. monocytogenes*[138–140] it is

conceivable that cell wall defects also contribute to ΔPDE virulence attenuation. Another well-established function of c-di-AMP in *L. monocytogenes* is the inhibition of the carnitine transporter OpuC and multiple potassium uptake channels[13,27]. However, mutants abolished for carnitine transport do not exhibit a systemic infection defect like the ΔPDE strain[141] and the cell cytosol is highly enriched in potassium[142].Therefore, reduced osmolyte uptake may not significantly impact *L. monocytogenes* replication in the cytosol. Among other c-di-AMP-binding proteins that have been studied in *L. monocytogenes*, PstA has a minor role in infection[63]; and the ΔPDE mutant does not have a growth defect that would be associated with a significantly reduced pyruvate carboxylase function[17,143]. The roles of other c-di-AMP molecular targets in *L. monocytogenes* pathogenesis should be investigated in future studies.

In addition to recognizing GSH as a virulence signal, *L. monocytogenes* also metabolizes GSH as a source of essential cysteine and uses GSH as antioxidant in broth cultures[128,132]. If these functions are relevant in the mammalian host, they can also explain why the ΔPDE *prfA** strain is not fully restored for virulence. Upon examining additional consequences of GSH deficiency, we found that ΔPDE was more sensitive to H_2O_2 than WT, suggesting that reduced oxidative stress resistance may contribute to attenuated virulence in ΔPDE. Furthermore, a reduced function of the GSH importers such as Ctp and OppDF at high c-di-AMP levels could also deprive *L. monocytogenes* of nutrient oligopeptides, which are also imported through these uptake channels[144,145]

It is curious that the PrfA* (G145S) variant, which is active independent of GSH binding, does not confer constitutive *actA* expression in ΔPDE in the absence of GSH supplementation. Outside of the allosteric activation site that binds GSH, PrfA has four cysteine residues that can be glutathionylated[105]. Although this modification modestly contributes to PrfA activation in the WT strain, it might have a more significant role at high c-di-AMP levels. Furthermore, the regulatory mechanisms of PrfA activity are complex, and PrfA can be inhibited by several

factors such as metals or oligopeptides that do not contain cysteine[114]. It is conceivable that the ΔPDE strain accumulates those PrfA inhibitors that can be identified in future metabolomics studies.

Altogether, our studies present an exciting avenue to investigate how c-di-AMP disrupts GSH metabolism in *L. monocytogenes*. Given the importance of GSH as a virulence signal, nutrient, and antioxidant in different bacteria[146]. it will be interesting to examine whether c-di-AMP regulates GSH metabolism in other species, and the consequences of such regulation on bacterial growth and infection.

Materials and Methods

Strains and culture conditions

L. monocytogenes strains are listed in **Table S2.2**. Listeria Synthetic Medium (LSM) was prepared based on published recipe[54]. Over-expression of genes was accomplished using the integrative plasmid pPL2[147]. Gene allelic exchange was performed using plasmid pKSV7. For all experiments related to broth cultures, *L. monocytogenes* was grown at 37°C with shaking and without antibiotics. For glycerol stocks and maintenance, strains carrying derivatives of the integrative plasmid pPL2 were grown in Brain Heart Infusion broth with 200μg/mL streptomycin and 10μg/mL chloramphenicol. For mouse and L2 cell infection, *L. monocytogenes* was grown static in BHI at 30°C.

RNAseq and analysis

L. monocytogenes cultures were grown to OD_{600} of ~ 0.5, and harvested by mixing 1:1 with cold methanol and centrifugation. RNA was extracted using acidified phenol:chloroform at pH 5.2 as previously described[148]. Contaminated DNA was removed from extracted RNA using Turbo DNase (Thermo Scientific). RNA sequencing and read mapping was performed by MiGS Sequencing Center (Pittsburgh, PA). Reads were mapped to the *L. monocytogenes* 10403S

genome (NCBI:txid393133). Differentially expressed gene (DEG) analysis was performed via EdgeR[149].

RT-qPCR for *L. monocytogenes* genes in broth

For quantification of PrfA activity upon activation by GSH, *L. monocytogenes* cultures were grown in LSM or LSM + 10mM GSH to OD_{600} ~0.5. For PrfA activation by TCEP, *L. monocytogenes* cultures were grown in LSM to OD ~0.5, then split into two aliquots of identical volumes. One culture aliquot was left untreated and the other was supplemented with 2mM TCEP for 2 hours, and both were shaken at 37°C. RNA was extracted, treated with Turbo DNase and converted to cDNA using iScript cDNA synthesis kit (BioRad). Gene expression was quantified using iTaq Universal SYBR Green (BioRad) with primers specific to each target, with *rplD* as the control housekeeping gene. Primers are listed in **Table S2.3**.

Quantification of GSH and GSSG

L. monocytogenes cultures were grown to an OD_{600} of ~0.5 and harvested by centrifugation. Cell pellets were washed three times in phosphate-buffered saline, and lysed by sonication. Lysates were centrifuged to remove cell debris. GSH and GSSG were quantified using the luminescence-based GSH-Glo assay kit (Promega). GSH standards of 0.5 – 20 μM were quantified to determine the linear range of luminescence readings, and bacterial lysates were diluted appropriately such that luminescence values were within the linear range.

^{3}H-GSH uptake assay

Cultures were grown in LSM to an OD_{600} of ~0.5, harvested by centrifugation, washed twice in uptake buffer (phosphate-buffered saline + 5mM glucose), and resuspended in an equivalent volume of LSM lacking cysteine. Cultures were grown an additional 45 minutes, then pelleted and resuspended in 52μL uptake buffer. 2μL of resuspension was reserved for OD_{600} measurement. 0.5μL 1μCi/μL ^{3}H-GSH, and 0.5μL10mM cold GSH was added to remaining 50μL

and incubated at room temperature for 30 minutes. Cells were added to a filter membrane fitted on a vacuum filter unit and washed with ~10mL phosphate-buffered saline. Filter membrane containing washed cells was transferred to a scintillation vial containing 3mL scintillation fluid, and counts per minute (CPM) were measured on a liquid scintillation counter and normalized to OD_{600}.

L2 plaque assay

Plaque formation upon *L. monocytogenes* infection of L2 cells was quantified as previously described[129,148]. Briefly, $1.2x10^6$ cells were infected with *L. monocytogenes* at multiplicity of infection (MOI) of 0.25. At 1 hour post infection, cells were washed, and fresh cell medium in 0.7% agarose was supplemented with 10µg/mL gentamicin to kill extracellular *L. monocytogenes*. At 5 days post infection, cells were stained with 0.3% crystal violet to visualize plaques. Plaque sizes were analyzed using ImageJ software.

P_{actA}::RFP assay

A pPL2 plasmid expressing red fluorescent protein from the *actA* promoter was used to quantify transcriptional activity. Fluorescence assays were performed based on published methods[107]. Briefly, *L. monocytogenes* strains carrying pPL2-P_{actA}::RFP were grown overnight at 37°C in LSM. Cultures were diluted 1:10 into fresh LSM or LSM + 10mM GSH and grown to OD_{600} of 1.5-2. For TCEP exposure, cultures were grown to OD_{600} of ~0.5 in LSM followed by addition of 2mM TCEP until OD_{600} of 1.5-2 was reached. Cultures were harvested by centrifugation and resuspended in phosphate-buffered saline to achieve a 5X concentration. Fluorescence was quantified in black-bottom 96-well plates (Greiner Bio) for fluorescence measurement (excitation 540nm, emission 650nm) (BioTek Synergy H1 Microplate Reader). Fluorescence values were normalized to OD_{600}.

Western Blot for *L. monocytogenes* proteins in broth and during macrophage growth.

For broth cultures, *L. monocytogenes* overnight cultures were subcultured 1:10 into LSM or LSM + 10mM GSH, and grown to OD_{600} of 1.5-2. Cultures were washed in one in 1x PBS and pellets were stored at -80C. For macrophage-infections, iBMMs were infected with *L. monocytogenes* strains at an MOI of 10. At 1hpi, iBMM media containing 10μg/mL gentamicin was added. At 8hpi, macrophages were lysed in 1x Tris-buffered saline + 0.5% Tween-20. Lysed cells were pelleted in a tabletop centrifuge at 4,700 RPM, washed 1x in PBS, and stored at -80C. Pellets were resuspended in 1x tris-buffered saline (TBS) + 0.05% BME and 1mM PMSF, and sonicated at 80% amplitude until lysates were clear. Saturated TCA was added to a final concentration of 6% and samples were precipitated on ice for one hour, pelleted in a microcentrifuge at 13,000 RPM, and washed 3x with 100% acetone. Pellets were fully dried in a SpeedVac, resuspended in 10% SDS + 0.05% BME, and boiled for 5 minutes. Redissolved pellet was mixed with SDS loading buffer and SDS-PAGE was run on a 12.5% acrylamide gel. Protein transfer onto nitrocellulose membrane was performed at 90V for 60 minutes. Membrane was incubated with primary antibodies overnight in 1x Tris-buffered saline + 0.1% Tween-20. αPrfA (ThermoFisher Scientific, #PA5-144446) was diluted 1:5000, and αRpoA (made in-house by Brianna Burton's research group at University of Wisconsin-Madison) was diluted 1:15,000. Secondary antibody (Anti-Rabbit IgG (H+L), HRP Conjugate, #W4011, Promega) was diluted 1:2500. Membrane was visualized using the Clarity Western ECL Substrate Kit (BioRad) and imaged with a BioRad system using the chemiluminescence setting. Images were quantified using ImageJ software to subtract background and measure band areas.

Mouse infection

All techniques were reviewed and approved by the University of Wisconsin—Madison Institutional Animal Care and Use Committee under the protocol M005916-R01-A01. Five 6-week-old female C57BL/6 mice (Charles River NCI facility) per bacterial strain were infected via tail vein injection with 0.2 cc of PBS with 1x105 of logarithmically growing bacteria. At 48hpi,

spleens and livers were harvested, and homogenized in organ lysis buffer. Organ homogenates were diluted, as necessary using PBS, spiral plated on LB agar, and CFU counts were obtained using the Q count. Bacterial CFUs per organ were calculated using known dilution factors.

H_2O_2 Susceptibility

Strains were grown overnight in LSM, washed once in PBS, and normalized to an OD_{600} of 0.01 in 1mL of LSM or LSM containing indicated concentrations of H_2O_2. Cultures were grown shaking at 37C for 16 hours, at which point OD_{600} was measured.

SUPPLEMENTARY INFORMATION

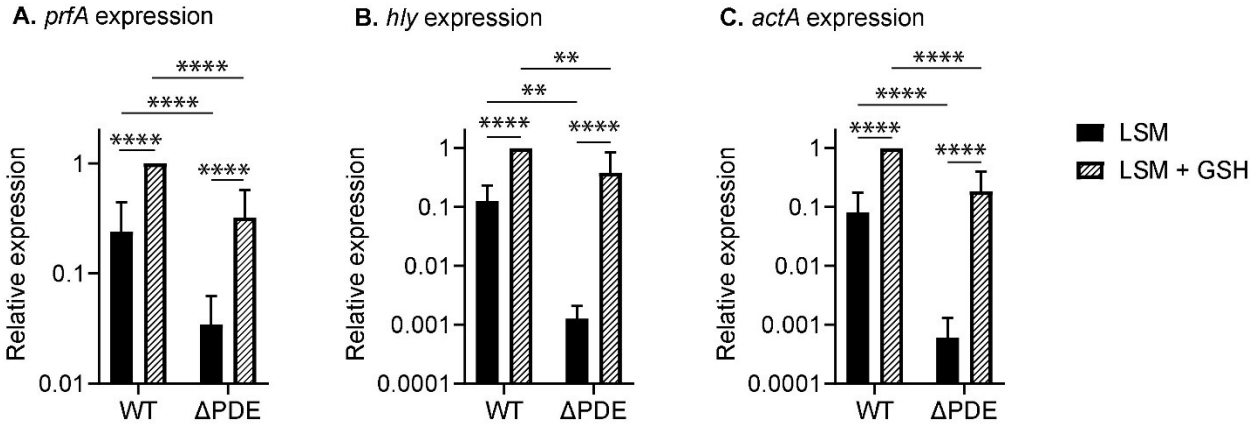

Figure S2.1. C-di-AMP accumulation inhibits gene expression within the PrfA core regulon. RT-qPCR for *prfA* (**A**), *hly* (**B**), and *actA* (**C**). Cultures were grown in LSM or LSM + 10mM GSH to mid-log phase. In each culture, gene expression levels was normalized to that of *rplD* as a housekeeping gene. Data are average of at least 5 independent experiments. Error bars show standard deviations. Statistical analyses were performed by two-way ANOVA with multiple comparisons for the indicated pairs: **, P < 0.01; ****, P < 0.0001

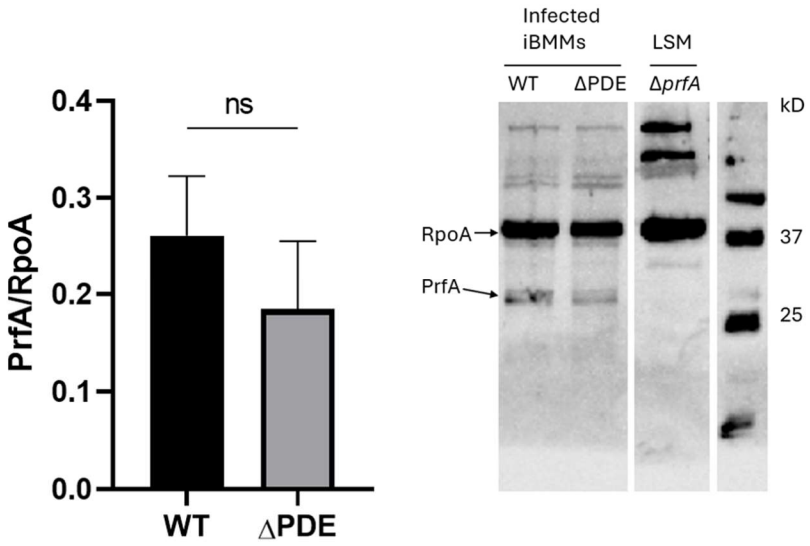

Figure S2.2. PrfA levels in an ex-vivo model of infection. iBMMs were infected with WT and ΔPDE at an MOI of 10, and harvested at 8hpi. iBMMs were lysed, and western blot was performed on lysates using rabbit antisera raised against PrfA and RpoA. Representative blot (left panel) is representative of 2 independent experiments. PrfA protein levels were quantified (right panel) by normalizing band intensity of PrfA/RpoA.

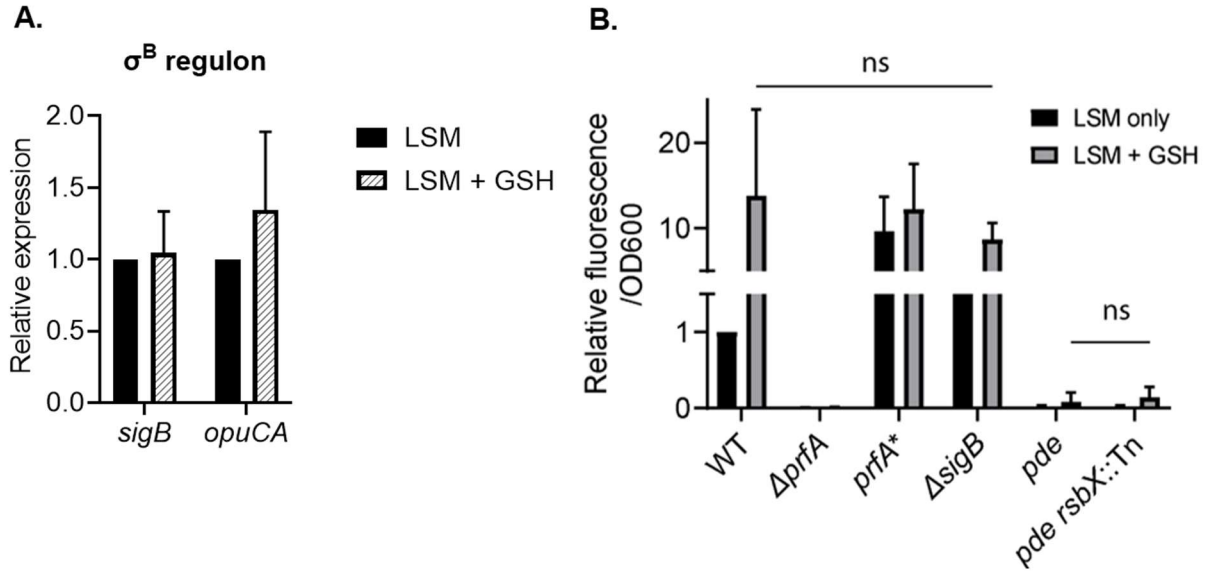

Figure S2.3. SigB activity does not influence PrfA-activation under the conditions used in this study. (A) *sigB* and *opuCA* gene expression measured by RT-qPCR. Cultures were grown in LSM or LSM + 10mM GSH to mid-log phase. In each culture, the expression level of target genes was normalized to that of *rplD* as a housekeeping gene. Error bars represent standard deviations. (B) P_{actA}::RFP transcriptional activity performed for strains grown in LSM or LSM + 10mM GSH.

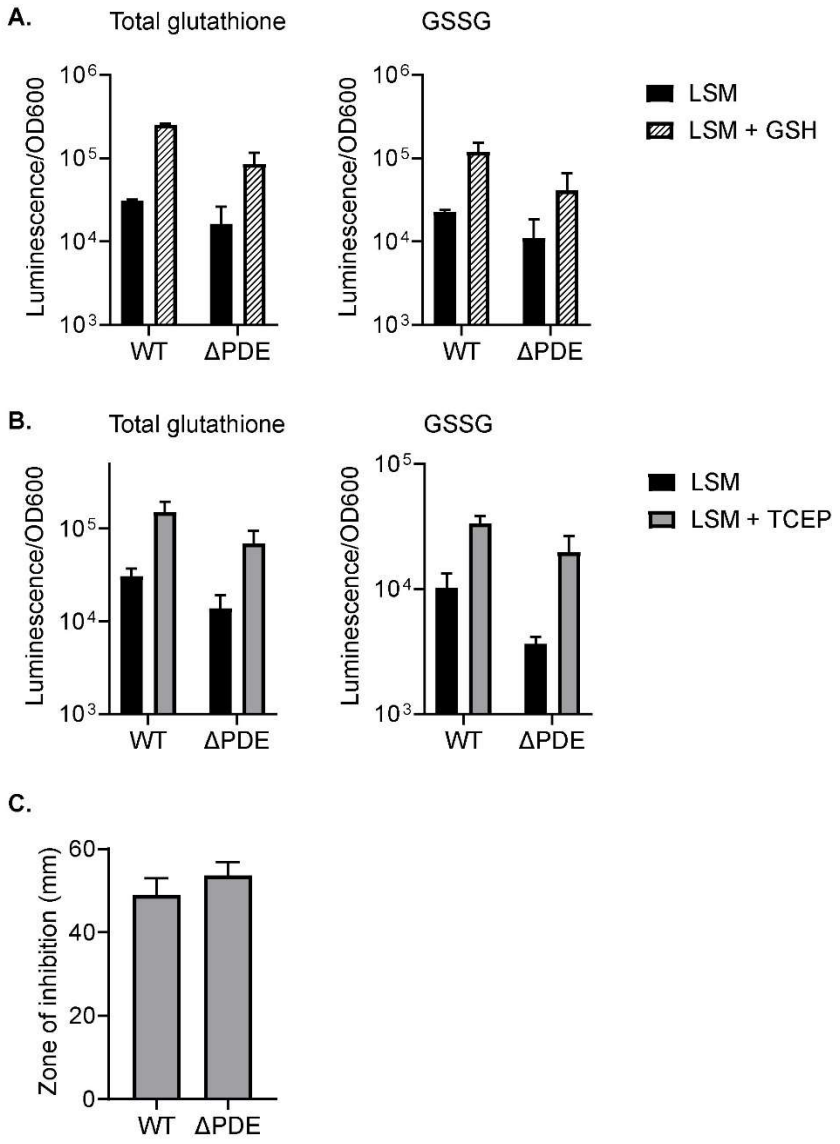

Figure S2.4. C-di-AMP accumulation causes a depletion of the total glutathione pool but not methylglyoxal susceptibility. A. Total glutathione and oxidized glutathione (GSSG) in cultures grown in LSM or LSM + 10mM GSH. **B.** Total glutathione and oxidized glutathione (GSSG) in cultures that were left untreated or treated with 2mM TCEP for 2 hours. **C.** Disk diffusion assay to assess methylglyoxal susceptibility. 1 x 10^7 cfu of each *L. monocytogenes* strain was grown on LSM agar with a sterile disk containing 10 µL of 40% methylglyoxal. Susceptibility was quantified as the diameter of zone of bacterial clearance. Error bars show standard deviations. Data in A are average of two independent experiments. Data in B and C are average of three independent experiments.

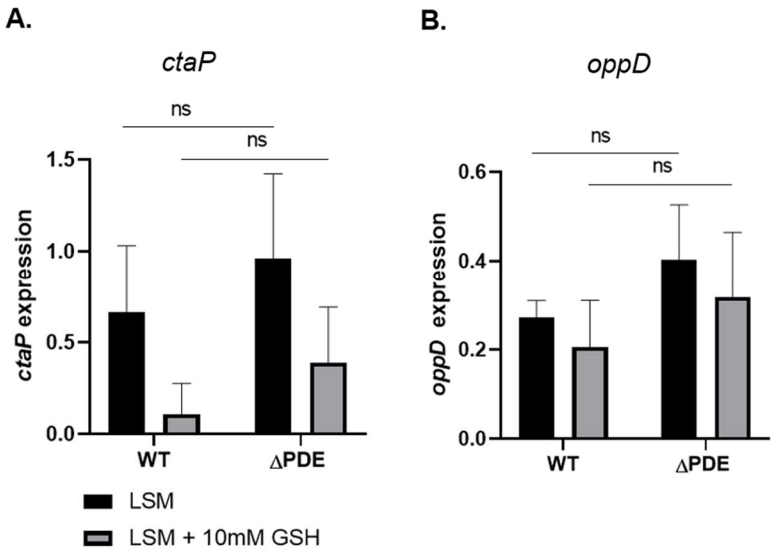

Figure S2.5 C-di-AMP accumulation does not inhibit expression of GSH transporters. RT-qPCR for *ctaP* (A) and *oppD* (B). Cultures were grown to mid-log phase in LSM or LSM + 10mM GSH. In each culture, gene expression level was normalized to *rplD* expression. Error bars represent standard deviations. Data represent averages of four biologically independent replicates.

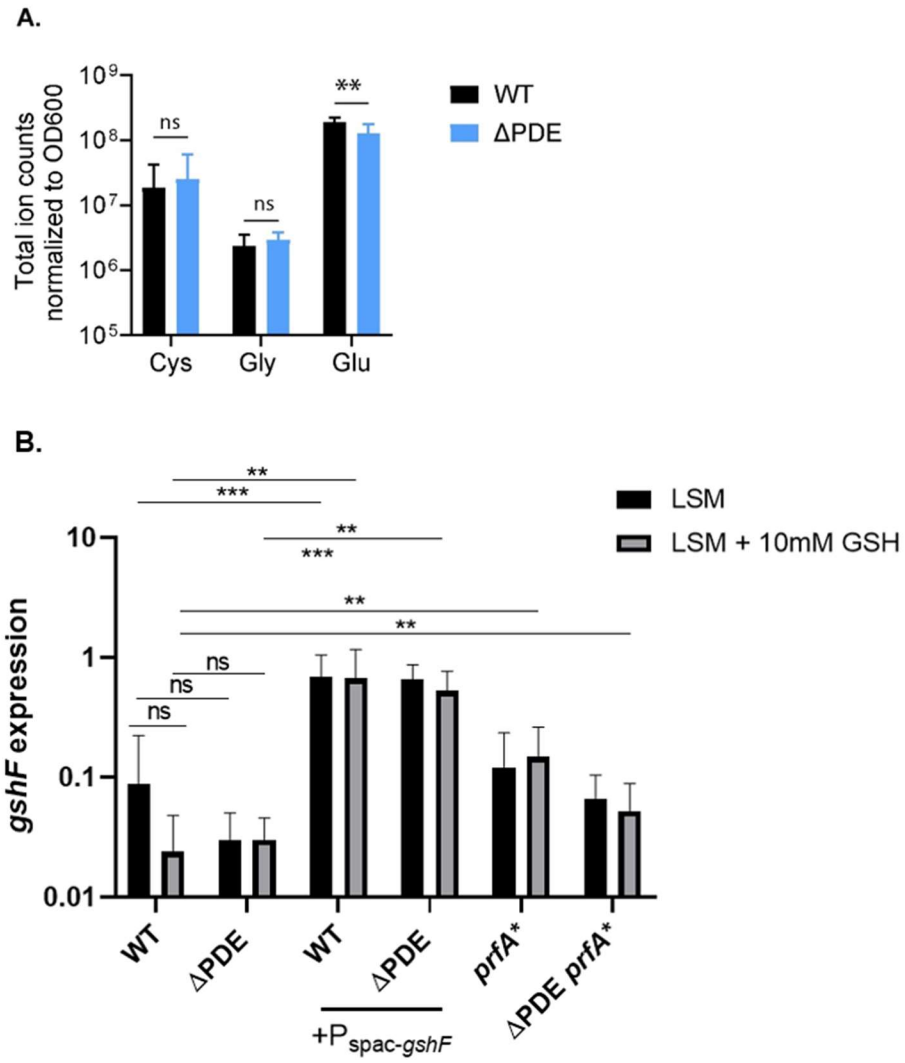

Figure S2.6. C-di-AMP accumulation does not inhibit *gshF* gene expression or deplete GshF substrates. A. Quantification of cysteine, glycine, and glutamate by LC-MS. Mid-log cultures grown in LSM were rapidly filtered and total metabolites were extracted by cold methanol. **B.** RT-qPCR for gshF. Cultures were grown to mid-log phase in LSM or LSM + 10mM GSH. In each culture, *gshF* expression level was normalized to *rplD* expression. Error bars represent standard deviations. Data in A are averages of three biologically independent replicates. Data in B are average of 9 independent biological replicates. Statistical analyses were performed by Student's t-test in A and two-way ANOVA in B.

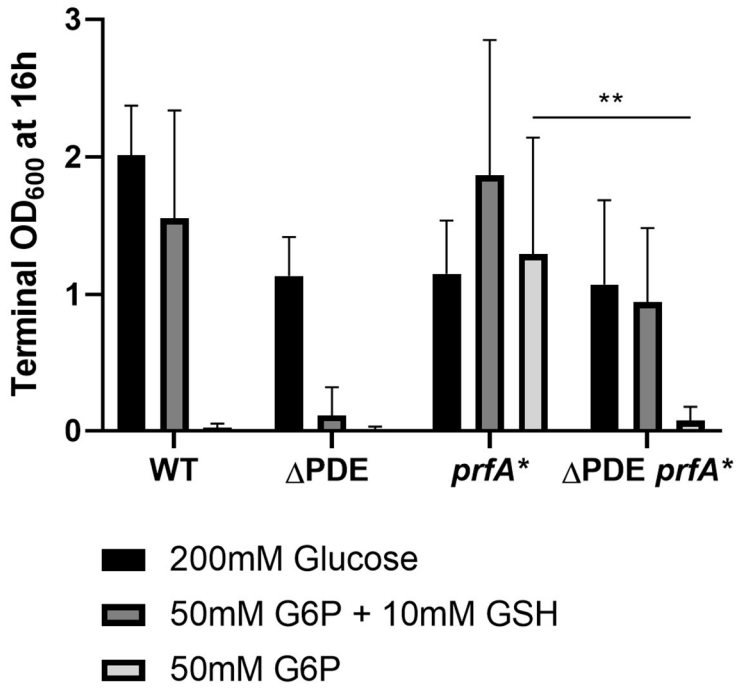

Figure S2.7. ΔPDE is unable to utilize G6P as a carbon source. Strains were normalized to OD_{600} 0.01 and grown for 16h in LSM (standard formulation contains ~200mM glucose), and LSM with 50mM G6P in place of glucose, with and without 10mM GSH. Terminal OD_{600} of strains was measured and normalized to WT grown in standard LSM. Data are representative of 3 independent experiments.

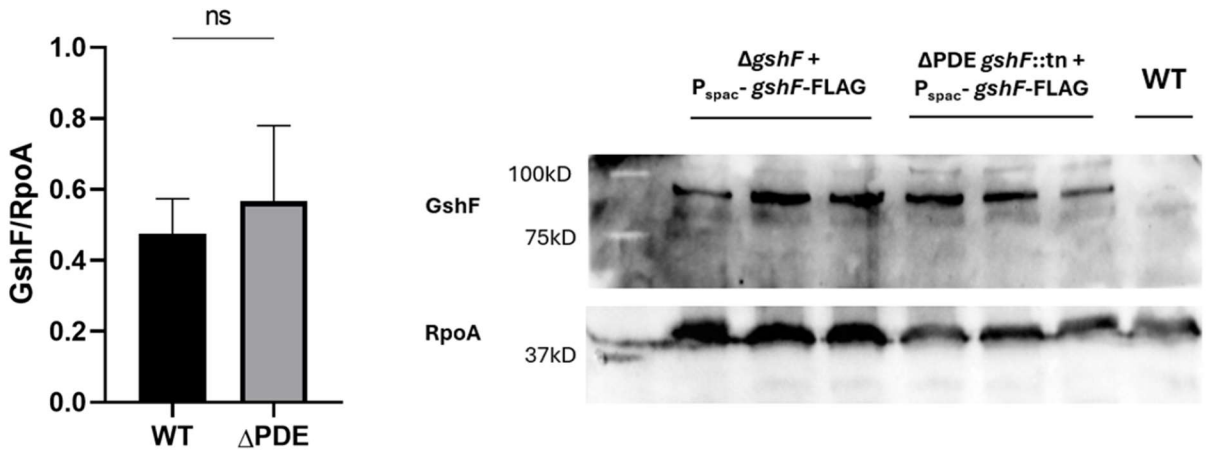

Figure S2.8: C-di-AMP accumulation does not alter GshF stability during growth in LSM. WT ΔgshF + gshF-FLAG and ΔPDE gshF::tn + gshF-FLAG were grown to OD_{600} ~1-1.5 in LSM. Western blot was performed on lysates using mouse antisera raised against FLAG and RpoA.

Representative blot (left panel) is is quantified (right panel) by normalizing band intensity of GshF-FLAG/RpoA.

Table S2.1. Differentially expressed genes in the ΔPDE strain with >4 fold-change in expression (FC) relative to WT.

10403S gene number	EGD-E gene number	Function	Log_2FC (ΔPDE/WT)	PValue
Upregulated genes:				
LMRG_01481	lmo2361	Rrf2 family protein	3.8	1.5E-08
LMRG_01482	lmo2360	membrane protein	3.5	4.4E-09
LMRG_01726	lmo2522, cell wall binding protein	hypothetical protein	2.7	5.8E-06
LMRG_02228	lmo2683	cellobiose-specific PTS system IIB component	2.6	9.0E-08
LMRG_02448	lmo0019	hypothetical protein	2.6	5.2E-07
LMRG_01989	lmo2708	cellobiose-specific PTS system IIC component	2.5	1.2E-06
LMRG_02229	lmo2684	cellobiose-specific PTS system IIC component	2.3	4.3E-07
LMRG_02230	lmo2685	cellobiose-specific PTS system IIA component	2.0	4.3E-06
LMRG_02751	lmo0186	hypothetical protein	2.0	6.0E-06
Downregulated genes:				
LMRG_02481	lmo0052	DHH subfamily 1 protein	-10.3	3.4E-11
LMRG_02626	lmo0204	actin-assembly inducing protein ActA	-9.0	9.7E-11
LMRG_02624	lmo0202	listeriolysin O	-8.7	1.6E-10
LMRG_02627	lmo0205	phospholipase C	-8.5	1.7E-10
LMRG_00918	lmo1466	hypothetical protein	-8.2	3.2E-09

LMRG_02623	lmo0201	1-phosphatidylinositol phosphodiesterase	-7.9	2.7E-11
LMRG_01542	lmo2290	gp13	-7.6	9.6E-08
LMRG_01541	lmo2291	major tail shaft protein	-7.1	1.6E-07
LMRG_01537	lmo2295	gp8	-7.0	1.4E-07
LMRG_01534	lmo2298	phage minor capsid protein	-6.8	3.8E-08
LMRG_01535	lmo2297	scaffolding protein	-6.7	4.2E-07
LMRG_01544	lmo2288	gp15	-6.7	5.8E-07
LMRG_01538	lmo2294	gp9	-6.6	3.8E-07
LMRG_01536	lmo2296	phage capsid protein	-6.4	2.0E-08
LMRG_01539	lmo2293	gp10	-6.3	6.3E-07
LMRG_01540	lmo2292	gp11	-6.3	2.7E-07
LMRG_01543	lmo2289	gp14	-6.3	1.3E-07
LMRG_01545	lmo2287	tail tape-measure protein	-6.0	1.6E-07
LMRG_01533	lmo2299	phage portal protein	-5.9	9.9E-09
LMRG_02628	lmo0206	hypothetical protein	-5.9	1.3E-09
LMRG_02261	lmo0838	MFS transporter	-5.8	7.5E-10
LMRG_01549	lmo2283	long tail fibre	-5.2	3.0E-07
LMRG_02629	lmo0207	hypothetical protein	-5.2	9.4E-10
LMRG_01550	lmo2282	short tail fibre	-5.1	1.0E-06
LMRG_02625	lmo0203	zinc metalloproteinase	-5.1	3.0E-10
LMRG_01551	lmo2281	gp22	-4.9	2.1E-05
LMRG_01546	lmo2286	tail or base plate protein gp17	-4.8	7.5E-07
LMRG_01547	lmo2285	tail or base plate protein gp18	-4.8	2.6E-07
LMRG_01548	lmo2284	tail or base plate protein gp19	-4.7	4.7E-07
LMRG_01531	lmo2303	terminase small subunit	-4.5	8.2E-07
LMRG_01527	lmo2321	gp32	-4.4	7.4E-06
LMRG_01529	lmo2303	gp66	-4.3	2.1E-07
LMRG_01528	lmo2304	gp65	-4.3	3.6E-05
LMRG_01521	lmo2323	gp43	-4.3	2.2E-06

LMRG_01526	lmo2321	gp49	-4.2	4.9E-06
LMRG_01532	lmo2300	phage terminase large subunit	-4.1	1.2E-07
LMRG_01515	lmo2329	hypothetical protein	-4.0	6.7E-05
LMRG_01525	lmo2321	recombination protein RecT	-4.0	4.0E-06
LMRG_02921	lmo2324	hypothetical protein	-4.0	9.3E-07
LMRG_01524	lmo2321	gp47	-4.0	4.8E-07
LMRG_02920	lmo2324	anti-repressor protein	-3.8	5.5E-06
LMRG_01516	lmo2329	hypothetical protein	-3.8	6.8E-05
LMRG_01553	lmo2279	phage holin	-3.7	2.3E-06
LMRG_01522	lmo2322	gp44	-3.4	7.1E-06
LMRG_02825	NA	internalin C	-3.3	1.8E-08
LMRG_02622	0	listeriolysin regulatory protein	-2.8	1.1E-08
LMRG_01559	NA	hypothetical protein	-2.7	1.1E-04
LMRG_02984	NA	hypothetical protein	-2.6	1.4E-05
LMRG_02915	NA	hypothetical protein	-2.6	1.9E-05
LMRG_02227	lmo2682	kdpA K+-transporting ATPase A subunit	-2.6	1.3E-07
LMRG_00127	0	internalin B	-2.6	2.5E-08
LMRG_01676	NA	hypothetical protein	-2.6	1.9E-05
LMRG_01558	NA	phage protein	-2.4	1.4E-05
LMRG_02367	NA	antigen A	-2.4	4.1E-07
LMRG_02369	NA	hypothetical protein	-2.4	4.1E-06
LMRG_01554	lmo2278	endolysin L-alanyl-D-glutamate peptidase	-2.4	5.7E-05
LMRG_01552	NA	gp23	-2.3	1.5E-04
LMRG_02377	NA	lmo0128 hypothetical protein	-2.2	5.4E-05
LMRG_01518	NA	gp41	-2.2	1.4E-04
LMRG_02370	NA	lmo0121 hypothetical protein	-2.2	6.5E-08
LMRG_02375	NA	lmo0126 hypothetical protein	-2.2	4.1E-07
LMRG_01523	NA	gp45	-2.1	8.6E-05

LMRG_00126	0	internalin A	-2.1	1.7E-07
LMRG_02376	NA	hypothetical protein	-2.1	6.3E-06
LMRG_02371	NA	hypothetical protein	-2.1	1.9E-06
LMRG_02366	NA	prophage LambdaLm01, antigen B	-2.0	4.1E-05
LMRG_02373	NA	hypothetical protein	-2.0	1.6E-05
LMRG_01165	NA	cold shock protein	-2.0	4.6E-05

Table S2.2. Strains used in this study

Strain number	Genotype	Source
L. monocytogenes **(Derivatives of strain 10403S)**		
TNHL22	Δ*pdeA* Δ*pgpH* (ΔPDE)	Huynh *et al*. 2015
TNHL425	PrfA G145S (PrfA*)	Gift from JD Sauer
TNHL876	ΔPDE PrfA*	This study
TNHL287	Δ*gshF*	This study
TNHL713	ΔPDE *gshF*::Tn	This study
TNHL829	WT + pPL2-Pspac-hly 5'UTR-*gshF*	This study
TNHL830	ΔPDE + pPL2-Pspac-hly 5'UTR-*gshF*	This study
TNHL831	Δ*gshF* + pPL2-Pspac-hly 5'UTR-*gshF*	This study
TNHL832	ΔPDE *gshF*::Tn + pPL2-Pspac-hly 5'UTR-*gshF*	This study
TNHL804	WT + pPL2-P_{actA}:RFP	This study
TNHL815	(ΔPDE) + pPL2-P_{actA}:RFP	This study
TNHL807	PrfA*+ pPL2-P_{actA}:RFP	This study
TNHL889	ΔPDE PrfA* pPL2-P_{actA}:RFP	This study
TNHL1020	ΔPDE PrfA* (reconstructed) + pPL2-P_{actA}:RFP	This study
TNHL1025	ΔPDE PrfA* (reconstructed) pPL2-P_{actA}:RFP	This study
TNHL1054	WT gshF::Tn + pPL2-Pspac-hly 5'UTR-gshF-FLAG	This study
TNHL1055	ΔPDE *gshF*::Tn + pPL2-Pspac-hly 5'UTR-*gshF*-FLAG	This study
TNHL875	Δ*sigB* + pPL2-P_{actA}:RFP	This study

TNHL859	ΔPDE rsbX::tn + pPL2-P_{actA}:RFP	This study
TNHL291	ΔprfA	This study
E. coli		
TNH895	pPL2 pPL2-P_{actA}:RFP in XL1B	Gift from JD Sauer
TNH920	pPL2-Pspac-hly 5'UTR-*gshF* in XL1B	This study
TNH1029	pPL2-Pspac-hly 5'UTR-*gshF*-FLAG in XL1B	This study

1. Huynh, T. N. *et al.* An HD-domain phosphodiesterase mediates cooperative hydrolysis of c-di-AMP to affect bacterial growth and virulence. *Proc Natl Acad Sci USA* **112**, E747–E756 (2015)

Table S2.3. Oligonucleotides used in this study

Primer	**Sequence 5'-3'**	**Target**
qRT-PCR		
TNH483	CGTTCAGAAGTACGTGGTG	Forward *rplD*
TNH484	AAGTCAAACCTTCAAGTACAACT	Reverse *rplD*
TNH538	CACGAGTATTAGCGAGAACGG	Forward *prfA*
TNH539	GATAACGTATGCGGTAGCCTGCTC	Reverse *prfA*
TNH792	ATTAACTCACGCAAATTCGGC	Forward *plcA*
TNH793	GTTTTCACACTCGGACCATTG	Reverse *plcA*
TNH784	TGCTCCTACTCCATCGGAAC	Forward *actA*
TNH785	CAAGAAGCATTGGCGTCTCT	Reverse *actA*
TNH782	TCAACCAGATGTTCTCCCTGTA	Forward *hly*
TNH783	CACTGTAAGCCATTTCGTCATC	Reverse *hly*
TNH827	CGACAAGATGAGCGACTTCA	Forward *gshF*
TNH828	GGGTGTAGCAGACGTTCTTT	Reverse *gshF*
TNH219	TGAAGCTGATTCGGATGGAAG	Forward *sigB*
TNH220	TTCTCGCTCATCTAAAACAGGG	Reverse *sigB*
TNH221	TCGGAATTGTTACTCGTGCC	Forward *opuC*
TNH222	GCTTCATTTCTGGTTCTGTCG	Reverse *opuC*

CES40	CGCATTTGCTGCACGTAATAA	Forward *oppD*
CES41	TCAGGATGAAGCAACCATGTAG	Reverse *oppD*
CES42	GCTGTATACGCACCGCTATT	Forward *ctaP*
CES43	ACCGTCGTGCCAAGTTAAA	Reverse *ctaP*
Cloning		
TNH838	gaccatgggcATAAAACTTGATATGACCATGCTTG	Forward *gshF*-NcoI
TNH839	gactcgagGTCAAATAAGAAATCTAAAATCTTATCAC	Reverse *gshF*-XhoI
CES29	gactgcagCCCTGAGGTGAAAACatgATAAAAC	Forward *gshF*-PstI
CES39	gaggatccttaGTCAAATAAGAAATCTAAAATCTTATC	Reverse *gshF-FLAG*-BamHI

Chapter 3. Utilization of glutathione as a sulfur source

Experiments and editing of this chapter were performed with the assistance of Tu Anh Huynh and Mallory Spencer

ABSTRACT

Cysteine is an essential sulfur-containing amino acid, and is necessary for protein synthesis, redox buffering in the cytosol, and is also a source of inorganic sulfur for synthesis of iron-sulfur clusters[128]. GSH, a tripeptide made up of cysteine, glycine, and glutamate, and is one of the most abundant antioxidants in both eukaryotes and prokaryotes[150]. It also serves as an important source of cysteine when broken down into its constituent amino acids[151]. *L. monocytogenes* is a cysteine auxotroph, and thus relies on exogenous sources of cysteine to survive. It was recently published that *L. monocytogenes* is able to utilize GSH as a cysteine source, indicating that it possesses the machinery to degrade exogenously supplied GSH and use the resulting cysteine[128]. However, the mechanisms by which *L. monocytogenes* breaks down GSH are not known. In Chapter 2, I found that in addition to being defective for GSH uptake, the ΔPDE strain is depleted for endogenously produced GSH compared to WT. This suggests that in ΔPDE, GshF activity is impaired, or GSH degradation is upregulated. In this chapter, I found ΔPDE to be to be impaired for growth when GSH is the sole source of cysteine, indicating that while GSH breakdown may be upregulated in ΔPDE. Following this discovery, a transcriptomic approach in addition to a negative selection screen were employed to better characterize utilization of GSH as a cysteine source in *L. monocytogenes*. While the majority of genes induced by GSH, regardless of cysteine availability, were involved in virulence*, lmo1132* was upregulated when GSH was the sole source of cysteine under hypoxic growth conditions. *lmo1132* shares homology with a low-molecular weight thiol transporter in *Enterococcaceae sp*, and thus represents a newly identified low-affinity GSH transporter in *L. monocytogenes*.

Additionally, *treA,* which is important for conversion of trehalose-6-phosphate to glucose-6 phosphate, was upregulated by GSH utilization as a cysteine source. This gene has not been implicated in *L. monocytognes* pathogenesis, and may represent a novel component of carbon acquisition during infection. Additionally, two genes of unknown function were downregulated by GSH utilization as a cysteine source, so identifying the function of these genes in relation to GSH metabolism represents an exciting subject for future studies.

INTRODUCTION

Low-molecular weight thiols (LMW) are molecules which contain reducing sulfhydryl groups, and enable detoxification of free radicals such as reactive oxygen species (ROS) and reactive nitrogen species (RNS)[152]. The nonribosomal tripeptide glutathione (GSH) is one such LMW composed of glutamate, cysteine and glycine[150]. GSH is the most important antioxidant produced by mammalian cells, and detoxifies reactive species such as superoxide and hydrogen peroxide. In fact, in both eukaryotes and prokaryotes, GSH is the most abundant thiol. In most mammalian cells, GSH levels range from 1-2mM, however in hepatocytes, which export GSH, levels can reach 10mM[153]. Given its abundance in mammalian tissues, many bacterial pathogens will encounter GSH during infection. In fact, GSH can serve as both a cysteine source and virulence-activating signal for many such species[154]. However, numerous bacteria also possess the ability to synthesize GSH on their own. In fact, de-novo GSH synthesis is vital for many bacteria to maintain redox homeostasis and also for full virulence potential of some pathogens[154].

Bacterial GSH synthesis

GSH is synthesized in a two-step reaction coupled with ATP hydrolysis, wherein glutamate and cysteine are covalently linked by glutamyl-cysteine ligase to form γ-glutamylcysteine by γ-ECL domain-containing enzymes. This is followed by binding of γ-

glutamylcysteine to glycine by glutathione synthase (GS) containing enzymes to form GSH[155]. In most organisms, the two steps of GSH synthesis are carried out by distinct enzymes, and this was long thought to be the primary mechanism of GSH synthesis by living organisms[156]. Interestingly, a number of bacteria across *Firmicutes, Desulfobacterales*, *Bacteroidetes*, and *Pasteurellaceaeare* phyla have been shown to synthesize GSH using a single, bifunctional enzyme containing both γ-ECL and GS domains (**Fig. 3.1**). These bifunctional enzymes are almost universally named GshF[127,157–159]. Importantly, it has been discovered that GshF is important for the pathogenesis of *L. monocytogenes,* as well as the resistance of a number of bacteria to oxidative stress[127]. Given its importance, the environmental signals which regulate GSH synthesis have been studied in a number of bacterial species. GSH synthesis in *E. coli* is carried out by the distinct enzymes GshA and GshB, containing γ-ECL and GS domains respectively, and is induced during oxidative stress by activation of the transcriptional regulator OxyR[160]. Furthermore, GSH synthesis is required by *E. coli* during stationary phase, but not in exponential phase[160]. In *Salmonella* species, GSH production is upregulated during the stringent response, possibly to counteract oxidative stress encountered during nutrient starvation[161]. In *L. monocytogenes*, GshF dependent GSH synthesis is upregulated by exposure to reducing agents. For instance, the reducing agent TCEP upregulates GSH synthesis, and this requires presence of the enzyme GshF[107]. Exposure to GSH, which in itself is reducing, also stimulates GSH synthesis in *L. monocytogenes*, though the mechanisms by which a reducing environment lead to increased GshF activity are not known[107].

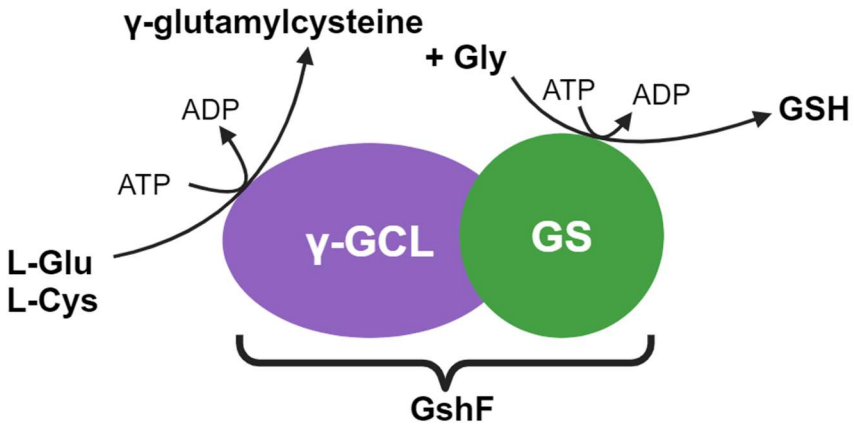

Figure 3.1. Synthesis of glutathione by GshF. GshF is a bifunctional enzyme which first synthesizes γ-glutamylcysteine from glutamate and cysteine via a γ-GCL domain, and then ligates glycine with γ-glutamylcysteine to form GSH via the GS domain. Both reactions are ATP-dependent.

GSH as a nutrient source

GSH is composed of a tripeptide, and serves as a source of amino acids for organisms capable of GSH breakdown. GSH degrading enzymes are well-characterized in a number of bacterial species. Perhaps the best characterized GSH degrading enzyme is gamma-glutamyltransferase (GGT), which converts GSH to glutamate and cysteinylglycine[162]. GGTs are ubiquitous across living organisms, being observed across all three domains of life. GGT was first noted as an enzyme whose dyfunction was the hallmark of metabolic disease in mammals[163]. However, more recent characterization of microbial metabolism has led to the discovery of GGT activity in bacteria. A number of pathogenic and nonpathogenic bacteria have been experimentally shown to encode GGT enzymes, though the localization and biological function of bacterial GGTs varies across species. Nonpathogenic *Bacillus* species secrete GGT where it can degrade extracellular GSH[164]. Conversely, GGT is membrane or periplasm associated in *Bacillus anthracis, Neisseria meningitides, Helicobacteri pylori, E. coli* and *Proteus mirabilis* and *Campylobacter jejuni*[165]. In fact, in *H. pylori*, GGT is in important virulence factor which promotes production of ammonia and reactive oxygen species that induce host cell

apoptosis[166]. For cysteine auxotrophs such as *Franciscella* species and *L. monocytogenes*, GSH is an important source of cysteine. In a forward genetic screen performed on a *Francisella tularensis* subspecies, GGT was found to be essential for intracellular replication[167], and L. monocytogenes was recently demonstrated to utilize GSH as an essential cysteine source[128] However, despite the ability to acquire cysteine from GSH, no GGT proteins or GSH degradation machinery have yet been identified in *L. monocytogenes*[128]

GSH as an antioxidant

GSH is a natural antioxidant, and can serve as an electron donor to neutralize reactive oxygen species and oxidizing agents such as H_2O_2. During this process, GSH is oxidized to form the disulfide molecule GSSG. In fact, GSH:GSSG ratios serve as an important indicator of the redox state of cells[168]. In addition to being a reducing agent on its own, numerous organisms encode glutathione-s-transferases (GSTs) which catalyze nucleophilic attack of toxic molecules by GSH[169]. In bacteria, GSTs serve many functions including protection from chemical and environmental stressors and antimicrobials[170]. GSTs are very diverse and can be characterized based on their substrates and pathway function[170]. In fact, numerous bacteria encode multiple GSTs with unknown functions, though some are predicted to be important for remediation of environmental pollutants[169]. While GSTs have been well-studied in gram-negative bacteria, their abundance and biological importance is less-well understood in gram-positive species[169]. However, it has been shown that GST homologs exist in a number of gram-positive bacteria. Interestingly, Fosfomycin resistance proteins bear homology to GSTs in *Bacilus subtilis,* once again illustrating the diverse functionality of GSTs[169]. Interestingly, *L. monocytogenes* has not been found to encode any GST proteins to date, despite the importance of GSH for *L. monocytogenes* virulence.

In addition to GSTs, glutathione peroxidases (GPx) are another class of GSH-utilizing enzymes. GPx proteins catalyze the conversion of GSH and peroxides to GSSG and a cognate

alcohol, respectively[171]. Similarly to GSTs, these proteins are widely distributed across the kingdom of life and are important for resistance to oxidative stressors. GPxs are encoded by a number of bacteria, including gram-positive pathogens such as *S. pyogenes* and *L. monocytogenes*[159,172]. Interestingly, while *S. pyogenes* mutants deleted for the GPx-ecoding gene *gpoA* are attenuated for virulence, a *L. monocytogenes* GPx mutant was more resistant to oxidative stress and exhibited enhanced virulence in mice[159]. Thus, while GSH, along with GST and GPx enzymes are important for resistance to oxidative stress, the function of GSH in different species and environments remains complex.

Pathogen interactions with host-derived GSH

GSH is an important virulence signal which mediates upregulation of virulence-genes in *Burkholderia pseudomallei, L. monocytognes,* and *Pseudomonas aureginosa*, though the mechanisms by which this occurs vary significantly between bacterial species[154]. In the cytosolic pathogen *B. pseudomallei*, the type-6 secretion system TYSS5 is upregulated only upon entry into the host cytosol. Expression of TYSS5 genes by *B. pseudomallei* can be induced by addition of GSH to defined medium, and is reduced when host-cells are deficient for GSH[173].

L. monocytogenes, which has a well-defined intracellular lifecycle, relies heavily on GSH for activation of virulence genes by the transcriptional regulator PrfA[105]. The helix-turn-helix domain of PrfA is stabilized when bound to GSH, priming PrfA for binding to the promoter regions of its core regulon, which includes important virulence genes such as *actA* and *hly*[106].

Pseudomonas aureginosa strains defective for GSH synthesis have been shown to be attenuated for virulence in multiple models of infection. Furthermore, GSH is important for reducing the five cysteine residues on the *P. auregionosa* virulence regulatory protein Vfr, which, in its reduced form, regulates expression of T3SS[174]. In addition, *B. pseudomallei* induces transcription of Type-4 secretion systems following sensing of GSH by the VirAG two-component system[173].

As discussed in Chapter 2, GSH is an important virulence signal for *L. monocytogenes*. GSH synthesis and uptake are important for *L. monocytogenes* virulence, and in Chapter 2 it was demonstrated that both processes are impaired in the ΔPDE strain, contributing, in part, to diminished virulence gene expression and attenuated virulence. Results from Chapter 2 also suggested that GSH degradation may be upregulated in the ΔPDE mutant. In this chapter, I set out to further explore GSH breakdown in the ΔPDE mutant, and found that it was modestly impaired for growth when using GSH as a sole source of cysteine. Because the processes by which GSH is catabolized *in L. monocytogenes* remain unknown, the remainder of this chapter aims to better define the mechanisms by which *L. monocytogenes* utilizes GSH as a source of the sulfur-containing amino acid cysteine. The results from this chapter will inform future studies aimed at exploring the effects of c-di-AMP on pathways important for utilization of GSH as a cysteine source.

RESULTS

C-di-AMP accumulation impairs utilization of GSH as a cysteine source when GSH concentrations are limiting.

To test the effect of c-di-AMP accumulation on GSH utilization, I measured the growth rate of WT and ΔPDE in LSM, which contains 2mM cysteine, and modified LSM lacking cysteine and supplemented with 10mM GSH. 10mM GSH was initially chosen as a physiologically relevant condition as this is similar to the concentration of GSH which exists in mammalian cells[150]. I found that WT and ΔPDE showed a negligible difference in growth rate when utilizing 10mM GSH as a cysteine source (**Fig. 3.2A-B).** However, I wondered if 10mM GSH was too high a concentration to identify small differences in growth between WT and ΔPDE, especially given the likely existence of low-affinity GSH transporters[128]. Therefore, I went on to test utilization of more limiting concentrations of GSH. WT and ΔPDE were grown for 16h in modified LSM lacking cysteine, with GSH levels ranging down to 0.05mM, and terminal OD_{600}

values were measured. During growth in 0.05 mM GSH, ΔPDE was more impaired than WT relative to standard, 2mM cysteine containing LSM (**Fig. 3.2C**). This is consistent with diminished GSH uptake in ΔPDE, but does not exclude the possibility that additional components involved in GSH utilization are impaired in ΔPDE. However, the mechanisms by which GSH is catabolized in *L. monocytogenes* have not yet been defined. Therefore, to lay groundwork for future studies on the effect of c-di-AMP accumulation on GSH catabolism, the remainder of this chapter will be focused on identifying mechanisms by which *L. monocytogenes* utilizes GSH as a cysteine source.

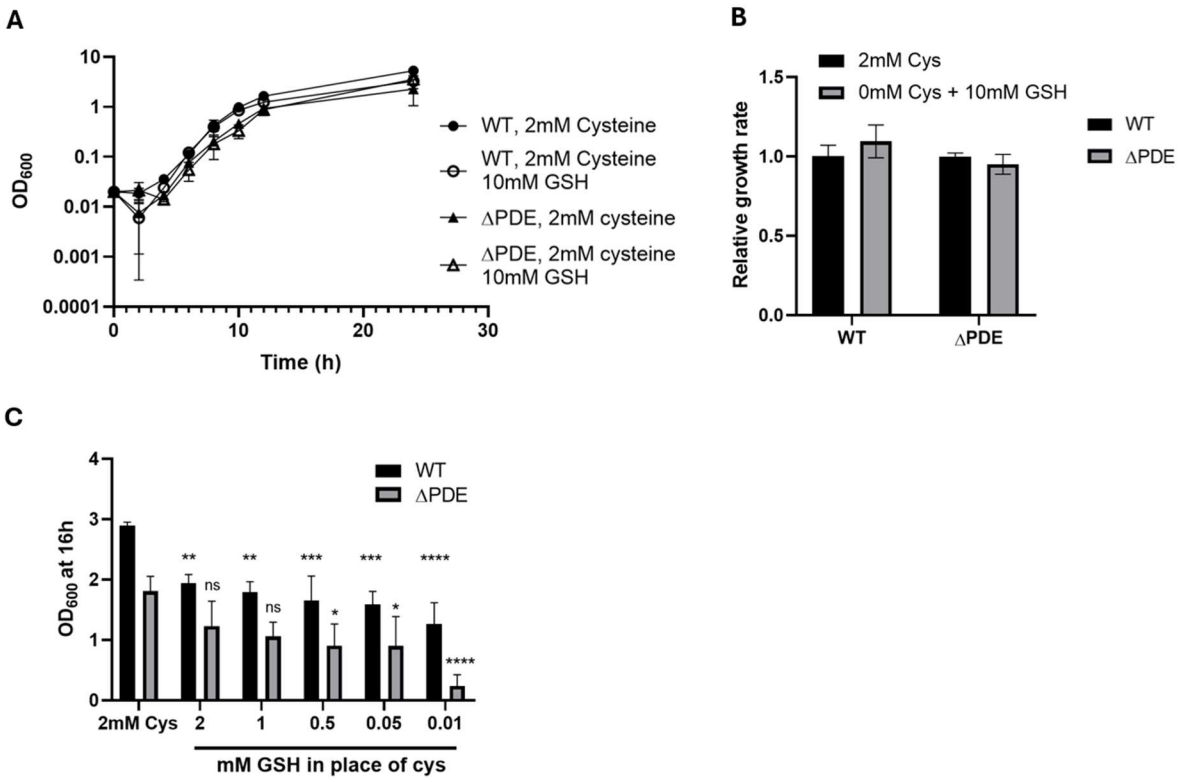

Figure 3.2. C-di-AMP accumulation impairs utilization of GSH as a nutrient source when GSH concentrations are limiting. A. Growth rate of WT and ΔPDE grown in LSM with 2mM cysteine, or modified LSM lacking cysteine, supplemented with 10mM GSH was relative growth rate in standard LSM for each strain. **B.** Relative growth rate calculated from growth curves shown in A. **C-D.** Terminal OD_{600} of cultures grown with in standard 2mM cysteine-containing LSM, or in LSM with indicated amount of GSH supplemented in place of cysteine. Data are

representative of 3-independent experiments. Error bars represent standard deviations. Statistical analyses were performed by two-way ANOVA with multiple comparisons between 2mM cysteine condition for each strain: ns, non-significant; *, P < 0.05; **, P < 0.01; ****, P < 0.0001.

Transcriptional changes induced during growth using GSH as the sole source of cysteine

I hypothesized that when forced to utilize GSH as a cysteine source, genes important for GSH degradation would be upregulated. To test this, biological duplicates of WT *L. monocytogenes* were grown to mid-exponential phase in LSM containing 2mM cysteine, LSM + 2mM cysteine + 10mM GSH, and LSM lacking cysteine + 10mm GSH. Total RNA was extracted and cDNA libraries were sequenced at the depth of 29-38 million reads, with 1433-1976x mapped read coverage of the *L. monocytogenes* genome. Genes which exhibited ≥2-fold change (P value < 0.05) relative to the control were considered differentially regulated. Compared to the LSM + 2mM Cysteine condition, genes in the core PrfA regulon were strongly upregulated when both GSH and cysteine were present, and also when GSH was the only available cysteine source (**Fig. 3.3A-B, Table S3.1**). Importantly, these results validated that the experimental conditions used elicited an expected biological response to GSH. In addition to the PrfA regulon, a number of genes were significantly upregulated in both conditions. These included glutamate dehydrogenase (*lmo0560*) and cysteine exporter CydD (*lmo2716*). A number of significantly downregulated genes were also shared between both conditions tested. Interestingly, compared to standard LSM, the cysteine transporter *ctaP* (*lmo0135*), exhibited a $\log_2$FC of -8.33 and -2.98 in the 2mM cysteine + 10mM GSH, and 0mM cysteine + 10mM GSH conditions respectively (**Table S3.1**). This was in agreement with qPCR data presented in Chapter 2 (**Fig. S2.5**), which confirmed downregulation of *ctaP* in response to GSH.

In addition to commonly differentially regulated genes, several genes exhibited strongly altered abundance in just one of the conditions tested. When GSH was the only cysteine source, tRNA modification GTPase TrmE (*lmo2811*), a Cas2 protein, and the PTS transporter subunit (*lmo2708*) were more strongly expressed than when both GSH and cysteine were present (**Fig. 3.3C**). Conversely, 16S pseudouridylate synthase (*lmo2342*), and response regulator ResD (*lmo1948*), as well as several proteins of unknown function were more strongly expressed when both GSH and cysteine were supplemented (**Fig. 3.3C**). As a complementary approach to these results, we next set out to identify genes essential for utilization of GSH as a cysteine source.

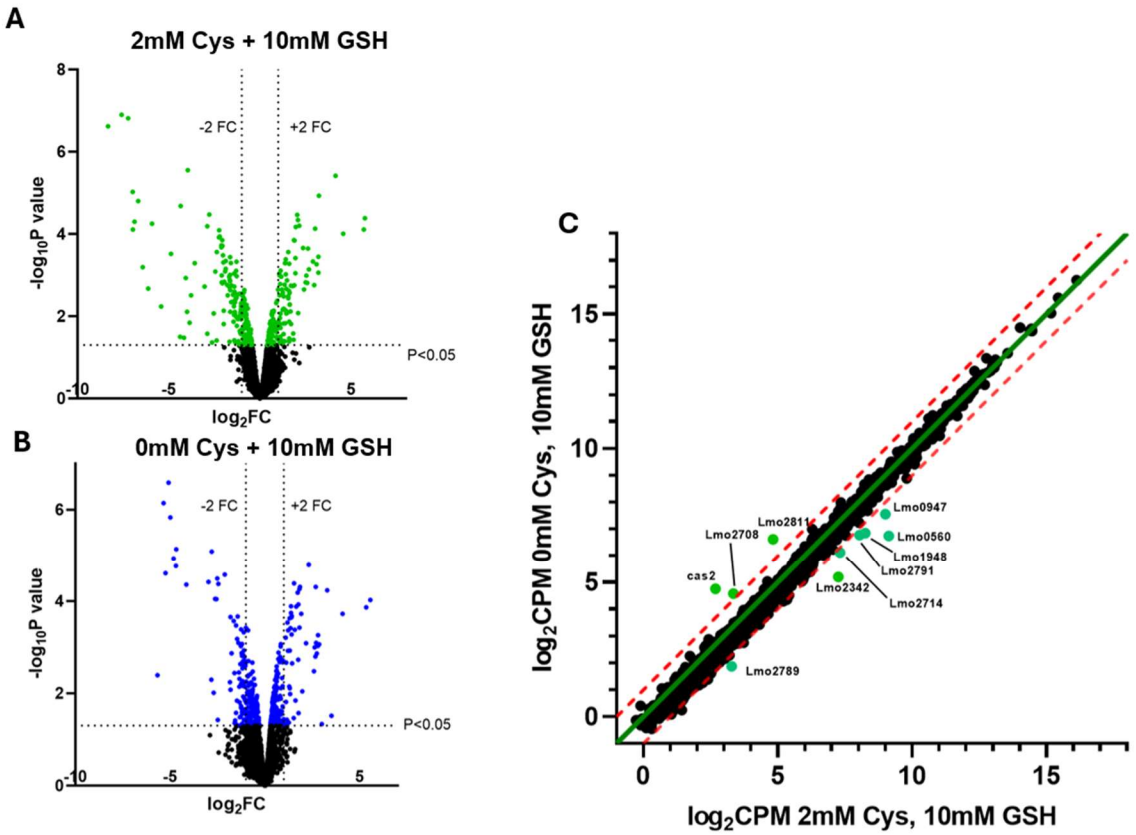

Figure 3.3. Differentially expressed genes induced by 10mM GSH with and without 2mM cysteine. A-B. Log_{10}Pvalue vs Log_2FC relative to standard LSM containing 2mM cysteine in

cultures grown with 10mM GSH (A) or 10mM GSH in place of cysteine (B). Dashed lines indicate >2-fold change in expression relative to control, and $p<0.05$. **C**. Log_2CPM of normalized read counts for 10mM GSH, 0mM cysteine vs. 10mM GSH + 2mM cysteine cultures. Green dashed line indicates 1:1 ratio of Log_2CPM, and red dashed lines indicate > 2-fold change. Lmo gene-symbols denote transcripts with >2-fold change.

Effects of hypoxic growth on GSH utilization

To explore potential genes which are required for growth when GSH is the sole cysteine source, a negative selection screen for genes required for utilization of GSH as a cysteine source was performed Mallory Spencer on a WT *L. monocytogenes* Himar1 transposon library[175] generously gifted to us by JD Sauer. Libraries were grown in standard LSM, and modified LSM in which 10mM GSH was the only source of cysteine. Transposon libraries were generated in the WT background using a *Himar-1 mariner* based transposon system as described previously[175]. Compared to growth in standard LSM, which contains 2mM cysteine, growth in LSM containing 10mM GSH as the sole cysteine source selected against insertions in *aroABCDE* (**Table S3.2**). Genes in the *aro* pathway are important for biosynthesis of menaquinone, which serves as an integral electron transporter during aerobic respiration, and is required for *L. monocytogenes* virulence[176]. Given these results, we hypothesized that genes in the *aro* pathway are required for utilization of GSH as a cysteine source. To test this, and to validate the TnSeq results, we tested the ability of Δ*aroE* and Δ*aroED* mutants to utilize GSH as a cysteine source during standard aerobic growth. We also attempted to test *aroB::tn* and *aroC::tn* mutants, pathway but their growth was too poor even in standard cysteine containing LSM to proceed. Neither Δ*aroE* nor Δ*aroED* appeared to have impaired growth when GSH was the sole cysteine source (**Fig. 3.4A-B**). Δ*aroED* was impaired for growth in standard LSM, as well as LSM containing GSH in place of cysteine, so its growth defect is likely independent of GSH utilization. Given that lack of *aro* genes may impair aerobic respiration and mask phenotypes related to GSH utilization, I repeated the experiment under hypoxic conditions (5%

CO_2, 2% O_2). While Δ*aroE*, and Δ*aroED* did not appear to be impaired for GSH utilization, I found that during hypoxic growth, all strains reached a higher terminal OD_{600} relative to cysteine-containing medium when GSH was the only source of cysteine (**Fig. 3.4A-B**). This indicates that *L. monocytogenes* is better able to utilize GSH as a cysteine source under hypoxic growth conditions. We went on repeat growth of just WT in LSM containing 2mM cysteine, and LSM in which 0.5mM GSH was the sole source of cysteine. While average growth of WT in the GSH-only media, assessed by terminal OD_{600} after 16-hours of growth, was higher than in standard LSM under hypoxic conditions, this difference was not statistically significant (**Fig 3.4C**). However, given the modest, albeit insignificant benefit hypoxic growth appeared to have for GSH utilization, we next hypothesized hypoxic growth may more robustly alter the expression of genes important for utilization of GSH as a cysteine source.

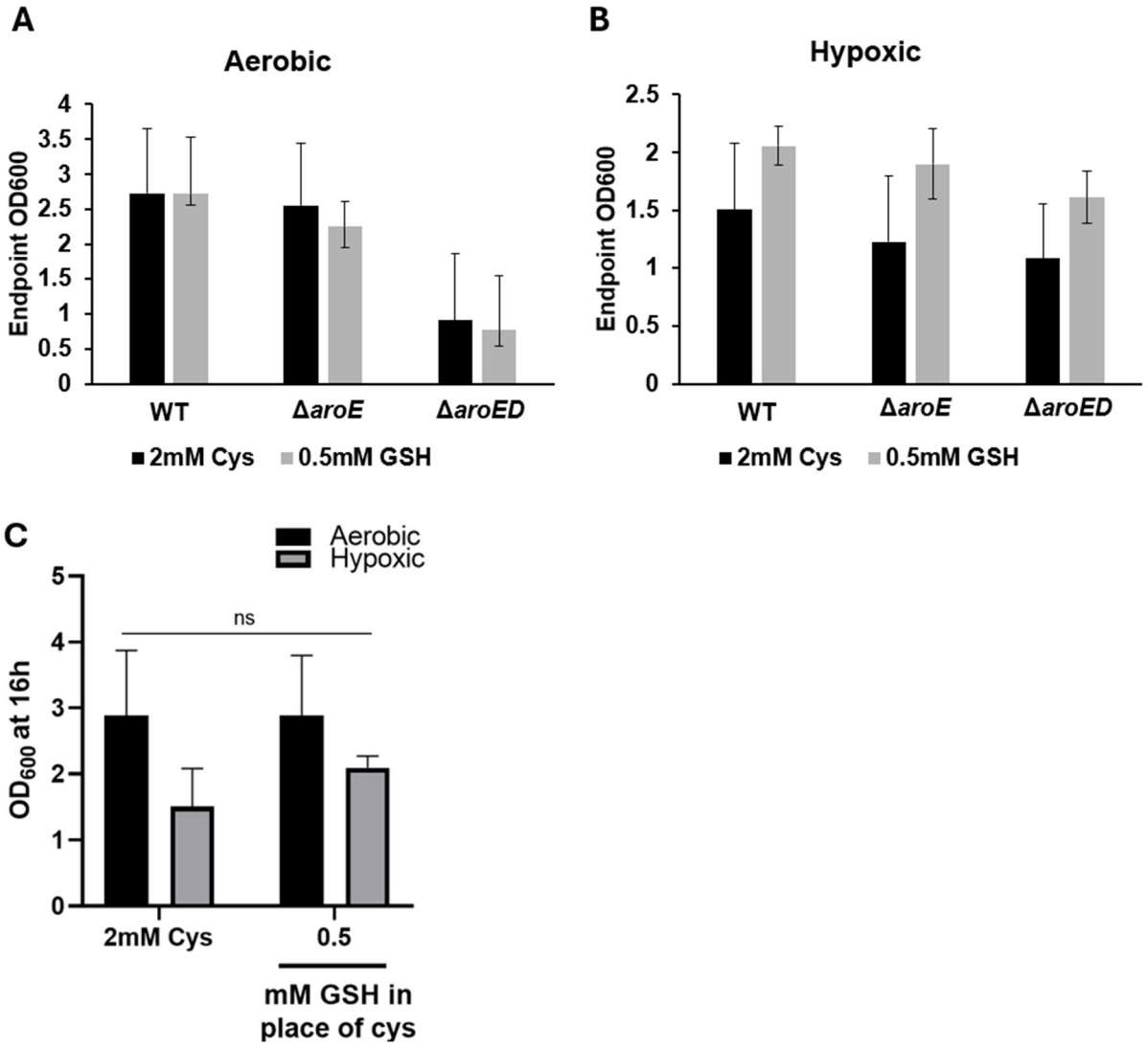

Figure 3.4. Utilization of GSH as a cysteine source during hypoxic growth. Endpoint OD_{600} of indicated strains grown under standard aerobic conditions (A) , or in a hypoxic chamber (B) (5% CO2, 2% O2), in standard LSM containing 2mM cysteine, or modified LSM lacking cysteine and supplemented with indicated concentrations of GSH. C. Endpoint OD_{600} of WT grown in standard LSM containing 2mM cysteine or modified LSM lacking cysteine and supplemented with indicated concentration of GSH. A-B are representative of two independent experiments. C is representative of 3 independent experiments. Error bars represent standard deviations. Statistical analyses in C were performed by two-way ANOVA with multiple comparisons between 2mM cysteine condition and modified LSM for either aerobic or hypoxic growth conditions: ns, non-significant; *, $P < 0.05$; **, $P < 0.01$; ****, $P < 0.0001$.

Differentially expressed genes when GSH is utilized as a cysteine source under hypoxic vs. aerobic conditions

Given that utilization of GSH as a cysteine source appeared improved during hypoxic growth, we wanted to assess what genes were differentially expressed aerobically vs. anaerobically when limiting cysteine was replaced with limiting GSH under both aerobic and hypoxic conditions. We hypothesized that genes necessary for breakdown and utilization of GSH for cysteine would be upregulated when GSH was the only cysteine source present, and provided in more limiting concentrations than the 10mM used previously. It was further hypothesized that under hypoxic growth conditions, genes important for GSH utilization would be more strongly upregulated than during aerobic growth. To test these hypotheses, RNAseq was performed on biological duplicates of WT *L. monocytogenes* grown to mid-exponential phase either aerobically, or in a hypoxic chamber, in LSM containing 0.2mM cysteine, or 0.2mM GSH in place of cysteine. cDNA libraries were sequenced to a depth of 15-25 million reads, with 225-518x coverage of the *L. monocytogenes* genome. Differential gene expression was calculated relative to aerobic growth with 0.2mM cysteine, as this is the closest to standard, aerobic growth conditions in LSM (**Table S3.3, Fig. 3.5**). Genes which exhibited ≥2-fold change ($log_2FC \geq 1$) (P value < 0.05) relative to the control were considered differentially expressed genes (DEGs). Gene expression relative to aerobic growth in 0.2mM cysteine appeared more similar between the two anaerobic conditions tested, however, each sample did exhibit a distinct transcriptional profile (**Fig. 3.5**).

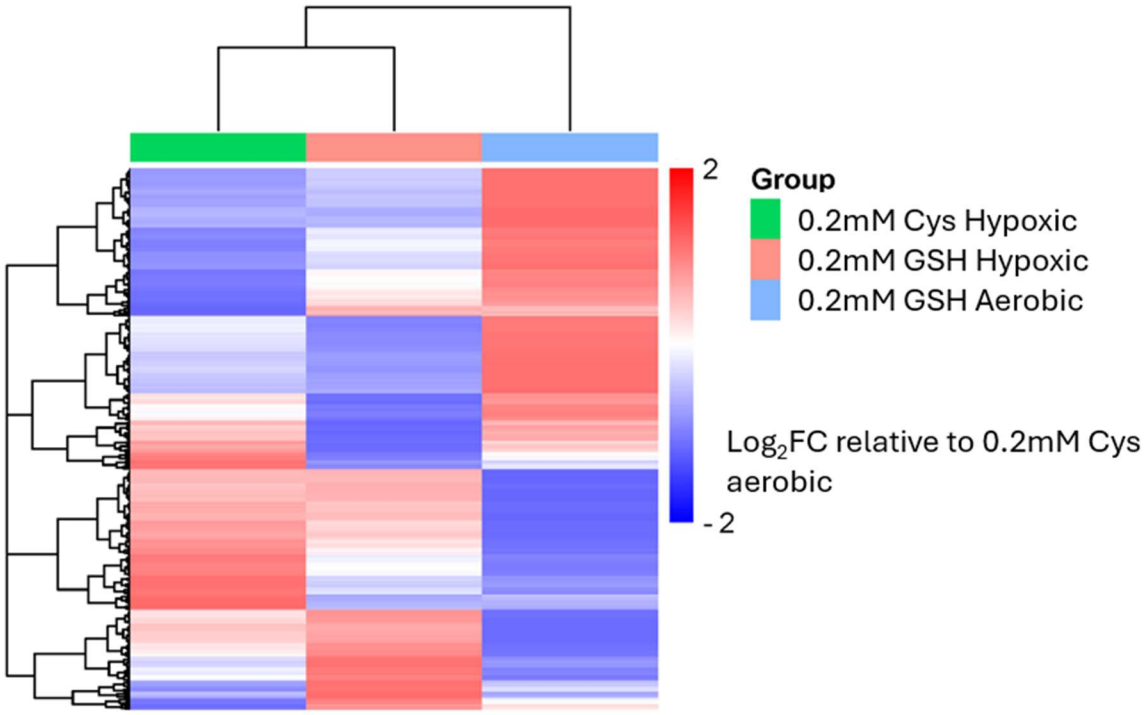

Figure 3.5. Transcriptional profile of *L. monocytogenes* grown using different cysteine sources in both aerobic and hypoxic conditions. Heatmap of significantly differentially expressed genes (>2Log_2FC, P<0.05) in at least one sample, relative to aerobic growth in 0.2mM cysteine. Color scale is Log_2FC relative to aerobic growth in 0.2mM cysteine. Left Y axis represents significant DEGs ordered by hierarchical clustering.

As expected, the PrfA regulon was strongly upregulated during aerobic growth in the presence of 0.2mM GSH compared to growth in 0.2mM cysteine (**Table S3.3**). Interestingly, this was also the case under hypoxic conditions, when either GSH or Cys was supplied (**Table S3.3**). Furthermore a number of genes in the *L. monocytogenes* A118 prophage locus were also strongly upregulated during GSH utilization. (**Table S3.3**). When medium was supplemented with cysteine under hypoxic growth, the *isdEC* genes involved in heme uptake were strongly downregulated compared to aerobic growth when either GSH or cysteine was supplemented (**Table S3.3**). Furthermore, *lmo1132* was upregulated during hypoxic GSH growth and downregulated during hypoxic cysteine growth. This gene is predicted to encode an ABC

transporter, whose protein sequence exhibits homology with CydC in Enterococcaceae bacteria. The CydDC system has been characterized in as an exporter of low molecular weight thiols such as cysteine and glutathione[177], so this may represent an undiscovered, low affinity GSH transporter in *L. monocytogenes*. Interestingly, expression of Lmo1132 was previously found to be important for Caco-2 cell adhesion[178] It is important to note that *lmo2715-lmo2716* are annotated as CydDC as well, though this ATP transport system is encoded in the same operon as the cytochrome *bd* type oxidase CydAB, and is important for correct insertion of CydAB into the cell-membrane[179].

GO enrichment analysis of differentially expressed genes revealed that genes involved with glutamate carboxylase activity and glutamate metabolism were upregulated upon growth in 0.2mM GSH, but only under hypoxic growth (**Fig. 3.6B**). Of note, iron-complex transport components were among the most significantly downregulated genes during hypoxic growth with 0.2mM cysteine(**Table S3.3, Fig. 3.5B**). Of the iron-transport related genes that were significantly downregulated under hypoxic growth with cysteine, only *lmo1959* and *lmo1849* were also significantly upregulated during both aerobic and hypoxic growth in 0.2mM GSH. Strikingly, *lmo2184* and *lmo2186*, which encode *isdEC* heme uptake system, were significantly downregulated during both hypoxic growth in 0.2mM cysteine, aerobic growth with 10mM GSH both with and without 2mM cysteine (**Table S3.3, Fig. 3.5B**). This suggests that both GSH and cysteine downregulates expression of iron uptake components, regardless of oxygen availability.

Finally, to better characterize gene expression across the conditions tested, shared and unique significantly differentially expressed genes across conditions relative to aerobic growth in 0.2mM cysteine were assessed. Surprisingly, only eight upregulated genes and two downregulated genes were shared between aerobic and hypoxic growth when 0.2mM GSH was the sole source of cysteine (**Fig. 3.7A**). Of the shared upregulated genes, one encoded *actA*,

which is in the core PrfA regulon and five belonged to the *L. monocytogenes* A118 prophage locus, which is associated with virulence (**Fig. 3.7B**)[104,180]. The remaining two shared upregulated genes, *lmo2023* and *lmo1254* encode L-aspartate oxidase (*nadB*), and alpha-phosphotrehalase *(treA*), respectively. *TreA* was previously found to be important for conversion of trehalose-6-phosphate to glucose-6 phosphate in *L. monocytogenes*[181]. Glucose-6-phosphate is an important carbon source for *L. monocytogenes* during host-cell infection[103], so *treA* upregulation in response to GSH may represent a new *L. monocytogenes* virulence strategy. *NadB* was shown in a prior study to be required for intracellular replication of *L. monocytogenes*,[182]. Aspartate is taken up by *L. monocytogenes* cells during macrophage infection[183], so upregulation of *NadB* is likely related to upregulation of virulence genes in response to GSH.

The shared downregulated genes during both aerobic and hypoxic growth in 0.2mM GSH were *lmo1225*, and *lmo1518*, both of which do not have known functions. However, *lmo1518* was found to be induced by cell-wall stress in *L. monocytogenes*[184]*.* Our finding that *lmo1518* is downregulated in response to GSH may suggest a link between GSH metabolism and cell-wall homeostasis.

A

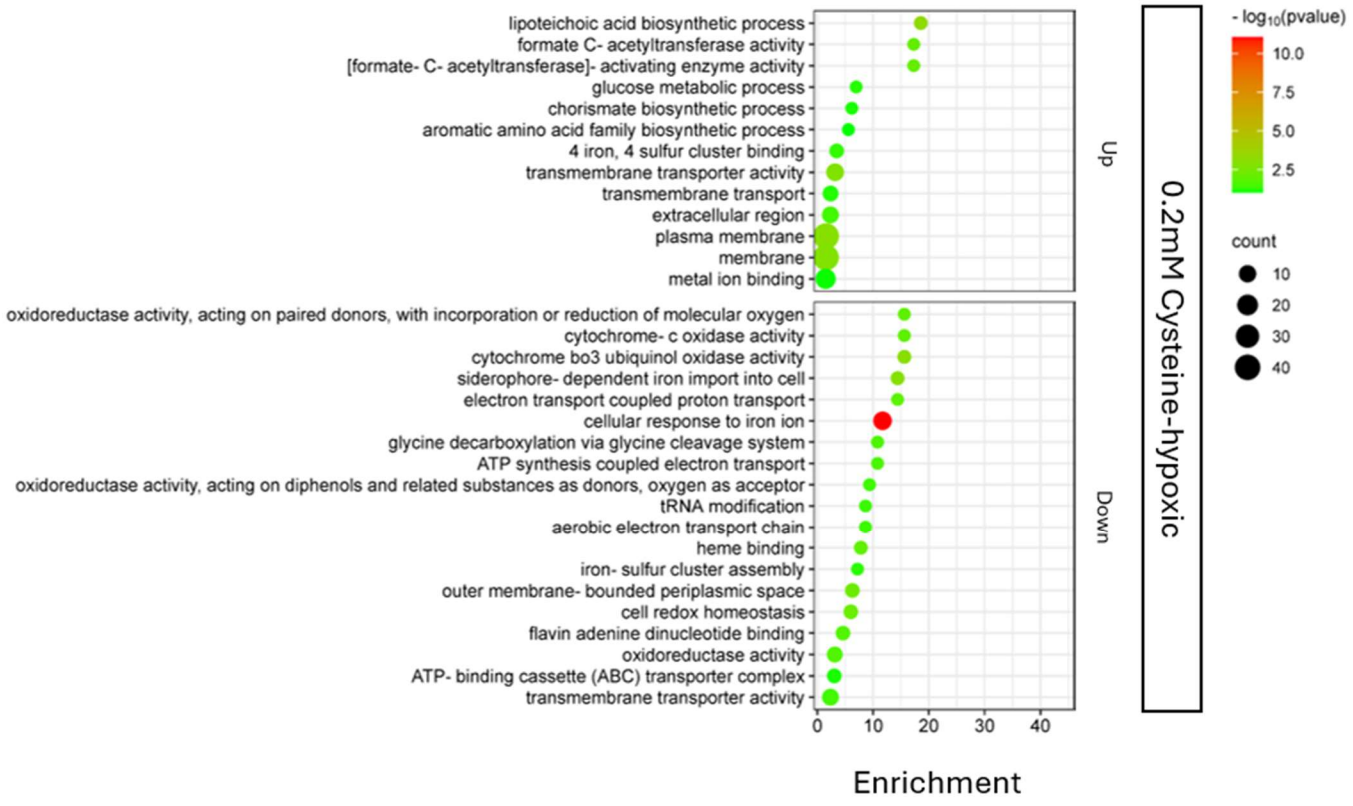
lipoteichoic acid biosynthetic process
formate C- acetyltransferase activity
[formate- C- acetyltransferase]- activating enzyme activity
glucose metabolic process
chorismate biosynthetic process
aromatic amino acid family biosynthetic process
4 iron, 4 sulfur cluster binding
transmembrane transporter activity
transmembrane transport
extracellular region
plasma membrane
membrane
metal ion binding
oxidoreductase activity, acting on paired donors, with incorporation or reduction of molecular oxygen
cytochrome- c oxidase activity
cytochrome bo3 ubiquinol oxidase activity
siderophore- dependent iron import into cell
electron transport coupled proton transport
cellular response to iron ion
glycine decarboxylation via glycine cleavage system
ATP synthesis coupled electron transport
oxidoreductase activity, acting on diphenols and related substances as donors, oxygen as acceptor
tRNA modification
aerobic electron transport chain
heme binding
iron- sulfur cluster assembly
outer membrane- bounded periplasmic space
cell redox homeostasis
flavin adenine dinucleotide binding
oxidoreductase activity
ATP- binding cassette (ABC) transporter complex
transmembrane transporter activity
0
10
20
30
40
Enrichment
Up
Down
0.2mM Cysteine-hypoxic
- log10(pvalue)
10.0
7.5
5.0
2.5
count
10
20
30
40

B

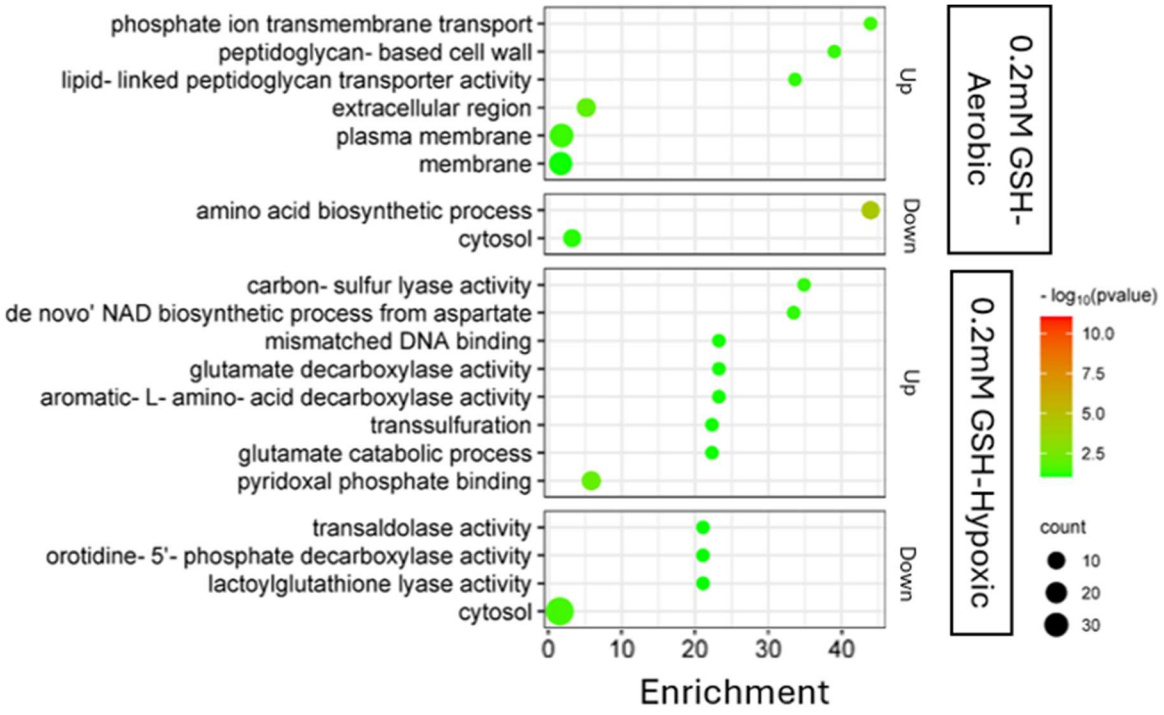

Figure 3.6. GO term enrichment analysis of differentially expressed genes in 0.2mM cysteine under hypoxic growth. (A), 0.2mM GSH under hypoxic growth (B), or 0.2mM GSH under aerobic growth, relative to 0.2mM cysteine under aerobic growth. GO enrichment analyses were performed using DAVID and visualized using SRplot.

A

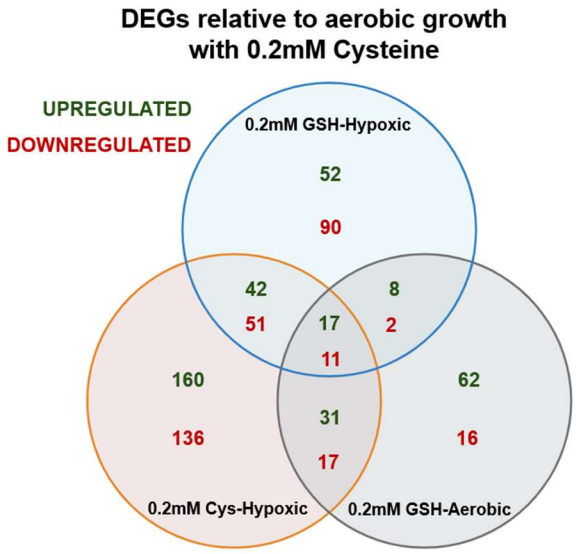

B

		Log2FC vs 0.2mM Cysteine, aerobic	
EGD-E Number	Function	0.2mM GSH, hypoxic	0.2mM GSH, aerobic
lmo1254	alpha-phosphotrehalase	1.08	1.03
lmo2294	gp9	1.26	2.74
lmo2283	long tail fiber	1.29	2.73
lmo2295	gp8	1.53	2.51
lmo2289	gp14	1.53	2.39
lmo2291	major tail shaft protein	1.60	2.62
lmo2023	L-aspartate oxidase	1.71	1.66
lmo0204	actin-assembly inducing protein ActA	3.85	3.96
lmo1225	hypothetical protein	-1.34	-1.13
lmo1518	hypothetical protein	-1.24	-1.45

Figure 3.7. A. Shared and unique significantly differentially expressed genes across conditions relative to aerobic growth in 0.2mM cysteine. B. Table of genes uniquely up and downregulated

genes shared among aerobic and hypoxic growth conditions when 0.2mM GSH is the sole source of cysteine.

DISCUSSION

GSH is an abundant antioxidant in the cells of most living organisms. It is important for neutralizing oxidative stressors, and is the cofactor for a number of GST and GPx enzymes with distinctive functions. In the cysteine auxotroph *L. monocytogenes*, GSH is an important virulence signal, and can also be utilized as a source of cysteine. In Chapter 2, it was demonstrated that during toxic accumulation of the second messenger, c-di-AMP, intracellular GSH is depleted in *L. monocytogenes* both due to reduced GSH synthesis and uptake. Upon testing WT and the ΔPDE strain for utilization of GSH as a cysteine source, I found that c-di-AMP accumulation modestly impairs growth when limiting GSH is supplemented in place of cysteine. This could indicate several things. One, it is possible that impaired GSH uptake by ΔPDE impairs use of GSH as a cysteine source. Additionally, c-di-AMP may inhibit yet undetermined mechanisms important for utilizing cysteine resulting from GSH degradation. However, the mechanisms by which GSH is catabolized have not been identified, making it challenging to discern the mechanisms by which c-di-AMP accumulation hinders GSH synthesis, uptake, and catabolism. In this chapter, I better characterized utilization of GSH as a cysteine source by *L. monocytogenes,* using a transcriptomic approach to identify differentially regulated genes during GSH utilization, as well as a negative selection screen to identify genes important for GSH utilization.

As an initial attempt to identify genes important for GSH degradation, RNAseq was performed on cDNA generated from WT *L. monocytogenes* grown in standard containing 2mM cysteine, 2mM cysteine + 10mM GSH, 10mM GSH in the place of cysteine. Differential gene

expression was calculated relative to the 2mM cysteine growth condition. As was expected, 10mM GSH in both the presence and absence of cysteine induced core PrfA regulon genes.

The negative selection screen results identified a number of underrepresented and overrepresented genes containing transposon insertions after outgrowth in LSM lacking cysteine, and supplemented with 10mM GSH. Of note, insertions in the *aroACED* were underrepresented in bacteria recovered from LSM with 0mM cysteine + 10mM GSH compared to standard LSM. This indicates that the electron transport chain, or perhaps, aerobic respiration in general is important for GSH catabolism. However, it should also be noted that the cultures used for the experiment were allowed to grow well into stationary phase. Thus, it is possible that over the course of exponential growth, mutants lacking components of a functional respiratory chain were naturally selected against. Also, given that *aroB::tn* and *aroC::tn* did not grow in standard LSM, and Δ*aroED* grew poorly, it is possible that underrepresentation of these mutants was due to a general growth defect rather than a GSH-specific phenotype. Nonetheless, the results from this experiment led us to question whether metabolic status in some way influences GSH metabolism.

Results from the negative selection screen were validated by growing *L. monocytogenes aro* mutants aerobically and hypoxically, when GSH was the only source of cysteine. Remarkably, hypoxic utilization of GSH in WT appeared somewhat improved under hypoxic growth conditions. This led to the hypothesis that hypoxic growth may more strongly upregulate genes important for GSH utilization. To test this, RNAseq was performed for WT grown aerobically or hypoxically, with either 0.2mM GSH or 0.2mM cysteine as the sole cysteine source. Perhaps the most striking result from this experiment was the downregulation of heme and iron uptake genes in response to hypoxic growth with 0.2mM cysteine, and to a lesser extent, hypoxic growth with 0.2mM GSH. Why this phenomenon may occur is still the subject of speculation. However, GSH and cysteine are known to be important for iron homeostasis,

forming complexes with iron, as well as aiding in the biosynthesis of iron cofactors[185]. Therefore, the results from this chapter potentially reveal a complex interplay between GSH, iron, and cysteine homeostasis. However, the mechanisms underlying this relationship are likely the subject of future research.

It was not surprising that both PrfA-regulated genes and A118 prophage genes were upregulated by 0.2mM GSH during aerobic growth, as previous studies have found prophage excision to be related to *L. monocytogenes* virulence[180]. Interestingly, a number virulence genes were upregulated during hypoxic growth with both 0.2mM GSH and 0.2mM cysteine. However, this is not entirely unexpected as hypoxic growth was previously shown to upregulate *L. monocytogenes* virulence genes[186]. We also identified two genes, *treA* and *nadB,* which are likely important for acquisition of nutrients during host-cell infection. GSH is abundant in the host cell cytosol, so it is tempting to speculate that genes important for utilization of GSH as a sulfur source are also important for virulence, and may share a similar expression profile with virulence-related genes outside of the core PrfA regulon. However, more studies are needed to determine if utilization of GSH for cysteine is required for full virulence of *L. monocytogenes*.

MATERIALS AND METHODS

Strains and Growth Conditions

L. monocytogenes strains are listed in (**Table S3.4)**. *Listeria* Synthetic Medium (LSM) was prepared based on published recipe[54]. For all experiments, unless otherwise indicated, *L. monocytogenes* was grown in LSM at 37°C with shaking.

Growth experiments in limiting cysteine and GSH

For aerobic growth experiments, strains were grown overnight in standard LSM. Overnight cultures were washed 3x in 1x phosphate-buffered-saline to remove exogenous cysteine, and then sub cultured into LSM medium modified as indicated to a final h2o of 0.01. For aerobic growth, cultures were grown shaking at 37C. For hypoxic growth, strains were grown stationary at 37C in a hypoxic chamber containing 5% CO_2, 2% O_2. OD_{600} was measured after 16 hours for endpoint measurements, or every 1.5h for 8h for kinetic growth assays.

Transposon sequencing of Himar1 libraries grown with 10mM GSH in place of cysteine.

An aliquot of a Himar1 transposon library in the WT *L. monocytogenes* background was generated as described previously in the lab of JD Sauer[175]. JD Sauer generously gifted us an aliquot. Library was grown in standard LSM containing 2mM cysteine or LSM in which cysteine was replaced with 10mM GSH. Cultures were grown to stationary phase and genomic gDNA was extracted and sent for Illumina sequencing at the University of Wisconsin Madison Biotechnology center. Insertion counts were analyzed using TRANSIT[187]

RNAseq under varying oxygen availability, GSH and Cysteine concentrations

WT *L. monocytogenes* in biological duplicate was prepared and grown to mid-logarithmic phase (OD_{600} = ~0.5) as described for previously growth kinetic assays, either aerobically or in hypoxic conditions with indicated concentrations of either cysteine or GSH. Cultures were pelleted and RNA was extracted and treated with Turbo DNase. RNAsequencing was performed by SeqCenter (Pittsburgh, PA). For experiment testing aerobic growth with and without 10mM GSH, read mapping to the *L. monocytogenes* 10403s genome (NC-017544.1) was performed by SeqCenter and differential gene expression analysis was performed with EdgeR[149]. For experiment testing aerobic and hypoxic growth with either 0.2mM GSH or 0.2mM cysteine, Galaxy[188] was used to perform read trimming with Fastp[189], read mapping with Bowtie2[190], mapped read counting with htseq[191], and differential gene expression analysis with Deseq2[192].

SUPPLEMENTARY MATERIAL

Table S3.1: Significantly differentially expressed genes (Log2FC > 1, p < 0.05) compared to standard LSM containing 2mM cysteine. Differentially expressed gene analysis was performed using EdgeR. Data is representative of two independent replicates.

		Log2FC relative to LSM containing 2mM cys, without GSH	
EGD-E Gene ID	**Function**	**10mM GSH, 2mM cys**	**10mM GSH, no cys**
lmo1786	internalin C	5.76	5.56
lmo0838	MFS transporter	5.70	5.34
lmo0203	zinc metalloproteinase	4.56	4.09
	CRISPR-associated protein cas2		3.51
lmo0641	cadmium-translocating P-type ATPase	3.02	3.28
lmo2811	tRNA modification GTPase TrmE		3.00
lmo0433	internalin A	3.11	2.86
lmo1962	TetR/AcrR family transcriptional regulator	3.21	2.80
lmo0206	hypothetical protein	2.54	2.79
lmo0205	phospholipase C	2.59	2.73
lmo0204	actin-assembly inducing protein ActA	2.69	2.70
lmo0947	MFS transporter	4.14	2.68
lmo0207	hypothetical protein	2.51	2.66
lmo2210	hypothetical protein	2.41	2.62
lmo0434	internalin B	2.97	2.58
lmo1746	hypothetical protein	3.23	2.31
	hypothetical protein (LMRG_02394)	3.20	2.17
lmo1124	hypothetical protein	2.10	1.97
lmo0212	acetyltransferase	2.36	1.91
lmo2115	hypothetical protein	1.46	1.84
lmo0415	peptidoglycan N-acetylglucosamine deacetylase	1.97	1.82
	CRISPR-associated protein		1.77
lmo2114	hypothetical protein	1.45	1.76
lmo0202	listeriolysin O	1.79	1.75
lmo1690	hypothetical protein	1.17	1.73
lmo0752	hypothetical protein	1.94	1.65
lmo2091	argininosuccinate lyase		1.61
lmo0200	listeriolysin regulatory protein	1.61	1.58
lmo1808	malonyl CoA-acyl carrier protein transacylase	2.04	1.53
lmo2643	hypothetical protein		1.51

lmo1309	hypothetical protein	1.62	1.43
lmo0972	D-alanine--poly(phosphoribitol) ligase subunit 2	1.95	1.41
lmo0201	1-phosphatidylinositol phosphodiesterase	1.55	1.41
lmo2177	hypothetical protein	1.48	1.40
lmo1807	3-oxoacyl-ACP reductase	1.90	1.37
lmo0973	membrane protein	1.59	1.37
lmo0626	hypothetical protein	1.86	1.35
lmo2439	hypothetical protein	1.12	1.33
lmo1254	alpha-phosphotrehalase	1.88	1.31
lmo0604	hypothetical protein	1.12	1.31
lmo0971	D-alanine transfer protein	1.69	1.30
lmo2469	APA family basic amino acid/polyamine antiporter	1.30	1.28
lmo1311	hypothetical protein	1.71	1.26
lmo1745	response regulator	2.16	1.23
lmo0974	D-alanine--poly(phosphoribitol) ligase subunit 1	1.56	1.22
lmo2785	catalase	2.09	1.19
lmo1310	hypothetical protein	1.68	1.16
lmo2773	beta-glucoside operon transcriptional antiterminator	1.25	1.12
lmo1993	pyrimidine-nucleoside phosphorylase		1.11
lmo2219	foldase prsA 2	1.42	1.10
lmo1802	hypothetical protein		1.08
lmo2497	phosphate ABC transporter permease	1.61	1.06
lmo2390	hypothetical protein	-1.29	-1.00
lmo2393	hypothetical protein		-1.01
	hypothetical protein (LMRG_01516)		-1.02
lmo0366	lipoprotein	-1.95	-1.03
lmo2325	hypothetical protein		-1.03
lmo0365	high-affinity iron transporter	-1.76	-1.04
lmo0760	hypothetical protein	-1.66	-1.04
lmo0591	hypothetical protein		-1.05
lmo2200	MarR family transcriptional regulator	-1.40	-1.05
lmo1733	glutamate synthase subunit small		-1.06
lmo2799	hypothetical protein		-1.06
lmo2324	anti-repressor protein		-1.08
lmo0485	hypothetical protein	-1.28	-1.09
lmo0119	hypothetical protein		-1.09
lmo2182	iron complex transport system ATP-binding protein	-2.00	-1.11
lmo0316	hydroxyethylthiazole kinase		-1.11
lmo2676	DNA polymerase V		-1.12
lmo2569	peptide/nickel transport system substrate-binding protein	-1.32	-1.13
lmo2102	glutamine amidotransferase subunit pdxT	-1.64	-1.13
lmo1007	hypothetical protein		-1.14
lmo2101	pyridoxine biosynthesis protein	-1.03	-1.14

lmo1734	glutamate synthase subunit large		-1.14
lmo2743	transaldolase	-1.26	-1.15
lmo2183	iron complex transport system permease	-2.05	-1.17
lmo1015	glycine betaine/proline transport system permease	-1.48	-1.19
lmo0223	cysteine synthase A	-2.37	-1.19
lmo1847	manganese-binding lipoprotein mntA		-1.19
lmo0116	hypothetical protein		-1.20
lmo0117	prophage LambdaLm01, antigen B		-1.20
lmo2184	heme ABC transporter heme-binding protein isdE	-2.03	-1.21
lmo1882	30S ribosomal protein S14	-1.36	-1.21
lmo0610	internalin	-1.42	-1.22
lmo1016	glycine betaine-binding protein	-1.29	-1.24
lmo0918	lichenan operon transcriptional antiterminator		-1.26
lmo0823	aldo/keto reductase	-2.12	-1.26
lmo0346	triosephosphate isomerase		-1.26
lmo1014	glycine betaine/proline transport system ATP-binding protein	-1.44	-1.26
lmo2683	cellobiose-specific PTS system IIB component		-1.27
lmo0508	galactitol-specific PTS system IIC component		-1.28
lmo2675	hypothetical protein		-1.29
lmo0019	hypothetical protein		-1.32
lmo1732	lactose/L-arabinose transport system permease		-1.33
lmo0761	hypothetical protein	-1.91	-1.34
lmo0115	hypothetical protein		-1.35
lmo2181	SrtB family sortase	-1.88	-1.37
lmo2186	heme uptake protein IsdC	-2.12	-1.40
lmo0791	hypothetical protein	-2.06	-1.44
lmo2185	hypothetical protein	-2.25	-1.46
lmo0484	heme-degrading monooxygenase IsdG	-1.12	-1.47
lmo0589	hypothetical protein		-1.52
lmo0612	hypothetical protein		-1.53
lmo0759	glyoxylase	-2.20	-1.53
lmo1848	manganese transport system membrane protein mntC	-1.40	-1.57
lmo1715	hypothetical protein		-1.60
lmo2437	hypothetical protein	-2.05	-1.61
lmo0130	hypothetical protein	-2.23	-1.65
lmo0758	hypothetical protein	-2.45	-1.76
lmo1849	manganese/iron transport system ATP-binding protein	-1.18	-1.81
lmo2829	hypothetical protein	-2.78	-1.82
lmo0140	hypothetical protein		-1.85
lmo0137	peptide/nickel transport system permease	-7.22	-2.12
lmo2433	tributyrin esterase	-2.89	-2.46
lmo2353	hypothetical protein	-2.38	-2.48

lmo0136	peptide/nickel transport system permease	-7.58	-2.52
lmo0903	OsmC/Ohr family protein	-4.34	-2.56
lmo2352	HTH-type transcriptional regulator ytlI	-3.58	-2.63
lmo2088	hypothetical protein		-2.70
lmo0152	peptide/nickel transport system substrate-binding protein	-3.95	-2.81
lmo0138	hypothetical protein	-3.78	-2.82
lmo0135	peptide/nickel transport system substrate-binding protein	-8.33	-2.98
lmo2343	monooxygenase moxC	-6.96	-4.15
lmo2346	polar amino acid transport system ATP-binding protein	-6.13	-4.67
lmo2345	hypothetical protein	-6.97	-4.69
lmo2344	hypothetical protein	-6.87	-4.82
lmo2347	polar amino acid transport system permease	-5.92	-4.99
lmo2348	polar amino acid transport system permease	-6.43	-5.08
lmo2350	hypothetical protein	-4.87	-5.25
lmo2349	polar amino acid transport system substrate-binding protein	-6.67	-5.35
lmo2351	FMN reductase	-5.41	-5.67
	hypothetical protein (LMRG_02074)	1.56	
	hypothetical protein (LMRG_01894)	1.82	
lmo0092	ATP synthase F1 beta subunit	1.36	
lmo0211	50S ribosomal protein L25 Ctc-form	-1.62	
lmo0279	anaerobic ribonucleoside-triphosphate reductase	1.30	
lmo0280	anaerobic ribonucleoside-triphosphate reductase activating protein	1.50	
lmo0361	twin arginine-targeting protein translocase TatC	-1.79	
lmo0362	sec-independent protein translocase tatAy	-1.58	
lmo0367	tat-translocated enzyme	-1.63	
lmo0375	hypothetical protein	-1.08	
lmo0416	transcriptional regulator	1.22	
lmo0541	iron complex transport system substrate-binding protein	-1.09	
lmo0551	hypothetical protein	1.08	
lmo0560	glutamate dehydrogenase	2.90	
lmo0611	FMN-dependent NADH-azoreductase 1	-1.31	
lmo0661	4-carboxymuconolactone decarboxylase	-1.35	
lmo0754	hypothetical protein	1.45	
lmo0781	mannose-specific PTS system IID component	-1.46	
lmo0782	mannose-specific PTS system IIC component	-1.43	
lmo0783	mannose-specific PTS system IIB component	-1.04	
lmo0841	hypothetical protein	1.06	
lmo0845	5-methyltetrahydropteroyltriglutamate/homocysteine S-methyltransferase	-1.07	
lmo0897	SulP family sulfate permease	1.26	

lmo0948	hypothetical protein	1.30
lmo0976	hypothetical protein	-1.05
lmo1123	hypothetical protein	1.17
lmo1251	crp/Fnr family transcriptional regulator	1.40
lmo1298	HTH-type transcriptional regulator glnR	-2.88
lmo1299	glutamine synthetase type I	-2.62
lmo1308	hypothetical protein	1.26
lmo1387	pyrroline-5-carboxylate reductase	-1.10
lmo1409	hypothetical protein	1.12
lmo1433	glutathione reductase	-1.00
lmo1516	amt familyammonium transporter	-4.37
lmo1517	nitrogen regulatory protein P-II	-4.17
lmo1518	hypothetical protein	-3.86
lmo1524	adenine phosphoribosyltransferase	1.59
lmo1539	glycerol uptake facilitator protein	-1.19
lmo1588	acetylornithine aminotransferase	1.38
lmo1590	ArgJ family protein	1.84
lmo1595	GAF domain-containing protein	-1.40
lmo1635	DNA binding 3-demethylubiquinone-9 3-methyltransferase domain-containing protein	1.10
lmo1649	hypothetical protein	1.08
lmo1741	hypothetical protein	1.13
lmo1743	hypothetical protein	1.42
lmo1744	hypothetical protein	1.38
lmo1761	neurotransmitter:Na+ symporter	1.21
lmo1806	acyl carrier protein	1.35
lmo1809	fatty acid/phospholipid synthesis protein PlsX	1.39
lmo1831	orotate phosphoribosyltransferase	-1.55
lmo1832	orotidine 5'-phosphate decarboxylase	-1.68
lmo1833	dihydroorotate oxidase	-1.60
lmo1834	dihydroorotate dehydrogenase electron transfer subunit	-1.64
lmo1835	carbamoyl-phosphate synthase large subunit	-1.87
lmo1836	carbamoyl-phosphate synthase small subunit	-2.10
lmo1837	dihydroorotase	-2.10
lmo1838	aspartate carbamoyltransferase	-1.99
lmo1846	multidrug resistance protein norM	1.02
lmo1945	hypothetical protein	1.12
lmo1983	dihydroxy-acid dehydratase	-1.41
lmo1984	acetolactate synthase large subunit	-1.27
lmo1985	acetolactate synthase small subunit	-1.35
lmo1986	ketol-acid reductoisomerase	-1.30
lmo1987	2-isopropylmalate synthase	-1.02
lmo1988	3-isopropylmalate dehydrogenase	-1.01
lmo1989	3-isopropylmalate dehydratase large subunit	-1.04

lmo1990	3-isopropylmalate dehydratase small subunit	-1.20
lmo2005	aryl-alcohol dehydrogenase	-1.03
lmo2025	quinolinate synthetase complex A subunit	1.29
lmo2110	mannose-6-phosphate isomerase class I	-1.20
lmo2180	hypothetical protein	-1.66
lmo2196	peptide/nickel transport system substrate-binding protein	-1.64
lmo2199	OsmC/Ohr family protein	-1.67
lmo2256	protease I	-1.10
lmo2295	gp8	1.08
lmo2391	hypothetical protein	-1.36
lmo2494	phosphate transport system regulatory protein PhoU	1.64
lmo2496	phosphate ABC transporter	1.63
lmo2539	serine hydroxymethyltransferase	-1.37
lmo2647	creatinine amidohydrolase	-2.54
lmo2648	hypothetical protein	-1.99
lmo2649	ascorbate-specific PTS system IIC component	-3.03
lmo2650	hypothetical protein	-3.99
lmo2651	mannitol-specific PTS system IIA component	-4.06
lmo2714	peptidoglycan bound protein	1.60
lmo2715	ABC transporter CydDC cysteine exporter CydC	1.10
lmo2716	ABC transporter CydDC cysteine exporter CydD	1.60
lmo2793	lipoprotein	1.10
lmo2804	hypothetical protein	1.08

Table S3.2: Log $_2$FC of number of transposon insertions detected in LSM + 0mM Cys, 10mM GSH vs. LSM containing 2mM Cysteine. Only genes with >2-fold change of insertion frequency are shown.

EGD-E Gene ID	Function	log2FC relative to 2mM cysteine
lmo1924	prephenate dehydrogenase	-5.53
lmo1619	D-amino acid aminotransferase	-5.46
lmo0491	3-dehydroquinate dehydratase type I	-5.31
lmo1490	shikimate 5-dehydrogenase	-4.42
lmo1923	3-phosphoshikimate 1-carboxyvinyltransferase	-4.39
lmo1568	hypothetical protein	-3.99

lmo1928	chorismate synthase	-3.77
lmo0886	alanine racemase	-3.64
lmo1600	bifunctional 3-deoxy-7-phosphoheptulonate synthase/chorismate mutase	-3.52
lmo1952	diaminopimelate decarboxylase	-3.35
lmo1956	fur family transcriptional regulator	-2.67
lmo0005	DNA replication and repair protein RecF	-2.58
lmo0004	hypothetical protein	-2.24
lmo1532	Holliday junction DNA helicase RuvB	-2.1
lmo2196	peptide/nickel transport system substrate-binding protein	-1.91
lmo1693	regulatory protein recX	-1.74
lmo1710	flavodoxin	-1.72
lmo1565	DNA polymerase I	-1.69
lmo2194	peptide/nickel transport system permease	-1.69
lmo2251	polar amino acid transport system ATP-binding protein	-1.66
lmo1758	DNA ligase	-1.65
lmo2856	50S ribosomal protein L34	-1.56
lmo1926	chorismate mutase	-1.55
lmo1756	aspartyl-tRNA(Asn)/glutamyl-tRNA amidotransferase subunit C	-1.51
lmo2250	hypothetical protein	-1.51
lmo1515	HTH-type transcriptional regulator cymR	-1.45
lmo2469	APA family basic amino acid/polyamine antiporter	-1.44
lmo2195	peptide/nickel transport system permease	-1.42
lmo1927	3-dehydroquinate synthase	-1.37
lmo1811	ATP-dependent DNA helicase RecG	-1.33
lmo0847	glutamine ABC transporter	-1.2
lmo0162	DNA polymerase III subunit delta	-1.18
lmo0287	response regulator VicR	-1.15
lmo2609	50S ribosomal protein L36	-1.12
lmo0848	polar amino acid transport system ATP-binding protein	-1.11
lmo0396	pyrroline-5-carboxylate reductase	-1.1
lmo1295	host factor-I protein	-1.05
lmo2327	hypothetical protein	-1.05
lmo0578	hypothetical protein	-1.01
lmo0641	cadmium-translocating P-type ATPase	-1
lmo1740	polar amino acid transport system permease	1
lmo2046	2-dehydropantoate 2-reductase	1
lmo2102	glutamine amidotransferase subunit pdxT	1
lmo2167	hydroxyacylglutathione hydrolase	1.01
lmo1371	dihydrolipoyl dehydrogenase	1.03
lmo2473	hypothetical protein	1.03
lmo2503	cardiolipin synthase	1.04
lmo0016	cytochrome aa3 quinol oxidase subunit IV	1.05
lmo0719	PadR family transcriptional regulator	1.05

lmo1373	2-oxoisovalerate dehydrogenase E1 component	1.05
lmo2016	cold shock protein	1.05
lmo2510	preprotein translocase subunit SecA	1.05
lmo0188	dimethyladenosine transferase	1.06
lmo1055	dihydrolipoyl dehydrogenase	1.07
lmo1934	DNA-binding protein HU-beta	1.07
lmo2560	DNA-directed RNA polymerase subunit delta	1.07
lmo2823	hypothetical protein	1.07
lmo0890	RsbT antagonist protein rsbS	1.08
lmo1366	hemolysin	1.08
lmo0787	amino acid transporter AAT family protein	1.09
lmo1688	enoyl-[acyl carrier protein] reductase III	1.09
lmo2806	hypothetical protein	1.1
lmo1739	polar amino acid transport system ATP-binding protein	1.12
lmo2810	tRNA uridine 5-carboxymethylaminomethyl modification protein GidA	1.12
lmo1360	hypothetical protein	1.13
lmo2511	sigma-54 modulation protein	1.13
lmo0943	starvation-inducible DNA-binding protein	1.15
lmo2217	hypothetical protein	1.15
lmo1764	phosphoribosylamine--glycine ligase	1.16
lmo1767	phosphoribosylformylglycinamidine cyclo-ligase	1.17
lmo2190	adapter protein mecA	1.17
lmo1327	ribosome-binding factor A	1.18
lmo0196	stage V sporulation protein G	1.19
lmo0210	L-lactate dehydrogenase	1.19
lmo1275	DNA topoisomerase I	1.19
lmo1683	fur family transcriptional regulator	1.19
lmo2048	hypothetical protein	1.19
lmo2426	arsenate reductase	1.19
lmo2562	hypothetical protein	1.19
lmo0266	hypothetical protein	1.21
lmo1064	MIT family metal ion transporter	1.21
lmo0200	listeriolysin regulatory protein	1.22
lmo0948	hypothetical protein	1.23
lmo1765	phosphoribosylaminoimidazolecarboxamide formyltransferase/IMP cyclohydrolase	1.24
lmo1771	phosphoribosylformylglycinamidine synthase	1.24
lmo0916	cellobiose-specific PTS system IIA component	1.28
lmo0055	adenylosuccinate synthetase	1.3
lmo2205	phosphoglycerate mutase	1.3
lmo1374	2-oxoisovalerate dehydrogenase E2 component	1.31
lmo1922	hypothetical protein	1.31
lmo2556	fructose-16-bisphosphate aldolase class II	1.31
lmo0598	biotin biosynthesis protein BioY	1.34

lmo0891	serine/threonine-protein kinase rsbT	1.34
lmo0555	Di/tripeptide permease DtpT	1.35
lmo0734	LacI family transcriptional regulator	1.36
lmo1687	hypothetical protein	1.36
lmo1546	rod shape-determining protein MreD	1.37
lmo2811	tRNA modification GTPase TrmE	1.4
lmo2041	methylase MraW	1.41
lmo1972	ascorbate-specific PTS system IIB component	1.49
lmo0964	hypothetical protein	1.5
lmo1328	tRNA pseudouridine synthase B	1.51
lmo1738	polar amino acid transport system substrate-binding protein	1.52
lmo2825	phosphoserine aminotransferase	1.54
lmo2538	uracil phosphoribosyltransferase	1.55
lmo2769	antibiotic transport system ATP-binding protein	1.55
lmo1389	simple sugar transport system ATP-binding protein	1.6
lmo0892	sigma-B regulation protein RsbU	1.67
lmo2770	glutamate-cysteine ligase/gamma-glutamylcysteine synthetase	1.67
lmo2824	D-3-phosphoglycerate dehydrogenase	1.67
lmo1993	pyrimidine-nucleoside phosphorylase	1.68
lmo2349	polar amino acid transport system substrate-binding protein	1.69
lmo2768	hypothetical protein	1.7
lmo1439	superoxide dismutase	1.71
lmo0044	30S ribosomal protein S6	1.75
lmo1774	phosphoribosylaminoimidazole carboxylase	1.75
lmo0895	RNA polymerase sigma-B factor	1.76
lmo0139	hypothetical protein	1.82
lmo1390	simple sugar transport system permease	1.88
lmo1391	simple sugar transport system permease	1.92
lmo1773	adenylosuccinate lyase	1.94
lmo1388	ABC transporter	2.06
lmo1772	phosphoribosylaminoimidazolesuccinocarboxamide synthase	2.14
lmo2692	hypothetical protein	2.25

Table S3.3. Significantly differentially expressed genes (Log2FC > 1, p < 0.05) relative to indicated condition. Abbreviations are as follows: LSM supplemented with 0.2mM cysteine (Cys) or 0.2mM glutathione (GSH) in place of cysteine, grown aerobically (O2) or under hypoxic conditions (A).

		Log2FC vs CysO2		
EGD-E Gene ID	**Function**	**CysA**	**GSHA**	**GSHO2**
lmo0138	hypothetical protein		-7.8	
	hypothetical protein (LMRG_01935)		-5.5	
lmo2650	hypothetical protein		-5.5	

lmo2432	hypothetical protein	-5.0	-5.1	
lmo2651	mannitol-specific PTS system IIA component	-3.5	-4.2	-2.6
lmo2852	hypothetical protein		-3.9	
lmo2648	hypothetical protein	-2.2	-3.9	-1.9
lmo2180	hypothetical protein	-6.1	-3.8	
lmo0139	hypothetical protein	-3.4	-3.8	-2.8
lmo1007	hypothetical protein	-8.6	-3.1	
lmo0349	hypothetical protein	-2.7	-3.1	
lmo2649	ascorbate-specific PTS system IIC component	-2.1	-3.0	-2.0
lmo0661	4-carboxymuconolactone decarboxylase	-3.1	-2.7	-1.6
lmo0609	hypothetical protein		-2.7	
lmo1245	hypothetical protein	-3.9	-2.6	
lmo0350	hypothetical protein		-2.5	
lmo0123	minor structural protein		-2.5	3.2
lmo0154	zinc transport system ATP-binding protein		-2.4	
lmo0622	hypothetical protein		-2.3	
lmo2094	hypothetical protein		-2.3	
lmo0880	peptidoglycan bound protein		-2.2	
lmo0121	hypothetical protein		-2.2	3.3
lmo0659	hypothetical protein		-2.1	
lmo0124	hypothetical protein		-2.1	2.9
lmo1849	manganese/iron transport system ATP-binding protein	-2.6	-2.1	
lmo0122	hypothetical protein	-1.2	-2.1	3.1
lmo2645	hypothetical protein		-2.1	
lmo1587	ornithine carbamoyltransferase		-2.1	
lmo2646	hypothetical protein		-2.0	
lmo0125	hypothetical protein		-1.9	2.9
lmo0120	hypothetical protein		-1.9	2.7
lmo0247	hypothetical protein		-1.8	
lmo0128	hypothetical protein		-1.8	3.5
lmo1872	rRNA (guanine-N1-)-methyltransferase		-1.8	
lmo0003	mate efflux family protein		-1.8	
lmo0019	hypothetical protein		-1.8	
lmo2743	transaldolase	-1.0	-1.8	
lmo2127	hypothetical protein	-1.1	-1.7	
lmo2676	DNA polymerase V	-1.9	-1.7	1.9
lmo0591	hypothetical protein		-1.7	
lmo0127	hypothetical protein		-1.7	3.5
lmo0129	N-acetylmuramoyl-L-alanine amidase		-1.7	3.4
lmo0518	membrane protein	-1.3	-1.6	
lmo2708	cellobiose-specific PTS system IIC component		-1.6	
lmo0372	beta-glucosidase		-1.6	
lmo0117	prophage LambdaLm01, antigen B		-1.6	3.2

lmo1889		hypothetical protein	-1.0	-1.6	
lmo1336		5-formyltetrahydrofolate cyclo-ligase	-1.3	-1.6	
lmo1618		hypothetical protein		-1.6	
lmo0346		triosephosphate isomerase		-1.6	
lmo2153		ribonucleotide reductase-associated flavodoxin		-1.6	
lmo2675		hypothetical protein	-1.6	-1.6	1.8
lmo1211		integral membrane protein		-1.6	
lmo0590		hypothetical protein		-1.5	
lmo2763		cellobiose-specific PTS system IIC component	-1.4	-1.5	
lmo0761		hypothetical protein		-1.5	
lmo2393		hypothetical protein		-1.5	
lmo2855		ribonuclease P		-1.5	
lmo1016		glycine betaine-binding protein		-1.5	
lmo1305		transketolase	-1.2	-1.5	
lmo2436		beta-glucoside operon transcriptional antiterminator		-1.5	
lmo0323		hypothetical protein	-1.0	-1.5	
lmo0373		cellobiose-specific PTS system IIC component		-1.5	
lmo0602		hypothetical protein		-1.5	
lmo1831		orotate phosphoribosyltransferase		-1.4	
lmo0377		hypothetical protein	-1.3	-1.4	-1.1
lmo0589		hypothetical protein		-1.4	
lmo1364		cold shock-like protein cspLA	-1.4	-1.4	
lmo1414		acetyl-CoA C-acetyltransferase	-1.3	-1.4	
lmo0343		transaldolase		-1.4	
lmo1568		hypothetical protein		-1.4	
lmo1832		orotidine 5'-phosphate decarboxylase		-1.4	
lmo1591		N-acetyl-gamma-glutamyl-phosphate reductase	-1.4	-1.4	
	0	internalin D		-1.4	
lmo2061		hypothetical protein	-1.1	-1.4	
lmo2202		3-oxoacyl-ACP synthase	-1.2	-1.4	
lmo1961		ferredoxin-NADP reductase 1	-3.3	-1.4	
lmo0675		flagellar motor switch protein FliN	-1.5	-1.4	
lmo0347		dihydroxyacetone kinase L subunit		-1.4	
lmo1978		glucose-6-phosphate dehydrogenase		-1.4	
lmo1209		ATP:cob(I)alamin adenosyltransferase	-1.2	-1.4	
lmo0227		tRNA-dihydrouridine synthase B	-1.8	-1.4	
lmo1835		carbamoyl-phosphate synthase large subunit		-1.3	
lmo0348		dihydroxyacetone kinase		-1.3	
lmo1225		hypothetical protein		-1.3	-1.1
lmo1370		butyrate kinase		-1.3	
lmo1836		carbamoyl-phosphate synthase small subunit		-1.3	
lmo2764		hypothetical protein	-1.6	-1.3	
lmo1920		hypothetical protein		-1.3	
lmo0901		cellobiose-specific PTS system IIC component	-1.5	-1.3	

lmo1330	30S ribosomal protein S15	-1.1	-1.3	-1.0
lmo2175	3-oxoacyl-ACP reductase	-2.0	-1.3	
lmo0806	hypothetical protein		-1.3	
lmo2043	MFS transporter	-1.3	-1.3	
lmo0652	hypothetical protein		-1.3	
lmo1469	30S ribosomal protein S21	-1.7	-1.3	-1.6
lmo2830	thioredoxin	-1.1	-1.3	
lmo0683	chemotaxis protein methyltransferase	-1.8	-1.3	
lmo1009	hypothetical protein		-1.3	
lmo0656	membrane protein		-1.3	
lmo1429	proton-coupled thiamine transporter YuaJ		-1.2	
lmo1518	hypothetical protein		-1.2	-1.4
lmo1539	glycerol uptake facilitator protein		-1.2	
lmo0766	multiple sugar transport system permease		-1.2	
lmo0844	endoribonuclease L-PSP	-1.4	-1.2	-1.0
lmo2243	ADA regulatory protein/Methylated-DNA-protein-cysteine methyltransferase	-1.0	-1.2	
lmo2737	catabolite control protein B		-1.2	
lmo0945	late competence protein ComEC	-1.0	-1.2	
lmo0222	chaperonin HslO		-1.2	
lmo2683	cellobiose-specific PTS system IIB component	-1.2	-1.2	-1.0
lmo1670	hypothetical protein	-2.1	-1.2	
lmo1371	dihydrolipoyl dehydrogenase		-1.2	
lmo2539	serine hydroxymethyltransferase		-1.2	
lmo1834	dihydroorotate dehydrogenase electron transfer subunit		-1.2	
lmo0185	Mg-dependent DNase	-1.1	-1.2	
lmo0976	hypothetical protein		-1.2	
lmo2014	alpha-mannosidase		-1.2	
lmo1281	4-hydroxybenzoyl-CoA thioesterase		-1.1	
lmo0226	7,8-dihydro-6-hydroxymethylpterin-pyrophosphokinase		-1.1	
lmo1567	citrate synthase		-1.1	
lmo0807	spermidine/putrescine transport system ATP-binding protein		-1.1	
lmo0679	flagellar biosynthetic protein FlhB	-1.3	-1.1	
lmo1958	iron complex transport system permease	-2.8	-1.1	
lmo0676	flagellar biosynthetic protein FliP	-1.3	-1.1	
lmo0905	hypothetical protein		-1.1	
lmo0936	oxygen-insensitive NADPH nitroreductase		-1.1	
lmo0538	N-acyl-L-amino acid amidohydrolase	-1.6	-1.1	
lmo2154	ribonucleoside-diphosphate reductase		-1.1	
lmo0342	transketolase	-1.0	-1.1	
lmo1910	D-amino-acid dehydrogenase	-1.4	-1.1	
lmo1732	lactose/L-arabinose transport system permease		-1.1	
lmo0935	TrmH family RNA methyltransferase group 2		-1.1	
lmo1933	GTP cyclohydrolase I		-1.1	

lmo2576	peptidoglycan bound protein	-1.2	-1.1	
lmo1959	iron complex transport system substrate-binding protein	-3.3	-1.1	
lmo2256	protease I		-1.1	
lmo1782	exodeoxyribonuclease III		-1.1	
lmo1538	glycerol kinase		-1.1	
lmo2641	trans-hexaprenyltranstransferase		-1.1	
lmo0193	HlyD family secretion protein		-1.1	
lmo0830	fructose-1,6-bisphosphatase class 3		-1.1	
lmo2557	hypothetical protein		-1.0	
lmo0686	chemotaxis protein MotB	-1.7	-1.0	
lmo0667	antibiotic transport system ATP-binding protein		-1.0	
lmo2692	hypothetical protein		-1.0	
	hypothetical protein (LMRG_01935)	-1.0	-1.0	-1.0
lmo1328	tRNA pseudouridine synthase B	-1.2	-1.0	
lmo0678	flagellar biosynthesis protein FliR	-1.2	-1.0	
lmo2261	hypothetical protein	-1.6	-1.0	
lmo2744	hypothetical protein	-1.1	-1.0	
lmo1955	tyrosine recombinase XerD		-1.0	
lmo0192	pur operon repressor	-1.3	-1.0	
lmo0277	hypothetical protein	-1.3	-1.0	
lmo2103	phosphate acetyltransferase		-1.0	
lmo0754	hypothetical protein		1.0	
lmo1576	hypothetical protein		1.0	
lmo2511	sigma-54 modulation protein	1.3	1.0	
lmo0900	hypothetical protein		1.0	
lmo1438	hypothetical protein		1.0	
lmo0242	hypothetical protein		1.0	
lmo2334	DNA-binding protein		1.0	
lmo1244	phosphoglycerate mutase		1.0	
lmo2591	N-acetylmuramoyl-L-alanine amidase		1.0	
lmo0480	hypothetical protein		1.0	
lmo2114	hypothetical protein	1.3	1.1	1.2
lmo0483	AraC/XylS family transcriptional regulator		1.1	
lmo0898	hypothetical protein		1.1	
lmo1254	alpha-phosphotrehalase		1.1	1.0
lmo2440	hypothetical protein		1.1	
lmo1142	hypothetical protein		1.1	
lmo1807	3-oxoacyl-ACP reductase		1.1	
lmo1679	cystathionine beta-lyase		1.1	
lmo2107	hypothetical protein		1.1	
lmo2498	phosphate ABC transporter permease		1.1	
lmo0862	trehalose-6-phosphate hydrolase		1.1	
lmo2040	cell division protein FtsL		1.1	

lmo2773	beta-glucoside operon transcriptional antiterminator		1.1	
lmo1403	DNA mismatch repair protein MutS		1.1	
lmo1131	ABC transporter	-1.6	1.1	
lmo1333	hypothetical protein		1.2	
lmo1166	propanol dehydrogenase PduQ		1.2	
lmo1143	hypothetical protein		1.2	
lmo0516	poly-gamma-glutamate synthesis protein		1.2	
lmo1251	crp/Fnr family transcriptional regulator		1.2	
lmo2717	cytochrome d ubiquinol oxidase subunit II	2.2	1.2	
lmo0417	hypothetical protein	1.9	1.2	
lmo2206	ATP-dependent chaperone ClpB	1.8	1.2	
lmo1632	anthranilate synthase component II		1.2	
lmo0533	ACT domain-containing protein	1.5	1.2	
lmo0802	hypothetical protein		1.2	
lmo0727	glutamine-fructose-6-phosphate transaminase		1.2	
lmo2816	hypothetical protein	1.4	1.2	
lmo1204	cobalamin biosynthesis protein CbiM	1.6	1.2	
lmo1132	ABC transporter	-1.5	1.2	
lmo0645	APA family basic amino acid/polyamine antiporter	1.1	1.2	
lmo2294	gp9		1.3	2.7
lmo2278	endolysin L-alanyl-D-glutamate peptidase	1.1	1.3	2.6
lmo2760	ABC transporter ATP-binding protein		1.3	
lmo0416	transcriptional regulator	2.1	1.3	
lmo0859	multiple sugar transport system substrate-binding protein		1.3	
lmo2283	long tail fiber		1.3	2.7
lmo2643	hypothetical protein	1.1	1.3	
lmo2494	phosphate transport system regulatory protein PhoU		1.3	
lmo2115	hypothetical protein	1.6	1.3	1.4
lmo1694	hypothetical protein	2.3	1.3	1.3
lmo1604	peroxiredoxin		1.3	
lmo1681	5-methyltetrahydropteroyltriglutamate/homocysteine S-methyltransferase		1.3	
lmo1484	competence protein ComEA		1.4	
lmo0973	membrane protein	2.2	1.4	
lmo0327	internalin	1.5	1.4	
lmo1050	hypothetical protein		1.4	
lmo1724	ABC transporter ATP-binding protein		1.4	
lmo2297	scaffolding protein	1.2	1.4	2.4
lmo0974	D-alanine--poly(phosphoribitol) ligase subunit 1	2.0	1.4	
lmo2581	hypothetical protein		1.4	
lmo2024	nicotinate-nucleotide diphosphorylase	1.0	1.4	1.1
lmo2487	hypothetical protein	2.7	1.4	1.2
lmo2025	quinolinate synthetase complex A subunit	1.5	1.4	1.2
lmo1745	response regulator	1.0	1.5	

lmo2817		aminoacylase		1.5	
lmo1586		inorganic polyphosphate/ATP-NAD kinase 2	1.3	1.5	
lmo2295		gp8		1.5	2.5
lmo0292		hypothetical protein	1.6	1.5	1.0
lmo2289		gp14		1.5	2.4
lmo2496		phosphate ABC transporter		1.5	
lmo0861		multiple sugar transport system permease		1.6	
lmo1031		hypothetical protein	2.4	1.6	
lmo0510		hypothetical protein		1.6	
lmo2291		major tail shaft protein		1.6	2.6
lmo1167		glycerol uptake facilitator protein		1.6	
lmo2288		gp15	1.5	1.6	2.9
lmo2486		hypothetical protein	2.5	1.6	1.4
lmo0383		methylmalonate-semialdehyde dehydrogenase		1.7	
lmo0860		multiple sugar transport system permease	1.1	1.7	
lmo2819		aminoacylase	1.4	1.7	
lmo1175		ethanolamine ammonia-lyase large subunit		1.7	
lmo2660		transketolase	1.7	1.7	
lmo0489		hypothetical protein		1.7	
lmo0520		hypothetical protein	1.3	1.7	
lmo2023		L-aspartate oxidase		1.7	1.7
lmo1170		hypothetical protein	1.1	1.7	
lmo1227		uracil-DNA glycosylase		1.7	
lmo2818		MFS transporter	1.4	1.8	
lmo0293		hypothetical protein		1.8	
lmo1165		aldehyde dehydrogenase	1.7	1.8	1.5
lmo0309		hypothetical protein	2.0	1.8	
lmo1413		peptidoglycan bound protein	1.8	1.8	
lmo2592		morphine 6-dehydrogenase	1.9	1.8	
lmo2567		hypothetical protein	3.8	1.9	
lmo2363		glutamate decarboxylase	2.3	1.9	
		hypothetical protein (LMRG_02594)	2.6	2.0	
lmo2593		transcriptional regulator	2.4	2.0	
lmo2174		hypothetical protein	2.6	2.1	
lmo1127		hypothetical protein	2.1	2.1	
lmo1125		hypothetical protein	2.4	2.3	
lmo2803		hypothetical protein	1.6	2.4	
lmo0303		hypothetical protein	1.8	2.4	
lmo1126		acetyltransferase	2.1	2.4	
lmo0056		hypothetical protein		2.4	
lmo2568		hypothetical protein	3.8	2.6	
lmo0306		hypothetical protein	2.7	2.8	1.6
	0	hypothetical protein (LMRG_02846)	3.9	2.9	

lmo0816		protease synthase and sporulation negative regulatory protein PAI 1	2.3	2.9	
lmo2281		gp22	3.3	3.1	3.4
lmo0202		listeriolysin O	3.8	3.4	2.7
	0	hypothetical protein (LMRG_01894)		3.5	
lmo0204		actin-assembly inducing protein ActA		3.8	4.0
lmo2280		gp23	4.5	3.9	5.6
lmo0205		phospholipase C	3.9	4.1	4.2
lmo0308		hypothetical protein	4.1	4.1	
	0	hypothetical protein (LMRG_02493)	4.5	4.2	
lmo2808		hypothetical protein	5.1	5.4	
lmo0058		secretion system component EssA	5.1	5.6	
lmo0838		MFS transporter	5.2		6.5
lmo1786		internalin C	6.3		5.8
lmo2210		hypothetical protein	4.5		5.1
lmo0207		hypothetical protein	4.9		4.6
lmo0206		hypothetical protein	4.5		4.4
lmo0203		zinc metalloproteinase	4.0		4.3
	0	gp32			3.7
lmo0118		antigen A			3.4
lmo2322		gp44			3.2
lmo2326		gp41			3.2
lmo0119		hypothetical protein			3.2
lmo2325		hypothetical protein			3.1
lmo0116		hypothetical protein			3.1
lmo0434		internalin B	4.4		3.0
lmo0126		hypothetical protein	-1.3		2.9
	0	hypothetical protein			2.9
	0	hypothetical protein			2.8
	0	hypothetical protein			2.7
lmo2324		anti-repressor protein			2.7
lmo2296		phage capsid protein			2.7
lmo2290		gp13	1.1		2.7
lmo0433		internalin A	3.5		2.7
lmo2287		tail tape-measure protein			2.7
lmo2303		gp66			2.7
lmo2285		tail or base plate protein gp18			2.6
lmo0947		MFS transporter			2.6
lmo2293		gp10			2.6
	0	recombination protein RecT			2.6
lmo2292		gp11			2.6
	0	gp47			2.6
lmo2286		tail or base plate protein gp17			2.6
lmo2298		phage minor capsid protein			2.5

lmo2299		phage portal protein		2.5
lmo2317		gp49		2.5
lmo2284		tail or base plate protein gp19		2.5
lmo2688		cell division protein FtsW/RodA/SpoVE	4.0	2.5
lmo1962		TetR/AcrR family transcriptional regulator	2.0	2.4
lmo2687		hypothetical protein	3.6	2.3
lmo2271		phage protein		2.3
lmo2300		phage terminase large subunit		2.2
lmo2279		phage holin		2.2
	0	gp68		2.1
	0	hypothetical protein (LMRG_01515)		2.1
lmo2282		short tail fiber		2.1
lmo2301		terminase small subunit		2.0
lmo2323		gp43		2.0
lmo1690		hypothetical protein	1.2	1.9
lmo0980		antibiotic transport system permease		1.9
lmo0647		hypothetical protein	3.5	1.8
lmo2689		magnesium-translocating P-type ATPase	3.6	1.8
lmo2071		hypothetical protein		1.7
lmo0937		hypothetical protein	2.5	1.6
lmo2495		phosphate ABC transporter ATP-binding protein		1.6
lmo0946		hypothetical protein		1.5
lmo2226		ABC-2 type transport system permease		1.5
lmo0415		peptidoglycan N-acetylglucosamine deacetylase	1.9	1.5
lmo0641		cadmium-translocating P-type ATPase	5.2	1.5
lmo0839		tetracycline resistance protein		1.5
lmo2497		phosphate ABC transporter permease		1.4
lmo2408		transcriptional regulator	1.5	1.4
lmo0995		YkrP protein		1.4
lmo2469		APA family basic amino acid/polyamine antiporter	1.7	1.4
lmo1307		hypothetical protein	3.5	1.3
lmo0421		hypothetical protein	1.1	1.3
lmo0626		hypothetical protein	1.9	1.3
lmo0280		anaerobic ribonucleoside-triphosphate reductase activating protein	3.2	1.3
	0	gp27	1.6	1.2
lmo2669		hypothetical protein	4.5	1.2
	0	hypothetical protein		1.2
lmo2219		foldase prsA 2	1.4	1.2
	0	hypothetical protein	2.5	1.1
lmo2204		hypothetical protein		1.1
lmo1037		hypothetical protein		1.1
lmo1746		hypothetical protein	1.0	1.1
lmo0998		hypothetical protein		1.1

lmo2586		formate dehydrogenase alpha subunit		1.1
lmo1975		DNA polymerase IV		1.1
lmo1311		hypothetical protein	3.2	1.1
lmo0897		SulP family sulfate permease	2.7	1.1
lmo2075		O-sialoglycoprotein endopeptidase		1.1
lmo1761		neurotransmitter:Na+ symporter		1.0
lmo0687		hypothetical protein	-1.5	-1.0
lmo0758		hypothetical protein	-1.3	-1.0
lmo0285		D-methionine transport system substrate-binding protein		-1.1
lmo0490		shikimate 5-dehydrogenase	3.5	-1.1
lmo2720		acetyl-CoA synthetase		-1.1
lmo1987		2-isopropylmalate synthase		-1.1
lmo0186		hypothetical protein	-1.9	-1.1
lmo2241		GntR family transcriptional regulator		-1.1
lmo1991		threonine dehydratase		-1.1
lmo2829		hypothetical protein	-1.2	-1.2
lmo1988		3-isopropylmalate dehydrogenase		-1.2
lmo2001		mannose-specific PTS system IIC component		-1.2
lmo1700		hypothetical protein		-1.2
	0	CRISPR-associated protein cas2	3.6	-1.2
lmo1369		phosphate butyryltransferase	-1.2	-1.3
lmo1983		dihydroxy-acid dehydratase	-1.4	-1.3
lmo2345		hypothetical protein	-4.4	-1.4
lmo0791		hypothetical protein	-2.4	-1.4
lmo2454		hypothetical protein		-1.4
lmo2350		hypothetical protein	-5.5	-1.4
lmo2437		hypothetical protein	-3.5	-1.5
lmo2346		polar amino acid transport system ATP-binding protein	-4.6	-1.5
lmo2348		polar amino acid transport system permease	-4.5	-1.5
lmo2343		monooxygenase moxC	-4.5	-1.6
lmo2349		polar amino acid transport system substrate-binding protein	-4.8	-1.6
lmo2351		FMN reductase	-5.1	-1.7
lmo2344		hypothetical protein	-4.1	-1.7
lmo2347		polar amino acid transport system permease	-5.0	-1.8
	0	GNAT family acetyltransferase		-1.9
lmo1854		hypothetical protein		-2.3
lmo2797		mannitol-specific PTS system IIA component		-3.2
lmo1172		response regulator NasT		-3.7
	0	hypothetical protein (LMRG_02841)		-4.3
lmo2186		heme uptake protein IsdC	-7.8	
lmo2185		hypothetical protein	-7.2	
lmo0541		iron complex transport system substrate-binding protein	-6.4	

lmo2184	heme ABC transporter heme-binding protein isdE	-6.0
lmo2183	iron complex transport system permease	-5.6
lmo2181	SrtB family sortase	-5.6
lmo2182	iron complex transport system ATP-binding protein	-5.4
lmo0362	sec-independent protein translocase tatAy	-5.3
lmo0365	high-affinity iron transporter	-5.1
lmo0484	heme-degrading monooxygenase IsdG	-4.9
lmo0367	tat-translocated enzyme	-4.9
lmo0366	lipoprotein	-4.8
lmo0485	hypothetical protein	-4.7
lmo0361	twin arginine-targeting protein translocase TatC	-4.4
lmo2569	peptide/nickel transport system substrate-binding protein	-4.3
lmo1960	iron complex transport system ATP-binding protein	-3.5
lmo0486	50S ribosomal protein L32	-3.4
lmo0016	cytochrome aa3 quinol oxidase subunit IV	-3.0
lmo0351	dihydroxyacetone kinase	-3.0
lmo0560	glutamate dehydrogenase	-3.0
lmo1384	hypothetical protein	-2.9
lmo1055	dihydrolipoyl dehydrogenase	-2.8
lmo0823	aldo/keto reductase	-2.7
lmo2006	acetolactate synthase catabolic	-2.7
lmo1957	iron complex transport system permease	-2.6
lmo2101	pyridoxine biosynthesis protein	-2.6
lmo2412	NifU family SUF system FeS assembly protein	-2.5
lmo0811	carbonic anhydrase	-2.4
lmo2102	glutamine amidotransferase subunit pdxT	-2.3
lmo2755	hypothetical protein	-2.3
lmo2390	hypothetical protein	-2.3
lmo1216	bax protein	-2.2
lmo2411	FeS assembly protein SufB	-2.2
lmo1054	pyruvate dehydrogenase E2 component	-2.2
lmo2005	aryl-alcohol dehydrogenase	-2.1
lmo2413	selenocysteine lyase	-2.1
lmo1052	pyruvate dehydrogenase E1 component	-2.1
lmo1992	alpha-acetolactate decarboxylase	-2.1
lmo2255	hypothetical protein	-2.1
lmo0519	lincomycin resistance protein lmrB	-2.1
lmo0013	quinol oxidase polypeptide II	-2.1
lmo2415	FeS assembly ATPase SufC	-2.0
lmo1053	pyruvate dehydrogenase E1 component subunit beta	-2.0

lmo2414	FeS assembly protein SufD	-2.0
lmo1816	50S ribosomal protein L28	-2.0
lmo1348	glycine cleavage system T protein	-1.9
lmo1956	fur family transcriptional regulator	-1.9
lmo1303	cell division suppressor protein yneA	-1.8
lmo0140	hypothetical protein	-1.8
lmo0014	cytochrome aa3 quinol oxidase subunit I	-1.8
lmo0800	hypothetical protein	-1.8
lmo0843	hypothetical protein	-1.8
lmo0015	cytochrome aa3 quinol oxidase subunit III	-1.8
lmo2199	OsmC/Ohr family protein	-1.7
lmo0213	peptidyl-tRNA hydrolase	-1.7
lmo1387	pyrroline-5-carboxylate reductase	-1.7
lmo1349	glycine cleavage system P-protein	-1.6
lmo2778	hypothetical protein	-1.6
lmo0597	transcription regulator CRP/FNR family protein	-1.6
lmo1233	thioredoxin	-1.6
lmo1733	glutamate synthase subunit small	-1.5
lmo2761	beta-glucosidase	-1.5
lmo0682	flagellar basal-body rod protein FlgG	-1.5
lmo2429	iron complex transport system ATP-binding protein	-1.5
lmo1882	30S ribosomal protein S14	-1.5
lmo0537	allantoate deiminase	-1.5
lmo1350	glycine dehydrogenase subunit 2	-1.5
lmo2055	hypothetical protein	-1.5
lmo2147	hypothetical protein	-1.4
lmo0689	hypothetical protein	-1.4
lmo0245	preprotein translocase subunit SecE	-1.4
lmo0623	hypothetical protein	-1.4
lmo1439	superoxide dismutase	-1.4
lmo2785	catalase	-1.4
lmo2200	MarR family transcriptional regulator	-1.4
lmo1688	enoyl-[acyl carrier protein] reductase III	-1.4
lmo0394	extracellular P60 protein	-1.3
lmo0685	chemotaxis protein MotA	-1.3
lmo0424	sugar uptake protein	-1.3
lmo2263	hypothetical protein	-1.3
lmo0688	hypothetical protein	-1.3
lmo2057	protoheme IX farnesyltransferase	-1.3
lmo0790	YbaK/EbsC family protein	-1.3
lmo2376	peptidyl-prolyl isomerase	-1.3
lmo1242	hypothetical protein	-1.3
lmo2056	hypothetical protein	-1.3

lmo1847	manganese-binding lipoprotein mntA	-1.3
lmo2749	anthranilate synthase component II	-1.3
lmo1418	nucleotide pyrophosphatase	-1.3
lmo2047	50S ribosomal protein L32	-1.2
lmo1420	UDP-N-acetylenolpyruvoylglucosamine reductase	-1.2
lmo2168	lactoylglutathione lyase	-1.2
lmo1329	riboflavin biosynthesis protein RibF	-1.2
lmo2597	50S ribosomal protein L13	-1.2
lmo0966	hypothetical protein	-1.2
lmo2072	AT-rich DNA-binding protein	-1.2
lmo0970	enoyl-[acyl-carrier protein] reductase I	-1.2
lmo0574	6-phospho-beta-glucosidase gmuD	-1.2
lmo0130	hypothetical protein	-1.2
lmo2506	cell division transport system permease	-1.2
lmo1002	phosphocarrier protein HPr	-1.2
lmo1617	hypothetical protein	-1.2
lmo1734	glutamate synthase subunit large	-1.2
lmo0198	UDP-N-acetylglucosamine diphosphorylase/glucosamine-1-phosphate N-acetyltransferase	-1.2
lmo0268	phosphoglycerate mutase	-1.2
lmo0799	hypothetical protein	-1.2
lmo0695	hypothetical protein	-1.1
lmo0221	type III pantothenate kinase	-1.1
lmo2522	hypothetical protein	-1.1
lmo2832	glycerate kinase	-1.1
lmo1357	acetyl-CoA carboxylase	-1.1
lmo2693	thymidylate kinase	-1.1
lmo2389	hypothetical protein	-1.1
lmo2430	iron complex transport system permease	-1.1
lmo1891	recombination protein U	-1.1
lmo1065	hypothetical protein	-1.1
lmo0611	FMN-dependent NADH-azoreductase 1	-1.1
lmo0513	hypothetical protein	-1.1
lmo0135	peptide/nickel transport system substrate-binding protein	-1.1
lmo1234	excinuclease ABC subunit C	-1.1
lmo0297	transcriptional antiterminator	-1.1
lmo1246	ATP-dependent RNA helicase dbpA	-1.1
lmo0846	hypothetical protein	-1.1
lmo1903	bacteriocin transport accessory protein	-1.0
lmo2148	hypothetical protein	-1.0
lmo1294	tRNA delta(2)-isopentenylpyrophosphate transferase	-1.0

lmo0672	hypothetical protein	-1.0
lmo1323	hypothetical protein	-1.0
lmo0238	serine O-acetyltransferase	-1.0
lmo1848	manganese transport system membrane protein mntC	-1.0
lmo0646	hypothetical protein	-1.0
lmo2176	hypothetical protein	-1.0
lmo0765	hypothetical protein	-1.0
lmo2664	L-iditol 2-dehydrogenase	1.0
lmo1723	hypothetical protein	1.0
lmo2554	glycosyl transferase family protein	1.0
lmo1649	hypothetical protein	1.0
lmo0234	hypothetical protein	1.0
lmo1501	hypothetical protein	1.0
lmo2547	homoserine dehydrogenase	1.0
lmo0829	pyruvate:ferredoxin oxidoreductase	1.0
lmo0732	internalin	1.0
lmo0984	hypothetical protein	1.0
lmo0655	serine/threonine protein phosphatase 1	1.1
lmo1643	hypothetical protein	1.1
lmo1035	hypothetical protein	1.1
lmo1068	hypothetical protein	1.1
lmo2637	pheromone lipoprotein	1.1
lmo2105	ferrous iron transporter B	1.1
lmo0212	acetyltransferase	1.1
lmo1967	hypothetical protein	1.1
lmo0235	2-C-methyl-D-erythritol 4-phosphate cytidylyltransferase	1.1
lmo0289	hypothetical protein	1.1
lmo0529	N-acetylglucosaminyltransferase	1.1
lmo0752	hypothetical protein	1.1
lmo0104	hypothetical protein	1.1
lmo2331	hypothetical protein	1.1
lmo1712	multidrug resistance protein	1.1
lmo1173	sensor histidine kinase	1.1
lmo1637	ABC-2 type transport system permease	1.2
lmo0236	YgbB family protein	1.2
lmo2719	tRNA-adenosine deaminase	1.2
lmo2553	hypothetical protein	1.2
lmo0975	ribose 5-phosphate isomerase A	1.2
lmo0274	hypothetical protein	1.2
lmo0610	internalin	1.2
lmo1261	hypothetical protein	1.2
lmo0531	hypothetical protein	1.2
lmo0625	hypothetical protein	1.2

lmo1433	glutathione reductase	1.2
lmo0593	formate/nitrite transporter	1.2
lmo1966	hypothetical protein	1.3
lmo0181	multiple sugar transport system substrate-binding protein	1.3
lmo2132	hypothetical protein	1.3
lmo0584	hypothetical protein	1.3
lmo2661	ribulose-phosphate 3-epimerase	1.3
lmo2444	hypothetical protein	1.3
lmo2069	chaperonin GroS	1.3
	hypothetical protein (LMRG_01512)	1.3
lmo2409	hypothetical protein	1.3
lmo0534	hypothetical protein	1.3
lmo0443	hypothetical protein	1.3
lmo0047	hypothetical protein	1.4
lmo0037	agmatine/putrescine antiporter	1.4
lmo0049	hypothetical protein	1.4
lmo2733	hypothetical protein	1.4
lmo2446	hypothetical protein	1.4
	hypothetical protein (LMRG_02892)	1.4
lmo2439	hypothetical protein	1.5
lmo2716	ABC transporter CydDC cysteine exporter CydD	1.5
lmo1138	Clp protease	1.5
lmo0231	ATP:guanido phosphotransferase	1.5
lmo0321	hypothetical protein	1.5
lmo0955	hypothetical protein	1.5
lmo2083	hypothetical protein	1.5
lmo2673	universal stress protein	1.6
lmo2157	hypothetical protein	1.6
lmo2231	hypothetical protein	1.6
lmo0960	hypothetical protein	1.7
lmo0994	hypothetical protein	1.7
lmo0491	3-dehydroquinate dehydratase type I	1.7
lmo0263	internalin C2	1.7
lmo2246	hypothetical protein	1.7
lmo1200	precorrin-6x reductase	1.8
lmo0515	universal stress protein	1.8
lmo0229	CtsR family transcriptional regulator	1.8
lmo2485	PspC domain-containing protein	1.8
lmo2484	membrane protein	1.8
lmo1444	foldase PrsA	1.8
lmo1750	hypothetical protein	1.9
lmo1198	cobalamin biosynthesis protein CbiG	1.9
lmo0954	hypothetical protein	1.9

lmo0751	hypothetical protein	1.9
lmo1308	hypothetical protein	1.9
lmo0061	DNA segregation ATPase FtsK/SpoIIIE	1.9
lmo0354	long-chain fatty acid CoA ligase (AMP-binding)	1.9
lmo1137	hypothetical protein	1.9
lmo1066	myo-inositol-1(or 4)-monophosphatase	1.9
lmo0554	hypothetical protein	1.9
lmo0997	ATP-dependent Clp protease ATP-binding subunit ClpE	1.9
lmo2387	hypothetical protein	2.0
lmo0459	hypothetical protein	2.0
lmo2156	hypothetical protein	2.0
lmo2085	peptidoglycan binding protein	2.0
lmo0881	hypothetical protein	2.1
lmo2445	internalin	2.1
lmo2718	cytochrome bd-I oxidase subunit I	2.1
lmo0265	succinyl-diaminopimelate desuccinylase	2.1
lmo0814	enoyl-(acyl carrier protein) reductase	2.2
lmo0133	hypothetical protein	2.2
	hypothetical protein (LMRG_01259)	2.2
	hypothetical protein (LMRG_02074)	2.2
lmo2362	glutamate/gamma-aminobutyrate antiporter	2.2
lmo0971	D-alanine transfer protein	2.3
lmo2642	serine/threonine protein phosphatase	2.3
lmo2804	hypothetical protein	2.4
lmo0961	protease	2.5
lmo0200	listeriolysin regulatory protein	2.6
lmo0972	D-alanine--poly(phosphoribitol) ligase subunit 2	2.6
lmo1651	ABC transporter	2.6
lmo1034	glycerol kinase	2.7
lmo1652	ABC transporter	2.8
lmo1033	transketolase	2.8
lmo1032	transketolase	2.9
lmo2434	glutamate decarboxylase	3.0
lmo1650	hypothetical protein	3.0
lmo0060	YukC protein	3.0
lmo2467	chitin-binding protein	3.1
lmo1506	hypothetical protein	3.2
lmo1309	hypothetical protein	3.2
lmo1310	hypothetical protein	3.2
lmo0057	hypothetical protein	3.2
lmo0279	anaerobic ribonucleoside-triphosphate reductase	3.3
lmo1505	hypothetical protein	3.5
lmo1120	hypothetical protein	3.5

lmo1121	hypothetical protein	3.6
lmo2170	enoyl-(acyl carrier protein) reductase	3.7
	hypothetical protein (LMRG_00561)	3.7
lmo0307	hypothetical protein	3.8
	hypothetical protein (LMRG_02863)	3.8
lmo1406	formate acetyltransferase	3.8
lmo0912	nitrite transporter NirC	3.9
lmo0788	hypothetical protein	3.9
lmo2686	hypothetical protein	3.9
lmo2238	hypothetical protein	4.0
	csn2 family CRISPR-associated protein	4.0
	hypothetical protein (LMRG_02864)	4.1
lmo1122	hypothetical protein	4.1
lmo1257	hypothetical protein	4.2
lmo1123	hypothetical protein	4.2
lmo1124	hypothetical protein	4.2
lmo2447	hypothetical protein	4.2
lmo2067	choloylglycine hydrolase (bsh)	4.2
lmo2594	hypothetical protein	4.3
lmo1407	pyruvate formate-lyase activating enzyme	4.3
lmo1312	hypothetical protein	4.3
lmo0412	hypothetical protein	4.4
	CRISPR-associated protein cas1	4.4
	CRISPR-associated protein	4.4
lmo1917	formate acetyltransferase	4.6
lmo2173	hypothetical protein	5.0
	hypothetical protein (LMRG_02908)	5.2
lmo2171	major facilitator family transporter	5.4
lmo2236	shikimate 5-dehydrogenase	5.5
lmo2410	hypothetical protein	6.2
lmo2172	propionate CoA-transferase	6.2
lmo2237	hypothetical protein	6.2
lmo0355	fumarate reductase flavoprotein subunit	6.7
lmo2235	NADH oxidase	7.3
lmo2234	hypothetical protein	7.6
lmo1634	bifunctional acetaldehyde-CoA/alcohol dehydrogenase	10.6

Table S3.4. Strains used in this study

Strain number	Genotype	Source
L. monocytogenes **(Derivatives of strain 10403S)**		

TNHL261	WT 10403s	This study
TNHL22	Δ*pdeA* Δ*pgpH* (ΔPDE)	Huynh *et al*. 2015
TNHL970	*ΔaroE*	Gift from JD Sauer
TNHL971	*ΔaroED*	Gift from JD Sauer
TNHL972	*aroA::tn*	Gift from JD Sauer
TNHL973	*aroE::tn*	Gift from JD Sauer
TNHL974	*aroB::tn*	Gift from JD Sauer

Chapter 4. Concluding remarks and future directions

CONCLUDING REMARKS

C-di-AMP is a critical component of *L. monocytogenes'* hallmark adaptability, and is essential for both growth in rich medium and full virulence, though many of its functions remain unknown. The ΔPDE mutant accumulates high levels of c-di-AMP, and has a number of defects whose underlying mechanisms can be studied to elucidate new functions of c-di-AMP. In this dissertation, I utilized the ΔPDE mutant to identify GSH metabolism and PrfA activation as newly discovered functions regulated by c-di-AMP. This work provides foundational knowledge for how c-di-AMP regulates both *L. monocytogenes* virulence and metabolism of the PrfA cofactor GSH. Major areas of focus for follow up studies, and proposed initial experimental steps are outlined below.

FUTURE DIRECTIONS

C-di-AMP homeostasis during *L. monocytogenes* infection

A major theme of the work presented in this thesis is the phenotypic consequences of artificially elevated c-di-AMP levels. In Chapters 2 and 3, I found that c-di-AMP accumulation impairs virulence-program activation, disrupts glutathione metabolism, and attenuates virulence in PrfA dependent and independent ways. However, c-di-AMP is also essential for full *L. monocytogenes* virulence[37]. This raises the question: How is c-di-AMP homeostasis maintained during virulence program activation and infection to both maintain essential functions and avoid detrimental effects? Studies which address this question will contribute to a better understanding of *L. monocytogenes* pathogenesis, and importantly, to a more complete picture of the biological functions of c-di-AMP. A first step to characterizing c-di-AMP homeostasis in the context of virulence is to quantify c-di-AMP levels upon virulence program activation and during host-cell infection. To do this, LC/MS/MS could be used to measure cytosolic c-di-AMP in

WT cultures grown in LSM and LSM + 10mM GSH. To assess secreted c-di-AMP during virulence-program activation, LC/MS/MS could also be performed on culture supernatants as well. As GSH is required for full activation of PrfA, and high levels of c-di-AMP reduce GSH availability, it is reasonable to hypothesize that under PrfA activating conditions, cytosolic c-di-AMP levels decrease to allow for increased GSH uptake and synthesis. However, secreted c-di-AMP is a potent activator of type I IFN response[4]. Following intravenous (IV) infection with *L. monocytogenes*, type I IFN results in rapid apoptosis and depletion of splenic lymphocytes, a phenomenon which promotes *L. monocytogenes* infection[193]. Conversely, type I IFN does not promote susceptibility to *L. monocytogenes* in an oral model of infection[194]. Therefore, c-di-AMP synthesis and secretion may be differentially regulated depending on stage of infection or host-cell niche. This possibility could be tested by utilizing LC/MS/MS to measure cytosolic and secreted c-di-AMP levels under culture conditions mimicking different host niches, or in different host cell-types infected with *Listeria* ex-vivo. Following baseline determination of how c-di-AMP levels fluctuate during PrfA activation and host-cell infection, future work will be aimed at determining the environmental signals to which c-di-AMP metabolizing proteins respond to maintain appropriate c-di-AMP levels during infection.

Saprophyte to host transition

In addition to modulating host-immune response during infection, c-di-AMP may mediate metabolic changes that occur when *L. monocytogenes* transitions between saprophyte and pathogen. Plant-derived sugars such as cellobiose can be taken up by phosphoenolpyruvate:carbohydrate phosphotransferase systems (PTS) and have been shown to suppress virulence gene activation in *L. monocytogenes*[195]. I found that genes encoding predicted cellobiose-specific PTS components (*lmo2683-2685*, *lmo2708*) were significantly upregulated in ΔPDE relative to WT grown in LSM (**Table S2.1**). It is tempting to speculate that naturally, very high levels of c-di-AMP mediate a saprophytic lifestyle, which could involve

uptake of plant-derived sugars in soil, while suppressing virulence-program activation. While *lmo2683-2685* and *lmo2708* are predicted cellobiose transporters, and cellobiose is not present in LSM, it is possible that these transporters have additional functions which affect PrfA activity. An initial experiment to address this would be to delete *lmo2683-2685* and *lmo2708* in ΔPDE, and test whether PrfA activity is affected in these mutants.

Mechanisms of c-di-AMP toxicity in bacterial virulence

In Chapter 2, I demonstrated that c-di-AMP accumulation impairs *L. monocytogenes* virulence, and that ΔPDE virulence could be modestly restored by PrfA* (**Fig. 2.6**). indicating that PrfA-independent factor(s) have a significant influence on ΔPDE survival in-vivo. Upon assessing additional consequences of GSH deficiency, I found that ΔPDE is more sensitive to H_2O_2 than WT, pointing to oxidative stress as an additional factor which renders ΔPDE attenuated in-vivo (**Fig. 2.7**). While H_2O_2 sensitivity assays indicated *gshF* deletion causes statistically equivalent H_2O_2 sensitivity in WT and ΔPDE, plaque data demonstrates that in the absence of *gshF,* plaque-size is more reduced in ΔPDE than in WT (**Fig. 2.4C**). This leads to the hypothesis that reduced GSH uptake contributes to impaired ΔPDE ex-vivo virulence. An immediate way to test this hypothesis would be to treat L2 cells with buthionine sulfoximine (BSO), which will deplete L2 intracellular GSH levels[196], prior to infection with WT, ΔPDE, Δ*gshF*, and ΔPDEΔ*gshF*. Δ*gshF* phenocopy of ΔPDEΔ*gshF* in BSO-treated cells will strongly support the hypothesis that impaired GSH uptake impairs ex-vivo virulence in ΔPDE.

Another unexplained finding in Chapter 2 is that PrfA* exhibited responsiveness to GSH in the ΔPDE background (Fig. 2.2A). While PrfA* responsiveness to GSH has never been reported, PrfA possesses four cysteine residues which could potentially be glutathionylated[105]. Previous studies have found that the PrfA$(C/A)_4$ mutant, in which all four cysteines are mutated to alanine, is very modestly attenuated for virulence in a mouse model[105]. While this may not be significant in the WT background, this phenotype may be more pronounced in ΔPDE, in which

GSH synthesis is diminished but not fully abolished. To test the hypothesis that decreased glutathionylation of PrfA causes PrfA* to be GSH responsive in ΔPDE, native PrfA can be replaced with PrfA* $(C/A)_4$ in the ΔPDE background, followed by assessment of PrfA activity via $P_{actA:}$::RFP reporter assay. If glutathionylation does in fact cause PrfA* to be GSH responsive in ΔPDE, $P_{actA:}$::RFP reporter activity in ΔPDE PrfA* $(C/4)_A$ is expected to be entirely unresponsive to GSH.

In addition to impaired GSH metabolism, ΔPDE is impaired for cell-wall homeostasis[64]. One hypothesis is that sensitivity to cell-wall targeting agents renders ΔPDE sensitive to host-cell defenses such as lysozyme, which target the bacterial cell wall. This would be difficult to directly test, as the underlying mechanism of lysozyme sensitivity in ΔPDE is not known. However, a previous study found that lysozyme-M deficient mice infected with the nonpathogenic, lysozyme sensitive bacteria *Micrococcus luteus* developed severely inflamed skin lesions due to reduced lysozyme inactivation of peptidoglycan[197]. If ΔPDE CFU counts in the liver and spleen are rescued to WT levels in a lysozyme-M deficient mouse, it will suggest that lysozyme sensitivity in ΔPDE contributes to attenuated virulence.

Forward genetic screen to identify underlying mechanisms of attenuated virulence in ΔPDE.

Given that c-di-AMP has many molecular targets in bacterial and host cells, we can anticipate that c-di-AMP accumulation attenuates virulence via multiple mechanisms. In addition to the targeted approaches described above, future studies can employ a forward genetic screen to identify suppressor mutations that rescue the ΔPDE strain for L2 plaque formation defect. I previously mutagenized ΔPDE pLIV2::*dacA*, which overexpresses a second copy of *dacA* and has a greater plaquing defect than ΔPDE alone, by treating it with ethyl methylsulfonate (EMS) for three minutes. While this treatment reliably generated 1-3 mutations within the genome, it appeared to be insufficient to yield suppressor mutations outside of the

dacA gene. Therefore, the screen can be repeated by treating this strain with EMS for longer. However, this approach may increase mutations/genome such that discerning what mutation rescues a single suppressor mutant will be challenging. Alternatively, a CRISPRi or CRISPRtOE approach[198,199] can also be performed to knock down or overexpress genes in ΔPDE respectively.

Elucidating GSH degradation machinery in *L. monocytogenes*

The aim of Chapter 3 was to identify components required for GSH breakdown into essential cysteine in *L. monocytogenes*. Initially, a transposon mutagenesis screen was employed to determine genes essential for utilization of 10mM GSH as a cysteine source in LSM. However, experimental challenges led us to question the validity of the screen hits. First, cultures used in this experiment were grown into stationary phase, which could have caused additional bottlenecks to select against insertions in genes unrelated to GSH utilization, or to select against GSH degradation genes in both culture conditions. To correct for this, a future TN-seq experiment can be performed in cultures grown to mid-logarithmic phase in LSM containing 0.2mM GSH in place of cysteine. Lowering supplied GSH concentrations and growing cultures for a shorter time will provide more stringent selective pressure against insertions in genes essential for breakdown of GSH to essential cysteine. In addition, identification of low-affinity GSH transporters could be carried out by performing a similar TN-seq experiment in the Δ*oppDF* background, with 10mM GSH supplied as a cysteine source. Insertions in low-affinity GSH transporters would be specifically selected against in the absence of OppDF at high GSH concentrations. Importantly, the effect of c-di-AMP on novel components of GSH uptake and degradation identified from these screens will aid in the understanding of how c-di-AMP regulates GSH metabolism and virulence-program activation.

Appendix A: C-di-AMP homeostasis under different growth and stress conditions.

BACKGROUND AND INTRODUCTION

Bacteria adapt to their surroundings by responding to environmental signals. To accomplish this, bacteria often utilize small nucleotide signaling molecules called second messengers to illicit a prompt physiological response to external conditions[200]. C-di-AMP is a widespread second messenger produced by many bacteria and some archaea[5]. It is synthesized by deadenylate cyclase (DAC) proteins, and degraded by phosphodiesterase (PDE) proteins. C-di-AMP is essential in rich medium, particularly for bacteria in the Firmicutes phylum[1], and this essentiality has been well-studied. Nonetheless, uncontrolled C-di-AMP accumulation can have detrimental effects on growth and stress-response in c-di-AMP producing bacteria[135,136]. In fact, toxicity of uncontrolled c-di-AMP accumulation is more widespread than c-di-AMP essentiality, and occurs in many bacteria for which c-di-AMP is dispensable[136,137]. Therefore, maintaining c-di-AMP homeostasis is of critical importance for bacteria that produce it. However, the mechanisms by which c-di-AMP levels are maintained in the cell, and ways in which c-di-AMP modifies cellular pathways to maintain optimal growth, are ill defined. The goal of the work presented here was to identify conditions under which c-di-AMP levels change significantly in WT *L. monocytogenes*, and to then systematically test mutants lacking c-di-AMP metabolic proteins for the same response. This work would have identified novel mechanisms by which c-di-AMP homeostasis is controlled in *L. monocytogenes.* Unfortunately, inconsistencies in LC/MS/MS measurements of intracellular c-di-AMP led to this work remaining largely incomplete. However, the data presented here could provide a useful basis for follow up studies on the regulation of DacA, PdeA, and PgpH in *L. monocytogenes*.

RESULTS AND DISCUSSION

C-di-AMP levels during growth in rich and defined medium

Initial work on this project was aimed at identifying stress conditions under which c-di-AMP levels change in WT *L. monocytogenes* relative to growth in standard BHI or LSM, and then systematically testing which c-di-AMP metabolic protein-DacA, PdeA, or PgpH-was responsible for sensing altered conditions and eliciting changes in nucleotide levels. Interestingly, in media alone, WT c-di-AMP levels appeared to be higher in LSM than in BHI (Fig. A1A-B). Curious if this was mediated by PdeA, PgpH, or DacA activity, c-di-AMP levels in BHI and LSM were measured for mutants with just one functional PDE, or conditionally depleted for *dacA.* Data in BHI was in agreement with previous findings that the ΔPDE mutant accumulates ~4-5x more c-di-AMP in BHI than WT and that PdeA and PgpH are both sufficient alone to restore c-di-AMP levels back to baseline[13]. Upon repeating additional experiments in LSM, I found that WT, and mutants with just one functional PDE, produced similar amounts of c-di-AMP in LSM and BHI (Fig. A1A-B). The ΔPDE mutant, however, produced ~10x more c-di-AMP compared to WT in LSM (Fig. A1A-B). These data suggest that DacA is more active in LSM, causing higher accumulation of c-d-AMP than in BHI when PDE activity is absent. Additionally, all results presented in the remainder of this section are from samples grown in LSM. This decision was made in the hopes that fewer molecular components were present in LSM than in BHI which could interfere with LC/MS/MS sensitivity.

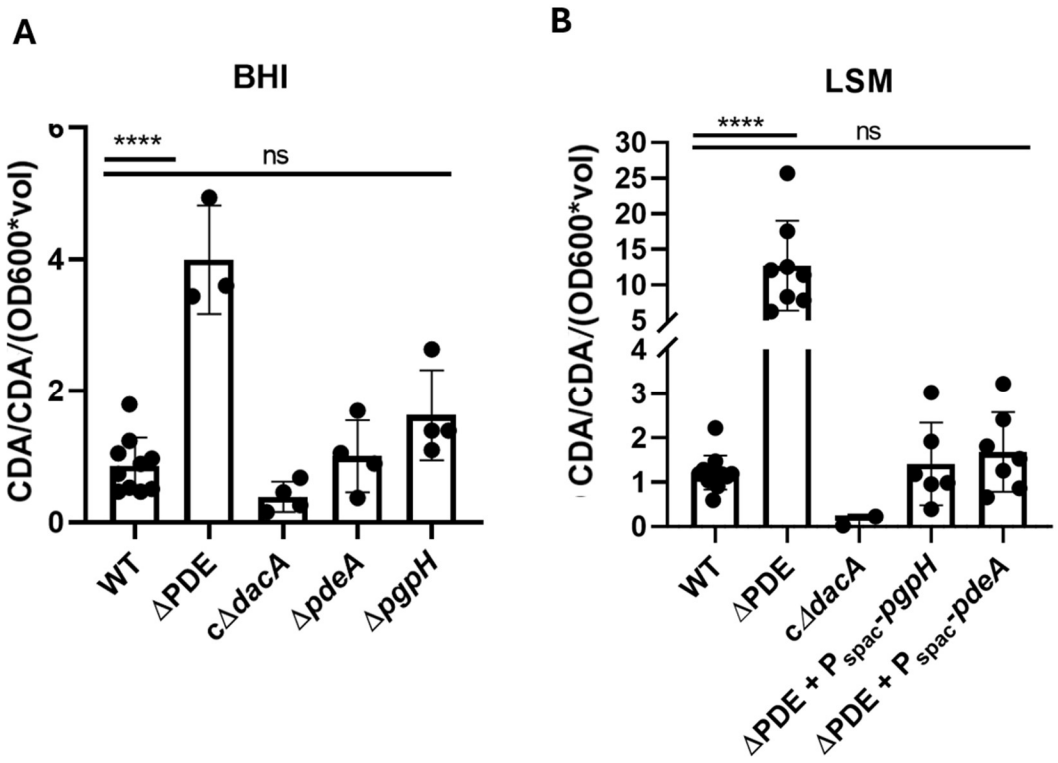

Figure A1. Intracellular c-di-AMP levels in BHI (A) and LSM (B). Methanol-extracted c-di-AMP was quantified via LC/MS/MS and normalized to the internal standard $C^{13}N^{15}$-c-di-AMP (CDA*). CDA/CDA* ratios were normalized to OD_{600} and volume of collected culture. Error bars show standard deviations. Statistical analyses were performed by two-way ANOVA with multiple comparisons for the indicated pairs: ns, non-significant; *, P < 0.05; **, P < 0.01; ****, P < 0.0001

C-di-AMP levels at different OD_{600} Values

Knowing that c-di-AMP regulates turgor pressure, which changes over the course of bacterial cell-division[47], I hypothesized that c-di-AMP levels may be dynamic depending on growth phase. To test this hypothesis, I re-analyzed c-di-AMP levels measured in LSM only by plotting them against exact OD_{600} at the time of culture collection. As expected, c-di-AMP levels were ~10-fold higher in ΔPDE than in WT across OD_{600} levels, whereas presence of either PdeA or PgpH was sufficient to maintain WT c-di-AMP levels. cΔ*dacA* also had the lowest c-di-AMP levels of all the strains, as was expected (Fig. A2A)

Next, Pearson correlation analysis was used to test for a linear relationship between OD_{600} and c-di-AMP levels and a linear regression line-of-best-fit was overlaid onto individual scatterplots (Fig. A2B-F). While fitted regression lines appeared to have a positive slope for WT, ΔPDE + P_{spac}-*pgpH*, and cΔ*dacA*, and a negative slope for ΔPDE, calculated Pearson R was only significant for WT (Fig. A2B-G). While this data indicates that c-di-AMP levels increase over the course of growth, there are several limitations that likely affected the results. First, sampling was uneven across strains, with WT having at least ~2x the number of replicates of any other strain (Figure A2G). The statistical significance of the Pearson's R calculated for WT is likely due to the higher number of samples compared to other strains. However, increasing replicates for other strains may reveal exciting relationships between OD_{600} and c-di-AMP levels that were not evident from this study. Additionally, OD_{600} levels at which samples were collected clustered largely between 0.5 and 1, which is considered mid-exponential phase for *L. monocytogenes*. Most of these samples were collected as media-only controls for stress-exposed samples, so growth to a constant OD_{600} was employed for consistency. To truly determine if c-di-AMP levels correlate with growth phase, additional sampling would have to be performed for cultures during lag-phase, as well as stationary phase.

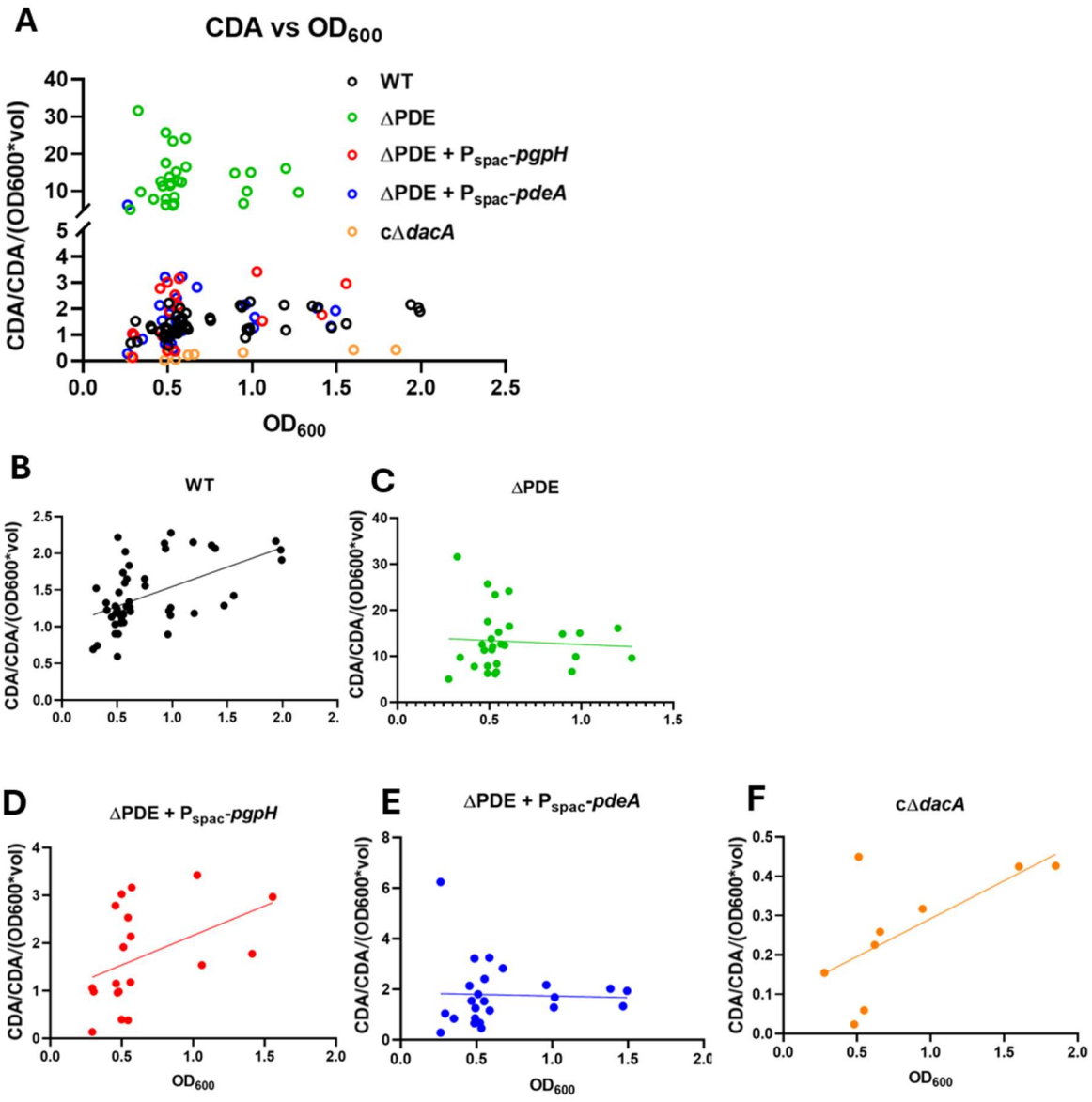

G

Pearson R	WT	ΔPDE	ΔPDE + P_{spac}-*pgpH*	ΔPDE + P_{spac}-*pdeA*	cΔ*dacA*
r	0.39	-0.07	0.45	-0.01	0.37
R squared	0.15	0.01	0.20	4.9E-05	0.14
P (two-tailed)	0.01	0.72	0.10	0.98	0.41
P value summary	*	ns	ns	ns	ns
Number of samples (n)	40	26	15	19	7

Figure A2: Normalized CDA vs. OD_{600}. Normalized CDA vs OD_{600} plotted for all strains (A), and for each strain individually (B-F). Linear regression analysis

was used to plot lines-of-best-fit. Pearson correlation analysis between OD_{600} and normalized CDA (G) was performed for each strain individually.

C-di-AMP levels following exposure to osmotic and cell-wall stress

C-di-AMP accumulation in ΔPDE leads to sensitivity to the cell-wall targeting β-lactam, cefuroxime[13], as well as osmotic stress induced by 4% NaCl[23] (Fig. A3A). However, how c-di-AMP levels naturally change in response to cefuroxime and NaCl stress is not known. I hypothesized that upon exposure to 10x the WT minimum inhibitory concentration (MIC) of cefuroxime, or to 4% NaCl, WT c-di-AMP levels would decrease to avoid the toxic effects on β-lactam and NaCl tolerance. I further hypothesized that this observation would be disrupted by removing function of one or both PDEs in *L. monocytogenes*. Because c-di-AMP levels were barely detectable in LSM via LC/MS/MS, cΔ*dacA* was excluded from this experiment. Before quantifying intracellular c-di-AMP following cefuroxime and NaCl exposure, it was first verified that cefuroxime and NaCl exposure did not significantly impair bacterial growth. To do this, CFU was assessed following 30 minutes of exposure to either 4% NaCl or 10x the MIC of cefuroxime (WT MIC in LSM=128μg/mL) for both WT and ΔPDE at mid-log phase (Fig. A3B-C). To ensure cefuroxime exposure conditions was sufficient to elicit a biological response in WT, qPCR on *lhrC*, the cell-wall stress responsive sRNA[201], was performed on both WT and ΔPDE grown to mid-log phase and exposed to 1280μg/mL cefuroxime as done before. *lhrC* expression was robustly induced in both WT and ΔPDE upon cefuroxime exposure (Fig A3D), indicating that 30-minutes of exposure to 1280μg/mL cefuroxime after mid-log phase was reached both induced a biological response and did not diminish growth.

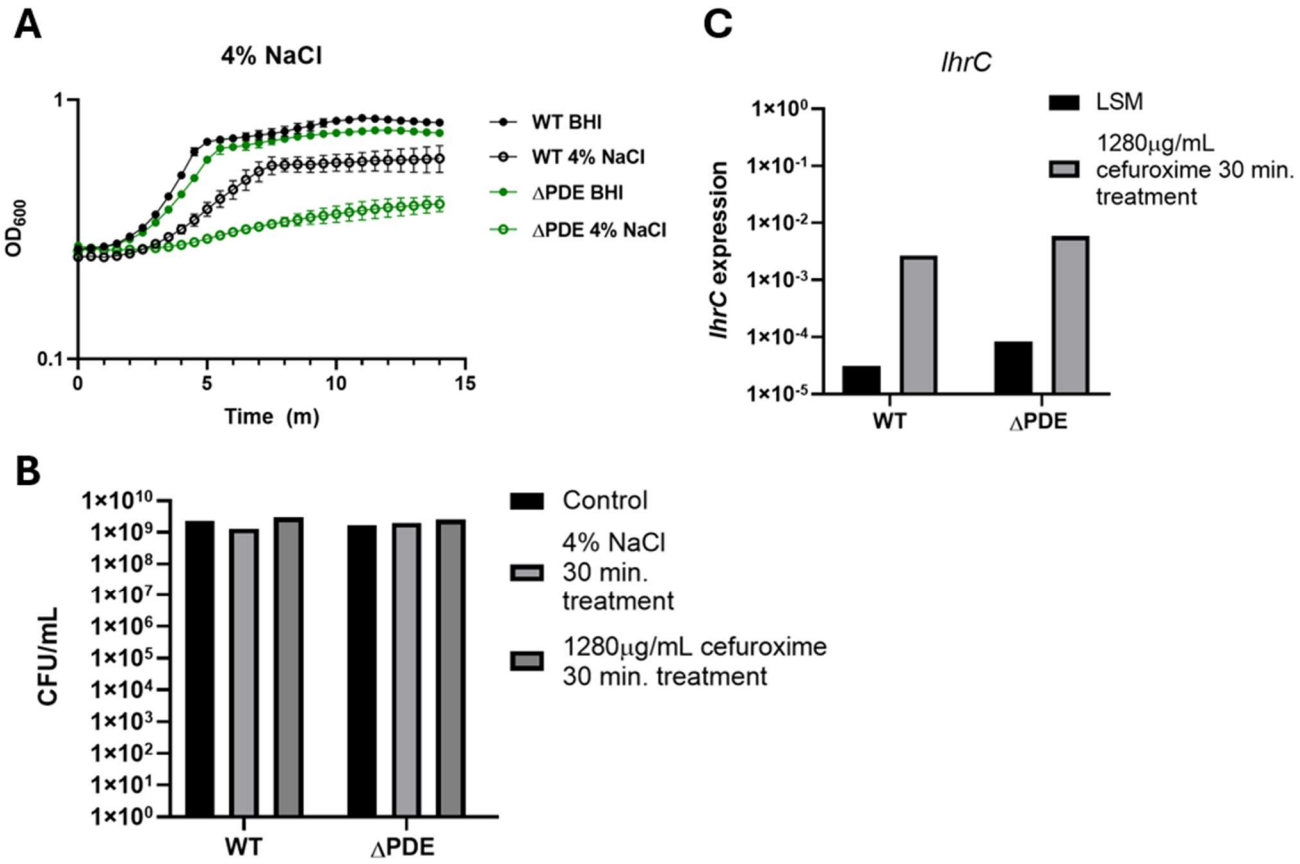

Figure A3. Growth and transcriptional response following exposure to NaCl and cefuroxime stress. A. 14h growth curve of WT and ΔPDE grown in BHI with and without indicated concentrations of NaCl. Data represents the average of three separate experiments. Error bars represent standard-deviations. B. CFU/mL in LSM only control, cultures exposed to either 4% NaCl or 1280μg/mL cefuroxime in LSM after reaching mid-logarithmic phase. C. qRT-PCR performed for *lhrC* in WT and ΔPDE strains in LSM only control, or cefuroxime-treated condition described in B. Experiments in B and C were performed once.

Following exposure to 4% NaCl, average c-di-AMP levels in all strains decreased. However, this difference was only statistically significant in the ΔPDE strain (Fig. A4A). Nonetheless, these results suggest that either increased DacA activity, or increased c-di-AMP export occurs in response to osmotic stress. It is tempting to speculate that increasing sample size would lead to significantly different c-di-AMP levels following NaCl exposure in WT, as well as additional mutants. Additionally, future experiments could attempt increasing percentage of NaCl used for exposure, to test if this would further suppress intracellular c-di-AMP levels.

WT c-di-AMP levels did change following exposure to cefuroxime. Interestingly, c-di-AMP significantly increased in the ΔPDE mutant following cefuroxime exposure, and the same phenomenon occurred to a lesser extent in a strain containing only a functional copy of PgpH, though this was not statistically significant (Fig. A4B). Similar to WT, c-di-AMP levels did not change in response to cefuroxime stress.

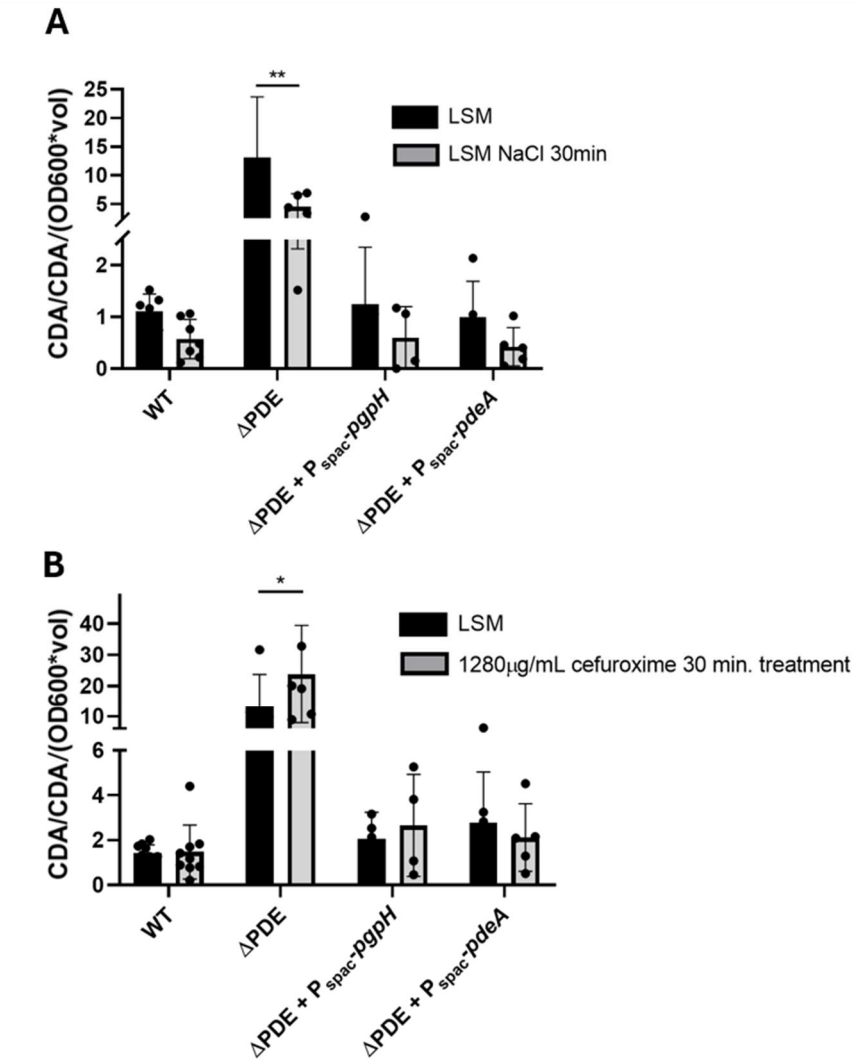

Figure A4. C-di-AMP levels in response to NaCl and cefuroxime stress. Normalized c-di-AMP levels in the indicated strains grown to mid-log phase and exposed to 4% NaCl (A), or 1280μg/mL cefuroxime (B) for 30 minutes. Error bars show standard deviations. Statistical analyses were performed by two-way ANOVA with multiple comparisons for the indicated pairs: ns, non-significant; *, P < 0.05; **, P < 0.01; ****, P < 0.0001.

Initially, it seemed puzzling that c-di-AMP does not increase following cefuroxime exposure, even though its accumulation causes cefuroxime sensitivity. However, in LSM, levels of c-di-AMP in ΔPDE strain are ~10x higher than in WT. It is probable that there is a threshold c-di-AMP concentration, that exists somewhere between those of WT and ΔPDE, at which cefuroxime sensitivity is induced. Basal, or even slightly elevated levels of c-di-AMP in WT may in fact be beneficial to resistance to cefuroxime sensitivity. Indeed, a previous study found that deletion of PgpH led to increased cefuroxime resistance in *L. monocytogenes*[71]

Overall, the results from this work demonstrate that c-di-AMP levels in *L. monocytogenes* are dynamic depending on media composition, growth phase, and stress conditions. However, to attain significant and reproducible results, sample size must be increased. Additional, stress conditions may need to be modified to induce c-di-AMP changes of greater magnitude.

MATERIALS AND METHODS

Strains and culture conditions

L. monocytogenes strains are listed in **Table SA1**. Listeria Synthetic Medium (LSM) was prepared based on published recipe[54]. Over-expression of genes was accomplished using the integrative plasmid pPL2[147]. For all experiments related to broth cultures, *L. monocytogenes* was grown at 37°C with shaking and without antibiotics. For glycerol stocks and maintenance, strains carrying derivatives of the integrative plasmid pPL2 were grown in Brain Heart Infusion broth with 200µg/mL streptomycin and 10µg/mL chloramphenicol.

RT-qPCR for *L. monocytogenes* genes in broth

For quantification of *lhrC* expression, *L. monocytogenes* cultures were grown in LSM or LSM to OD_{600} ~0.5. RNA was extracted, treated with Turbo DNase and converted to cDNA using iScript cDNA synthesis kit (BioRad). Gene expression was quantified using iTaq Universal

SYBR Green (BioRad) with primers specific to each target, with *rplD* as the control housekeeping gene. Sequence of RT-qPCR *lhrC* forward (TNH303) and reverse (TNH304) primers are, respectively, as follows: ATAAGCTAACAACAAGCAAAACATTT, TAAAAAACCAGTGTGGAAAAAGGGAG.

Quantification of c-di-AMP by LC/MS/MS

Quantification of c-di-AMP from *L. monocytogenes* cultures was carried out as described previously[13] In short, *L. monocytogenes* strains were grown in either BHI or LSM to mid-log phase (OD600, ~0.5). Cell pellets from 0.5-ml cultures were resuspended in 50 µl of 0.25 µM $C^{13}N^{15}$-c-di-AMP, which is an internal standard, and lysed via sonication. Methanol extracted fractions were pooled, dried in a SpeedVac, and resuspended in 50 µl of MilliQ H_2O. Liquid chromatography-tandem mass spectrometry (LC-MS/MS) was performed on an Agilent 6460 Triple Quad LC-MS/MS with a 1260 HPLC. Chromatographic separation was done with an analytical Synergi 4u Hydro-RP 80A column (50 by 2 mm, 4 µm; Phenomenex). Mass transitions for c-di-AMP quantification are previously published. Peak areas of the c-di-AMP transition were divided by that of C13N15-c-di-AMP (+689/146) in the same sample.

SUPPLEMENTARY MATERIAL

Table SA1: Strains used in this study

Strain number	Genotype	Source
***L. monocytogenes* (Derivatives of strain 10403S)**		
TNHL261	WT 10403s	This study
TNHL22	Δ*pdeA* Δ*pgpH* (ΔPDE)	Huynh *et al*. 2015
TNHL261	cΔdacA	This study
TNHL12	ΔpdeA	This study
TNHL295	ΔpgpH	This study
TNHL27	ΔPDE + pPL2-Pspac-pdeA	This study
TNHL28	ΔPDE + pPL2-Pspac-pgpH	This study

Appendix B: Transcriptional response of WT, cΔ*dacA* and ΔPDE to cefuroxime stress.

BACKGROUND AND INTRODUCTION

Our lab has previously published that the ΔPDE strain, which accumulates ~4x more c-di-AMP than WT in BHI, and ~10x more c-di-AMP than WT in the defined medium LSM, is more susceptible than WT to the β-lactam cefuroxime[64]. While the ΔPDE mutant does have a number of cell-wall defects, such as decreased abundance of muropeptides, a thinner cell wall, and reduced total peptidoglycan, the exact mechanisms underlying cefuroxime sensitivity in ΔPDE remain unknown. We hypothesized that in ΔPDE, expression of genes important for cell-wall homeostasis and cefuroxime resistance would be differentially expressed compared to WT following cefuroxime stress. We further hypothesized that certain gene expression patterns in cΔ*dacA,* which is severely depleted for c-di-AMP, would be inverse to those in ΔPDE upon cefuroxime stress, as well as in media alone. Thus, the aim of the work presented in this appendix was driven by two main goals: 1) To identify differentially regulated genes in ΔPDE which contribute to cefuroxime sensitivity, and 2) to identify genes whose expression level could serve as a reporter of c-di-AMP levels, either in the presence of absence of cefuroxime stress.

RESULTS AND DISCUSSION

Biological duplicates of WT, ΔPDE, and cΔ*dacA* were grown to mid-log (OD_{600}=~0.5) phase in LSM. Upon reaching mid-log phase, cultures were split, and cefuroxime was added to one of the cultures to a final concentration of 1280µg/mL. Both cefuroxime treated and untreated controls were grown an additional 30 minutes before being harvested for RNA

extraction. The cDNA libraries were sequenced at the depth of 17 – 20 million reads, and had 852x-1042x mapped read coverage. Differential expression analysis was performed via EdgeR, and genes were considered significant if they exhibited >2-fold change relative to the control, and a P-value <0.05.

Differential gene expression was calculated for each strain exposed to cefuroxime, relative to WT in cefuroxime, and for each strain in LSM relative to WT in LSM (**Table SB1**). DEGs in ΔPDE grown in LSM relative to WT LSM are presented in **Table SB.1**. Additional differential gene expression analysis was performed for each strain following cefuroxime stress relative to itself in LSM (**Table SB2**).

In all comparisons with WT, both with and without cefuroxime stress, ΔPDE exhibited a similar transcriptional profile wherein A118 phage genes and the PrfA virulence regulon were downregulated, and PTS-system genes were upregulated. Interestingly, *lmo2683-2685*, which encode cellobiose-specific PTS system IIA, B, and C components, which were significantly upregulated in all comparisons of ΔPDE to WT, were the most highly significantly downregulated genes in all comparisons of c*ΔdacA* to WT. Thus, transcription of these genes could potentially serve as a useful indicator of c-di-AMP levels as an alternative to LC/MS/MS. However, given the complex involvement of PTS systems in *L. monocytogenes* in growth and virulence, and their regulation by multiple sigma factors[202], it is unlikely that these genes would serve as a reliable c-di-AMP reporter in variable growth conditions. It is interesting to note that in WT exposed to cefuroxime, compared to itself in LSM, PrfA regulon genes and phage genes were significantly downregulated. This is similar the transcriptional profile of ΔPDE in the absence of cell-wall stress. This finding suggests that cell-wall stress, induced by either cefuroxime, c-di-AMP accumulation, or both, causes downregulation of the *L. monocytogenes* PrfA regulon as well as A118 prophage genes. Whether the underlying mechanism is the same in WT and ΔPDE has yet to be determined.

While results from this experiment did not yield any differentially expressed genes of interest which could help explain ΔPDE cefuroxime sensitivity, further analyses of this dataset could still yield promising results. Upon discovering that the PrfA regulon was downregulated in ΔPDE, work aimed at characterizing cell-wall homeostasis in ΔPDE was deprioritized. Nonetheless, this dataset will hopefully serve as a useful reference for other researchers investigating the role of c-di-AMP in *L. monocytogenes* growth.

MATERIALS AND METHODS

L. monocytogenes cultures were grown to OD_{600} of ~ 0.5, and cultures were split. To one half of culture, filter-sterilized cefuroxime stock was added to a final concentration of 1280µg/mL. Both cultures were allowed to grow an additional 30 minutes and then harvested by mixing 1:1 with cold methanol and centrifugation. RNA was extracted using acidified phenol:chloroform at pH 5.2 as previously described[148]. Contaminated DNA was removed from extracted RNA using Turbo DNase (Thermo Scientific). RNA sequencing and read mapping was performed by MiGS Sequencing Center (Pittsburgh, PA). Reads were mapped to the *L. monocytogenes* 10403S genome (NCBI:txid393133). Differentially expressed gene (DEG) analysis was performed via EdgeR[149].

Table SB1: Significantly (P<0.05) differentially expressed genes (Fold-change >2) relative to WT in the indicated condition. Samples appended with “cef” were grown to mid-log phase in LSM, and then cefuroxime was added to culture to a concentration of 1280µg/mL for 30 minutes prior to harvest. Samples appended with “LSM” indicate paired, untreated control.

		Log2Fold change		
		vs WT cef		vs WT in LSM
EGD-E Gene ID	**Gene function**	**ΔPDE cef**	**cΔ*dacA* cef**	**cΔ*dacA* LSM**
lmo0001	chromosomal replication initiator protein DnaA		1.16	
lmo0019	hypothetical protein	1.60		
lmo0021	mannose-specific PTS system IIA component			1.15
lmo0022	mannose-specific PTS system IIB component	1.18		
lmo0024	mannose-specific PTS system IID component			
lmo0037	agmatine/putrescine antiporter		2.50	3.42
lmo0042	membrane-associated protein			-1.06

lmo0047	hypothetical protein			
lmo0052	DHH subfamily 1 protein	-9.75		
lmo0059	YukD protein			
lmo0072	hypothetical protein	1.22		
lmo0083	hypothetical protein		-1.09	
lmo0085	hypothetical protein		1.54	
lmo0087	hypothetical protein		1.05	1.40
lmo0088	ATP synthase subunit C	1.24		
lmo0095	hypothetical protein		-1.47	-1.10
lmo0096	mannose-specific PTS system IIAB component manL			
lmo0097	mannose-specific PTS system IIC component			-1.30
lmo0098	F-type H+-transporting ATPase subunit delta			-1.05
lmo0101	hypothetical protein		-2.07	-1.44
lmo0104	hypothetical protein			-1.17
lmo0105	chitinase			
lmo0107	ABC transporter		1.19	1.68
lmo0115	hypothetical protein		1.36	
lmo0116	hypothetical protein	-1.56		
lmo0117	prophage LambdaLm01, antigen B	-1.25		
lmo0118	antigen A	-1.89	1.15	
lmo0119	hypothetical protein	-1.54	1.40	1.46
lmo0120	hypothetical protein	-1.49	1.37	1.27
lmo0121	hypothetical protein	-1.58	1.27	
lmo0122	hypothetical protein	-1.36	1.14	1.02
lmo0123	minor structural protein	-1.52	1.32	1.53
lmo0124	hypothetical protein	-1.37	1.13	1.17
lmo0125	hypothetical protein	-1.41	1.14	1.18
lmo0126	hypothetical protein	-1.30	1.27	1.05
lmo0127	hypothetical protein	-1.34	1.22	
lmo0128	hypothetical protein	-1.60	1.04	
lmo0129	N-acetylmuramoyl-L-alanine amidase	-1.25	1.29	1.16
lmo0130	hypothetical protein			
lmo0134	hypothetical protein		-1.35	-1.02
lmo0135	peptide/nickel transport system substrate-binding protein			
lmo0136	peptide/nickel transport system permease			
lmo0137	peptide/nickel transport system permease			-1.23
lmo0138	hypothetical protein			
lmo0139	hypothetical protein			
lmo0143	hypothetical protein			
lmo0149	hypothetical protein			
lmo0152	peptide/nickel transport system substrate-binding protein	-1.82		
lmo0160	peptidoglycan bound protein		-1.05	

lmo0161	hypothetical protein			
lmo0186	hypothetical protein	1.46	-1.17	-1.42
lmo0197	stage V sporulation protein G			-1.08
lmo0200	listeriolysin regulatory protein	-1.16		
lmo0201	1-phosphatidylinositol phosphodiesterase	-6.30	-1.06	
lmo0202	listeriolysin O	-6.97		-1.35
lmo0203	zinc metalloproteinase	-4.15		
lmo0204	actin-assembly inducing protein ActA	-6.38		-1.80
lmo0205	phospholipase C	-6.14		-1.88
lmo0206	hypothetical protein	-3.80		-1.98
lmo0207	hypothetical protein	-2.64		-1.89
lmo0223	cysteine synthase A	-1.10		
lmo0229	CtsR family transcriptional regulator		-1.29	
lmo0230	hypothetical protein		-1.21	
lmo0231	ATP:guanido phosphotransferase			1.26
lmo0232	ATP-dependent Clp protease ATP-binding subunit ClpC			
lmo0233	DNA repair protein RadA			1.07
lmo0238	serine O-acetyltransferase			2.33
lmo0239	cysteinyl-tRNA synthetase			1.95
lmo0240	ribonuclease III family protein			1.40
lmo0241	TrmH family RNA methyltransferase group 3			1.39
lmo0242	hypothetical protein			1.11
lmo0243	RNA polymerase sporulation-specific sigma factor			
lmo0244	50S ribosomal protein L33			
lmo0266	hypothetical protein		1.77	2.30
lmo0267	hypothetical protein		1.05	1.77
lmo0279	anaerobic ribonucleoside-triphosphate reductase		1.43	1.72
lmo0280	anaerobic ribonucleoside-triphosphate reductase activating protein		1.31	1.52
lmo0286	aminotransferase		-1.20	
lmo0292	hypothetical protein		-1.15	
lmo0300	beta-glucosidase		1.67	2.01
lmo0301	cellobiose-specific PTS system IIA component			2.29
lmo0303	hypothetical protein		-1.79	
lmo0309	hypothetical protein			
lmo0316	hydroxyethylthiazole kinase		1.08	1.35
lmo0323	hypothetical protein	1.19		
lmo0324	lipoprotein			
lmo0325	hypothetical protein		-1.57	
lmo0326	transcriptional regulator			
lmo0328	hypothetical protein			
lmo0331	internalin			-1.05
lmo0332	hypothetical protein			-1.41
lmo0334	hypothetical protein			

lmo0336	hypothetical protein	1.11		
lmo0340	hypothetical protein		-1.11	-1.46
lmo0342	transketolase		1.50	1.02
lmo0343	transaldolase		1.72	1.13
lmo0344	short chain dehydrogenase		1.53	
lmo0345	ribose 5-phosphate isomerase B		1.32	
lmo0346	triosephosphate isomerase		1.85	1.24
lmo0347	dihydroxyacetone kinase L subunit		1.65	
lmo0348	dihydroxyacetone kinase		1.70	1.15
lmo0349	hypothetical protein		1.41	
lmo0350	hypothetical protein		1.80	1.28
lmo0351	dihydroxyacetone kinase	-1.15	1.70	1.39
lmo0355	fumarate reductase flavoprotein subunit		1.25	
lmo0357	fructose-specific PTS system IIA component	1.14		
lmo0361	twin arginine-targeting protein translocase TatC	-1.15		
lmo0362	sec-independent protein translocase tatAy	-1.31		
lmo0365	high-affinity iron transporter	-1.85		
lmo0366	lipoprotein	-1.57		
lmo0367	tat-translocated enzyme	-1.61		
lmo0372	beta-glucosidase	1.34	1.66	1.70
lmo0373	cellobiose-specific PTS system IIC component	1.00		
lmo0374	cellobiose-specific phosphotransferase enzyme IIB component	1.56	2.21	
lmo0378	hypothetical protein		1.97	2.67
lmo0383	methylmalonate-semialdehyde dehydrogenase		1.09	
lmo0384	5-deoxy-glucuronate isomerase			1.68
lmo0385	5-dehydro-2-deoxygluconokinase			1.37
lmo0386	3D-(3,5/4)-trihydroxycyclohexane-1,2-dione hydrolase		1.41	1.91
lmo0394	extracellular P60 protein		-1.25	-2.04
lmo0398	fructose-specific PTS system IIA component			
lmo0400	fructose-specific PTS system IIC component		4.27	4.73
lmo0406	lactoylglutathione lyase		-1.01	
lmo0408	hypothetical protein		-1.13	
lmo0415	peptidoglycan N-acetylglucosamine deacetylase	-1.08		
lmo0425	PRD/PTS system IIA 2 domain-containing regulatory protein		1.28	1.37
lmo0426	fructose-specific PTS system IIA component		1.24	1.01
lmo0427	fructose-specific PTS system IIB component			1.48
lmo0433	internalin A	-1.27		
lmo0434	internalin B	-1.66		
lmo0436	hypothetical protein		-1.09	
lmo0440	hypothetical protein			-1.36
lmo0442	hypothetical protein	1.05		
lmo0443	hypothetical protein			

lmo0444	membrane protein			
lmo0479	secreted protein	1.01	-1.25	-1.46
lmo0485	hypothetical protein			
lmo0489	hypothetical protein		2.08	2.07
lmo0490	shikimate 5-dehydrogenase			1.01
lmo0492	transcription regulator LysR		-1.07	-1.23
lmo0498	ribose 5-phosphate isomerase B		1.04	
lmo0500	hypothetical protein			1.21
lmo0502	hypothetical protein		1.10	
lmo0504	hypothetical protein		1.04	1.09
lmo0517	phosphoglycerate mutase			1.41
lmo0518	membrane protein		-1.46	
lmo0544	glucitol/sorbitol-specific PTS system IIC component		4.45	4.99
lmo0545	glucitol operon activator protein			1.47
lmo0546	sorbitol-6-phosphate 2-dehydrogenase		2.15	2.38
lmo0548	hypothetical protein			1.27
lmo0549	internalin		1.00	
lmo0550	peptidoglycan bound protein			
lmo0559	hypothetical protein			
lmo0560	glutamate dehydrogenase			1.09
lmo0573	AGZA family MFS transporter xanthine/uracil permease			-1.31
lmo0579	hypothetical protein		-1.16	
lmo0582	invasion associated secreted endopeptidase			
lmo0584	hypothetical protein			-1.08
lmo0586	hypothetical protein		1.83	2.15
lmo0587	secreted protein			1.38
lmo0592	hypothetical protein		-1.31	
lmo0598	biotin biosynthesis protein BioY			-1.12
lmo0604	hypothetical protein	-2.18		
lmo0609	hypothetical protein		-1.43	
lmo0629	hypothetical protein		-1.02	
lmo0635	2-haloalkanoic acid dehalogenase		-1.16	-1.27
lmo0642	hypothetical protein		-1.08	-1.01
lmo0647	hypothetical protein		1.28	1.25
lmo0659	hypothetical protein		1.16	1.89
lmo0665	hypothetical protein			1.32
lmo0669	hypothetical protein			
lmo0670	hypothetical protein			
lmo0675	flagellar motor switch protein FliN			-1.57
lmo0681	flagellar biosynthesis regulator FlhF			
lmo0683	chemotaxis protein methyltransferase			
lmo0684	hypothetical protein		1.03	
lmo0685	chemotaxis protein MotA			-1.03

lmo0686	chemotaxis protein MotB			
lmo0687	hypothetical protein			
lmo0688	hypothetical protein			
lmo0689	hypothetical protein			
lmo0692	chemotaxis protein cheA		1.09	
lmo0694	hypothetical protein			1.09
lmo0695	hypothetical protein			1.02
lmo0696	flagellar hook capping protein		1.35	
lmo0697	flagellar hook protein FlgE		1.47	1.10
lmo0698	hypothetical protein		1.49	1.21
lmo0699	flagellar motor switch protein FliM		1.44	1.39
lmo0700	flagellar motor switch protein FliN/FliY		1.51	1.14
lmo0701	hypothetical protein		1.39	1.12
lmo0702	hypothetical protein		1.55	1.24
lmo0703	hypothetical protein		1.25	1.15
lmo0704	hypothetical protein		1.12	1.09
lmo0705	flagellar hook-associated protein FlgK		1.20	
lmo0706	flagellar hook-associated protein 3		1.01	
lmo0716	flagellar protein export ATPase FliI		1.22	
lmo0731	hypothetical protein		1.14	
lmo0741	hypothetical protein		1.28	2.80
lmo0742	ABC transporter ATP-binding protein		2.60	2.43
lmo0745	hypothetical protein			
lmo0758	hypothetical protein		1.49	2.05
lmo0759	glyoxylase		1.60	2.00
lmo0760	hypothetical protein		1.47	1.76
lmo0761	hypothetical protein		1.55	1.46
lmo0762	GTP-binding protein HflX			1.20
lmo0765	hypothetical protein			-1.12
lmo0766	multiple sugar transport system permease			
lmo0767	maltose/maltodextrin ABC transporter permease MalG			
lmo0778	hypothetical protein			-1.04
lmo0786	FMN-dependent NADH-azoreductase 2			-1.10
lmo0788	hypothetical protein		1.53	1.69
lmo0791	hypothetical protein			-1.37
lmo0794	hypothetical protein	1.01		
lmo0797	hypothetical protein			
lmo0798	AAT family amino acid transporter		-1.06	-1.38
lmo0802	hypothetical protein		-1.53	
lmo0806	hypothetical protein		-1.61	-1.77
lmo0807	spermidine/putrescine transport system ATP-binding protein		-1.42	-2.10
lmo0808	spermidine/putrescine transport system permease		-1.49	-1.90
lmo0809	spermidine/putrescine transport system permease		-1.55	-2.31

lmo0810	spermidine/putrescine transport system substrate-binding protein		-1.68	-2.23
lmo0824	hypothetical protein			1.21
lmo0829	pyruvate:ferredoxin oxidoreductase		1.02	1.16
lmo0833	hypothetical protein		-1.64	-1.53
lmo0835	peptidoglycan bound protein			1.52
lmo0836	hypothetical protein		-1.22	-1.89
lmo0838	MFS transporter	-4.49	-1.14	-1.98
lmo0839	tetracycline resistance protein	-1.15		
lmo0840	MarR family transcriptional regulator			-1.14
lmo0843	hypothetical protein		-1.50	-1.86
lmo0847	glutamine ABC transporter			-1.47
lmo0848	polar amino acid transport system ATP-binding protein			-1.46
lmo0850	hypothetical protein			-2.42
lmo0864	hypothetical protein			1.08
lmo0867	hypothetical protein			-1.29
lmo0869	hypothetical protein		1.02	1.03
lmo0874	cellobiose-specific PTS system IIA component			
lmo0875	cellobiose-specific PTS system IIB component			2.90
lmo0880	peptidoglycan bound protein		-1.82	-1.55
lmo0881	hypothetical protein			
lmo0903	OsmC/Ohr family protein	-2.20		
lmo0908	hypothetical protein			-1.03
lmo0916	cellobiose-specific PTS system IIA component	1.25	1.77	1.14
lmo0917	beta-glucosidase	1.14		
lmo0920	ABC transporter permease		-1.19	-1.14
lmo0921	membrane protein		-1.15	-1.16
lmo0929	sortase A		-1.28	
lmo0937	hypothetical protein			-2.43
lmo0941	hypothetical protein			
lmo0942	hypothetical protein			
lmo0950	hypothetical protein		-1.05	
lmo0952	hypothetical protein			-1.02
lmo0953	hypothetical protein			-1.07
lmo0954	hypothetical protein			
lmo0955	hypothetical protein			
lmo0971	D-alanine transfer protein			1.35
lmo0972	D-alanine--poly(phosphoribitol) ligase subunit 2			1.56
lmo0973	membrane protein			1.38
lmo0974	D-alanine--poly(phosphoribitol) ligase subunit 1			1.28
lmo0989	hypothetical protein			-1.12
lmo0994	hypothetical protein			-1.13
lmo0995	YkrP protein			

lmo0997	ATP-dependent Clp protease ATP-binding subunit ClpE	1.10	-1.50	
lmo0999	hypothetical protein		-1.06	-1.56
lmo1007	hypothetical protein		-1.02	
lmo1014	glycine betaine/proline transport system ATP-binding protein	-1.09		
lmo1023	ktr system potassium uptake protein C			-1.02
lmo1030	hypothetical protein			1.24
lmo1031	hypothetical protein		1.04	
lmo1032	transketolase			1.06
lmo1033	transketolase		1.25	1.31
lmo1037	hypothetical protein			
lmo1038	molybdopterin-guanine dinucleotide biosynthesis protein MobA			-1.22
lmo1052	pyruvate dehydrogenase E1 component		1.31	
lmo1053	pyruvate dehydrogenase E1 component subunit beta		1.35	
lmo1054	pyruvate dehydrogenase E2 component		1.21	1.19
lmo1055	dihydrolipoyl dehydrogenase		1.29	1.17
lmo1069	hypothetical protein			-1.19
lmo1070	hypothetical protein			-1.52
lmo1074	teichoic acid transport system permease		-1.17	-1.61
lmo1075	teichoic acids export ATP-binding protein tagH		-1.12	-1.38
lmo1079	hypothetical protein			-1.01
lmo1116	hypothetical protein			
lmo1117	hypothetical protein			
lmo1127	hypothetical protein			-1.13
lmo1131	ABC transporter	-1.15	1.53	1.31
lmo1132	ABC transporter		1.43	1.24
lmo1133	hypothetical protein			
lmo1138	Clp protease		-1.04	
lmo1139	hypothetical protein		-1.07	
lmo1151	propanediol utilization protein pduA			
lmo1155	propanediol dehydratase small subunit		1.24	
lmo1162	propanediol utilization protein PduM			1.37
lmo1174	ethanolamine utilization protein EutA			1.17
lmo1182	ethanolamine utilization protein		3.69	4.00
lmo1191	cobyrinic acid a,c-diamide synthase		1.06	
lmo1192	cobalamin biosynthesis protein CobD		1.44	
lmo1197	precorrin-4 C(11)-methyltransferase			
lmo1199	precorrin-3B C(17)-methyltransferase			1.48
lmo1203	precorrin-2 C(20)-methyltransferase			1.56
lmo1204	cobalamin biosynthesis protein CbiM		1.81	1.40
lmo1208	cobyric acid synthase CobQ			1.18
lmo1211	integral membrane protein			-1.17

lmo1216	bax protein	1.05		
lmo1229	hypothetical protein		-1.02	
lmo1236	hypothetical protein		2.12	2.24
lmo1237	glutamate racemase		2.01	2.11
lmo1238	ribonuclease PH		2.38	2.49
lmo1239	rdgB/HAM1 family non-canonical purine NTP pyrophosphatase		2.28	2.42
lmo1240	hypothetical protein		3.25	3.57
lmo1254	alpha-phosphotrehalase			1.28
lmo1255	trehalose-specific PTS system IIBC component		1.15	1.72
lmo1263	transcriptional regulator			
lmo1266	hypothetical protein			-1.03
lmo1284	hypothetical protein			-1.08
lmo1295	host factor-I protein		-1.18	-1.48
lmo1297	aluminum resistance protein			-1.01
lmo1306	hypothetical protein		-1.13	-1.90
lmo1309	hypothetical protein			1.35
lmo1310	hypothetical protein		1.07	1.67
lmo1311	hypothetical protein			1.02
lmo1314	ribosome recycling factor			-1.06
lmo1315	di-trans,poly-cis-decaprenylcistransferase		-1.16	
lmo1316	phosphatidate cytidylyltransferase			
lmo1317	1-deoxy-D-xylulose 5-phosphate reductoisomerase			
lmo1318	RIP metalloprotease RseP			
lmo1328	tRNA pseudouridine synthase B	-1.08		
lmo1333	hypothetical protein		-1.19	-1.60
lmo1334	secreted protein		-1.38	-1.47
lmo1335	50S ribosomal protein L33			-1.01
lmo1341	late competence protein ComGG		-1.10	
lmo1364	cold shock-like protein cspLA			-1.19
lmo1369	phosphate butyryltransferase			
lmo1384	hypothetical protein		-1.13	-1.37
lmo1388	ABC transporter			-1.18
lmo1389	simple sugar transport system ATP-binding protein			-1.48
lmo1390	simple sugar transport system permease			-1.66
lmo1391	simple sugar transport system permease			-1.67
lmo1406	formate acetyltransferase		2.34	2.39
lmo1407	pyruvate formate-lyase activating enzyme		1.99	2.08
lmo1409	hypothetical protein		1.35	
lmo1410	hypothetical protein			-1.32
lmo1411	transcriptional regulator			
lmo1412	DNA topology modulation protein FlaR			
lmo1416	hypothetical protein			

lmo1438	hypothetical protein			
lmo1440	hypothetical protein			-1.39
lmo1460	DNA repair protein RecO			1.29
lmo1461	hypothetical protein			-1.27
lmo1466	hypothetical protein	-8.13		
lmo1468	hypothetical protein			
lmo1478	MarR family transcriptional regulator			-1.11
lmo1480	30S ribosomal protein S20			-1.43
lmo1504	alanyl-tRNA synthetase	-1.04		-1.00
lmo1505	hypothetical protein	1.32		
lmo1506	hypothetical protein	1.02	-1.17	
lmo1515	HTH-type transcriptional regulator cymR		-1.05	
lmo1516	amt familyammonium transporter		-1.22	-1.66
lmo1517	nitrogen regulatory protein P-II		-1.15	-1.24
lmo1518	hypothetical protein		-1.21	-1.15
lmo1526	hypothetical protein			-1.02
lmo1546	rod shape-determining protein MreD			
lmo1551	folylpolyglutamate synthase			-1.03
lmo1584	hypothetical protein			
lmo1585	protease IV			-1.27
lmo1587	ornithine carbamoyltransferase	-1.32		
lmo1588	acetylornithine aminotransferase			
lmo1589	acetylglutamate kinase	-1.01		
lmo1590	ArgJ family protein	-1.35		
lmo1591	N-acetyl-gamma-glutamyl-phosphate reductase	-1.26		
lmo1597	hypothetical protein			1.02
lmo1601	hypothetical protein		-1.17	
lmo1603	aminopeptidase			-1.07
lmo1622	hypothetical protein		-1.29	
lmo1628	tryptophan synthase	-1.12		
lmo1629	N-(5'phosphoribosyl)anthranilate isomerase	-1.18		
lmo1631	anthranilate phosphoribosyltransferase	-1.11		
lmo1632	anthranilate synthase component II	-1.07		
lmo1634	bifunctional acetaldehyde-CoA/alcohol dehydrogenase		1.52	1.33
lmo1635	DNA binding 3-demethylubiquinone-9 3-methyltransferase domain-containing protein		-1.01	
lmo1649	hypothetical protein	1.23		
lmo1653	cellsurface protein		1.73	
lmo1654	cellsurface protein		1.67	
lmo1655	hypothetical protein		2.13	2.20
lmo1665	hypothetical protein		-1.19	-2.08
lmo1666	peptidoglycan bound protein			
lmo1669	nucleoside triphosphatase YtkD			1.06
lmo1671	zinc transport system substrate-binding protein			-1.10

lmo1682	hypothetical protein	-1.05		
lmo1690	hypothetical protein			
lmo1700	hypothetical protein			-1.31
lmo1710	flavodoxin		-1.08	
lmo1713	rod shape-determining protein MreB		-1.24	-2.07
lmo1727	LacI family transcriptional regulator			1.09
lmo1734	glutamate synthase subunit large			1.28
lmo1738	polar amino acid transport system substrate-binding protein	-1.78		
lmo1739	polar amino acid transport system ATP-binding protein	-1.87		
lmo1740	polar amino acid transport system permease	-1.80		
lmo1764	phosphoribosylamine--glycine ligase			
lmo1765	phosphoribosylaminoimidazolecarboxamide formyltransferase/IMP cyclohydrolase			
lmo1766	phosphoribosylglycinamide formyltransferase			
lmo1767	phosphoribosylformylglycinamidine cyclo-ligase			
lmo1768	amidophosphoribosyltransferase			
lmo1769	phosphoribosylformylglycinamidine synthase II			
lmo1770	phosphoribosylformylglycinamidine synthase I			
lmo1771	phosphoribosylformylglycinamidine synthase		-1.16	
lmo1772	phosphoribosylaminoimidazolesuccinocarboxamide synthase			
lmo1775	AIR carboxylase			
lmo1776	hypothetical protein		-1.05	-1.23
lmo1786	internalin C	-1.47		-1.25
lmo1799	hypothetical protein		1.36	
lmo1816	50S ribosomal protein L28			-1.07
lmo1841	uracil phosphoribosyltransferase			-1.16
lmo1850	hypothetical protein			-1.10
lmo1867	pyruvate, phosphate dikinase		1.53	1.02
lmo1868	lactoylglutathione lyase			-1.03
lmo1879	cold shock protein			-1.60
lmo1882	30S ribosomal protein S14			1.11
lmo1890	hypothetical protein			
lmo1892	penicillin binding protein 1A		-1.22	
lmo1917	formate acetyltransferase		1.73	1.31
lmo1919	hypothetical protein			
lmo1934	DNA-binding protein HU-beta			-1.65
lmo1938	30S ribosomal protein S1			-1.15
lmo1943	hypothetical protein		1.02	1.32
lmo1966	hypothetical protein			
lmo1971	ascorbate-specific PTS system IIC component			1.73
lmo1972	ascorbate-specific PTS system IIB component			
lmo1975	DNA polymerase IV		1.41	1.44

lmo1983	dihydroxy-acid dehydratase	1.17		
lmo1984	acetolactate synthase large subunit	1.02		
lmo1986	ketol-acid reductoisomerase	1.09		
lmo2011	sensor histidine kinase YesM			1.12
lmo2014	alpha-mannosidase		1.19	1.55
lmo2016	cold shock protein			-2.33
lmo2022	cysteine desulfurase			1.03
lmo2023	L-aspartate oxidase	-1.44		1.91
lmo2024	nicotinate-nucleotide diphosphorylase	-1.57	1.07	2.04
lmo2025	quinolinate synthetase complex A subunit	-1.55		1.70
lmo2038	UDP-N-acetylmuramoyl-L-alanyl-D-glutamate-2			1.13
lmo2039	penicillin binding protein 2B			1.07
lmo2040	cell division protein FtsL			1.45
lmo2041	methylase MraW			1.61
lmo2042	mraZ protein			1.82
lmo2063	hypothetical protein			
lmo2071	hypothetical protein		1.68	1.53
lmo2079	hypothetical protein			
lmo2083	hypothetical protein			
lmo2084	hypothetical protein			1.22
lmo2085	peptidoglycan binding protein	1.02		
lmo2090	argininosuccinate synthase	-1.62		
lmo2091	argininosuccinate lyase	-1.65		
lmo2093	hypothetical protein	-1.29		2.11
lmo2094	hypothetical protein		1.70	3.04
lmo2095	1-phosphofructokinase			-1.48
lmo2096	galactitol-specific PTS system IIC component			1.27
lmo2097	galactitol-specific PTS system IIB component			1.68
lmo2098	galactitol-specific PTS system IIA component		2.17	1.59
lmo2099	hypothetical protein		2.08	1.50
lmo2101	pyridoxine biosynthesis protein		1.26	1.06
lmo2102	glutamine amidotransferase subunit pdxT		1.09	1.25
lmo2104	ferrous iron transporter A		2.11	2.52
lmo2105	ferrous iron transporter B		1.94	1.89
lmo2107	hypothetical protein			1.34
lmo2108	N-acetylglucosamine-6-phosphate deacetylase			1.01
lmo2114	hypothetical protein	-1.91		1.49
lmo2115	hypothetical protein	-1.79		1.31
lmo2116	hypothetical protein			-1.10
lmo2120	hypothetical protein		-2.00	-1.40
lmo2127	hypothetical protein		-1.89	-1.71
lmo2129	hypothetical protein			
lmo2131	hypothetical protein			-1.61
lmo2132	hypothetical protein	1.24		

lmo2133	fructose-bisphosphate aldolase class II	1.17		
lmo2134	fructose-bisphosphate aldolase class II	1.01		
lmo2135	fructose-specific PTS system IIC component	1.35		
lmo2136	fructose-specific PTS system IIB component	1.66		
lmo2137	fructose-specific PTS system IIA component	1.43		
lmo2147	hypothetical protein			
lmo2150	hypothetical protein	-1.23		-1.19
lmo2151	hypothetical protein			1.25
lmo2156	hypothetical protein	-1.71		2.25
lmo2158	hypothetical protein		-1.55	
lmo2160	sugar phosphate isomerase/epimerase			1.00
lmo2163	hypothetical protein		1.12	
lmo2172	propionate CoA-transferase			
lmo2173	hypothetical protein		1.07	
lmo2175	3-oxoacyl-ACP reductase	1.05		-1.24
lmo2177	hypothetical protein	-1.52		
lmo2178	peptidoglycan bound protein			
lmo2180	hypothetical protein		2.40	1.50
lmo2181	SrtB family sortase			
lmo2182	iron complex transport system ATP-binding protein	-1.02		
lmo2183	iron complex transport system permease			
lmo2184	heme ABC transporter heme-binding protein isdE			
lmo2185	hypothetical protein			
lmo2186	heme uptake protein IsdC	-1.25		
lmo2187	hypothetical protein			
lmo2196	peptide/nickel transport system substrate-binding protein			-1.30
lmo2197	hypothetical protein			-1.83
lmo2202	3-oxoacyl-ACP synthase		-1.03	
lmo2203	hypothetical protein		-1.82	
lmo2204	hypothetical protein			-1.70
lmo2210	hypothetical protein		-1.28	
lmo2218	hypothetical protein			-1.26
lmo2219	foldase prsA 2	-1.02	-1.84	-1.51
lmo2221	hypothetical protein		1.27	1.29
lmo2222	hypothetical protein		1.55	1.37
lmo2223	hypothetical protein			-1.40
lmo2228	hypothetical protein	-1.27		-1.37
lmo2230	hypothetical protein	1.17		
lmo2234	hypothetical protein		1.07	1.31
lmo2235	NADH oxidase			1.56
lmo2236	shikimate 5-dehydrogenase			1.07
lmo2245	hypothetical protein			1.37
lmo2247	oxidoreductase			1.35

lmo2250	hypothetical protein			
lmo2251	polar amino acid transport system ATP-binding protein			
lmo2252	aspartate aminotransferase			
lmo2254	AGZA family MFS transporter xanthine/uracil permease		-1.92	-2.93
lmo2255	hypothetical protein			-1.02
lmo2257	hypothetical protein			-1.49
lmo2268	ATP-dependent nuclease subunit B			1.01
lmo2271	phage protein	-1.50		
lmo2278	endolysin L-alanyl-D-glutamate peptidase	-1.65	1.07	
lmo2279	phage holin	-2.18		
lmo2280	gp23	-1.35	1.15	
lmo2281	gp22	-2.88	1.29	
lmo2282	short tail fiber	-3.78	1.31	
lmo2283	long tail fiber	-4.07	1.36	
lmo2284	tail or base plate protein gp19	-3.66	1.12	
lmo2285	tail or base plate protein gp18	-3.82	1.24	
lmo2286	tail or base plate protein gp17	-3.79	1.04	
lmo2287	tail tape-measure protein	-5.02		
lmo2288	gp15	-4.59		
lmo2289	gp14	-5.48		
lmo2290	gp13	-5.95		
lmo2291	major tail shaft protein	-5.38	1.21	
lmo2292	gp11	-5.38	1.32	
lmo2293	gp10	-5.49	1.21	
lmo2294	gp9	-5.33	1.47	
lmo2295	gp8	-5.17	1.32	
lmo2296	phage capsid protein	-5.49	1.11	
lmo2297	scaffolding protein	-5.58		
lmo2298	phage minor capsid protein	-5.54	1.23	
lmo2299	phage portal protein	-4.97	1.29	
lmo2300	phage terminase large subunit	-2.73	1.11	
lmo2301	terminase small subunit	-3.47		
lmo2303	gp66	-2.71	1.93	1.38
lmo2304	gp65	-2.95	1.70	1.46
lmo2317	gp49	-3.33	1.76	1.39
lmo2321	gp45	-1.87		
lmo2322	gp44	-3.01	1.94	1.61
lmo2323	gp43	-3.33	1.71	1.09
lmo2324	anti-repressor protein	-2.87	1.50	
lmo2325	hypothetical protein	-1.78	1.38	
lmo2326	gp41	-1.67	1.63	
lmo2327	hypothetical protein	1.03	1.03	
lmo2343	monooxygenase moxC			-1.45

lmo2344	hypothetical protein			
lmo2345	hypothetical protein			-1.19
lmo2346	polar amino acid transport system ATP-binding protein			-1.18
lmo2347	polar amino acid transport system permease			-1.01
lmo2348	polar amino acid transport system permease			-1.23
lmo2349	polar amino acid transport system substrate-binding protein			
lmo2350	hypothetical protein			-1.22
lmo2351	FMN reductase			
lmo2352	HTH-type transcriptional regulator ytlI			
lmo2356	hypothetical protein	1.02		
lmo2360	membrane protein	1.84		
lmo2361	Rrf2 family protein	1.81		
lmo2375	hypothetical protein		-1.09	
lmo2376	peptidyl-prolyl isomerase			-1.09
lmo2378	multicomponent Na+:H+ antiporter subunit A		1.04	
lmo2380	multicomponent Na+:H+ antiporter subunit C		1.05	
lmo2385	ComA operon protein 2			
lmo2395	hypothetical protein		-1.24	-3.10
lmo2402	hypothetical protein			1.28
lmo2403	hypothetical protein			1.07
lmo2407	hypothetical protein			-1.02
lmo2408	transcriptional regulator			-1.74
lmo2409	hypothetical protein			-1.22
lmo2410	hypothetical protein			
lmo2412	NifU family SUF system FeS assembly protein			1.10
lmo2414	FeS assembly protein SufD			1.17
lmo2415	FeS assembly ATPase SufC			1.28
lmo2427	rod shape-determining protein RodA			
lmo2428	rod shape-determining protein RodA			
lmo2432	hypothetical protein	1.11		
lmo2433	tributyrin esterase	-1.57	1.07	1.11
lmo2437	hypothetical protein	1.41	-1.18	
lmo2439	hypothetical protein	-2.05		
lmo2440	hypothetical protein			
lmo2442	hypothetical protein	-1.06		
lmo2443	hypothetical protein			-1.28
lmo2444	hypothetical protein		1.45	1.66
lmo2446	hypothetical protein		1.68	1.47
lmo2447	hypothetical protein		1.29	
lmo2450	carboxylesterase			1.34
lmo2454	hypothetical protein	1.06	-1.25	
lmo2460	transcriptional regulator		1.06	1.28
lmo2466	hypothetical protein			-1.33

lmo2470	internalin		1.27	1.22
lmo2474	hypothetical protein			1.15
lmo2484	membrane protein			
lmo2485	PspC domain-containing protein			
lmo2486	hypothetical protein			
lmo2487	hypothetical protein			
lmo2489	excinuclease ABC subunit B		1.14	1.27
lmo2494	phosphate transport system regulatory protein PhoU	1.01		
lmo2495	phosphate ABC transporter ATP-binding protein	1.10		
lmo2498	phosphate ABC transporter permease	1.28		
lmo2499	phosphate transport system substrate-binding protein	1.47	1.03	
lmo2502	hypothetical protein			
lmo2504	hypothetical protein		-1.06	-1.40
lmo2505	D-glutamyl-L-m-Dpm peptidase P45			-1.18
lmo2506	cell division transport system permease			
lmo2507	cell division ATP-binding protein FtsE			
lmo2511	sigma-54 modulation protein			-1.00
lmo2512	competence protein ComFC			
lmo2518	transcriptional regulator LytR		-1.35	
lmo2522	hypothetical protein	2.28	-1.17	-1.59
lmo2527	hypothetical protein	2.12		
lmo2548	50S ribosomal protein L31		-1.05	-1.46
lmo2567	hypothetical protein			
lmo2568	hypothetical protein			1.47
lmo2569	peptide/nickel transport system substrate-binding protein			-1.15
lmo2584	formate dehydrogenase family accessory protein FdhD		1.09	1.92
lmo2587	hypothetical protein			
lmo2591	N-acetylmuramoyl-L-alanine amidase		-1.13	-1.40
lmo2594	hypothetical protein		1.09	1.49
lmo2636	thiamine biosynthesis lipoprotein		-1.04	-1.09
lmo2649	ascorbate-specific PTS system IIC component		1.21	
lmo2651	mannitol-specific PTS system IIA component		1.44	
lmo2660	transketolase			1.10
lmo2661	ribulose-phosphate 3-epimerase		1.49	2.41
lmo2662	ribose 5-phosphate isomerase B		2.15	1.09
lmo2663	L-iditol 2-dehydrogenase			1.09
lmo2664	L-iditol 2-dehydrogenase		1.18	
lmo2665	galactitol-specific PTS system IIC component		1.69	1.01
lmo2666	galactitol-specific PTS system IIB component			1.47
lmo2667	hypothetical protein			1.33
lmo2668	hypothetical protein		1.58	1.42

lmo2675	hypothetical protein		1.28	1.12
lmo2676	DNA polymerase V		1.13	
lmo2680	K+-transporting ATPase C subunit	-1.05		
lmo2681	K+-transporting ATPase B subunit	-1.02		
lmo2682	K+-transporting ATPase A subunit	-2.16		
lmo2683	cellobiose-specific PTS system IIB component	2.21	-2.35	-2.71
lmo2684	cellobiose-specific PTS system IIC component	2.04	-2.23	-2.99
lmo2685	cellobiose-specific PTS system IIA component	2.17	-2.37	-3.54
lmo2688	cell division protein FtsW/RodA/SpoVE		1.80	1.85
lmo2689	magnesium-translocating P-type ATPase	-1.56		1.41
lmo2691	autolysin			
lmo2708	cellobiose-specific PTS system IIC component	2.10	-1.18	-1.55
lmo2712	gluconokinase			1.01
lmo2714	peptidoglycan bound protein			
lmo2716	ABC transporter CydDC cysteine exporter CydD		1.22	
lmo2717	cytochrome d ubiquinol oxidase subunit II		1.31	
lmo2718	cytochrome bd-I oxidase subunit I		1.24	
lmo2719	tRNA-adenosine deaminase		1.13	
lmo2720	acetyl-CoA synthetase		-1.10	
lmo2721	6-phosphogluconolactonase			
lmo2735	sucrose phosphorylase		1.08	
lmo2744	hypothetical protein			-1.46
lmo2762	cellobiose-specific PTS system IIB component		1.23	
lmo2786	ADP-ribosylglycohydrolase			-1.74
lmo2787	beta-glucoside-specific phosphotransferase enzyme II ABC component			-1.25
lmo2796	hypothetical protein		-1.11	
lmo2798	hypothetical protein			
lmo2801	N-acetylmannosamine-6-phosphate 2-epimerase		1.01	1.01
lmo2812	hypothetical protein			
lmo2836	hypothetical protein	1.18		
lmo2837	multiple sugar transport system permease		1.46	1.05
lmo2850	MFS transporter			
lmo2856	50S ribosomal protein L34			-1.40

Table SB2: Significantly (P<0.05) differentially expressed genes (Fold-change >2) relative to strains exposed to 1280µg/mL cefuroxime for 30 minutes (appended "cef") vs the same strain in untreated control condition ("LSM").

		vs self in LSM		
EGD-E Gene ID	**Gene function**	**ΔPDE cef**	**cΔdac A cef**	**WT Cef**
lmo2210	hypothetical protein	5.11	3.58	4.70
lmo2156	hypothetical protein	4.26	1.32	3.42
lmo2114	hypothetical protein	3.77	1.85	4.18
lmo2115	hypothetical protein	3.62	1.98	3.87
lmo0974	D-alanine--poly(phosphoribitol) ligase subunit 1	3.27		2.39
lmo0973	membrane protein	3.20		2.35
lmo0971	D-alanine transfer protein	3.12		2.47
lmo0972	D-alanine--poly(phosphoribitol) ligase subunit 2	3.06		2.66
lmo2720	acetyl-CoA synthetase	2.68		1.97
lmo2568	hypothetical protein	2.45	1.24	2.17
lmo2567	hypothetical protein	2.37	1.53	1.88
lmo0604	hypothetical protein	2.36	1.88	3.37
lmo1690	hypothetical protein	2.21	1.66	2.42
lmo0292	hypothetical protein	2.15	1.83	3.10
lmo0954	hypothetical protein	2.05	1.75	1.65
lmo2203	hypothetical protein	1.97		2.11
lmo2487	hypothetical protein	1.86	1.10	1.51
lmo2486	hypothetical protein	1.82	1.15	1.49
lmo0955	hypothetical protein	1.81	1.49	1.65
lmo0802	hypothetical protein	1.75	1.43	2.20
lmo2219	foldase prsA 2	1.59	1.22	1.55
lmo2714	peptidoglycan bound protein	1.59		1.90
lmo2202	3-oxoacyl-ACP synthase	1.49		1.04
lmo2177	hypothetical protein	1.49	2.72	2.79
lmo1890	hypothetical protein	1.40		1.97
lmo2721	6-phosphogluconolactonase	1.34		1.14
lmo0443	hypothetical protein	1.33	1.41	1.38
lmo1315	di-trans,poly-cis-decaprenylcistransferase	1.32	1.13	1.75
lmo2093	hypothetical protein	1.30		1.79
lmo0088	ATP synthase subunit C	1.29		
lmo0047	hypothetical protein	1.27		
lmo0997	ATP-dependent Clp protease ATP-binding subunit ClpE	1.27		1.72
lmo2812	hypothetical protein	1.25	3.10	2.58
lmo1369	phosphate butyryltransferase	1.25		
lmo1037	hypothetical protein	1.22	2.36	1.57
lmo1597	hypothetical protein	1.18		

lmo2485	PspC domain-containing protein	1.14		1.10
lmo1589	acetylglutamate kinase	1.14	1.91	2.36
lmo1919	hypothetical protein	1.10	1.35	1.62
lmo1972	ascorbate-specific PTS system IIB component	1.09		
lmo0095	hypothetical protein	1.08		1.26
lmo1438	hypothetical protein	1.07	1.01	1.16
lmo0560	glutamate dehydrogenase	1.06		1.13
lmo2836	hypothetical protein	1.04		
lmo1587	ornithine carbamoyltransferase	1.04	1.95	2.27
lmo0303	hypothetical protein	1.03		
lmo0559	hypothetical protein	1.01		
lmo0229	CtsR family transcriptional regulator	1.01		1.18
lmo1588	acetylornithine aminotransferase	1.01	2.06	2.50
lmo0550	peptidoglycan bound protein	1.01		
lmo2182	iron complex transport system ATP-binding protein	-0.90		-1.61
lmo2184	heme ABC transporter heme-binding protein isdE	-0.91		-1.32
lmo0138	hypothetical protein	-0.92		
lmo0687	hypothetical protein	-0.94		-1.20
lmo2504	hypothetical protein	-0.95		
lmo0995	YkrP protein	-0.97		
lmo0670	hypothetical protein	-0.97		
lmo1653	cellsurface protein	-1.00		-1.30
lmo1155	propanediol dehydratase small subunit	-1.00		
lmo2024	nicotinate-nucleotide diphosphorylase	-1.01		
lmo2025	quinolinate synthetase complex A subunit	-1.04		
lmo0684	hypothetical protein	-1.04		-1.19
lmo2129	hypothetical protein	-1.05		-2.00
lmo0731	hypothetical protein	-1.06		-2.00
lmo0243	RNA polymerase sporulation-specific sigma factor	-1.10	-2.34	-1.13
lmo2691	autolysin	-1.11		-1.02
lmo0130	hypothetical protein	-1.12		-1.62
lmo0139	hypothetical protein	-1.14		
lmo2505	D-glutamyl-L-m-Dpm peptidase P45	-1.16		-1.12
lmo0240	ribonuclease III family protein	-1.18	-2.00	
lmo0669	hypothetical protein	-1.18		

lmo2651	mannitol-specific PTS system IIA component	-1.21		-1.22
lmo2506	cell division transport system permease	-1.23		-1.11
lmo2522	hypothetical protein	-1.25		
lmo1388	ABC transporter	-1.26		-2.16
lmo2507	cell division ATP-binding protein FtsE	-1.29		-1.13
lmo2352	HTH-type transcriptional regulator ytlI	-1.32		
lmo0394	extracellular P60 protein	-1.38		-1.20
lmo0242	hypothetical protein	-1.50	-2.51	-1.16
lmo2433	tributyrin esterase	-1.51		
lmo0239	cysteinyl-tRNA synthetase	-1.60	-2.38	
lmo0241	TrmH family RNA methyltransferase group 3	-1.61	-2.36	-1.24
lmo0238	serine O-acetyltransferase	-1.74	-2.38	
lmo0137	peptide/nickel transport system permease	-1.79		-1.10
lmo0136	peptide/nickel transport system permease	-1.89		
lmo0152	peptide/nickel transport system substrate-binding protein	-1.93		
lmo2343	monooxygenase moxC	-2.06		-1.26
lmo0135	peptide/nickel transport system substrate-binding protein	-2.07		
lmo2360	membrane protein	-2.08		
lmo2344	hypothetical protein	-2.16		-1.10
lmo2345	hypothetical protein	-2.18		-1.22
lmo0903	OsmC/Ohr family protein	-2.21		-1.27
lmo2351	FMN reductase	-2.27		
lmo2346	polar amino acid transport system ATP-binding protein	-2.35		-1.53
lmo2361	Rrf2 family protein	-2.36		
lmo2350	hypothetical protein	-2.39		-1.08
lmo2347	polar amino acid transport system permease	-2.49	-1.05	-1.52
lmo2349	polar amino acid transport system substrate-binding protein	-2.58	-1.07	-1.28
lmo2348	polar amino acid transport system permease	-2.58		-1.55
lmo2685	cellobiose-specific PTS system IIA component			
lmo2683	cellobiose-specific PTS system IIB component			

lmo2684	cellobiose-specific PTS system IIC component		
lmo0101	hypothetical protein		
lmo2120	hypothetical protein		
lmo2254	AGZA family MFS transporter xanthine/uracil permease	-1.06	-2.08
lmo2127	hypothetical protein		
lmo0880	peptidoglycan bound protein		
lmo0810	spermidine/putrescine transport system substrate-binding protein		
lmo0833	hypothetical protein		
lmo0806	hypothetical protein		
lmo0325	hypothetical protein		
lmo0809	spermidine/putrescine transport system permease		
lmo2158	hypothetical protein		
lmo0843	hypothetical protein		
lmo0808	spermidine/putrescine transport system permease		
lmo0518	membrane protein		1.58
lmo0609	hypothetical protein		
lmo0807	spermidine/putrescine transport system ATP-binding protein		
lmo1334	secreted protein		
lmo0134	hypothetical protein		
lmo2518	transcriptional regulator LytR		
lmo0592	hypothetical protein		
lmo1622	hypothetical protein		
lmo0929	sortase A		
lmo0479	secreted protein		
lmo2454	hypothetical protein		
lmo1713	rod shape-determining protein MreB		
lmo2395	hypothetical protein		
lmo0836	hypothetical protein		
lmo1892	penicillin binding protein 1A		
lmo1516	amt familyammonium transporter		
lmo0230	hypothetical protein		1.40
lmo1518	hypothetical protein		
lmo0286	aminotransferase		
lmo1333	hypothetical protein		
lmo1665	hypothetical protein		
lmo0920	ABC transporter permease		
lmo2708	cellobiose-specific PTS system IIC component		
lmo1295	host factor-I protein		
lmo2437	hypothetical protein		
lmo1506	hypothetical protein		
lmo0186	hypothetical protein		
lmo1601	hypothetical protein		

lmo1074	teichoic acid transport system permease		
lmo0635	2-haloalkanoic acid dehalogenase		
lmo0579	hypothetical protein		1.23
lmo1771	phosphoribosylformylglycinamidine synthase	-1.13	
lmo0921	membrane protein		
lmo1517	nitrogen regulatory protein P-II		
lmo0838	MFS transporter		-1.22
lmo0408	hypothetical protein		
lmo1384	hypothetical protein		
lmo1306	hypothetical protein		
lmo2591	N-acetylmuramoyl-L-alanine amidase		
lmo1075	teichoic acids export ATP-binding protein tagH		
lmo0340	hypothetical protein		
lmo2796	hypothetical protein		1.05
lmo1341	late competence protein ComGG		
lmo2375	hypothetical protein		
lmo0083	hypothetical protein		
lmo0436	hypothetical protein		
lmo0642	hypothetical protein		
lmo1710	flavodoxin		
lmo1139	hypothetical protein		
lmo0492	transcription regulator LysR		
lmo0201	1-phosphatidylinositol phosphodiesterase	-1.56	-1.64
lmo0798	AAT family amino acid transporter		
lmo0999	hypothetical protein		
lmo2548	50S ribosomal protein L31		
lmo0160	peptidoglycan bound protein		
lmo0950	hypothetical protein		
lmo1776	hypothetical protein		
lmo1515	HTH-type transcriptional regulator cymR		
lmo2636	thiamine biosynthesis lipoprotein		
lmo1138	Clp protease		
lmo0629	hypothetical protein		
lmo1229	hypothetical protein		
lmo1007	hypothetical protein		
lmo1635	DNA binding 3-demethylubiquinone-9 3-methyltransferase domain-containing protein		1.12
lmo0406	lactoylglutathione lyase		
lmo0549	internalin		
lmo0706	flagellar hook-associated protein 3		
lmo2801	N-acetylmannosamine-6-phosphate 2-epimerase		
lmo1943	hypothetical protein		
lmo0869	hypothetical protein		

lmo0829	pyruvate:ferredoxin oxidoreductase	
lmo2327	hypothetical protein	-2.03
lmo2499	phosphate transport system substrate-binding protein	
lmo2378	multicomponent Na+:H+ antiporter subunit A	
lmo0128	hypothetical protein	
lmo0498	ribose 5-phosphate isomerase B	
lmo0504	hypothetical protein	
lmo2286	tail or base plate protein gp17	
lmo1031	hypothetical protein	
lmo0267	hypothetical protein	
lmo0087	hypothetical protein	
lmo2380	multicomponent Na+:H+ antiporter subunit C	
lmo1191	cobyrinic acid a,c-diamide synthase	
lmo2460	transcriptional regulator	
lmo2278	endolysin L-alanyl-D-glutamate peptidase	
lmo2234	hypothetical protein	
lmo2173	hypothetical protein	
lmo1310	hypothetical protein	
lmo0316	hydroxyethylthiazole kinase	
lmo2735	sucrose phosphorylase	
lmo2594	hypothetical protein	
lmo2102	glutamine amidotransferase subunit pdxT	
lmo0692	chemotaxis protein cheA	
lmo2584	formate dehydrogenase family accessory protein FdhD	
lmo0383	methylmalonate-semialdehyde dehydrogenase	
lmo0502	hypothetical protein	
lmo2296	phage capsid protein	-1.32
lmo2300	phage terminase large subunit	-1.12
lmo0704	hypothetical protein	
lmo2284	tail or base plate protein gp19	-1.05
lmo2163	hypothetical protein	
lmo2719	tRNA-adenosine deaminase	
lmo2676	DNA polymerase V	
lmo0124	hypothetical protein	
lmo2489	excinuclease ABC subunit B	
lmo0122	hypothetical protein	
lmo0125	hypothetical protein	
lmo1255	trehalose-specific PTS system IIBC component	
lmo2280	gp23	
lmo0118	antigen A	

lmo0001	chromosomal replication initiator protein DnaA		
lmo0659	hypothetical protein		
lmo2664	L-iditol 2-dehydrogenase		
lmo2014	alpha-mannosidase		
lmo0107	ABC transporter		
lmo0705	flagellar hook-associated protein FlgK		
lmo1054	pyruvate dehydrogenase E2 component		
lmo2649	ascorbate-specific PTS system IIC component		-1.25
lmo2291	major tail shaft protein		-1.31
lmo2293	gp10		-1.01
lmo2716	ABC transporter CydDC cysteine exporter CydD		
lmo0127	hypothetical protein		
lmo0716	flagellar protein export ATPase FliI		
lmo2298	phage minor capsid protein		-1.26
lmo2762	cellobiose-specific PTS system IIB component		
lmo2285	tail or base plate protein gp18		
lmo2718	cytochrome bd-I oxidase subunit I		
lmo0426	fructose-specific PTS system IIA component		
lmo1033	transketolase		
lmo0703	hypothetical protein		
lmo0355	fumarate reductase flavoprotein subunit		-1.93
lmo2101	pyridoxine biosynthesis protein		
lmo2470	internalin		
lmo0121	hypothetical protein		
lmo2221	hypothetical protein		
lmo0126	hypothetical protein		
lmo0425	PRD/PTS system IIA 2 domain-containing regulatory protein		
lmo2675	hypothetical protein		
lmo0741	hypothetical protein		
lmo0647	hypothetical protein	1.28	1.24
lmo1055	dihydrolipoyl dehydrogenase		
lmo2447	hypothetical protein		
lmo0129	N-acetylmuramoyl-L-alanine amidase		
lmo2299	phage portal protein		-1.36
lmo2281	gp22		-1.35
lmo1052	pyruvate dehydrogenase E1 component		
lmo2282	short tail fiber		-1.02

lmo2717	cytochrome d ubiquinol oxidase subunit II	
lmo0280	anaerobic ribonucleoside-triphosphate reductase activating protein	
lmo0123	minor structural protein	
lmo0345	ribose 5-phosphate isomerase B	
lmo2295	gp8	-1.16
lmo2292	gp11	-1.10
lmo1053	pyruvate dehydrogenase E1 component subunit beta	
lmo0696	flagellar hook capping protein	
lmo1409	hypothetical protein	
lmo2283	long tail fiber	-1.11
lmo1799	hypothetical protein	-1.14
lmo0115	hypothetical protein	
lmo0120	hypothetical protein	
lmo2325	hypothetical protein	-1.03
lmo0701	hypothetical protein	
lmo0119	hypothetical protein	
lmo0386	3D-(3,5/4)-trihydroxycyclohexane-1,2-dione hydrolase	
lmo0349	hypothetical protein	
lmo1975	DNA polymerase IV	
lmo0279	anaerobic ribonucleoside-triphosphate reductase	
lmo1132	ABC transporter	
lmo1192	cobalamin biosynthesis protein CobD	
lmo0699	flagellar motor switch protein FliM	
lmo2444	hypothetical protein	
lmo2837	multiple sugar transport system permease	
lmo2294	gp9	
lmo0697	flagellar hook protein FlgE	
lmo0760	hypothetical protein	
lmo0758	hypothetical protein	
lmo0698	hypothetical protein	
lmo2661	ribulose-phosphate 3-epimerase	
lmo2324	anti-repressor protein	
lmo0342	transketolase	
lmo0700	flagellar motor switch protein FliN/FliY	
lmo1634	bifunctional acetaldehyde-CoA/alcohol dehydrogenase	
lmo1867	pyruvate, phosphate dikinase	
lmo0344	short chain dehydrogenase	

lmo0788	hypothetical protein		
lmo1131	ABC transporter		
lmo0085	hypothetical protein		-1.43
lmo0761	hypothetical protein		
lmo2222	hypothetical protein		
lmo0702	hypothetical protein		
lmo2668	hypothetical protein		
lmo0759	glyoxylase		
lmo2326	gp41		-1.04
lmo0347	dihydroxyacetone kinase L subunit		
lmo0372	beta-glucosidase		
lmo1654	cellsurface protein		-1.60
lmo0300	beta-glucosidase		
lmo2446	hypothetical protein		
lmo2071	hypothetical protein		
lmo2665	galactitol-specific PTS system IIC component		
lmo0351	dihydroxyacetone kinase		
lmo2304	gp65		
lmo2094	hypothetical protein		1.28
lmo0348	dihydroxyacetone kinase		
lmo2323	gp43		-1.00
lmo0343	transaldolase		
lmo1917	formate acetyltransferase		
lmo2317	gp49		
lmo0916	cellobiose-specific PTS system IIA component		
lmo0266	hypothetical protein		
lmo0350	hypothetical protein		
lmo2688	cell division protein FtsW/RodA/SpoVE		
lmo1204	cobalamin biosynthesis protein CbiM		
lmo0586	hypothetical protein		
lmo0346	triosephosphate isomerase		
lmo2303	gp66		-1.01
lmo2322	gp44		
lmo2105	ferrous iron transporter B		
lmo0378	hypothetical protein		
lmo1407	pyruvate formate-lyase activating enzyme		
lmo1237	glutamate racemase		
lmo0489	hypothetical protein		
lmo2099	hypothetical protein		
lmo2104	ferrous iron transporter A	-1.08	

lmo1236	hypothetical protein		
lmo1655	hypothetical protein		
lmo2662	ribose 5-phosphate isomerase B		
lmo0546	sorbitol-6-phosphate 2-dehydrogenase		
lmo2098	galactitol-specific PTS system IIA component		
lmo0374	cellobiose-specific phosphotransferase enzyme IIB component		-1.28
lmo1239	rdgB/HAM1 family non-canonical purine NTP pyrophosphatase		
lmo1406	formate acetyltransferase		
lmo1238	ribonuclease PH		
lmo2180	hypothetical protein		-1.22
lmo0037	agmatine/putrescine antiporter		
lmo0742	ABC transporter ATP-binding protein		
lmo1240	hypothetical protein		
lmo1182	ethanolamine utilization protein		
lmo0400	fructose-specific PTS system IIC component		
lmo0544	glucitol/sorbitol-specific PTS system IIC component		
lmo0019	hypothetical protein		
lmo0021	mannose-specific PTS system IIA component		
lmo0022	mannose-specific PTS system IIB component	-1.26	
lmo0024	mannose-specific PTS system IID component		
lmo0042	membrane-associated protein		
lmo0052	DHH subfamily 1 protein		
lmo0059	YukD protein		
lmo0072	hypothetical protein		
lmo0096	mannose-specific PTS system IIAB component manL	1.03	
lmo0097	mannose-specific PTS system IIC component	1.23	
lmo0098	F-type H+-transporting ATPase subunit delta	1.11	
lmo0104	hypothetical protein		-1.13
lmo0105	chitinase		1.20
lmo0116	hypothetical protein		
lmo0117	prophage LambdaLm01, antigen B		
lmo0143	hypothetical protein		-1.05
lmo0149	hypothetical protein		
lmo0161	hypothetical protein		-1.01
lmo0197	stage V sporulation protein G		
lmo0200	listeriolysin regulatory protein		-1.30
lmo0202	listeriolysin O		-1.55

lmo0203	zinc metalloproteinase		-1.45
lmo0204	actin-assembly inducing protein ActA		-2.63
lmo0205	phospholipase C		-2.46
lmo0206	hypothetical protein		-2.13
lmo0207	hypothetical protein		-2.16
lmo0223	cysteine synthase A		
lmo0231	ATP:guanido phosphotransferase		1.52
lmo0232	ATP-dependent Clp protease ATP-binding subunit ClpC		1.26
lmo0233	DNA repair protein RadA		
lmo0244	50S ribosomal protein L33	-1.28	
lmo0301	cellobiose-specific PTS system IIA component		
lmo0309	hypothetical protein		-1.24
lmo0323	hypothetical protein		
lmo0324	lipoprotein		
lmo0326	transcriptional regulator		
lmo0328	hypothetical protein		
lmo0331	internalin		
lmo0332	hypothetical protein		
lmo0334	hypothetical protein		-1.16
lmo0336	hypothetical protein		
lmo0357	fructose-specific PTS system IIA component		
lmo0361	twin arginine-targeting protein translocase TatC		
lmo0362	sec-independent protein translocase tatAy		
lmo0365	high-affinity iron transporter		
lmo0366	lipoprotein		
lmo0367	tat-translocated enzyme		
lmo0373	cellobiose-specific PTS system IIC component		
lmo0384	5-deoxy-glucuronate isomerase		
lmo0385	5-dehydro-2-deoxygluconokinase		
lmo0398	fructose-specific PTS system IIA component		
lmo0415	peptidoglycan N-acetylglucosamine deacetylase		
lmo0427	fructose-specific PTS system IIB component		
lmo0433	internalin A		-1.19
lmo0434	internalin B		-1.11
lmo0440	hypothetical protein		
lmo0442	hypothetical protein		
lmo0444	membrane protein		1.19

lmo0485	hypothetical protein	1.04
lmo0490	shikimate 5-dehydrogenase	
lmo0500	hypothetical protein	
lmo0517	phosphoglycerate mutase	
lmo0545	glucitol operon activator protein	
lmo0548	hypothetical protein	
lmo0573	AGZA family MFS transporter xanthine/uracil permease	
lmo0582	invasion associated secreted endopeptidase	-1.03
lmo0584	hypothetical protein	
lmo0587	secreted protein	
lmo0598	biotin biosynthesis protein BioY	
lmo0665	hypothetical protein	
lmo0675	flagellar motor switch protein FliN	-1.10
lmo0681	flagellar biosynthesis regulator FlhF	-1.06
lmo0683	chemotaxis protein methyltransferase	-1.12
lmo0685	chemotaxis protein MotA	-1.48
lmo0686	chemotaxis protein MotB	-1.21
lmo0688	hypothetical protein	-1.32
lmo0689	hypothetical protein	-1.20
lmo0694	hypothetical protein	
lmo0695	hypothetical protein	
lmo0745	hypothetical protein	-1.05
lmo0762	GTP-binding protein HflX	
lmo0765	hypothetical protein	-1.02
lmo0766	multiple sugar transport system permease	-1.26
lmo0767	maltose/maltodextrin ABC transporter permease MalG	-1.10
lmo0778	hypothetical protein	
lmo0786	FMN-dependent NADH-azoreductase 2	
lmo0791	hypothetical protein	-1.21
lmo0794	hypothetical protein	
lmo0797	hypothetical protein	-1.00
lmo0824	hypothetical protein	
lmo0835	peptidoglycan bound protein	

lmo0839	tetracycline resistance protein	
lmo0840	MarR family transcriptional regulator	
lmo0847	glutamine ABC transporter	
lmo0848	polar amino acid transport system ATP-binding protein	
lmo0850	hypothetical protein	-1.46
lmo0864	hypothetical protein	
lmo0867	hypothetical protein	
lmo0874	cellobiose-specific PTS system IIA component	
lmo0875	cellobiose-specific PTS system IIB component	2.77
lmo0881	hypothetical protein	1.03
lmo0908	hypothetical protein	-1.06
lmo0917	beta-glucosidase	
lmo0937	hypothetical protein	-1.24
lmo0941	hypothetical protein	1.29
lmo0942	hypothetical protein	1.31
lmo0952	hypothetical protein	
lmo0953	hypothetical protein	
lmo0989	hypothetical protein	
lmo0994	hypothetical protein	
lmo1014	glycine betaine/proline transport system ATP-binding protein	
lmo1023	ktr system potassium uptake protein C	
lmo1030	hypothetical protein	
lmo1032	transketolase	
lmo1038	molybdopterin-guanine dinucleotide biosynthesis protein MobA	
lmo1069	hypothetical protein	
lmo1070	hypothetical protein	-1.37
lmo1079	hypothetical protein	
lmo1116	hypothetical protein	-1.12
lmo1117	hypothetical protein	-1.26
lmo1127	hypothetical protein	
lmo1133	hypothetical protein	
lmo1151	propanediol utilization protein pduA	
lmo1162	propanediol utilization protein PduM	
lmo1174	ethanolamine utilization protein EutA	
lmo1197	precorrin-4 C(11)-methyltransferase	-1.02
lmo1199	precorrin-3B C(17)-methyltransferase	
lmo1203	precorrin-2 C(20)-methyltransferase	

lmo1208	cobyric acid synthase CobQ		
lmo1211	integral membrane protein		
lmo1216	bax protein		
lmo1254	alpha-phosphotrehalase		
lmo1263	transcriptional regulator		
lmo1266	hypothetical protein		
lmo1284	hypothetical protein		
lmo1297	aluminum resistance protein		
lmo1309	hypothetical protein		
lmo1311	hypothetical protein		
lmo1314	ribosome recycling factor		
lmo1316	phosphatidate cytidylyltransferase		1.07
lmo1317	1-deoxy-D-xylulose 5-phosphate reductoisomerase		1.05
lmo1318	RIP metalloprotease RseP		1.05
lmo1328	tRNA pseudouridine synthase B		
lmo1335	50S ribosomal protein L33		
lmo1364	cold shock-like protein cspLA		
lmo1389	simple sugar transport system ATP-binding protein		
lmo1390	simple sugar transport system permease		
lmo1391	simple sugar transport system permease		
lmo1410	hypothetical protein		-1.48
lmo1411	transcriptional regulator		-1.22
lmo1412	DNA topology modulation protein FlaR		-1.03
lmo1416	hypothetical protein	2.14	1.14
lmo1440	hypothetical protein		
lmo1460	DNA repair protein RecO		
lmo1461	hypothetical protein		-1.07
lmo1466	hypothetical protein		
lmo1468	hypothetical protein		-1.05
lmo1478	MarR family transcriptional regulator		
lmo1480	30S ribosomal protein S20		
lmo1504	alanyl-tRNA synthetase		
lmo1505	hypothetical protein		
lmo1526	hypothetical protein		
lmo1546	rod shape-determining protein MreD	1.05	
lmo1551	folylpolyglutamate synthase		
lmo1584	hypothetical protein		-1.49
lmo1585	protease IV		-1.54
lmo1590	ArgJ family protein	2.29	2.64

lmo1591	N-acetyl-gamma-glutamyl-phosphate reductase	2.41	2.70
lmo1603	aminopeptidase		
lmo1628	tryptophan synthase		
lmo1629	N-(5'phosphoribosyl)anthranilate isomerase		
lmo1631	anthranilate phosphoribosyltransferase		
lmo1632	anthranilate synthase component II		
lmo1649	hypothetical protein		
lmo1666	peptidoglycan bound protein		-1.03
lmo1669	nucleoside triphosphatase YtkD		
lmo1671	zinc transport system substrate-binding protein		
lmo1682	hypothetical protein		
lmo1700	hypothetical protein		
lmo1727	LacI family transcriptional regulator		
lmo1734	glutamate synthase subunit large		
lmo1738	polar amino acid transport system substrate-binding protein		
lmo1739	polar amino acid transport system ATP-binding protein		
lmo1740	polar amino acid transport system permease		
lmo1764	phosphoribosylamine--glycine ligase	-1.10	-1.16
lmo1765	phosphoribosylaminoimidazolecarboxamide formyltransferase/IMP cyclohydrolase	-1.07	-1.20
lmo1766	phosphoribosylglycinamide formyltransferase	-1.19	-1.06
lmo1767	phosphoribosylformylglycinamidine cyclo-ligase	-1.25	-1.04
lmo1768	amidophosphoribosyltransferase	-1.15	
lmo1769	phosphoribosylformylglycinamidine synthase II	-1.23	
lmo1770	phosphoribosylformylglycinamidine synthase I	-1.10	
lmo1772	phosphoribosylaminoimidazolesuccinocarboxamide synthase	-1.11	
lmo1775	AIR carboxylase	-1.15	
lmo1786	internalin C		-1.97
lmo1816	50S ribosomal protein L28		
lmo1841	uracil phosphoribosyltransferase		
lmo1850	hypothetical protein		
lmo1868	lactoylglutathione lyase		
lmo1879	cold shock protein		
lmo1882	30S ribosomal protein S14		
lmo1934	DNA-binding protein HU-beta		
lmo1938	30S ribosomal protein S1		
lmo1966	hypothetical protein		1.07
lmo1971	ascorbate-specific PTS system IIC component		

lmo1983	dihydroxy-acid dehydratase		
lmo1984	acetolactate synthase large subunit		
lmo1986	ketol-acid reductoisomerase		
lmo2011	sensor histidine kinase YesM		
lmo2016	cold shock protein		-2.09
lmo2022	cysteine desulfurase		
lmo2023	L-aspartate oxidase		
lmo2038	UDP-N-acetylmuramoyl-L-alanyl-D-glutamate-2		
lmo2039	penicillin binding protein 2B		
lmo2040	cell division protein FtsL		
lmo2041	methylase MraW		
lmo2042	mraZ protein		
lmo2063	hypothetical protein		-1.23
lmo2079	hypothetical protein		-1.77
lmo2083	hypothetical protein		1.14
lmo2084	hypothetical protein		
lmo2085	peptidoglycan binding protein		
lmo2090	argininosuccinate synthase	2.09	2.44
lmo2091	argininosuccinate lyase	2.38	2.46
lmo2095	1-phosphofructokinase		
lmo2096	galactitol-specific PTS system IIC component		
lmo2097	galactitol-specific PTS system IIB component		
lmo2107	hypothetical protein		
lmo2108	N-acetylglucosamine-6-phosphate deacetylase		
lmo2116	hypothetical protein		
lmo2131	hypothetical protein		-1.34
lmo2132	hypothetical protein		
lmo2133	fructose-bisphosphate aldolase class II		
lmo2134	fructose-bisphosphate aldolase class II		
lmo2135	fructose-specific PTS system IIC component		
lmo2136	fructose-specific PTS system IIB component		
lmo2137	fructose-specific PTS system IIA component		
lmo2147	hypothetical protein		-1.38
lmo2150	hypothetical protein		
lmo2151	hypothetical protein		
lmo2160	sugar phosphate isomerase/epimerase		
lmo2172	propionate CoA-transferase		-1.03
lmo2175	3-oxoacyl-ACP reductase		
lmo2178	peptidoglycan bound protein	1.41	1.42

lmo2181	SrtB family sortase		-1.43
lmo2183	iron complex transport system permease		-1.44
lmo2185	hypothetical protein		-1.65
lmo2186	heme uptake protein IsdC		-1.41
lmo2187	hypothetical protein	-1.33	
lmo2196	peptide/nickel transport system substrate-binding protein		-1.88
lmo2197	hypothetical protein		
lmo2204	hypothetical protein		-1.13
lmo2218	hypothetical protein		
lmo2223	hypothetical protein		
lmo2228	hypothetical protein		
lmo2230	hypothetical protein		
lmo2235	NADH oxidase		
lmo2236	shikimate 5-dehydrogenase		
lmo2245	hypothetical protein		
lmo2247	oxidoreductase		
lmo2250	hypothetical protein	1.18	
lmo2251	polar amino acid transport system ATP-binding protein	1.17	
lmo2252	aspartate aminotransferase	1.26	
lmo2255	hypothetical protein		
lmo2257	hypothetical protein		-1.11
lmo2268	ATP-dependent nuclease subunit B		
lmo2271	phage protein		-1.21
lmo2279	phage holin		-1.04
lmo2287	tail tape-measure protein		-1.11
lmo2288	gp15		-1.08
lmo2289	gp14		-1.11
lmo2290	gp13		
lmo2297	scaffolding protein		-1.20
lmo2301	terminase small subunit		-1.19
lmo2321	gp45		
lmo2356	hypothetical protein		
lmo2376	peptidyl-prolyl isomerase		

lmo2385	ComA operon protein 2		-1.21
lmo2402	hypothetical protein		
lmo2403	hypothetical protein		
lmo2407	hypothetical protein		
lmo2408	transcriptional regulator		-1.14
lmo2409	hypothetical protein		
lmo2410	hypothetical protein		-1.05
lmo2412	NifU family SUF system FeS assembly protein		
lmo2414	FeS assembly protein SufD		
lmo2415	FeS assembly ATPase SufC		
lmo2427	rod shape-determining protein RodA		1.04
lmo2428	rod shape-determining protein RodA		1.20
lmo2432	hypothetical protein		
lmo2439	hypothetical protein	2.07	2.92
lmo2440	hypothetical protein		1.03
lmo2442	hypothetical protein	1.36	1.78
lmo2443	hypothetical protein		
lmo2450	carboxylesterase		
lmo2466	hypothetical protein		
lmo2474	hypothetical protein		
lmo2484	membrane protein	1.10	1.13
lmo2494	phosphate transport system regulatory protein PhoU		
lmo2495	phosphate ABC transporter ATP-binding protein		
lmo2498	phosphate ABC transporter permease		
lmo2502	hypothetical protein		-1.03
lmo2511	sigma-54 modulation protein		
lmo2512	competence protein ComFC		1.16
lmo2527	hypothetical protein		-2.02
lmo2569	peptide/nickel transport system substrate-binding protein		-1.12
lmo2587	hypothetical protein		1.00
lmo2660	transketolase		
lmo2663	L-iditol 2-dehydrogenase		
lmo2666	galactitol-specific PTS system IIB component		
lmo2667	hypothetical protein		
lmo2680	K+-transporting ATPase C subunit		
lmo2681	K+-transporting ATPase B subunit		
lmo2682	K+-transporting ATPase A subunit		
lmo2689	magnesium-translocating P-type ATPase		
lmo2712	gluconokinase		
lmo2744	hypothetical protein		

lmo2786	ADP-ribosylglycohydrolase		
lmo2787	beta-glucoside-specific phosphotransferase enzyme II ABC component		-1.09
lmo2798	hypothetical protein	1.04	1.00
lmo2850	MFS transporter		
lmo2856	50S ribosomal protein L34		

REFERENCES

1. Fahmi, T., Port, G. C. & Cho, K. H. c-di-AMP: An Essential Molecule in the Signaling Pathways that Regulate the Viability and Virulence of Gram-Positive Bacteria. *Genes* **8**, 197 (2017).
2. Structural and Biophysical Analysis of the Soluble DHH/DHHA1-Type Phosphodiesterase TM1595 from Thermotoga maritima: Structure. https://www.cell.com/structure/fulltext/S0969-2126(17)30329-5.
3. Witte, G., Hartung, S., Büttner, K. & Hopfner, K.-P. Structural Biochemistry of a Bacterial Checkpoint Protein Reveals Diadenylate Cyclase Activity Regulated by DNA Recombination Intermediates. *Molecular Cell* **30**, 167–178 (2008).
4. Woodward, J. J., Iavarone, A. T. & Portnoy, D. A. c-di-AMP secreted by intracellular Listeria monocytogenes activates a host type I interferon response. *Science* **328**, 1703–1705 (2010).
5. Aline Dias da, P., Nathalia Marins de, A., Gabriel Guarany de, A., Robson Francisco de, S. & Cristiane Rodrigues, G. The World of Cyclic Dinucleotides in Bacterial Behavior. *Molecules* **25**, 2462 (2020).
6. Yin, W. *et al.* A decade of research on the second messenger c-di-AMP. *FEMS Microbiology Reviews* **44**, 701–724 (2020).
7. Commichau, F. M., Heidemann, J. L., Ficner, R. & Stülke, J. Making and Breaking of an Essential Poison: the Cyclases and Phosphodiesterases That Produce and Degrade the Essential Second Messenger Cyclic di-AMP in Bacteria. *J Bacteriol* **201**, e00462-18, /jb/201/1/JB.00462-18.atom (2018).
8. Corrigan, R. M. & Gründling, A. Cyclic di-AMP: another second messenger enters the fray. *Nature Reviews Microbiology* **11**, 513–524 (2013).
9. Rosenberg, J. *et al.* Structural and Biochemical Analysis of the Essential Diadenylate Cyclase CdaA from Listeria monocytogenes. *J. Biol. Chem.* **290**, 6596–6606 (2015).

10. Pham, T. H., Liang, Z.-X., Marcellin, E. & Turner, M. S. Replenishing the cyclic-di-AMP pool: regulation of diadenylate cyclase activity in bacteria. *Curr Genet* **62**, 731–738 (2016).
11. Mehne, F. M. P. *et al.* Cyclic Di-AMP Homeostasis in *Bacillus subtilis*: BOTH LACK AND HIGH LEVEL ACCUMULATION OF THE NUCLEOTIDE ARE DETRIMENTAL FOR CELL GROWTH. *J. Biol. Chem.* **288**, 2004–2017 (2013).
12. Mudgal, S., Manikandan, K., Mukherjee, A., Krishnan, A. & Sinha, K. M. Cyclic di-AMP: Small molecule with big roles in bacteria. *Microbial Pathogenesis* **161**, 105264 (2021).
13. Huynh, T. N. *et al.* An HD-domain phosphodiesterase mediates cooperative hydrolysis of c-di-AMP to affect bacterial growth and virulence. *Proc Natl Acad Sci USA* **112**, E747–E756 (2015).
14. Bai, Y. *et al.* Two DHH Subfamily 1 Proteins in Streptococcus pneumoniae Possess Cyclic Di-AMP Phosphodiesterase Activity and Affect Bacterial Growth and Virulence. *J Bacteriol* **195**, 5123–5132 (2013).
15. F, R. *et al.* YybT is a signaling protein that contains a cyclic dinucleotide phosphodiesterase domain and a GGDEF domain with ATPase activity. *The Journal of biological chemistry* **285**, (2010).
16. F, R., Q, J., I, S. & Zx, L. Unusual heme-binding PAS domain from YybT family proteins. *Journal of bacteriology* **193**, (2011).
17. Sureka, K. *et al.* The cyclic di-nucleotide c-di-AMP is an allosteric regulator of metabolic enzyme function. *Cell* **158**, 1389–1401 (2014).
18. Blötz, C. *et al.* Identification of the Components Involved in Cyclic Di-AMP Signaling in Mycoplasma pneumoniae. *Front. Microbiol.* **8**, (2017).
19. Ar, G., By, H., C, S., Cm, W. & Tn, H. NrnA Is a Linear Dinucleotide Phosphodiesterase with Limited Function in Cyclic Dinucleotide Metabolism in Listeria monocytogenes. *Journal of bacteriology* **204**, (2022).

20. Yamamoto, T. *et al.* Listeria monocytogenes Strain-Specific Impairment of the TetR Regulator Underlies the Drastic Increase in Cyclic di-AMP Secretion and Beta Interferon-Inducing Ability. *Infection and Immunity* **80**, 2323 (2012).

21. Gries, C. M. *et al.* Cyclic di-AMP Released from Staphylococcus aureus Biofilm Induces a Macrophage Type I Interferon Response. *Infection and Immunity* **84**, 3564–3574 (2016).

22. Schuster, C. F. *et al.* The second messenger c-di-AMP inhibits the osmolyte uptake system OpuC in Staphylococcus aureus. *Sci Signal* **9**, ra81 (2016).

23. Huynh, T. N. *et al.* Cyclic di-AMP targets the cystathionine beta-synthase domain of the osmolyte transporter OpuC. *Molecular Microbiology* **102**, 233–243 (2016).

24. Wetzel, K. J., Bjorge, D. & Schwan, W. R. Mutational and Transcriptional Analyses of the Staphylococcus aureus Low Affinity Proline Transporter OpuD During in vitro Growth and Infection of Murine Tissues. *FEMS Immunol Med Microbiol* **61**, 346–355 (2011).

25. Gundlach, J. *et al.* Sustained sensing in potassium homeostasis: Cyclic di-AMP controls potassium uptake by KimA at the levels of expression and activity. *J Biol Chem* **294**, 9605–9614 (2019).

26. Faozia, S., Fahmi, T., Port, G. C. & Cho, K. H. c-di-AMP-Regulated K+ Importer KtrAB Affects Biofilm Formation, Stress Response, and SpeB Expression in Streptococcus pyogenes. *Infect Immun* **89**, e00317-20 (2021).

27. Gibhardt, J. *et al.* c-di-AMP assists osmoadaptation by regulating the Listeria monocytogenespotassium transporters KimA and KtrCD. *J. Biol. Chem.* jbc.RA119.010046 (2019) doi:10.1074/jbc.RA119.010046.

28. Krüger, L. *et al.* Essentiality of c-di-AMP in Bacillus subtilis: Bypassing mutations converge in potassium and glutamate homeostasis. *PLOS Genetics* **17**, e1009092 (2021).

29. Devaux, L. *et al.* Cyclic di-AMP regulation of osmotic homeostasis is essential in Group B Streptococcus. *PLOS Genetics* **14**, e1007342 (2018).

30. Moscoso, J. A. *et al.* Binding of Cyclic Di-AMP to the Staphylococcus aureus Sensor Kinase KdpD Occurs via the Universal Stress Protein Domain and Downregulates the Expression of the Kdp Potassium Transporter. *Journal of Bacteriology* **198**, 98–110 (2015).

31. Rubin, B. E. *et al.* High-throughput interaction screens illuminate the role of c-di-AMP in cyanobacterial nighttime survival. *PLoS Genet* **14**, e1007301 (2018).

32. Chin, K.-H. *et al.* Structural Insights into the Distinct Binding Mode of Cyclic Di-AMP with SaCpaA_RCK. *Biochemistry* **54**, 4936–4951 (2015).

33. Wright, M. J. & Bai, G. Bacterial second messenger cyclic di-AMP in streptococci. *Molecular Microbiology* **120**, 791–804 (2023).

34. Quintana, I. M. *et al.* The KupA and KupB Proteins of Lactococcus lactis IL1403 Are Novel c-di-AMP Receptor Proteins Responsible for Potassium Uptake. *Journal of Bacteriology* **201**, (2019).

35. Cereija, T. B., Guerra, J. P. L., Jorge, J. M. P. & Morais-Cabral, J. H. c-di-AMP, a likely master regulator of bacterial K+ homeostasis machinery, activates a K+ exporter. *Proc Natl Acad Sci U S A* **118**, e2020653118 (2021).

36. Bai, Y. *et al.* Cyclic Di-AMP Impairs Potassium Uptake Mediated by a Cyclic Di-AMP Binding Protein in Streptococcus pneumoniae. *Journal of Bacteriology* **196**, 614–623 (2014).

37. Whiteley, A. T. *et al.* c-di-AMP modulates Listeria monocytogenes central metabolism to regulate growth, antibiotic resistance and osmoregulation. *Molecular Microbiology* **104**, 212–233 (2017).

38. L, Z., W, L. & Zg, H. DarR, a TetR-like transcriptional factor, is a cyclic di-AMP-responsive repressor in Mycobacterium smegmatis. *The Journal of biological chemistry* **288**, (2013).

39. Peterson, B. N. *et al.* (p)ppGpp and c-di-AMP Homeostasis Is Controlled by CbpB in Listeria monocytogenes. *mBio* **11**, e01625-20 (2020).

40. Krüger, L. *et al.* A meet-up of two second messengers: the c-di-AMP receptor DarB controls (p)ppGpp synthesis in Bacillus subtilis. *Nat Commun* **12**, 1210 (2021).

41. Ren, A. & Patel, D. J. c-di-AMP binds the ydaO riboswitch in two pseudo-symmetry-related pockets. *Nat Chem Biol* **10**, 780–786 (2014).

42. McFarland, A. P. *et al.* Sensing of Bacterial Cyclic Dinucleotides by the Oxidoreductase RECON Promotes NF-κB Activation and Shapes a Proinflammatory Antibacterial State. *Immunity* **46**, 433–445 (2017).

43. Barker, J. R. *et al.* STING-Dependent Recognition of Cyclic di-AMP Mediates Type I Interferon Responses during Chlamydia trachomatis Infection. *mBio* **4**, (2013).

44. Parvatiyar, K. *et al.* DDX41 recognizes bacterial secondary messengers cyclic di-GMP and cyclic di-AMP to activate a type I interferon immune response. *Nat Immunol* **13**, 1155–1161 (2012).

45. M, M., Kp, H. & G, W. c-di-AMP recognition by Staphylococcus aureus PstA. *FEBS letters* **589**, (2015).

46. Warneke, R. *et al.* DarA—the central processing unit for the integration of osmotic with potassium and amino acid homeostasis in Bacillus subtilis. *Journal of Bacteriology* **0**, e00190-24 (2024).

47. Rojas, E. R. & Huang, K. C. Regulation of microbial growth by turgor pressure. *Current Opinion in Microbiology* **42**, 62–70 (2018).

48. Chen, C. & Beattie, G. A. Characterization of the Osmoprotectant Transporter OpuC from Pseudomonas syringae and Demonstration that Cystathionine-β-Synthase Domains Are Required for Its Osmoregulatory Function. *J Bacteriol* **189**, 6901–6912 (2007).

49. J, G. *et al.* Control of potassium homeostasis is an essential function of the second messenger cyclic di-AMP in Bacillus subtilis. *Science signaling* **10**, (2017).

50. Rm, C. *et al.* Systematic identification of conserved bacterial c-di-AMP receptor proteins. *Proceedings of the National Academy of Sciences of the United States of America* **110**, (2013).

51. Quintana, I. *et al.* Genetic Engineering of Lactococcus lactis Co-producing Antigen and the Mucosal Adjuvant 3’ 5’- cyclic di Adenosine Monophosphate (c-di-AMP) as a Design Strategy to Develop a Mucosal Vaccine Prototype. *Frontiers in Microbiology* **9**, (2018).

52. Commichau, F. M., Gibhardt, J., Halbedel, S., Gundlach, J. & Stülke, J. A Delicate Connection: c-di-AMP Affects Cell Integrity by Controlling Osmolyte Transport. *Trends in Microbiology* **26**, 175–185 (2018).

53. Nelson, J. W. *et al.* Riboswitches in eubacteria sense the second messenger c-di-AMP. *Nat Chem Biol* **9**, 834–839 (2013).

54. Whiteley, A. T., Pollock, A. J. & Portnoy, D. A. The PAMP c-di-AMP Is Essential for Listeria monocytogenes Growth in Rich but Not Minimal Media due to a Toxic Increase in (p)ppGpp. *Cell Host & Microbe* **17**, 788–798 (2015).

55. Pham, H. T. *et al.* Cyclic di-AMP Oversight of Counter-Ion Osmolyte Pools Impacts Intrinsic Cefuroxime Resistance in Lactococcus lactis. *mBio* **12**, 10.1128/mbio.00324-21 (2021).

56. Zeden, M. S. *et al.* Identification of the main glutamine and glutamate transporters in Staphylococcus aureus and their impact on c-di-AMP production. *Molecular Microbiology* **n/a**,.

57. Bacillus subtilis DisA regulates RecA-mediated DNA strand exchange - PMC. https://www-ncbi-nlm-nih-gov.ezproxy.library.wisc.edu/pmc/articles/PMC6547438/.

58. Oppenheimer-Shaanan, Y., Wexselblatt, E., Katzhendler, J., Yavin, E. & Ben-Yehuda, S. c-di-AMP reports DNA integrity during sporulation in Bacillus subtilis. *EMBO Rep* **12**, 594–601 (2011).

59. Zheng, C. *et al.* Functional analysis of the sporulation-specific diadenylate cyclase CdaS in Bacillus thuringiensis. *Frontiers in Microbiology* **6**, (2015).

60. Torres, R., Serrano, E., Tramm, K. & Alonso, J. C. Bacillus subtilis RadA/Sms contributes to chromosomal transformation and DNA repair in concert with RecA and circumvents replicative stress in concert with DisA. *DNA Repair (Amst)* **77**, 45–57 (2019).

61. Schär, J. *et al.* Pyruvate Carboxylase Plays a Crucial Role in Carbon Metabolism of Extra- and Intracellularly Replicating Listeria monocytogenes. *Journal of Bacteriology* **192**, 1774–1784 (2010).

62. Campeotto, I., Zhang, Y., Mladenov, M. G., Freemont, P. S. & Gründling, A. Complex Structure and Biochemical Characterization of the Staphylococcus aureus Cyclic Diadenylate Monophosphate (c-di-AMP)-binding Protein PstA, the Founding Member of a New Signal Transduction Protein Family*. *Journal of Biological Chemistry* **290**, 2888–2901 (2015).

63. Choi, P. H., Sureka, K., Woodward, J. J. & Tong, L. Molecular basis for the recognition of cyclic-di-AMP by PstA, a PII-like signal transduction protein. *MicrobiologyOpen* **4**, 361–374 (2015).

64. Massa, S. M. *et al.* C-di-AMP accumulation impairs muropeptide synthesis in Listeria monocytogenes. *Journal of Bacteriology* (2020) doi:10.1128/JB.00307-20.

65. Corrigan, R. M., Abbott, J. C., Burhenne, H., Kaever, V. & Gründling, A. c-di-AMP Is a New Second Messenger in Staphylococcus aureus with a Role in Controlling Cell Size and Envelope Stress. *PLoS Pathog* **7**, e1002217 (2011).

66. Witte, C. E. *et al.* Cyclic di-AMP Is Critical for Listeria monocytogenes Growth, Cell Wall Homeostasis, and Establishment of Infection. *mBio* **4**, e00282-13 (2013).

67. Fernandes-Alnemri, T., Yu, J.-W., Datta, P., Wu, J. & Alnemri, E. S. AIM2 activates the inflammasome and cell death in response to cytoplasmic DNA. *Nature* **458**, 509–513 (2009).

68. Sauer, J.-D. *et al.* Listeria monocytogenes Triggers AIM2-Mediated Pyroptosis upon Infrequent Bacteriolysis in the Macrophage Cytosol. *Cell Host & Microbe* **7**, 412–419 (2010).

69. Zeevi, M. K. *et al.* Listeria monocytogenes Multidrug Resistance Transporters and Cyclic Di-AMP, Which Contribute to Type I Interferon Induction, Play a Role in Cell Wall Stress. *Journal of Bacteriology* **195**, 5250–5261 (2013).

70. Wang, M. *et al.* Adaptation of Listeria monocytogenes to perturbation of c-di-AMP metabolism underpins its role in osmoadaptation and identifies a fosfomycin uptake system. *Environmental Microbiology* **24**, 4466–4488 (2022).

71. Zhang, X. *et al.* Biochemical and molecular regulatory mechanism of the pgpH gene on biofilm formation in Listeria monocytogenes. *Journal of Applied Microbiology* **134**, lxac086 (2023).

72. Bécavin, C. *et al.* Comparison of Widely Used Listeria monocytogenes Strains EGD, 10403S, and EGD-e Highlights Genomic Differences Underlying Variations in Pathogenicity. *mBio* **5**, e00969-14 (2014).

73. Pandey, N. & Cascella, M. Beta-Lactam Antibiotics. in *StatPearls* (StatPearls Publishing, Treasure Island (FL), 2024).

74. Prosser, G. A. & de Carvalho, L. P. S. Kinetic mechanism and inhibition of Mycobacterium tuberculosis D-alanine:D-alanine ligase by the antibiotic D-cycloserine. *FEBS J* **280**, 1150–1166 (2013).

75. Archer, K. A., Durack, J. & Portnoy, D. A. STING-Dependent Type I IFN Production Inhibits Cell-Mediated Immunity to Listeria monocytogenes. *PLOS Pathogens* **10**, e1003861 (2014).

76. Ye, M. *et al.* DhhP, a Cyclic di-AMP Phosphodiesterase of Borrelia burgdorferi, Is Essential for Cell Growth and Virulence. *Infection and Immunity* **82**, 1840–1849 (2014).

77. Cho, K. H. & Kang, S. O. Streptococcus pyogenes c-di-AMP Phosphodiesterase, GdpP, Influences SpeB Processing and Virulence. *PLoS One* **8**, (2013).

78. Fahmi, T., Faozia, S., Port, G. C. & Cho, K. H. The Second Messenger c-di-AMP Regulates Diverse Cellular Pathways Involved in Stress Response, Biofilm Formation, Cell Wall Homeostasis, SpeB Expression, and Virulence in *Streptococcus pyogenes*. *Infect Immun* **87**, e00147-19, /iai/87/6/IAI.00147-19.atom (2019).

79. Yang, J. *et al.* Deletion of the cyclic di-AMP phosphodiesterase gene (cnpB) in Mycobacterium tuberculosis leads to reduced virulence in a mouse model of infection. *Mol Microbiol* **93**, 65–79 (2014).

80. Jackson-Litteken, C. D. *et al.* The Diadenylate Cyclase CdaA Is Critical for Borrelia turicatae Virulence and Physiology. *Infection and Immunity* **89**, e00787-20 (2021).

81. Kundra, S. *et al.* c-di-AMP Is Essential for the Virulence of Enterococcus faecalis. *Infection and Immunity* **89**, e00365-21 (2021).

82. Colomer-Winter, C., Flores-Mireles, A. L., Kundra, S., Hultgren, S. J. & Lemos, J. A. (p)ppGpp and CodY Promote Enterococcus faecalis Virulence in a Murine Model of Catheter-Associated Urinary Tract Infection. *mSphere* **4**, 10.1128/msphere.00392-19 (2019).

83. Moradali, M. F. *et al.* Atypical cyclic di-AMP signaling is essential for Porphyromonas gingivalis growth and regulation of cell envelope homeostasis and virulence. *npj Biofilms Microbiomes* **8**, 1–11 (2022).

84. Hu, J., Zhang, G., Liang, L., Lei, C. & Sun, X. Increased Excess Intracellular Cyclic di-AMP Levels Impair Growth and Virulence of Bacillus anthracis. *Journal of Bacteriology* **202**, (2020).

85. Hu, J., Yao, J., Lei, C. & Sun, X. c-di-AMP accumulation impairs toxin expression of Bacillus anthracis by down-regulating potassium importers. *Microbiology Spectrum* **0**, e03786-23 (2024).

86. Du, B. *et al.* Functional analysis of c-di-AMP phosphodiesterase, GdpP, in Streptococcus suis serotype 2. *Microbiological Research* **169**, 749–758 (2014).

87. Rørvik, G. H., Naemi, A., Edvardsen, P. K. T. & Simm, R. The c-di-AMP signaling system influences stress tolerance and biofilm formation of Streptococcus mitis. *Microbiologyopen* **10**, e1203 (2021).

88. Oberkampf, M. *et al.* c-di-AMP signaling is required for bile salt resistance, osmotolerance, and long-term host colonization by Clostridioides difficile. *Science Signaling* **15**, eabn8171 (2022).

89. W, Z., At, W. & Pj, K. Analysis of human cGAS activity and structure. *Methods in enzymology* **625**, (2019).

90. Andrade, W. A. *et al.* Group B Streptococcus Degrades Cyclic-di-AMP to Modulate STING-Dependent Type I Interferon Production. *Cell Host & Microbe* **20**, 49–59 (2016).

91. Zagorac, G. B. & Kezele, T. G. Ceftriaxone and Doxycycline induced Seroconversion in Previously Seronegative Patient with Clinically Suspected Disseminated Lyme Disease: Case Report. *Infect Chemother* **53**, 582 (2021).

92. Sharma, A. K. *et al.* Bacterial Virulence Factors: Secreted for Survival. *Indian J Microbiol* **57**, 1–10 (2017).

93. Carrasco, S. E. *et al.* Outer Surface Protein OspC Is an Antiphagocytic Factor That Protects Borrelia burgdorferi from Phagocytosis by Macrophages. *Infect Immun* **83**, 4848–4860 (2015).

94. Brouwer, S. *et al.* Pathogenesis, epidemiology and control of Group A Streptococcus infection. *Nat Rev Microbiol* **21**, 431–447 (2023).

95. Kapur, V., Majesky, M. W., Li, L. L., Black, R. A. & Musser, J. M. Cleavage of interleukin 1 beta (IL-1 beta) precursor to produce active IL-1 beta by a conserved extracellular cysteine protease from Streptococcus pyogenes. *Proc Natl Acad Sci U S A* **90**, 7676–7680 (1993).

96. Kapur, V. *et al.* A conserved Streptococcus pyogenes extracellular cysteine protease cleaves human fibronectin and degrades vitronectin. *Microb. Pathog.* **15**, 327–346 (1993).

97. Moayeri, M., Leppla, S. H., Vrentas, C., Pomerantsev, A. P. & Liu, S. Anthrax Pathogenesis*. *Annual Review of Microbiology* **69**, 185–208 (2015).

98. Fioravanti, A. *et al.* Structure of S-layer protein Sap reveals a mechanism for therapeutic intervention in anthrax. *Nat Microbiol* **4**, 1805–1814 (2019).

99. Mignot, T., Mock, M. & Fouet, A. A plasmid-encoded regulator couples the synthesis of toxins and surface structures in Bacillus anthracis. *Molecular Microbiology* **47**, 917–927 (2003).

100. Strauch, M. A. & Hoch, J. A. Transition-state regulators: sentinels of *Bacillus subtilis* post-exponential gene expression. *Molecular Microbiology* **7**, 337–342 (1993).

101. Wertheim, H. F. L., Nghia, H. D. T., Taylor, W. & Schultsz, C. *Streptococcus suis:* An Emerging Human Pathogen. *CLIN INFECT DIS* **48**, 617–625 (2009).

102. Portnoy, D. A., Auerbuch, V. & Glomski, I. J. The cell biology of Listeria monocytogenes infection. *J Cell Biol* **158**, 409–414 (2002).

103. Chico-Calero, I. *et al.* Hpt, a bacterial homolog of the microsomal glucose- 6-phosphate translocase, mediates rapid intracellular proliferation in Listeria. *Proc Natl Acad Sci U S A* **99**, 431–436 (2002).

104. de las Heras, A., Cain, R. J., Bielecka, M. K. & Vázquez-Boland, J. A. Regulation of Listeria virulence: PrfA master and commander. *Current Opinion in Microbiology* **14**, 118–127 (2011).

105. Reniere, M. L. *et al.* Glutathione activates virulence gene expression of an intracellular pathogen. *Nature* **517**, 170–173 (2015).

106. Hall, M. *et al.* Structural basis for glutathione-mediated activation of the virulence regulatory protein PrfA in Listeria. *Proc Natl Acad Sci U S A* **113**, 14733–14738 (2016).

107. Portman, J. L., Dubensky, S. B., Peterson, B. N., Whiteley, A. T. & Portnoy, D. A. Activation of the Listeria monocytogenes Virulence Program by a Reducing Environment. *mBio* **8**, e01595-17 (2017).

108. *Enterococci: From Commensals to Leading Causes of Drug Resistant Infection*. (Massachusetts Eye and Ear Infirmary, Boston, 2014).

109. Basaranoglu, S. T. *et al.* Streptococcus mitis/oralis Causing Blood Stream Infections in Pediatric Patients. *Jpn J Infect Dis* **72**, 1–6 (2019).

110. Schubert, A. M., Sinani, H. & Schloss, P. D. Antibiotic-Induced Alterations of the Murine Gut Microbiota and Subsequent Effects on Colonization Resistance against Clostridium difficile. *mBio* **6**, 10.1128/mbio.00974-15 (2015).

111. Chowdhury, R., Sahu, G. K. & Das, J. Stress response in pathogenic bacteria. *J Biosci* **21**, 149–160 (1996).

112. Foodborne Illness Acquired in the United States—Major Pathogens - PMC. https://www-ncbi-nlm-nih-gov.ezproxy.library.wisc.edu/pmc/articles/PMC3375761/.

113. Radoshevich, L. & Cossart, P. Listeria monocytogenes: towards a complete picture of its physiology and pathogenesis. *Nat Rev Microbiol* **16**, 32–46 (2018).

114. Johansson, J. & Freitag, N. E. Regulation of Listeria monocytogenes Virulence. *Microbiol Spectr* **7**, (2019).

115. Eiting, M., Hagelüken, G., Schubert, W.-D. & Heinz, D. W. The mutation G145S in PrfA, a key virulence regulator of Listeria monocytogenes, increases DNA-binding affinity by stabilizing the HTH motif. *Molecular Microbiology* **56**, 433–446 (2005).

116. Louie, A., Bhandula, V. & Portnoy, D. A. Secretion of c-di-AMP by Listeria monocytogenes Leads to a STING-Dependent Antibacterial Response during Enterocolitis. *Infect Immun* **88**, e00407-20 (2020).

117. Peignier, A. & Parker, D. Impact of Type I Interferons on Susceptibility to Bacterial Pathogens. *Trends in Microbiology* **29**, 823–835 (2021).

118. Schwedt, I., Wang, M., Gibhardt, J. & Commichau, F. M. Cyclic di-AMP, a multifaceted regulator of central metabolism and osmolyte homeostasis in Listeria monocytogenes. *microLife* **4**, uqad005 (2023).

119. Milohanic, E. *et al.* Transcriptome analysis of Listeria monocytogenes identifies three groups of genes differently regulated by PrfA. *Mol Microbiol* **47**, 1613–1625 (2003).

120. Quereda, J. J., Ortega, A. D., Pucciarelli, M. G. & García-Del Portillo, F. The Listeria Small RNA Rli27 Regulates a Cell Wall Protein inside Eukaryotic Cells by Targeting a Long 5'-UTR Variant. *PLoS Genet* **10**, e1004765 (2014).

121. Chen, G. Y., Pensinger, D. A. & Sauer, J.-D. Listeria monocytogenes cytosolic metabolism promotes replication, survival, and evasion of innate immunity. *Cellular Microbiology* **19**, e12762 (2017).

122. Gaballa, A., Guariglia-Oropeza, V., Wiedmann, M. & Boor, K. J. Cross Talk between SigB and PrfA in Listeria monocytogenes Facilitates Transitions between Extra- and Intracellular Environments. *Microbiol. Mol. Biol. Rev.* **83**, (2019).

123. Bergholz, T. M., Bowen, B., Wiedmann, M. & Boor, K. J. Listeria monocytogenes Shows Temperature-Dependent and -Independent Responses to Salt Stress, Including Responses That Induce Cross-Protection against Other Stresses. *Applied and Environmental Microbiology* **78**, 2602–2612 (2012).

124. Chaturongakul, S. & Boor, K. J. σB Activation under Environmental and Energy Stress Conditions in Listeria monocytogenes. *Appl Environ Microbiol* **72**, 5197–5203 (2006).

125. Xia, Y., Xin, Y., Li, X. & Fang, W. To Modulate Survival under Secondary Stress Conditions, Listeria monocytogenes 10403S Employs RsbX To Downregulate σB Activity in the Poststress Recovery Stage or Stationary Phase. *Appl Environ Microbiol* **82**, 1126–1135 (2016).

126. Anaya-Sanchez, A., Feng, Y., Berude, J. C. & Portnoy, D. A. Detoxification of methylglyoxal by the glyoxalase system is required for glutathione availability and virulence activation in Listeria monocytogenes. *PLoS Pathog* **17**, e1009819 (2021).

127. Gopal, S. *et al.* A multidomain fusion protein in Listeria monocytogenes catalyzes the two primary activities for glutathione biosynthesis. *J Bacteriol* **187**, 3839–3847 (2005).

128. Berude, J. C., Kennouche, P., Reniere, M. L. & Portnoy, D. A. Listeria monocytogenes utilizes glutathione and limited inorganic sulfur compounds as a source of essential L-cysteine. *bioRxiv* 2023.10.16.562582 (2023) doi:10.1101/2023.10.16.562582.

129. Reniere, M. L., Whiteley, A. T. & Portnoy, D. A. An In Vivo Selection Identifies Listeria monocytogenes Genes Required to Sense the Intracellular Environment and Activate Virulence Factor Expression. *PLoS Pathog* **12**, e1005741 (2016).

130. Brenner, M. *et al.* Listeria monocytogenes TcyKLMN Cystine/Cysteine Transporter Facilitates Glutathione Synthesis and Virulence Gene Expression. *mBio* **13**, e0044822 (2022).

131. Slauch, J. M. How does the oxidative burst of macrophages kill bacteria? Still an open question. *Mol Microbiol* **80**, 580–583 (2011).

132. Chen, M. *et al.* Listeria monocytogenes GshF contributes to oxidative stress tolerance via regulation of the phosphoenolpyruvate-carbohydrate phosphotransferase system. *Microbiol Spectr* **11**, e0236523 (2023).

133. Dey, B. *et al.* A bacterial cyclic dinucleotide activates the cytosolic surveillance pathway and mediates innate resistance to tuberculosis. *Nat Med* **21**, 401–406 (2015).

134. Savage, C. R. *et al.* Intracellular Concentrations of Borrelia burgdorferi Cyclic Di-AMP Are Not Changed by Altered Expression of the CdaA Synthase. *PLOS ONE* **10**, e0125440 (2015).

135. Commichau, F. M. & Stülke, J. Coping with an Essential Poison: a Genetic Suppressor Analysis Corroborates a Key Function of c-di-AMP in Controlling Potassium Ion Homeostasis in Gram-Positive Bacteria. *J Bacteriol* **200**, e00166-18, /jb/200/12/e00166-18.atom (2018).

136. Huynh, T. N. & Woodward, J. J. Too much of a good thing: regulated depletion of c-di-AMP in the bacterial cytoplasm. *Curr Opin Microbiol* **30**, 22–29 (2016).

137. Stülke, J. & Krüger, L. Cyclic di-AMP Signaling in Bacteria. *Annual Review of Microbiology* **74**, (2020).

138. Kelliher, J. L. *et al.* PASTA kinase-dependent control of peptidoglycan synthesis via ReoM is required for cell wall stress responses, cytosolic survival, and virulence in Listeria monocytogenes. *PLOS Pathogens* **17**, e1009881 (2021).

139. Rismondo, J. *et al.* Discrete and overlapping functions of peptidoglycan synthases in growth, cell division and virulence of Listeria monocytogenes. *Mol Microbiol* **95**, 332–351 (2015).

140. Pensinger, D. A. *et al.* Listeria monocytogenes GlmR Is an Accessory Uridyltransferase Essential for Cytosolic Survival and Virulence. *mBio* **14**, e0007323 (2023).

141. Wemekamp-Kamphuis, H. H. *et al.* Multiple deletions of the osmolyte transporters BetL, Gbu, and OpuC of Listeria monocytogenes affect virulence and growth at high osmolarity. *Applied and Environmental Microbiology* **68**, 4710–4716 (2002).

142. Do, E. A. & Gries, C. M. Beyond Homeostasis: Potassium and Pathogenesis during Bacterial Infections. *Infect Immun* **89**, e0076620 (2021).

143. J, S. *et al.* Pyruvate carboxylase plays a crucial role in carbon metabolism of extra- and intracellularly replicating Listeria monocytogenes. *Journal of bacteriology* **192**, (2010).

144. Borezee, E., Pellegrini, E. & Berche, P. OppA of Listeria monocytogenes, an Oligopeptide-Binding Protein Required for Bacterial Growth at Low Temperature and Involved in Intracellular Survival. *Infection and Immunity* **68**, 7069–7077 (2000).

145. Xayarath, B., Marquis, H., Port, G. C. & Freitag, N. E. Listeria monocytogenes CtaP is a multifunctional cysteine transport-associated protein required for bacterial pathogenesis. *Mol Microbiol* **74**, 956–973 (2009).

146. Ku, J. W. & Gan, Y.-H. Modulation of bacterial virulence and fitness by host glutathione. *Current Opinion in Microbiology* **47**, 8–13 (2019).

147. Lauer, P., Chow, M. Y. N., Loessner, M. J., Portnoy, D. A. & Calendar, R. Construction, characterization, and use of two Listeria monocytogenes site-specific phage integration vectors. *J Bacteriol* **184**, 4177–4186 (2002).

148. Gall, A. R., Hsueh, B. Y., Siletti, C., Waters, C. M. & Huynh, T. N. NrnA Is a Linear Dinucleotide Phosphodiesterase with Limited Function in Cyclic Dinucleotide Metabolism in Listeria monocytogenes. *J Bacteriol* **204**, e0020621 (2022).

149. Robinson, M. D., McCarthy, D. J. & Smyth, G. K. edgeR: a Bioconductor package for differential expression analysis of digital gene expression data. *Bioinformatics* **26**, 139–140 (2010).

150. Forman, H. J., Zhang, H. & Rinna, A. Glutathione: Overview of its protective roles, measurement, and biosynthesis. *Mol Aspects Med* **30**, 1–12 (2009).

151. A Resourceful Race: Bacterial Scavenging of Host Sulfur Metabolism during Colonization - PMC. https://www-ncbi-nlm-nih-gov.ezproxy.library.wisc.edu/pmc/articles/PMC9119060/.

152. New roles for glutathione: Modulators of bacterial virulence and pathogenesis - ScienceDirect. https://www.sciencedirect.com/science/article/pii/S2213231721001701.

153. Meister, A. Glutathione metabolism and its selective modification. *Journal of Biological Chemistry* **263**, 17205–17208 (1988).

154. Ku, J. W. K. & Gan, Y.-H. New roles for glutathione: Modulators of bacterial virulence and pathogenesis. *Redox Biol* **44**, 102012 (2021).

155. Lu, S. C. Glutathione synthesis. *Biochimica et Biophysica Acta (BBA) - General Subjects* **1830**, 3143–3153 (2013).

156. Stout, J., Vos, D. D., Vergauwen, B. & Savvides, S. N. Glutathione Biosynthesis in Bacteria by Bifunctional GshF Is Driven by a Modular Structure Featuring a Novel Hybrid ATP-Grasp Fold. *Journal of Molecular Biology* **416**, 486–494 (2012).

157. Ge, S., Zhu, T. & Li, Y. Expression of Bacterial GshF in Pichia pastoris for Glutathione Production. *Appl Environ Microbiol* **78**, 5435–5439 (2012).

158. Vergauwen, B., De Vos, D. & Van Beeumen, J. J. Characterization of the Bifunctional γ-Glutamate-cysteine Ligase/Glutathione Synthetase (GshF) of *Pasteurella multocida**. *Journal of Biological Chemistry* **281**, 4380–4394 (2006).

159. Brenot, A., King, K. Y., Janowiak, B., Griffith, O. & Caparon, M. G. Contribution of Glutathione Peroxidase to the Virulence of Streptococcus pyogenes. *Infection and Immunity* **72**, 408–413 (2004).

160. Carmel-Harel, O. & Storz, G. Roles of the glutathione- and thioredoxin-dependent reduction systems in the Escherichia coli and saccharomyces cerevisiae responses to oxidative stress. *Annu Rev Microbiol* **54**, 439–461 (2000).

161. Henard, C. A., Bourret, T. J., Song, M. & Vázquez-Torres, A. Control of Redox Balance by the Stringent Response Regulatory Protein Promotes Antioxidant Defenses of Salmonella*. *Journal of Biological Chemistry* **285**, 36785–36793 (2010).

162. Suzuki, H., Kumagai, H. & Tochikura, T. gamma-Glutamyltranspeptidase from Escherichia coli K-12: purification and properties. *Journal of Bacteriology* **168**, 1325–1331 (1986).

163. Gupta, S. *et al.* Glutathione is a potential therapeutic target for acrolein toxicity in the cornea. *Toxicology Letters* **340**, 33–42 (2021).

164. Minami, H., Suzuki, H. & Kumagai, H. γ-Glutamyltranspeptidase, but Not YwrD, Is Important in Utilization of Extracellular Glutathione as a Sulfur Source in Bacillus subtilis. *J Bacteriol* **186**, 1213–1214 (2004).

165. Saini, M., Kashyap, A., Bindal, S., Saini, K. & Gupta, R. Bacterial Gamma-Glutamyl Transpeptidase, an Emerging Biocatalyst: Insights Into Structure–Function Relationship and Its Biotechnological Applications. *Front. Microbiol.* **12**, (2021).

166. Ricci, V., Giannouli, M., Romano, M. & Zarrilli, R. Helicobacter pylori gamma-glutamyl transpeptidase and its pathogenic role. *World J Gastroenterol* **20**, 630–638 (2014).

167. Wang, Y. *et al.* Discovery of a glutathione utilization pathway in Francisella that shows functional divergence between environmental and pathogenic species. *Cell Host Microbe* **31**, 1359-1370.e7 (2023).

168. Giustarini, D. *et al.* Pitfalls in the analysis of the physiological antioxidant glutathione (GSH) and its disulfide (GSSG) in biological samples: An elephant in the room. *Journal of Chromatography B* **1019**, 21–28 (2016).

169. Allocati, N., Federici, L., Masulli, M. & Di Ilio, C. Distribution of glutathione transferases in Gram-positive bacteria and *Archaea*. *Biochimie* **94**, 588–596 (2012).

170. Allocati, N., Federici, L., Masulli, M. & Di Ilio, C. Glutathione transferases in bacteria. *The FEBS Journal* **276**, 58–75 (2009).

171. Glutathione Peroxidase - an overview | ScienceDirect Topics. https://www.sciencedirect.com/topics/neuroscience/glutathione-peroxidase.

172. Zhang, Y. *et al.* Destroying glutathione peroxidase improves the oxidative stress resistance and pathogenicity of Listeria monocytogenes. *Front. Microbiol.* **14**, (2023).

173. Wong, J., Chen, Y. & Gan, Y.-H. Host Cytosolic Glutathione Sensing by a Membrane Histidine Kinase Activates the Type VI Secretion System in an Intracellular Bacterium. *Cell Host & Microbe* **18**, 38–48 (2015).

174. Vallis, A. J., Yahr, T. L., Barbieri, J. T. & Frank, D. W. Regulation of ExoS Production and Secretion byPseudomonas aeruginosa in Response to Tissue Culture Conditions. *Infection and Immunity* **67**, 914–920 (1999).

175. Zemansky, J. *et al.* Development of a mariner-Based Transposon and Identification of Listeria monocytogenes Determinants, Including the Peptidyl-Prolyl Isomerase PrsA2, That Contribute to Its Hemolytic Phenotype. *J Bacteriol* **191**, 3950–3964 (2009).

176. Meganathan, R. Biosynthesis of menaquinone (vitamin K2) and ubiquinone (coenzyme Q): a perspective on enzymatic mechanisms. *Vitam Horm* **61**, 173–218 (2001).

177. Holyoake, L. V., Poole, R. K. & Shepherd, M. The CydDC Family of Transporters and Their Roles in Oxidase Assembly and Homeostasis. *Adv Microb Physiol* **66**, 1–53 (2015).

178. Schardt, J. *et al.* Comparison between Listeria sensu stricto and Listeria sensu lato strains identifies novel determinants involved in infection. *Sci Rep* **7**, 17821 (2017).

179. Corbett, D. *et al.* Listeria monocytogenes Has Both Cytochrome bd-Type and Cytochrome aa3-Type Terminal Oxidases, Which Allow Growth at Different Oxygen Levels, and Both Are Important in Infection. *Infect Immun* **85**, e00354-17 (2017).

180. Rabinovich, L., Sigal, N., Borovok, I., Nir-Paz, R. & Herskovits, A. A. Prophage Excision Activates *Listeria* Competence Genes that Promote Phagosomal Escape and Virulence. *Cell* **150**, 792–802 (2012).

181. Ells, T. C. & Truelstrup Hansen, L. Increased thermal and osmotic stress resistance in Listeria monocytogenes 568 grown in the presence of trehalose due to inactivation of the phosphotrehalase-encoding gene treA. *Appl Environ Microbiol* **77**, 6841–6851 (2011).

182. Schauer, K. *et al.* Deciphering the intracellular metabolism of Listeria monocytogenes by mutant screening and modelling. *BMC Genomics* **11**, 573 (2010).

183. Eylert, E. *et al.* Carbon metabolism of Listeria monocytogenes growing inside macrophages. *Molecular Microbiology* **69**, 1008–1017 (2008).

184. Nielsen, P. K. *et al.* Genome-wide transcriptional profiling of the cell envelope stress response and the role of LisRK and CesRK in Listeria monocytogenes. *Microbiology,* **158**, 963–974 (2012).

185. Berndt, C. & Lillig, C. H. Glutathione, Glutaredoxins, and Iron. *Antioxidants & Redox Signaling* **27**, 1235–1251 (2017).

186. Toledo-Arana, A. *et al.* The Listeria transcriptional landscape from saprophytism to virulence. *Nature* **459**, 950–956 (2009).

187. TRANSIT - A Software Tool for Himar1 TnSeq Analysis | PLOS Computational Biology. https://journals.plos.org/ploscompbiol/article?id=10.1371/journal.pcbi.1004401.

188. Sloggett, C., Goonasekera, N. & Afgan, E. BioBlend: automating pipeline analyses within Galaxy and CloudMan. *Bioinformatics* **29**, 1685–1686 (2013).

189. Chen, S., Zhou, Y., Chen, Y. & Gu, J. fastp: an ultra-fast all-in-one FASTQ preprocessor. *Bioinformatics* **34**, i884–i890 (2018).

190. Langmead, B. & Salzberg, S. L. Fast gapped-read alignment with Bowtie 2. *Nat Methods* **9**, 357–359 (2012).

191. Anders, S., Pyl, P. T. & Huber, W. HTSeq—a Python framework to work with high-throughput sequencing data. *Bioinformatics* **31**, 166–169 (2015).

192. Love, M. I., Huber, W. & Anders, S. Moderated estimation of fold change and dispersion for RNA-seq data with DESeq2. *Genome Biology* **15**, 550 (2014).

193. Carrero, J. A., Calderon, B. & Unanue, E. R. Lymphocytes are detrimental during the early innate immune response against Listeria monocytogenes. *Journal of Experimental Medicine* **203**, 933–940 (2006).

194. Pitts, M. G., Myers-Morales, T. & D'Orazio, S. E. F. Type I IFN Does Not Promote Susceptibility to Foodborne Listeria monocytogenes. *The Journal of Immunology* **196**, 3109–3116 (2016).

195. Cao, T. N., Joyet, P., Aké, F. M. D., Milohanic, E. & Deutscher, J. Studies of the Listeria monocytogenes Cellobiose Transport Components and Their Impact on Virulence Gene Repression. *MIP* **29**, 10–26 (2019).

196. Depletion of glutathione selectively inhibits synthesis of leukotriene C by macrophages. - PMC. https://www.ncbi.nlm.nih.gov/pmc/articles/PMC319382/.

197. Ganz, T. *et al.* Increased inflammation in lysozyme M–deficient mice in response to Micrococcus luteus and its peptidoglycan. *Blood* **101**, 2388–2392 (2003).

198. Peters, J. M. *et al.* A Comprehensive, CRISPR-based Functional Analysis of Essential Genes in Bacteria. *Cell* **165**, 1493–1506 (2016).

199. Banta, A. B. *et al.* A Targeted Genome-scale Overexpression Platform for Proteobacteria. *bioRxiv* 2024.03.01.582922 (2024) doi:10.1101/2024.03.01.582922.

200. Zarrella, T. M. & Bai, G. The Many Roles of the Bacterial Second Messenger Cyclic di-AMP in Adapting to Stress Cues. *J Bacteriol* **203**, e00348-20 (2020).

201. Sievers, S. *et al.* A multicopy sRNA of Listeria monocytogenes regulates expression of the virulence adhesin LapB. *Nucleic Acids Res* **42**, 9383–9398 (2014).

202. Wang, S. *et al.* Phosphotransferase System-Dependent Extracellular Growth of Listeria monocytogenes Is Regulated by Alternative Sigma Factors σL and σH. *Appl Environ Microbiol* **80**, 7673–7682 (2014).